UNIVERSITY OF LATVIA
FACULTY OF CHEMISTRY

DEVELOPMENT AND APPLICATION OF NANOFLOW LIQUID CHROMATOGRAPHY AND MASS SPECTROMETRY METHODS FOR THE DETERMINATION OF CHEMICAL CONTAMINANTS IN FOOD AND ENVIRONMENT

DOCTORAL THESIS

NANOPLŪSMAS ŠĶIDRUMA HROMATOGRĀFIJAS UN MASSPEKTROMETRIJAS METOŽU IZSTRĀDE UN PIELIETOŠANA ĶĪMISKO PIESĀRŅOTĀJU NOTEIKŠANAI PĀRTIKĀ UN VIDĒ

PROMOCIJAS DARBS

Author: **Deniss Fedorenko**
Scientific supervisor: Prof., *Dr. chem.* Vadims Bartkevičs

RIGA
2024

Promocijas darbs izstrādāts Pārtikas drošības, dzīvnieku veselības un vides zinātniskā institūtā "BIOR" laika posmā no 2019. līdz 2023. gadam.

Darbs sastāv no ievada, 3 nodaļām, secinājumiem, literatūras saraksta, 14 pielikumiem.
Darba forma: disertācija dabaszinātnēs (ķīmijas nozarē), analītiskās ķīmijas apakšnozarē.

Darba vadītājs: Prof., *Dr. Chem.*, Vadims Bartkevičs

Recenzenti:

1) Prof., *Dr.habil.chem.* Māris Kļaviņš (Latvijas Universitāte);
2) Asoc. prof., *Dr. chem.* Kristaps Kļaviņš (Rīgas Tehniskā Universitāte);
3) *Dr. chem.* Osvalds Pugovičs (Latvijas Organiskās sintēzes institūts).

Promocijas darba aizstāvēšana notiks 2024. gada 22. februārī, plkst. 14:00 Latvijas Universitātes Ķīmijas nozares promocijas padomes atklātā sēdē Latvijas Universitātē Ķīmijas fakultātē Jelgavas ielā 1, Rīgā, 217. telpā.

Ar promocijas darbu un tā kopsavilkumu var iepazīties Latvijas Universitātes Bibliotēkā Latvijā, Rīgā, Raiņa bulvārī 19.

The doctoral thesis was carried out at the Institute of Food Safety, Animal Health and Environment "BIOR" from 2019 to 2023.

The thesis contains the introduction, 3 chapters, a reference list and 14 appendices.

Form of the thesis: dissertation in Natural Sciences (in the field of Chemistry), subfield of Analytical Chemistry.

Supervisor: Prof., *Dr. chem.*, Vadims Bartkevičs

Reviewers:

1) Prof., *Dr.habil.chem.* Māris Kļaviņš (University of Latvia);
2) Asoc. prof., *Dr. chem.* Kristaps Kļaviņš (Riga Technical University);
3) *Dr. chem.* Osvalds Pugovičs (Latvian Institute of Organic Synthesis).

The thesis will be defended at the public session of the Doctoral Committee of Chemistry, University of Latvia, Jelgavas Str. 1, Riga, at 14:00 on February 22nd, 2024, room 217.

The thesis and the summary of the thesis are available at the Library of the University of Latvia, Raiņa Blvd. 19.

CONTENTS

CONTENTS 4
ABSTRACT 7
ANOTĀCIJA 8
ABBREVIATIONS 9
INTRODUCTION 13
1. LITERATURE REVIEW 22
1.1. Introduction to nanoflow liquid chromatography 22
1.2. Instrumental setups in nano-LC 26
1.3. The applicability of nanoflow liquid chromatography 28
1.4. Chemical contaminants in food and environment 37
1.4.1. Mycotoxins 37
1.4.2. Pyrrolizidine alkaloids 40
1.4.3. Perfluorinated compounds 44
1.4.4. Biomarkers and pharmaceuticals 46
2. EXPERIMENTAL PART 50
2.1. Chemicals and materials 50
2.2. Samples 51
2.3. Determination of mycotoxins 53
2.3.1. Sample preparation 53
2.3.2. Instrumental analysis 54
2.4. Determination of pyrrolizidine alkaloids 54
2.4.1. Investigation of SPE procedure 54
2.4.2. Investigation of QuEChERS procedure 55
2.4.3. Sample preparation procedure 55
2.4.4. Instrumental analysis using conventional flow LC-MS method 56
2.4.5. Instrumental analysis using nano-LC method 57

2.4.6. The use of target ion screening for the determination of pyrrolizidine alkaloids ..58
2.5. Determination of biomarkers and pharmaceuticals 60
2.5.1. Sample preparation..... 60
2.5.2. Instrumental analysis..... 60
2.6. Determination of PFAS 61
2.6.1. Sample preparation..... 61
2.6.2. Instrumental analysis..... 62
3. RESULTS AND DISCUSSION..... 64
3.1. Determination of mycotoxins 64
3.1.1. Optimization of nano-LC setup and MS procedure 64
3.1.2. Method performance evaluation..... 66
3.1.3. The occurrence of mycotoxins in grain cereal and pulses harvested in Latvia..... 68
3.2. Determination of pyrrolizidine alkaloids 72
3.2.1. Evaluation of method performance and different sample preparation procedures 72
3.2.2. The occurrence of pyrrolizidine alkaloids in tea, honey, herbal tinctures, and milk from the Latvian market 74
3.2.3. Target ion screening approach 76
3.3. Determination of biomarkers and pharmaceuticals 80
3.3.1. Method development and optimization of LC 80
3.3.2. Optimization of the Orbitrap MS parameters..... 81
3.3.3. Method performance evaluation..... 83
3.3.4. The occurrence of biomarkers and pharmaceuticals in wastewater..... 85
3.4. Determination of PFAS 86
3.4.1. Control of background contamination..... 86
3.4.2. Selection of the nano-LC fluidics setup 87
3.4.3. Method performance evaluation..... 89
3.4.4. The occurrence of PFAS in food..... 94
CONCLUSIONS 97

ACKNOWLEDGMENTS 100

REFERENCE 101

ANNEXES 130

PUBLICATIONS 146

Application of nano-LC – nano-ESI – Orbitrap-MS for trace determination of four priority PFAS in food products considering recently established tolerable weekly intake (TWI) limits 146

Dilute-and-shoot approach for determination of several biomarkers and pharmaceuticals in wastewater using nanoflow liquid chromatography – Orbitrap mass spectrometry 157

Nanoflow Liquid Chromatography Mass Spectrometry Method for Quantitative Analysis and Target Ion Screening of Pyrrolizidine Alkaloids in Honey, Tea, Herbal Tinctures, and Milk 166

Mycotoxins in cereals and pulses harvested in Latvia by nanoLC-Orbitrap MS 176

Recent Applications of Nano-Liquid Chromatography in Food Safety and Environmental Monitoring: A Review 187

ABSTRACT

Development and application of nanoflow liquid chromatography and mass spectrometry methods for the determination of chemical contaminants in food and environment. Fedorenko, D., scientific supervisor *Dr. chem.*, Prof. Bartkevičs, V. Doctoral thesis in analytical chemistry, 129 pages, 16 figures, 7 tables, 202 literature references, 14 annexes. In English.

In this doctoral thesis, novel analytical methods employing nanoflow liquid chromatography (nano-LC) and Orbitrap mass spectrometry were developed to determine various chemical contaminants in food and the environment. A literature review has been conducted on recent applications of nano-LC methods in the field of food safety and environmental analysis, highlighting the variety of analytes, matrices, and analytical methodologies.

Quantitative analytical methods for determining mycotoxins, pyrrolizidine alkaloids, pharmaceuticals, population-health related biomarkers, and perfluorinated compounds were developed. Different nano-LC instrumental setups were evaluated, including post-column solvent addition. A variety of sample preparation techniques was applied, including solid-phase extraction, quick, easy, cheap, effective, rugged, and safe (QuEChERS) extraction, and dilute-and-shoot approach. A target ion screening approach was developed using selective fragment ions specific to pyrrolizidine alkaloids. Improved retention of ionic and highly polar compounds on reversed-phase nano-LC column has been demonstrated in the analysis of biomarkers and pharmaceuticals by the in-sample addition of tetrabutylammonium bromide as an ion pair reagent.

The developed nano-LC methods were applied to study the occurrence of mycotoxins, pyrrolizidine alkaloids, and perfluorinated compounds in food from the Latvian market, and the occurrence of pharmaceuticals and biomarkers in wastewater from the wastewater treatment plants of different cities in Latvia was studied.

NANOFLOW LIQUID CHROMATOGRAPHY, ORBITRAP MASS SPECTROMETRY, CHEMICAL CONTAMINANTS, WASTEWATER-BASED EPIDEMIOLOGY, TARGET ION SCREENING

ANOTĀCIJA

Nanoplūsmas šķidruma hromatogrāfijas un masspektrometrijas metožu izstrāde un pielietošana ķīmisko piesārņotāju noteikšanai pārtikā un vidē. Fedorenko, D., zinātniskais vadītājs *Dr. chem.*, Prof. Bartkevičs, V. Promocijas darbs, 129 lappuses, 16 attēli, 7 tabulas, 202 literatūras avoti, 14 pielikumi. Angļu valodā.

Šajā promocijas darbā tika izstrādātas jaunas analītiskās metodes, izmantojot nanoplūsmas šķidrumu hromatogrāfiju (nano-LC) un Orbitrap masspektrometriju, lai noteiktu dažādus ķīmiskos piesārņotājus pārtikā un vidē. Tika veikts literatūras apskats par jaunākajiem nano-LC metožu pielietojumiem pārtikas nekaitīguma un vides analīžu jomā, uzsverot analizējamo savienojumu, matricu un analītisko metodoloģiju daudzveidību.

Tika izstrādātas kvantitatīvas analītiskās metodes mikotoksīnu, pirolizidīna alkaloīdu, farmaceitisko savienojumu, populācijas veselības stāvokļa biomarķieru un perfluorētu savienojumu noteikšanai. Tika novērtētas dažādas nano-LC instrumentālās konfigurācijas, tostarp šķīdinātāja pievienošana pēc kolonnas. Ir izmantotas dažādas paraugu sagatavošanas pieejas, tostarp cietfāzes ekstrakcija, ātra, viegla, lēta, efektīva, izturīga un droša (QuEChERS) ekstrakcija un *dilute-and-shoot* pieeja. Tika izstrādāta mērķa jonu skrīninga metode, izmantojot selektīvus fragmentu jonus, kas ir specifiski pirolizidīna alkaloīdiem sadursmju izraisītas disociācijas apstākļos. Uzlabotā polāru savienojumu izdalīšana ar apgrieztās fazes nano-LC kolonnu ir demonstrēta biomarķieru un farmaceitisko savienojumu analīzē, paraugam pievienojot tetrabutilamonija bromīdu kā jonu pāra reaģentu.

Izstrādātās nano-LC metodes tika pielietotas mikotoksīnu, pirolizidīna alkaloīdu un perfluorētu savienojumu noteikšanai pārtikas produktos no Latvijas veikaliem, kā arī tika pētīta farmaceitisko vielu un biomarķieru sastopamība notekūdeņos no dažādām Latvijas pilsētām.

NANOPLŪSMAS ŠĶIDRUMA HROMATOGRĀFIJA, ORBITRAP MASSPEKTROMETRIJA, ĶĪMISKIE PIESĀRŅOTĀJI, NOTEKŪDEŅU EPIDEMIOLOĢIJA, MĒRĶA JONU SKRĪNINGS.

ABBREVIATIONS

15-AcDON	15-Acetyldeoxynivalenol
15-MAS	15-Monoacetoxyscirpenol
3-AcDON	3-Acetyldeoxynivalenol
5-HIAA	5-hydroxyindolic acid
AFB_1	Aflatoxin B_1
AFB_2	Aflatoxin B_2
AFG_1	Aflatoxin G_1
AFG_2	Aflatoxin G_2
AFL	Aflatoxicol
AGC	Automatic gain control
AIF	All ion fragmentation
ALT	Altenuene
AME	Alternariol monomethyl ether
ANOVA	Analysis of variance
AOH	Alternariol
ATX I	Altertoxin I
BEA	Beauvericin
d	dilution factor
D3G	Deoxynivalenol-3-glucoside
dd-MS^2	Data-dependent mass spectrometry method
DON	Deoxynivalenol
dSPE	Disperse solid-phase extraction
ENN B	Enniatin B
ENN B_1	Enniatin B_1

ESI	Electrospray ionization
FB_1	Fumonisin B_1
FB_2	Fumonisin B_2
FB_3	Fumonisin B_3
FS	Full scan
FUS X	Fusarenon X
HPLC	High performance liquid chromatography
HRMS	High-resolution mass spectrometry
HT-2	HT-2 toxin
i.d.	Internal diameter
IL	Ionic liquid
i-LOD	Instrumental LOD
i-LOQ	Instrumental LOQ
LC	Liquid chromatography
LLE	Liquid-liquid extraction
LOD	Limit of detection
LOQ	Limit of quantification
m/z	Mass-to-charge ratio
ME	Matrix effect
m-LOD	LOD of a method
m-LOQ	LOQ of a method
MS	Mass spectrometry
MS/MS	Tandem mass spectrometry
Nano-LC	Nanoflow liquid chromatography
NEO	Neosolaniol
NIV	Nivalenol

Orbitrap-MS	Orbitrap mass spectrometry
OTA	Ochratoxin A
OTB	Ochratoxin B
PFAS	Perfluorinated compounds
PFCA	perfluoroalkyl carboxylic acid
PFHxS	Perfluorohexane sulfonic acid
PFNA	Perfluorononanoic acid
PFOA	Perfluorooctanoic acid
PFOS	Prefluorooctane sulfonate
PFSA	perfluoroalkyl sulfonic acid
PT	Proficiency testing
PVDF	Polyvinylidene fluoride
QC	Quality control
QqQ	Triple quadrupole mass spectrometer
QuEChERS	Analytical approach Quick Easy Cheap Effective Rugged Safe
S/N	Signal-to-noise ratio
SIM	Single reaction monitoring
SPE	Solid phase extraction
T-2	T-2 toxin
T-2TETR	T-2 tetraol
T-2TRI	T-2 toxin triol
TBAB	Tetrabutylammonium bromide
TEN	Tentoxin
TOF	Time-of-flight mass spectrometer
TWI	Tolerable weekly intake
UHPLC	Ultra-high performance liquid chromatography

VBA	Visual Basic for Applications
WW	Wastewater
ZEN	Zearalenone

INTRODUCTION

Nowadays, liquid chromatography and mass spectrometry are widely used analytical chemistry methodologies. This combination provides unique opportunities for a wide variety of applications. Recent technological advances made the reliable, efficient, and robust analysis of various analytes in complex matrices using such techniques possible. Since the dawn of this approach, several factors remained substantial, namely, sensitivity and matrix effects, as they impede the possible implementations, and many advances have been achieved in breaking the gap between innovation and real-world applications. On the one hand, the analytes of interest are usually present in samples at low concentrations, making the sensitivity crucial for the analysis. On the other hand, the ability to analyze complicated matrices is typically limited by the matrix effects.

Miniaturized liquid chromatography systems, such as recently developed nanoflow liquid chromatography (nano-LC) instrumentation combined with a modern mass spectrometry system, for example, Orbitrap, aim to solve both problems. In this work, the nano-LC methodology is evaluated to find possibilities for achieving better sensitivity and reducing matrix effects. Three main model groups of analytes were considered: perfluorinated compounds (PFAS), biomarkers, and pharmaceuticals, as well as pyrrolizidine alkaloids (PAs) and mycotoxins. The advances in the healthcare and food production field resulted in the availability of various chemical compounds for providing quality products for consumers. Different chemical contaminants can be found in foods and the environment, raising concerns over public health. The origins of the chemical contamination could be associated not only with the direct use of some compounds. Still, they could originate from the product itself, for example, during improper storage conditions, such as mycotoxins from the filamentous fungi [8] or pyrrolizidine alkaloids occurring through natural processes in plants [9]. There are several pathways for the entry of pharmaceuticals into the environment, for example, incomplete wastewater treatment, the use of wastewater sludge in agricultural soil, and improper disposal

of unused drugs [1–3]. The presence of antibiotics in foods and the environment is a significant concern, especially in light of emerging antibiotic resistance in pathogens[4]. Industrial processes and production in the previous years used PFAS in various products, contaminating food and the environment [5–7]. This type of environmental contamination not only may exert a significant impact on living organisms but also represents a potential threat to human health.

Not only are these compounds common chemical contaminants found in food products or the environment, but they represent some of the critical analytical challenges. The analysis of PFAS is demanding due to the difficulties in reaching the necessary sensitivity, and, combined with the new legislative requirements for PFAS monitoring in regard to even lower levels of interest, currently, this group of contaminants is challenging. The analysis of complex matrix, such as wastewater, is problematic due to the significant matrix effects as well as the low concentration of analytes. Therefore, dilution of the samples instead of commonly used preconcentration is preferable, provided the sensitivity is sufficient for the analysis. Additionally, PAs and mycotoxins are widely studied groups of contaminants in literature, with great availability of analytical methods for the determination of these compounds. Consequently, a comparison between a nano-LC method and other established methods is beneficial. Moreover, a perspective target ion screening approach for the analysis of chemical compounds without available reference standards is becoming more favorable in the literature, which could be especially useful in the case of PAs due to the great variety of these compounds in nature and the relatively low availability of analytical standards. Therefore, the combination of nano-LC methodology with sensitive and selective high-resolution Orbitrap mass spectrometry could be favorable in providing analytical methods with good sensitivity and low matrix effects, allowing the analysis of complex matrices and a wide variety of analytes.

The practical relevance of the problem.

Chemical contaminants in food and the environment have a significant impact on public health and well-being. Therefore, there is a need to develop novel analytical methods to provide

the necessary sensitivity, reliability, and efficiency to infallibly identify and elucidate the occurrence of contaminants even at low concentrations. The legislation imposes the essential requirements for both analytical performance and the levels of interest for different groups of chemical compounds. However, not all groups of chemical compounds are covered by legislation, and literature data suggest possible risks to health and the environment. Competent authorities have yet to evaluate the data, provide their opinion, and establish the limits of the compounds, for example, in the cases of mycotoxins [10,11] and pharmaceuticals [12,13]. Therefore, occurrence data allow a reliable assessment of the risk associated with exposure to such contaminants. Wastewater-based epidemiology approach (WBE) provides a comprehensive view of the population's well-being and lifestyle habits. It considers biological or chemical indicators for the estimation of consumption patterns of illicit drugs, pharmaceuticals, and other substances, as well as outbreaks of infectious diseases such as COVID-19, which makes this approach multidisciplinary between analytical chemistry, environmental, and social sciences. This approach is cost-effective, non-invasive, and protects personal privacy, meaning the data cannot be associated with an individual and personal privacy is not compromised. Several classes of food, stress, lifestyle, health, and population biomarkers are commonly analyzed in WBE [14]. Analysis of wastewater is challenging due to the complexity of the matrix and the typically low concentrations of the analytes of interest in the sample. Therefore, analytical methods should provide the required sensitivity at the typically low concentrations present in the sample for reliable determination of compounds in complex matrices.

Several analytical techniques are available; however, innovative techniques such as nano-LC provide similar or better sensitivity compared to other types of liquid chromatography, low solvent consumption that reduces both environmental impact and the cost of analysis, and ensures low matrix effects that, in combination with Orbitrap mass spectrometry provide the capability of performing efficient, reliable and sensitive determination of various contaminants in complex matrices [15,16].

The aim of this work. The following aims were proposed during this work:

i. The development of novel analytical methodologies employing nanoflow liquid chromatography – mass spectrometry to evaluate possible sensitivity improvements and reduction of matrix effects in determining model compounds such as mycotoxins, pyrrolizidine alkaloids, and PFAS in food, as well as pharmaceuticals and biomarkers in environmental samples.

ii. The application of the developed methods for the analysis of food products from the Latvian market, studying the occurrence of selected groups of analytes, as well as the analysis of wastewater.

The approach used. The following objectives have been set to fulfil the aims of the thesis:

i. Evaluation of literature data on nano-LC and its recent applications for the determination of various contaminants in food and environmental samples.

ii. Comparison of applications of different optimized instrumental setups of nano-LC.

iii. The development of analytical methods for the determination of mycotoxins, pyrrolizidine alkaloids, PFAS, biomarkers, and pharmaceuticals by employing nano-LC Orbitrap MS.

iv. Investigation of the applicability of target ion screening approach for the screening of the pyrrolizidine alkaloids content using high-resolution Orbitrap mass spectrometry.

v. Investigation of the possibility of improving retention of highly polar analytes with the use of an ion pair reagent with an in-sample addition methodology.

vi. Application of the developed analytical methods for the characterization of occurrence of mycotoxins, pyrrolizidine alkaloids, and PFAS in foods and for the determination of biomarkers and pharmaceuticals in environmental samples.

vii. Expanding the knowledge on the occurrence of such compounds in foods and environmental samples.

Scientific novelty. The scientific novelty of the thesis is expressed as follows:

i. Different instrumental setups were investigated to evaluate the possibilities of improving a nano-electrospray process during highly aqueous gradient conditions and the application of a post-column solvent addition configuration in nano-LC allowed to improve nano-electrospray stability, which has not been reported in the literature to date.

ii. The determination of pyrrolizidine alkaloids in foods using a novel quantitative nano-LC method with post-column solvent addition and small sample loop to improve chromatography of polar compounds, which has not been previously reported in the literature to date.

iii. Applying a novel developed nano-LC Orbitrap MS method for the determination of pyrrolizidine alkaloids provided data on the occurrence of pyrrolizidine alkaloids in food products from the Latvian market, which has been published in the literature for the first time.

iv. The application of in-sample addition of tetrabutylammonium bromide as an ion pair reagent to improve the retention of highly polar compounds in nano-LC has not been previously investigated in the literature, which allowed to analyze both polar and ionic analytes within one chromatographic run using a single reversed-phase C18 nano-LC column.

v. The literature data on the use of nano-LC combined with Orbitrap MS for the wastewater sample analysis is rather limited. The application of the dilute-and-shoot methodology for the quantitative determination of pharmaceuticals, population, and lifestyle biomarkers in wastewater samples using nano-LC was reported in the literature for the first time, which demonstrated that this approach can be successfully applied for WW matrices avoiding time and resource consuming clean-up procedures and providing great accuracy, sensitivity, and simplicity of the method.

vi. A novel nano-LC Orbitrap MS method for the determination of PFAS in food samples was developed and reported in the literature for the first time, allowing the trace determination of four priority PFAS in a wide range of food product groups. The method was selective, sensitive, and reliable which was demonstrated in validation and by the analysis of proficiency testing materials.

vii. The method was applied to analyze different food products from the Latvian market and the occurrence data of PFAS was provided, which has not been reported in the literature to date.

Practical application of the work. The developed nano-LC Orbitrap MS methods were applied to the analysis of chemical contaminants in food products from the Latvian market and wastewater from wastewater treatment plants of Latvian cities. The developed method for the determination of biomarkers and pharmaceuticals is in use in the Institute of Food Safety, Animal Health and Environment "BIOR" for the analysis of wastewater within a monitoring program of lifestyle habits, population health and wellbeing biomarkers. Additionally, the developed methodology will be extended to include other analytes to broaden the scope of application and to extend the method to analyze other types of environmental samples, such as hospital wastewater. The analytical performance of the nano-LC method demonstrated the capabilities that it could be used for quantitative analysis of four priority PFAS in food products at the levels suggested by the new legislative requirements for both monitoring purposes and compliance testing of maximum levels for selected food groups, allowing the routine monitoring program to comply with the new requirements.

Scientific publications.

Publication	Contribution*, %
1. Zacs, D.; **Fedorenko, D.**; Pasecnaja, E.; Bartkevics, V. Application of nano-LC – nano-ESI – Orbitrap-MS for trace determination of four priority PFAS in food products considering recently established tolerable weekly intake (TWI) limits. *Analytica Chimica Acta*[1] **2023**, 341027. *D. Fedorenko has developed 60% of the experimental work, contributed to the writing of the publication (50%), provided the research results in accordance with the requirements of the journal, and also contributed by preparing answers to reviewers' questions and suggestions.*	50
2. **Fedorenko, D.**; Podjava, A.; Prikulis, A.; Bartkevics, V. Dilute-and-shoot approach for determination of several biomarkers and pharmaceuticals in wastewater using nanoflow liquid chromatography – Orbitrap mass spectrometry. *Journal of Separation Science*[2] **2023**, 46:2201002. *D. Fedorenko has developed 80% of the experimental work, contributed to the writing of the publication (80%), provided the research results in accordance with the requirements of the journal, and also contributed by preparing answers to reviewers' questions and suggestions.*	100
3. Jansons, M.; **Fedorenko, D.**; Pavlenko, R.; Berzina, Z.; Bartkevics, V. Nanoflow Liquid Chromatography Mass Spectrometry Method for Quantitative Analysis and Target Ion Screening of Pyrrolizidine Alkaloids in Honey, Tea, Herbal Tinctures, and Milk. *Journal of Chromatography A*[3] **2022**, *1676*, 463269. *D. Fedorenko has developed 50% of the experimental work, contributed to the writing of the publication (60%), provided the research results in accordance with the requirements of the journal, and also contributed by preparing answers to reviewers' questions and suggestions.*	50

[1] *Peer reviewed journal, imprint of Elsevier (IF= 6.911 (2022)), ISSN: 1873-4324*
[2] *Peer reviewed journal, imprint of John Wiley & Sons (IF= 3.614 (2022)), ISSN: 1615-9314*
[3] *Peer reviewed journal, imprint of Elsevier (IF=4.601 (2022)), ISSN: 0021-9673*

4. Reinholds, I; Jansons, M.; **Fedorenko, D.**; Pugajeva, I.; Zute, S.; Bartkiene, E.; Bartkevics, V. Mycotoxins in cereals and pulses harvested in Latvia by nanoLC-Orbitrap MS. *Food Additives & Contaminants: Part B*[4], **2021**, *14(2)*, 115-123. *D. Fedorenko has developed 50% of the experimental work, contributed to the writing of the publication (50%), provided the research results in accordance with the requirements of the journal, and also contributed by preparing answers to reviewers' questions and suggestions.*	100
5. **Fedorenko, D.**; Bartkevics, V. Recent Applications of Nano-Liquid Chromatography in Food Safety and Environmental Monitoring: A Review. *Critical Reviews in Analytical Chemistry*[5] **2021**, 1–25. *D. Fedorenko has developed 90% of the work, contributed to the writing of the publication (90%), provided the research results in accordance with the requirements of the journal, and also contributed by preparing answers to reviewers' questions and suggestions.*	100

* - expressed as part of the publication, included or planned for inclusion in PhD students' thesis

List of conferences.

1. 16th Baltic Conference on Food Science and Technology FOODBALT 2023, Jelgava, Latvia. **Fedorenko, D.**; Jansons, M.; Pavlenko, R.; Berzina, Z.; Bartkevičs, V. The quantitative analysis of pyrrolizidine alkaloids in food products using nanoflow liquid chromatography mass spectrometry (in book of abstracts/oral presentation).
2. 81st International Scientific Conference of the University of Latvia, Section of Analytical Chemistry, Riga, Latvia, 2023. **Fedorenko, D.;** Podjava, A.; Prikulis, A.; Bartkevičs, V. The applicability of the dilute-and-shoot methodology for the determination of several biomarkers and pharmaceuticals in wastewater using nanoflow liquid chromatography – orbitrap mass spectrometry (in book of abstracts/oral presentation).
3. 81st International Scientific Conference of the University of Latvia, Section of Analytical Chemistry, Riga, Latvia, 2023. Skrastiņa, A.; **Fedorenko, D.;** Prikulis, A.;

[4] *Peer reviewed journal, imprint of Taylor & Francis (IF=3.964 (2022)), ISSN: 1939-3229*
[5] *Peer reviewed journal, imprint of Taylor & Francis (IF=5.686 (2022)), ISSN: 1547-6510*

Bartkevičs, V. Occurrence of antibiotics and antiviral drugs in wastewater from 14 Latvian cities (in book of abstracts/oral presentation).

4. 79th International Scientific Conference of the University of Latvia, Section of Analytical Chemistry, Riga, Latvia, 2021. **Fedorenko, D.**; Jansons, M.; Bartkevičs, V. Application of nanoflow liquid chromatography for improvements of mass spectrometric detection sensitivity (in book of abstracts/oral presentation).

1. LITERATURE REVIEW

1.1. Introduction to nanoflow liquid chromatography

Nanoflow liquid chromatography (nano-LC) represents a new step in miniaturization and automation in liquid chromatography achieved by the rapid development of separation science and the availability of advanced chromatography instrumentation. The theoretical background of capillary and nano-LC methods was developed by research groups, including those of Novotny and Karlsson [17,18] and Knox et al.[19,20], who studied separation processes on microcolumns. Since then, the technological development trends have been aimed toward the miniaturization of column size, decreasing the sorbent particle size, and improving the separation efficiency.

The term "nano-liquid chromatography" refers to nanoflow liquid chromatography, and it is agreed that this type of liquid chromatography is characterized by the flow rate that is generally measured in nano litres per minute and the injection volume is also in nano litres [16,21]. During the initial period of development of nano-LC, no clear definition of nano liquid chromatography was established [21,22]. Later on, it was agreed that nano-LC is characterized not only by the flow rate but also by the diameter of an analytical column that typically is below 100 μm, and the injection volume that is measured in nano litres; however, depending on the analytical procedure the injection volume on a micro litre scale could be used, especially when a pre-concentration step is implemented, therefore, improving the sensitivity [23–27].

On the one hand, nano-LC is similar to other types of liquid chromatography in the process of separation of chemical compounds and theoretical background, but on the other hand, it differs from other types of liquid chromatography by the size of capillaries, analytical column, and coupling to detectors. The main points of interest include chromatographic dilution, which depends on the internal diameter (i.d.) of a column, as well on the internal

diameter of other capillaries and the flow rate. Figure 1.1 (A) demonstrates the effect of decreasing i.d. of a column, resulting in radial diameter reduction and increasing the concentration of analyte entering a detector [28]. The effect of the reduced diameter of an analytical column provides better chromatographic separation, demonstrated in Figure 1.1. (B) by Van Deemter plot, and using a flow rate of 175 nL min^{-1}, maximum column plate counts of more than 100000 m^{-1} was achieved [22]. Equation 1.1. demonstrates the relationship between chromatographic dilution *D* that decreases proportionally to the square of column i.d. (denoted as *d*) if other parameters stay the same [29–32] :

$$D = \frac{\pi d_c^2 \varepsilon (1+k)\sqrt{2HL\pi}}{4V_{inj}} \quad (1.1)$$

where *D* is chromatographic dilution, *d* is column i.d., *H* and *L* are the plate height and column length respectively, ε is the column porosity, and V_{inj} is the injection volume.

The decreased flow rate provides several benefits, including improved sensitivity as well as lower solvent consumption, and better coupling to mass spectrometric (MS) detectors [15]. This effect was demonstrated by studying low flow rates that are typical in nano-LC [33]. The signal intensity dependence on the flow rate was investigated, and it was found that the signal intensity in the MS detector improved with a slower flow rate, demonstrated in Figure 1.1. (B). Several explanations of this phenomenon were proposed and it was concluded that a lower flow rate resulted in a more stable spray, improved ionization, and better coupling with MS since the droplet size was smaller at a lower flow rate [29,30,34,35].

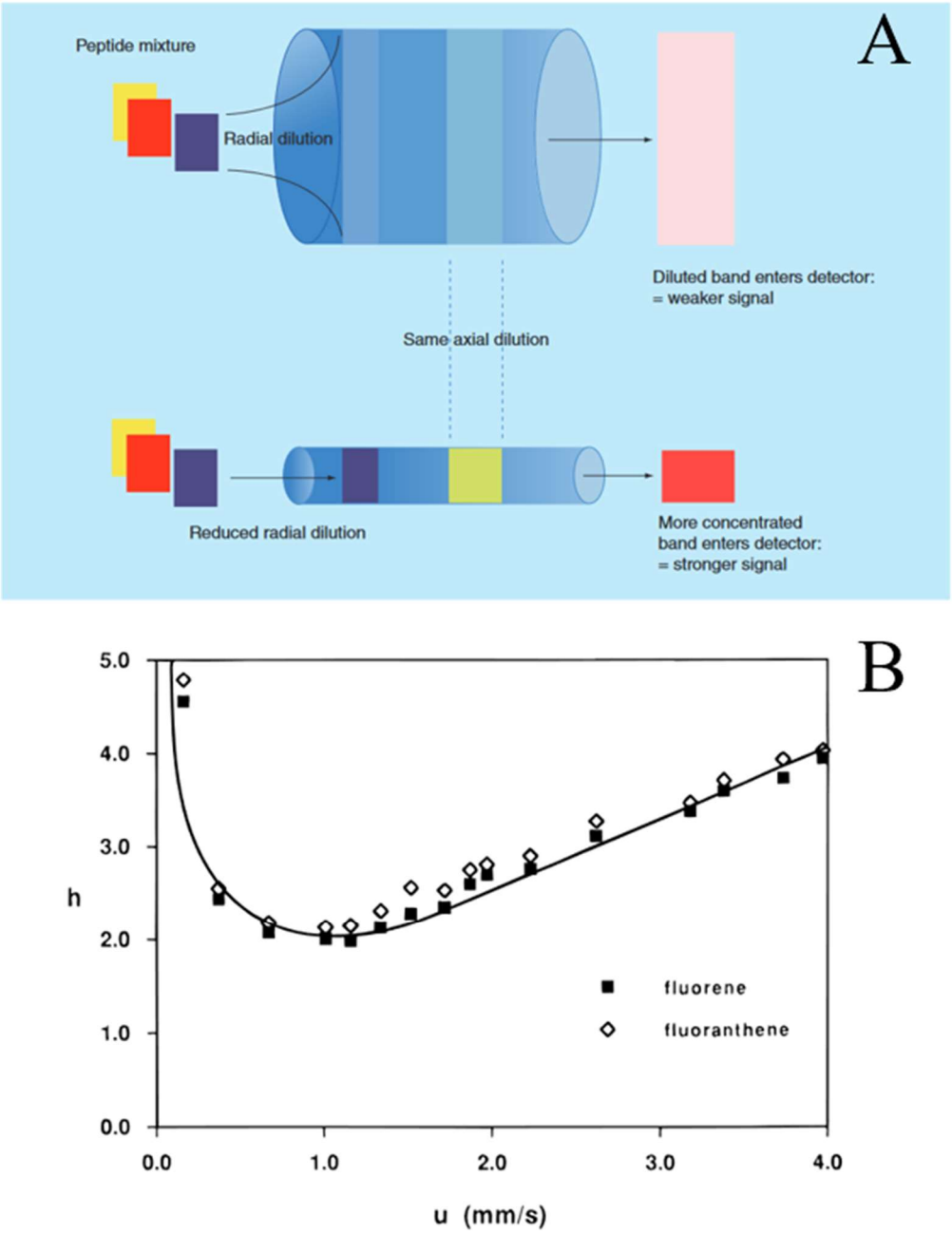

Figure 1.1. **The effect of reducing chromatographic dilution on the sensitivity of a detector (A) and the Van Deemter plot (B) for fluorene and fluoranthene using nanoflow liquid chromatography** [22,28]

The effect of the decreased flow rate is demonstrated in Figure 1.2, where the sensitivity gains of nano-LC were evaluated using Cytochrome C tryptic peptides and compared to analytical LC, micro LC, and capillary LC. Additionally, the number of protein groups identified using nano-LC methodology was significantly larger, and considerably better signal

intensities for nano-LC were achieved for the analyzed HeLa cell lysate digest [36]. Therefore, the use of nano-LC provides more opportunities in the analysis of complex matrices due to the combination of both chromatographic separation and sensitivity.

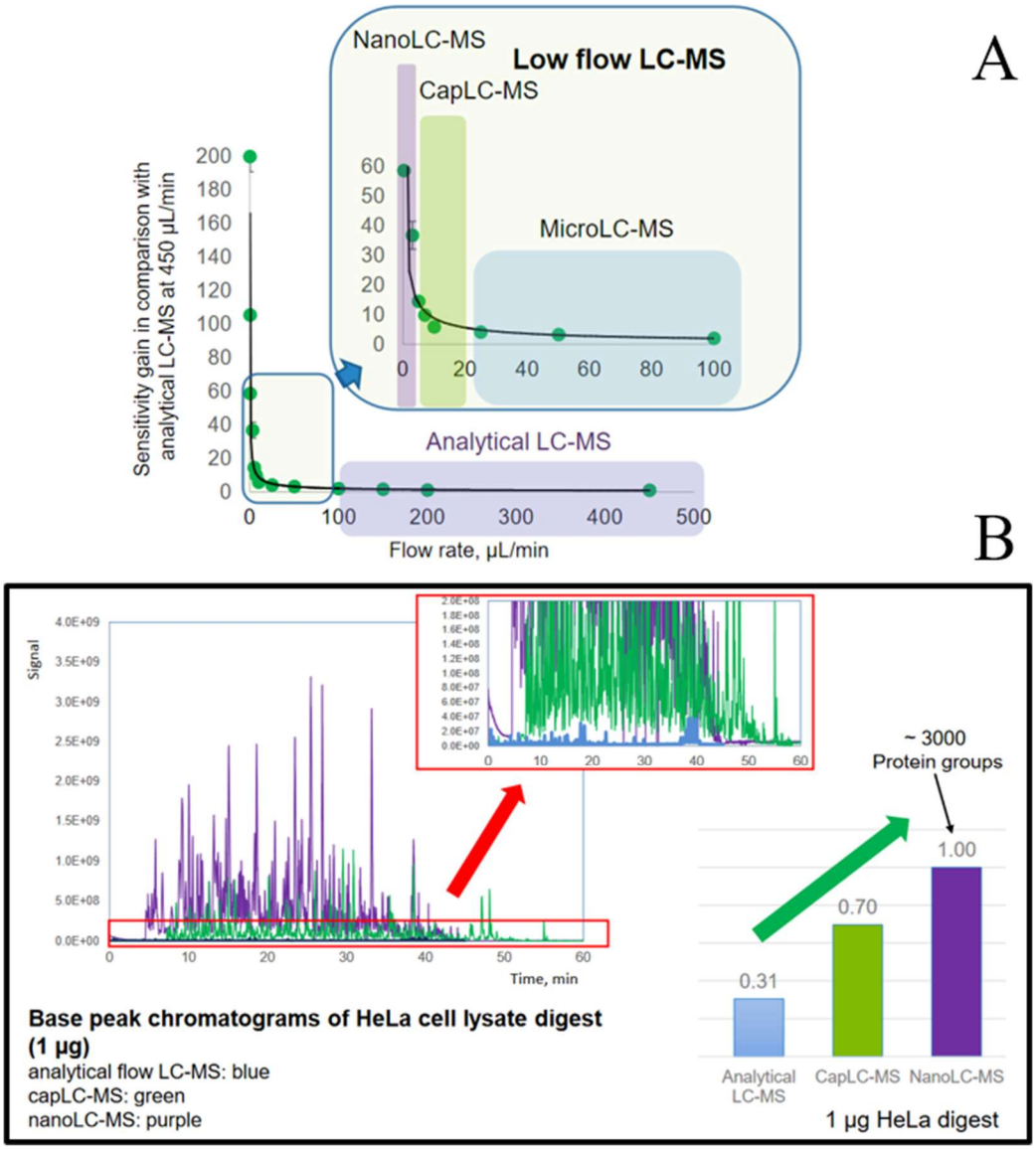

Figure 1.2. **The sensitivity gains of nano-LC in comparison to other types of liquid chromatography (A), and the significantly improved sensitivity and the number of protein groups identified in comparison to analytical and capillary LC [36]**

The initial development and applications of nano-LC included in-house packed analytical columns and pumps with passive split, meaning that the flow from the pump was mechanically

split into two using capillaries with different diameters. The smaller diameter tube led to the column, while the larger diameter tube led to waste, meaning that most of the solvent was discarded [29,30,37]. This approach was not feasible for a broader scale of application since not only the cost of analysis was increased, but also the efficiency and reproducibility of the flow during a chromatographic run under gradient conditions were limited. Consequently, new splitless types of pumps were developed, such as continuous flow and solvent refill pumps [29,30,38], that allowed an accurate, stable, and reproducible flow.

1.2. Instrumental setups in nano-LC

Similar to other conventional types of liquid chromatography, the typical instrumental setup consists of a pump connected to an autosampler, an analytical column, and a detector. Various instrumental setups are implemented in nano-LC and Figure 1.3. demonstrates the fluidics setup used for direct injection and the use of preconcentration on a trap column. Preconcentration or on-column focusing is a widely employed method for increased sensitivity [39]. Similar to other liquid chromatography techniques, preconcentration is also a common method in nano-LC. Two columns with different stationary phases are usually used employing preconcentration technique: analytical column for separation of compounds, and trap column or pre-column for focusing of analytes. On-column focusing allows the analysis of diluted samples, and this is a way of overcoming a low sensitivity issue that is likely to occur in the method with low injection volume or low concentration of analytes in an extract [39–41].

The application of highly aqueous part of a chromatographic gradient combined with the injection of a sample with low organic content and high preconcentration factors may provide instability of nano-electrospray, resulting in decreased sensitivity, reproducibility, and even loss of analytical signal [42,43]. The proper voltage selection for the analysis is important since the changing mobile phase composition under gradient conditions leads to changes in viscosity and surface tension. This phenomenon was investigated [44], and the application of voltage-control

algorithms was proposed. The other approaches for resolving this issue include the use of post-column solvent addition, demonstrated in Figure 1.4, and the use of dilution of the samples [42]. Post-column solvent addition provides increased content of organic phase reaching the ion source during a chromatographic gradient with a highly aqueous part, thus stabilizing nano-electrospray [43].

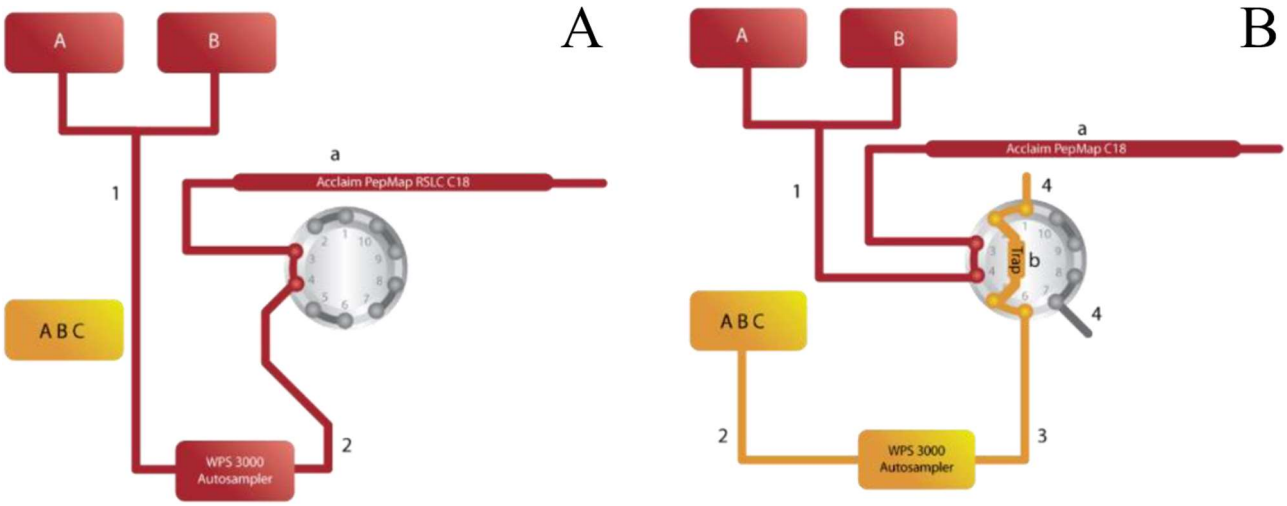

Figure 1.3. **Instrumental setups in nano-LC: the application of direct injection (A) and pre-concentration (B)** [45]

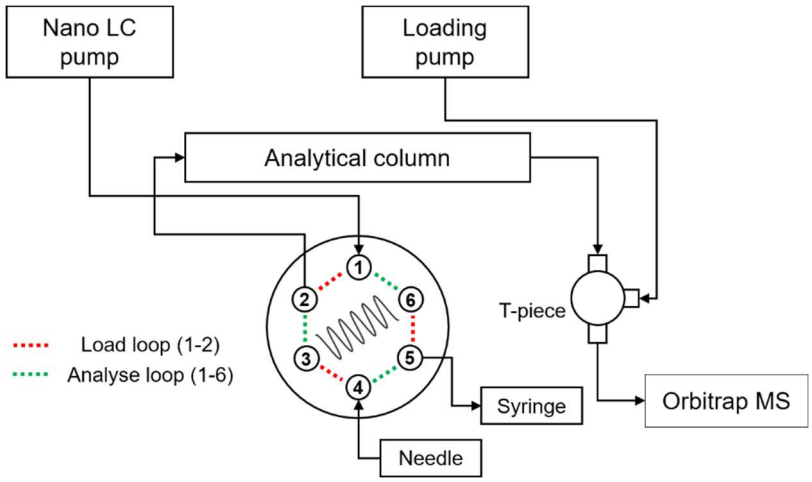

Figure 1.4. **Instrumental setups in nano-LC featuring post-column solvent addition to ensure nanoelectrospray stability**

Applications of nano-LC methodology could be extended to even more miniaturized technology, such as a lab-on-chip approach. This design features a chromatographic column etched out of a flat substrate (chip) and several auxiliary elements, such as a sample preparation section and connection to MS detector [46–49]. This application of the nano-LC concept has several advantages, for example, easier connectivity with separation and reaction processes either before or after the column, as well as reduced connector volumes, which can eliminate dead volumes [48,49]. There is an ongoing research and development effort aimed at providing more practical applications of this type of liquid chromatography for food safety analysis, and several methods have been reported for the determination of mycotoxins [46], pesticides [50], and pharmaceutical compounds [51]. Such iterative optimization and the implementation of innovative ideas expand the possibilities and the applicability of the nano-LC method and facilitate the future development in liquid chromatography miniaturization that is aimed towards further decrease of column internal diameter, as well as the application of lab-on-chip designs and improving robustness that could be beneficial in food and environmental sample analysis.

1.3. The applicability of nanoflow liquid chromatography

Over the years, the interest in nano-LC applications has shifted from mostly in proteomics to other fields, for example, in biochemistry and analysis of pharmaceutical compounds, including chiral compounds [16,29]. Additionally, it is used to analyze environmental samples in forensics and in food safety applications. The number of publications related to nano-LC methods in food analysis initially was significantly lower, despite the key benefit that all sample types currently analyzed by conventional HPLC and UHPLC can also be analyzed by nano-LC methods [29], as shown by the variety of sample types and analytes that have been described in the literature. Nano-LC can be successfully used with a variety of detectors, for example,

ultraviolet diode array detectors (UV-DAD) [52,53] and MS detectors, for example, MS-MS, time of flight (TOF), Q-Trap, and Orbitrap [54].

Nano-LC methods provide numerous advantages, for example, due to the reduced flow rates, consumption of solvents is decreased [21,38,39], in line with the green chemistry principles, reducing both the environmental impact and the cost of analysis. The other significant benefits of nano-LC are sensitivity and low matrix effects, demonstrated by numerous examples in the literature. Table 1.1 lists recent literature sources reporting the applications of nano-LC methods for the analysis of various contaminants and drug residues relevant to food safety, as well as some applications for environment sample analysis. Table 1.1 also provides an overview of the liquid chromatography (LC) conditions and detector types employed in nano-LC analysis by various researchers. MS detectors are used the most frequently, but UV detectors also have been applied. Among the MS detectors, Orbitrap MS is the most implemented detection method in nano-LC. The composition of mobile phases is generally MeCN and H_2O with or without some additives. Both gradient and isocratic conditions are implemented in the nano-LC analytical methods, with the typical injection volumes and flow rates also shown in Table 1.1. Additionally, it should be mentioned that some studies involve a pre-concentration step for sensitivity improvements. It should be noted that the time of nano-LC analysis varies significantly, similar to other liquid chromatography methods. Based on the literature precedents listed in Table 1.1, possibilities for nano-LC method optimization are apparent, and such methods do not always have to be time-consuming despite the slower flow rate.

An additional advantage is the opportunity to use stationary phases that are commonly available for HPLC, such as reversed phase C18 sorbents with 3 – 5 μm or smaller particle size, which are known to enable high separation efficiency [16,30,39]. Other types of columns, such as monolithic and open tubular columns, can be also used with nano-LC methods [29,39,55].

Matrix effects are one of the critical parameters of analytical performance. The sample preparation usually does not eliminate all matrix components, and the final extract typically

contains some matrix components that interfere with analytes during the electrospray ionization process. As a result, the presence of residual matrix components may affect the analytical signal, leading to signal suppression or enhancement [56]. One of the benefits of the nano-LC methods is attributed to the potential for a significant decrease of matrix effects. There are many similarities in the sample preparation procedures for applying with nano-LC and other methods. Sample preparation for nano-LC usually has fewer steps [15], and the reduction of matrix effect is associated with the application of larger dilution factors than in conventional flow LC-MS methods, which is possible due to the better sensitivity. Therefore, dilution is useful for decreasing matrix effects, for instance, a dilution factor of up to 100 resulted in a significant reduction of matrix effects [23]. Dilution factors of 10, 20, and 50 are also reported to substantially decrease matrix effects [24,57]. It has been demonstrated that applying large dilution factors decreased the matrix effects while maintaining reasonable sensitivity.

Sample preparation procedures for nano-LC analysis mostly rely on fewer sample preparation steps compared to other techniques. This brings several benefits, such as shortened sample preparation time, lighter workload of laboratory equipment, and lower consumption of reagents, allowing to reduce the costs of analysis while maintaining the level or improving the analytical performance.

Table 1.1

Several applications of nano-LC methods and their overall characteristics [15]

Analytes	Samples	Instruments	LC mobile phase	Column	Conditions and flow rate	Injection volume	Time of analysis	Reference
Antibiotics (penicillin group)	Pharmaceuticals, bovine milk, porcine tissues (liver and kidney)	UltiMate 3000 nano LC system; Dionex VWD-3000 UV detector; Bruker Ion trap MS Esquire 2000	0.1% FA in H_2O and MeCN	In-house packed C_{18} column, 3 µm, 100 µm i.d. × 100 mm	Gradient, 200 nL min^{-1}	50 –1000 nL	45 min	[53]
Antibiotics and pesticides (two methods)	Milk and honey	UltiMate 3000 nano-LC; UltiMate 3000 RS Variable Wavelength Detector and Exactive Plus Orbitrap MS	MeCN:MeOH:H_2O, 75:15:10 with 3 – 5 % (v/v) FA	In-house packed monolith column with multiwalled carbon nanotubes (MWCNTs), 75 µm i.d. × 100 mm	Isocratic, 800 nL min^{-1}	1000 nL	20 – 25 min	[58]
Phenolic acids, flavonoids	Cranberry syrup	Bruker EASY-nLC; Bruker micrOTOF MS	1 % FA in H_2O and MeCN	NanoSeparations C_{18} column, 3 µm, i.d. 75 µm, with preconcentration	Gradient, 300 nL min^{-1}	1000 nL	40 min	[59]
Antibiotics (sulfonamides)	Pasteurized bovine milk	LC Packing Dionex Ultimate Capillary HPLC with UV detector; Thermo LCQ ion-trap MS	0.1 % FA in H_2O and 0.1 % FA in MeCN	In-house packed C_{18} column, core-shell, 2.6 µm, 100 µm i.d. × 250 mm, with preconcentration	190 nL min^{-1}	200 – 1200 nL	40 min	[60]

Analytes	Samples	Instruments	LC	Column	Conditions and flow rate	Injection volume	Time of analysis	Source
64 multiclass pesticides	Tomato, orange, fruit-based jam, baby food and olive oil	Thermo EASY-nLC 1000 nano-LC, Thermo Q-Exactive Orbitrap MS	0.1 % FA in H_2O and 0.1 % FA in MeCN	Thermo EASY-Spray C_{18} PepMap column, 3 µm, i.d. 75 µm, with preconcentration	Gradient, 300 nL min^{-1}	1000 nL	48 min	[24]
162 multiclass pesticides	Olive oil	Thermo EASY-nLC 1000 nano-LC, Thermo Q-Exactive Orbitrap MS	0.1 % FA in H_2O and 0.1 % FA in MeCN	Thermo EASY-Spray PepMap C_{18} column, 3 µm, i.d. 75 µm	Gradient, 200 nL min^{-1}	1000 nL	37 min	[25]
Pesticides	Apples and baby food	AB Sciex Eksigent Ekspert nano-LC 400, Thermo LTQ-Orbitrap MS with ambient dielectric barrier discharge ionization source	H_2O:MeCN, 95:5 with 0.05 % FA and MeCN with 0.05 % FA	AB Sciex C_{18} column, 3 µm, 75 µm i.d. × 150 mm	Gradient, 800 nL min^{-1}	5000 nL	33 min	[61]
Pharmaceuticals	Benthic invertebrates (*Potamopyrgus antipodarum* and *Valvata piscinalis*)	Thermo Ultimate3000 nano LC, Sciex Qtrap 3200 MS	H_2O:MeCN, 98:2 with 0.1% FA and MeCN:H_2O, 80:20 with 0.1% FA	Themo PepMap C_{18} column, 3 µm, i.d. 75 µm, with preconcentration	Gradient, 300 nL min^{-1}	1000 nL	35 min	[62]

Analytes	Samples	Instruments	LC	Column	Conditions and flow rate	Injection volume	Time of analysis	Source
Pharmaceuticals	Wastewater and sludge	Sciex Eksigent nano LC, Thermo LTQ XL-ETD ion trap MS	0.3 % FA and 0.1 % ammonium formate in H_2O, MeCN with 0.1 % FA	In-house packed column, 3 µm, i.d. 75 µm × 110 mm	Gradient, 300 nL min^{-1}	1000 nL	33 min	[63]
35 emerging pollutants (various classes of pharmaceuticals, steroids, pesticides and others)	Benthic invertebrates (*Potamopyrgus antipodarum*, *Gammarus fossarum*, and *Chironomus riparius*)	Thermo Ultimate 3000 nano-LC, AB Sciex Qtrap 5500	For positive ion mode: 0.1 % FA in H_2O and MeOH:MeCN:H_2O, 45:45:10 with 0.1% FA. For negative ion mode: 0.1 mM NH_4OAc in H_2O and 0.1 mM NH_4OAc in MeCN:MeOH:H_2O, 45:45:10	Thermo PepMap C_{18} column, 3 µm, i.d. 75 µm × 150 mm, with preconcentration	Gradient, 300 nL min^{-1}	1000 nL	64 and 57 min	[27]
Perfluorooctanoic acid, perfluorooctane sulfonate	River water	Agilent Series 1100 capillary gradient pump, Micromass LCT TOF MS	10 mM NH_4OAc in MeCN:H_2O, 10:90; 10 mM NH_4OAc in MeCN:H_2O, 90:10	G&T Septech C_{18} column, 3.5 µm, i.d. 100 µm × 150 mm, with preconcentration	Gradient, 700 nL min^{-1}	0.02 – 1000 µL	14 min	[64]
Mycotoxins	Edible nuts (peanuts, pistachios, almonds)	Thermo EASY-nLC 1000 nano-LC system and Thermo Q-Exactive Orbitrap MS	0.1 % FA in H_2O and 0.1 % FA in MeCN	Thermo PepMap C_{18} column, 3 µm, i.d. 75 µm× 150 mm, with preconcentration	Gradient, 200 nL min^{-1}	100 nL	28 min	[65]

Analytes	Samples	Instruments	LC	Column	Conditions and flow rate	Injection volume	Time of analysis	Source
Pesticides (aldicarb, atrazine, methomyl, propazine)	River water	Agilent 1100 series nano LC system; direct-EI-MS; Agilent 5975B Inert MSD MS	H_2O and MeCN	Agilent C_{18} Zorbax-SB, 3.5 µm, 75µm i.d. × 150 mm	Gradient, 300 nL min^{-1}	60 nL	40 min	[56]
Veterinary drugs and antibiotics	Honey, veal muscle, eggs and milk	Thermo EASY-nLC 1000 nano-LC system, Thermo Q-Exactive Orbitrap MS	0.1 % FA in H_2O and 0.1 % FA in MeCN	Thermo EASY-Spray PepMap C_{18} column, 3 µm, 75 µm i.d. × 150 mm	Gradient, 200 nL min^{-1}	1000 nL	35 min	[23]
Pesticides	Milli-Q water (spiked)	LC Packings Dionex Ultimate Capillary HPLC; mechanical split; UV detector; Thermo nano pump	0.1 % FA in H_2O and 0.1 % FA in MeCN	In-house packed phenyl column, 3 µm, 100 µm i.d., 250 mm, with preconcentration	Gradient, 500 nL min^{-1}	20 µL	25 min	[66]
Pesticides	Honeybees	Thermo EASY-nLC 1000 nano-LC system, Thermo Q-Exactive Orbitrap MS	0.1 % FA in H_2O and 0.1 % FA in MeCN	Thermo EASY-Spray PepMap C_{18} column, 3 µm, 75 µm i.d. × 150 mm	Gradient, 200 nL min^{-1}	1000 nL	37 min	[26]
Insecticides and pesticides	Honey and pollen	Thermo EASY-nLC 1000 nano-LC system, Thermo Q-Exactive Orbitrap MS	0.1 % FA in H_2O and 0.1 % FA in MeCN	Thermo EASY-Spray PepMap C_{18} column, 3 µm, 75 µm i.d. × 150 mm	Gradient, 300 nL min^{-1}	1000 nL	37 min	[67]

Analytes	Samples	Instruments	LC	Column	Conditions and flow rate	Injection volume	Time of analysis	Source
Pesticides	Baby food	LC Packings Dionex Ultimate Capillary HPLC unit with mechanical spilt and UV detector	H_2O and MeCN (20:80, v/v)	In-house packed phenyl column, 3 µm, 100 µm i.d. × 255 mm, with preconcentration	Isocratic, 300 nL min^{-1}	1000 nL	32 min	[68]
Pesticides, drugs of abuse, performance enhancing drugs, environmental contaminants	Food (leek, lemon, olive oil), human urine, wastewater	Thermo EASY-nLC 1000 nano-LC system, Thermo Q-Exactive Orbitrap MS	0.1 % FA in H_2O and 0.1 % FA in MeCN	Thermo EASY-Spray PepMap C_{18} column, 2 µm, 75 µm i.d. × 500 mm and 3 µm, 75 µm i.d. × 150 mm	Gradient, 300 nL min^{-1}	1000 nL	45 min and 37 min	[57]
Aflatoxins	Peanut products (peanuts, peanut butter, peanut powder)	Agilent 1200 nano-HPLC; Agilent 6410 series TripleQuad MS	0.1 mM NH_4OAc in H_2O and MeCN:MeOH (25:75, v/v) with 1mM NH_4OAc	Agilent nanoLC-chips with Zorbax SB-C_8 stationary phase, 5 µm, 75 µm i.d. × 150 mm, with preconcentration	Gradient, 300 nL min^{-1}	8000 nL	25 min	[46]

Abbreviations: FA – formic acid; MeCN – acetonitrile; MeOH – methanol; UV – ultraviolet; TOF – time of flight; i.d. – internal diameter; NH_4OAc – ammonium acetate; IAC – immunoaffinity cartridges

Despite its aforementioned advantages, several drawbacks are present with this type of miniaturized liquid chromatography that affect the applicability of this method. Some parameters of nano-LC methods require more attention than regular HPLC. Since lower flow rates are applied, longer equilibration and analysis time are required, resulting in decreased sample throughput. Another concern is that it is essential to pay attention to the void volume and dead volume [29,30,39] by ensuring that all fittings are correct and the length of the capillaries is appropriate. In regular high performance liquid chromatography (HPLC), leakages usually can be spotted easily. However, the flow rates in nano-LC are significantly slower, and leakages are harder to spot [69]. Therefore, precisely matching fittings must be used, and more attention should be given to this problem. Smaller capillaries also result in higher chances of clogging; therefore, filtering of the samples is crucial. Analytical column in nano-LC has smaller dimensions and less amount of sorbent, meaning that a high concentration of matrix components could easily oversaturate a column, reducing efficiency and decreasing its lifespan. Therefore, sample dilution is often used [23,24,57]. Narrower bands in nano-LC, compared with HPLC and ultra-high performance liquid chromatography (UHPLC), indicate that a detector must be fast enough to have sufficient scanning time to obtain the adequate number of scans per band. Another concern regarding nano-ESI is the selection of the proper voltage for the analysis. Under isocratic conditions, an acceptable voltage for ionization can be found experimentally and is equally applicable throughout the chromatographic run. However, the changing mobile phase composition under gradient conditions leads to viscosity and surface tension changes, which affect electrospray efficiency. This phenomenon was studied, and the application of voltage-control algorithms was proposed[44]. The robustness of the technique is considered in practical applications [70]; therefore, the limitations must be assessed to evaluate whether a method is fit for purpose.

1.4. Chemical contaminants in food and environment

1.4.1. Mycotoxins

Mycotoxins represent the class of naturally occurring contaminants and are secondary metabolites originating from filamentous fungi, including such species as *Aspergillus, Penicillium, Fusarium,* and *Claviceps* [8]. Grain cereals are the most susceptible crops to mycotoxins. Filamentous fungi produce mycotoxins during pre-harvest and post-harvest periods under certain environmental and microclimatic conditions, such as high temperatures and humidity, elevated moisture, and CO_2 levels. This causes economic losses to agriculture worldwide [71] and increases the health-associated risks for consumers since exposure to mycotoxins is associated with acute and chronic health effects in humans [72].

While many mycotoxins are known, the maximum levels (MLs) of mycotoxins in European non-processed and processed cereals have been set only for nine compounds under the Commission Regulation (EC) No 1881/2006 [11]. Mycotoxin exposure is associated with increased health risks for humans and other animal species. Table 1.2 provides a brief overview of the toxicity, including the carcinogenic classification of several groups of mycotoxins widely reported in the literature. The International Agency for Research on Cancer (IARC) classified some of them as group 1 human carcinogen, such as aflatoxin B_1 (AFB_1) and the combination of four aflatoxins (AFs: $AFB_1 + AFB_2 + AFG_1 + AFG_2$), as possible human carcinogens (group 2B) for ochratoxin A (OTA) and not classifiable as to its carcinogenicity to humans for the fumonisins FB_1 and FB_2 and the *Fusarium* toxins deoxynivalenol (DON) and zearalenone (ZEN) [73]. According to Commission Recommendation 2013/165/EU [74], the data on the toxicity of type A trichothecenes T-2 and HT-2 are limited, and further extended screening of these toxins has been advised due to their relatively high prevalence and contamination levels in the cereals harvested in Europe [75,76].

Table 1.2

A brief overview on the classification of the mycotoxins and the health risks [72,73,77]

Toxin	Examples	Carcinogenic group	Toxicities of the mycotoxins	Producing fungi
Aflatoxins	Aflatoxins AFB_1, AFB_2, AFG_1, AFG_2, AFM_1, AFM_2	Group 1 (except for AFM_2)	Genotoxicity, hepatotoxicity, mutagenic	*Aspergillus Emericella*
Ochratoxins (OTA, OTB, OTC)	Ochratoxin A	Group 2B (OTA)	Nephrotoxicity, carcinogenic (OTA)	*Aspergillus Neopetromyces muricatus, Penicillium*
Citrinin (CT)	CT	ND	Nephrotoxicity	*Penicillium, Aspergillus, Monascus purpureus*
Fumonisins	FB_1, FB_2, FB_3, FB_4	Group 2B (FB_1, FB_2)	Esophagus cancer, neural tube defects	*Fusarium Aspergillus Alternaria*
Trichothecenes (T-2, HT-2, DAS, NIV, DON)	T-2, HT-2, DAS, NIV, DON	Group 3 (DON)	Severe GI toxicity (DON), lymphocytic, carcinogenic, cytotoxic, and immunosuppressive (T-2), bone marrow toxicity and toxicity of lymphoid organs (NIV)	*Fusarium Cephalosporium sp., Myrothecium sp., Trichoderma sp., Verticimonosporium sp. Phomopsis sp., Stachybotrys sp. Graminearum sp.*
Zearalenone (ZEN)	ZEN	Group 3	Genotoxici*ty*, carcinogenic	*Fusarium Gibberella*
Patulin (PAT)	PAT	Group 3	Immunotoxicity, nephrotoxicity, hepatotoxicity, genotoxicity	*Aspergillums, Penicillium, Byssochlamys, Paecilomyces*
Ergot alkaloids	Ergocryptine, ergocornine, ergocristine, etc.	ND	Ergotism	*Claviceps Neotyphodium coenophialum*

OTA – ochratoxin A; OTB – ochratoxin B; OTC – ochratoxin C; DON – deoxynivalenol; CT – citrinin; DAS – diacetoxyscirpenol; NIV – nivalenol, ZEN – zearalenone, PAT – patulin; GI – gastrointestinal; Group 1: the agent is carcinogenic to humans; Group 2B: the argent is possibly carcinogenic to humans; Group 3: the agent is not classifiable as to its carcinogenicity to humans; ND – no data

Compared to cereals, legumes are a wider group of protein-rich crop varieties and include lentils, beans, cowpeas, peas, soybeans, lupin beans, and others. However, no limits have been set in Europe for the mycotoxin levels in processed grain legumes and unprocessed pulses. The consumption of legume products has been growing steadily in recent years, driven by the trend of shifting towards vegetarian and vegan food preferences and the increase in consumption

among adults and children following grain-free diets due to specific allergies or intolerances. These growth conditions of these crops are considered mycotoxin growth-inducing climatic conditions, thus being more susceptible to cross-contamination with filamentous fungi that produce mycotoxins [78].

Type A and type B trichothecenes T-2, HT-2, DON, nivalenol (NIV), and acetylated DON forms (3-AcDON, 15-AcDON) have been associated with certain acute human and animal health disorders such as gastroenteritis outbreaks, immune suppression, and haemorrhaging effects. ZEN, a mycoestrogenic toxin, has been associated with adverse effects such as reproductive disorders in domestic animals and hyperestrogenic syndrome in humans [77,79]. Emerging *Fusarium* enniatins (ENNs), beauvericin (BEA), and *Alternaria* toxins have also raised concerns about health-endangering effects because of their high prevalence in non-processed crops and cereal products [80,81], including infant food products [82].

Multi-mycotoxin LC-MS methods have been extensively employed over the last years, and improvements in terms of sample preparation, selectivity, and sensitivity for the qualitative and quantitative mycotoxin analyses were achieved. Various instrumental methods are reported in the literature for the determination of mycotoxins, while the most common approach is the use of HPLC-MS/MS methodology [83]. High-resolution mass spectrometry techniques (HRMS) based on TOF and the Orbitrap-MS systems have been introduced for multi-mycotoxin analysis, including both targeted and non-targeted applications. Compared to tandem mass spectrometry (MS/MS) methods based on low-resolution multi-monitoring, such applications provide advantages of improved selectivity achieved by applying high-resolution detection using different available mass spectrometric modes such as full scan (FS) or parallel reaction monitoring (PRM) and facilitate accurate mass measurement, as well as the elimination or reduction of the interference impact on analyte signal intensity during multi-compound analysis [84,85]. While improvements in method specificity of HRMS can be attributed to the increase in MS resolution, ion suppression or enhancement phenomena due to matrix effects may occur in

both MS/MS and HRMS approaches [86]. The use of nano-LC methodology for determining mycotoxins allowed to achieve low matrix effects, low solvent consumption, and great sensitivity as reported in recent literature [46,65].

1.4.2. Pyrrolizidine alkaloids

Pyrrolizidine alkaloids (PAs) are 1,2-saturated, 1,2-unsaturated necine bases, or 1,2-saturated otonecine bases that represent a group of compounds found in the *Fabaceae*, *Boraginaceae, Apocynaceae, Jacobeae,* and *Asteraceae* plant families. While being open-chain monoesters and diesters or macrocyclic diesters regarding the chemical structure, there is a great variety of PAs occurring in nature. PAs are produced by plants as secondary metabolites for defense purposes against herbivores and insects. These compounds can be oxidized to form *N*-oxides [87–89]. Figure 1.5. demonstrates the main structural differences between the various types of PAs [90].

The main contamination pathways of plant food with PAs are reported to be co-harvesting of plants containing PAs, contamination through horizontal natural transfer from PA-producing plants via the soil, or intended adulteration [89,91,92]. However, the presence of PAs is not only limited to plant-based products but also could occur in animal products, such as milk, meat, eggs, and others. This is explained by the consequence of the presence of PA-producing plants in animal feed and by the intake of PA-containing herbs [93–95]. A Commission Regulation (EU) 2020/2040 provided maximum levels of PAs in different types of food products expressed as a total concentration of PAs (including *N*-oxides) [96]. Based on the occurrence data, exposure to PAs in humans is considered to be mainly through plant-based food products, including different types of teas, herbal teas, honey, pollen, food supplements, spices, and aromatic herbs. Additionally, it is reported that PAs could be transferred from contaminated ingredients during food treatment such as fermentation or brewing [89]; however, differences in stability data of the

PAs in the ingredients and difficulties in providing data on transfer rates suggest that unambiguous data on this subject is yet to be provided.

The toxicity of PAs is associated with the bioactivation through an oxidation process in liver, resulting in the formation of dehydropyrrolizidine alkaloids and 6,7-dihydro-7-hydroxy-1-hydroxymethyl-5H-pyrrolizine (DHP) which are especially toxic [92]. As a result, PAs are hepatotoxic, pneumotoxic, genotoxic, carcinogenic, and exhibit developmental toxicity [97]. The formation of DHP-derived DNA adducts causes gene and chromosomal mutations responsible for tumorigenesis, according to the data from studies *in vitro* and *in vivo* [98].

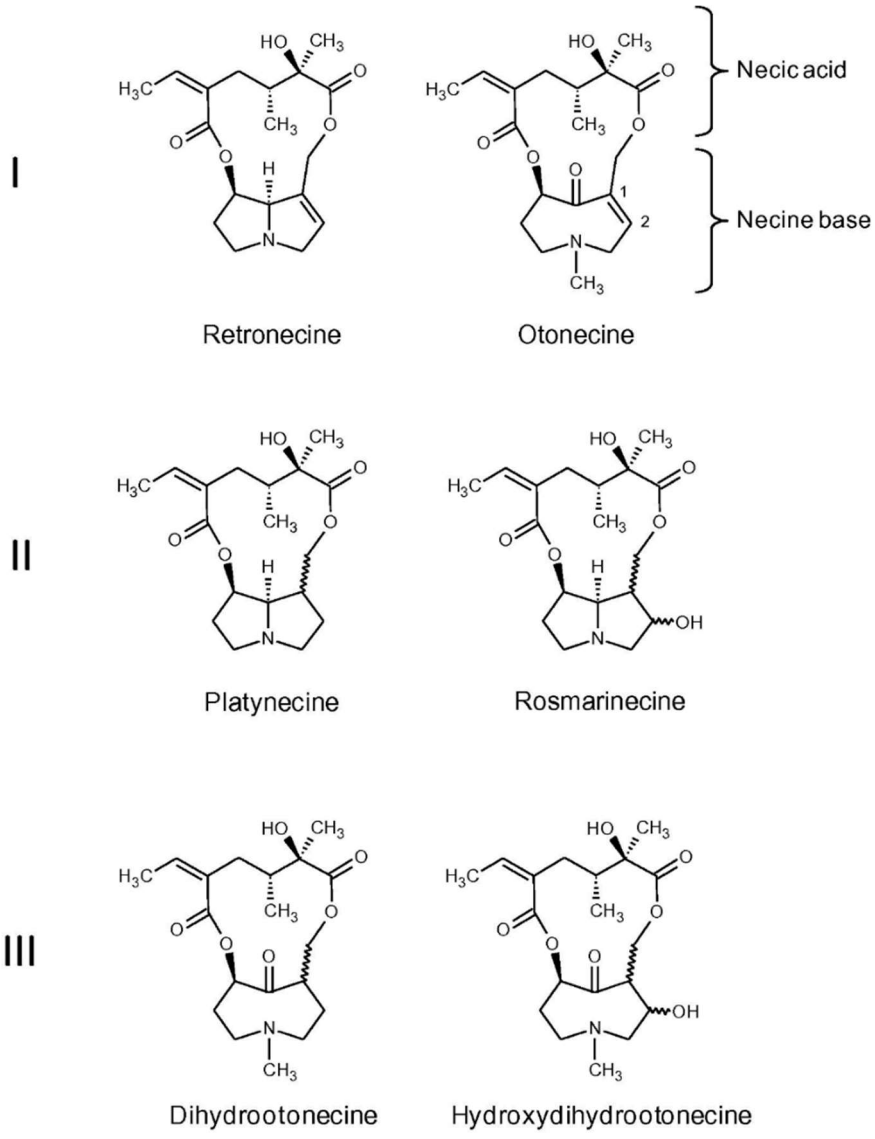

Figure 1.5. **Different variations of chemical structures of the PAs with 1,2-unsaturated necine bases (I), with 1,2-saturated retronecine bases (II), and containing 1,2-saturated otonecine bases (III)** [90]

The quantitative determination of PAs in food matrices is challenging, considering the complexity of the matrices, the similarity of chemical structures of closely related compounds, and the availability of analytical standards. Different methods for determination of PAs are available, such as UV–VIS spectrometry, thin-layer chromatography, nuclear magnetic resonance, GC–MS, LC-MS, and immunology-based methods [99], as well as capillary electrophoresis, and enzyme-linked immunosorbent assay (ELISA). LC-MS methods are the most common in the determination of PAs since they provide more reliable data, are selective and sensitive, and sample preparation is simplified in comparison with LC-UV methods or GC–MS methods. Additionally, electrospray ionization (ESI), common with LC-MS analyses, provides better sensitivity due to easily ionizable nitrogen atoms in the chemical structure of PAs, thus being analyzed mainly in positive ionization mode [100]. In comparison to GC–MS, no thermal degradation of *N*-oxides is present in LC-MS analysis, making it suitable not only for free bases but also for *N*-oxide form [101].

Taking into account the fact that the variety of PAs is significant, but the availability of analytical standards for each compound is rather limited, several different approaches have been used to analyze pyrrolizidine alkaloids. The quantitation of the alkaloids can be performed using a single available standard; therefore, the obtained concentrations are only estimations [100]. Different types of PAs produce characteristic mass spectras, such as retronecine-type PAs have common ion at *m/z* 94, 120, 138, otonecine-type PAs – at *m/z* 150, 168, platynecine-type – at *m/z* 122, 140, and other fragments [100,102]. Based on the fact that structurally, the PAs could have common structural elements, and under fragmentation process in collision cell in MS, different compounds could provide fragments with the same *m/z*; therefore, the signal could indicate the presence of a PA compound that does not have an available analytical standard. This non-targeted approach for analysis and quantitation is based on characteristic target ions and fragmentation patterns, and it allows to perform analysis without analytical standards [99,102,103].

The comparison between the limits of quantification and extraction procedures of the methods presented in scientific literature is provided in Table 1.3. Most published methods use UHPLC with 50–150 mm long columns and particles in size < 3 μm, and sample preparation procedures include extraction with acidified water or methanol, as well as different types of solid phase extraction (SPE) procedures. The use of nano-LC methodology has not been reported in the literature to date.

Table 1.3

Limits of quantification from methods reported in scientific literature for determination of pyrrolizidine alkaloids in different matrices and comparison to this study

Method	Mass spectrometry	Samples	Analytical column	LOQ	Reference
Nano-LC	**Orbitrap**	**Honey, tea, herbal infusions, milk**	**PepMap C18, 3 μm, 150 × 0.075 mm**	**0.32 - 3.6 μg kg^{-1}**	43
HPLC	Ion trap	Honey	Hypersil Gold C18, 3 μm, 150 × 2.1 mm	0.045 - 0.10 μg kg^{-1}	104
UHPLC	Single quadrupole	Honey	Ascentis Express C8, 2.7 μm, 150 × 5 mm	0.081 - 4.35 μg kg^{-1}	105
UHPLC	Triple quadrupole	Tea, honey	Hypersil Gold C18, 1.9 μm, 150 × 2.1 mm	1.7 - 6.4 μg kg^{-1} (tea), 0.18 - 0.62 μg kg^{-1} (honey)	106
UHPLC	Triple quadrupole	Salads, herbs, tea	Acquity BEH C18, 1.7 μm, 100 × 2.1 mm	0.1 - 1 μg kg^{-1}	107
UHPLC	Triple quadrupole	Honey and pollen	Hypersil Gold C18, 1.9 μm, 50 × 2.1 mm	1 - 3 μg kg^{-1}	108
UHPLC	Triple quadrupole	Tea	Kinetex pentafluorophenyl, 1.7 μm, 50 × 2.1 mm	1 - 5 μg L^{-1}	109
UHPLC	Triple quadrupole	Feed	Acquity BEH C18, 1.7 μm, 50 × 2.1 mm	5 μg kg^{-1}	110
HPLC	Single quadrupole	Feed	Gemini NX-C18, 3 μm, 150 × 4.6 mm	5 μg kg^{-1}	111
HPLC	Triple quadrupole	Honey	ZORBAX Eclipse XDB C18, 3 μm, 150 × 4.6 mm	8.6 - 18 μg kg^{-1}	112
UHPLC	Triple quadrupole	Tea	Hypersil Gold C18, 1.9 μm, 150 × 2.1 mm	10 μg kg^{-1}	113

1.4.3. Perfluorinated compounds

Per- and polyfluoroalkyl compounds (PFAS) are synthetic organic chemicals that contain at least one perfluoroalkyl group [114]. PFAS are persistent contaminants with hydrophobic and oleophobic properties. There are short-chained (less than 8 carbon atoms) and long-chained PFAS (8 carbon atoms or more) [115]. Over the decades, extensive commercial production of these compounds resulted in the availability of various commercial products such as disposable food packaging, cookware, outdoor gear, and furniture, as well as in aqueous film forming foams for firefighting [114,116]. The high usage of PFAS is associated with their useful chemical properties since a strong fluorine-carbon bond is present in the chemical structure, resulting in excellent stability. However, the same chemical and physical properties facilitating the wide application of such compounds are also the cause of the persistence of the compounds in the environment as degradation under environmental conditions is limited and, therefore, is also the cause for health concerns in humans [117,118].

Both long and short-chained perfluoroalkyl carboxylic acids (PFCAs) and perfluoroalkyl sulfonic acids (PFSAs) raise concerns in terms of their effects on the environment and health since the body of evidence of adverse effects to human health is accumulated [116,118]. Main industrial production of PFAS is through electrochemical fluorination and telomerization processes resulting in a variety of isomers, homologues, and byproducts that have a potential to enter the environment through the direct emission of PFAS or through the indirect emission by degradation process of other precursors [119]. The occurrence of PFAS in groundwater [120], food [121], drinking water [122], soil [123], and aquatic biota [124] has been investigated, and considerable PFAS concentrations were detected, contributing to the total exposure assessment. Dietary exposure through seafood and drinking water consumption is considered one of the most common pathways of PFAS exposure for humans [120]. Other ways of exposure include indoor environment such as through dust and air [116].

The adverse effects are reported not only in humans but also in various plants and animals, as exposure from contaminated water sources could result in decreased growth rates, reproduction rates, and survival rates [125]. The high bioaccumulation potential, together with the high detection rate of such compounds in environmental samples, including bodies of water, results in elevated concentrations of these compounds throughout food chains [116,126].

Exposure to PFAS has demonstrated various toxic effects during animal studies, including hepatotoxicity, developmental toxicity, immunotoxicity, and hormonal effects [127]. It was reported that exposure to PFAS could provide an increased risk of cancer and different reproductive effects observed *in vitro* and *in vivo* [116,128]. Additionally, toxic effects in humans were reported, including high cholesterol levels, pregnancy-induced hypertension, ulcerative colitis, as well as kidney and testicular cancer. The compound-specific toxic impact of PFAS on the thyroid, inhibiting iodide uptake, was found [116,116,129–131]. Moreover, children were found to be more susceptible to PFAS exposure, resulting in developing dyslipidemia [131,132].

Legislative initiatives were implemented for human health protection with an aim to limit exposure to PFAS, and in 2008, the European Food Safety Authority (EFSA) established a tolerable daily intake (TDI) of 150 ng kg^{-1} bw d^{-1} for PFOS and 1500 ng kg^{-1} bw d^{-1} for PFOA, respectively [133]. The TDI was derived from the available occurrence data at that time which was limited, and in 2018 EFSA derived separate tolerable weekly intakes (TWI) for PFOS and PFOA by evaluation of recent toxicological studies, examining the possible impact on human health and taking into account recent occurrence data; therefore, the recommended intakes were dramatically decreased [134], for example, for PFOS from 1050 ng kg^{-1} bw.wk^{-1} to 13 ng kg^{-1} bw.wk^{-1} and for PFOA from 10500 ng kg^{-1} bw.wk^{-1} to 6 ng kg^{-1} bw.wk^{-1} [135]. EFSA Panel on Contaminants in the Food Chain (CONTAM Panel) addressed the risk assessment for other PFAS and reviewed the risk assessment of the previous Opinion, and based on similar effects in animals, toxicokinetic, observed levels in human blood as well as the occurrence data, two additional compounds were included in the PFAS priority list namely, perfluorononanoic acid

(PFNA) and perfluorohexane sulfonic acid (PFHxS) apart from PFOA and PFOS that were already present, and TWI of 4.4 ng kg^{-1} $bw.wk^{-1}$ for the sum of selected four PFAS was established [136].

Currently, liquid chromatography methods coupled with mass spectrometry are applied to PFAS analysis at low concentrations, and sub-ppb detection limits achieved [121,137]; however, the suggested TWI values by EFSA for exposure assessment require lower detection limits. Typically, for chromatographic separation, high performance or ultra-high performance is used, while selective detection is ensured by applying tandem MS/MS or HRMS systems equipped with electrospray ionization sources [137]. Sample preparation protocols often include SPE clean-up procedures [138]. Moreover, the use of HRMS for nontarget detection of PFAS in complex food matrixes at low levels is reported, which allows to perform the analysis without reference standards, providing the possibility of assessment of PFAS for which the availability of reference standards is limited [139].

1.4.4. Biomarkers and pharmaceuticals

Wastewater-based epidemiology approach (WBE) considers biological or chemical indicators for the estimation of consumption patterns of illicit drugs, pharmaceuticals, and other substances. The analysis of metabolites and pharmaceutical compounds found in wastewater (WW) from human excretion provides a comprehensive view of the well-being and lifestyle habits of a population. The human consumption of various pharmaceuticals undoubtedly provides benefits in enabling a better quality of life as well as disease prevention and treatment. WBE includes quantification of biological or chemical indicators for the estimation of consumption patterns of illicit drugs, pharmaceuticals, and other substances, as well as outbreaks of infectious diseases such as COVID-19. Due to the multidisciplinary nature of this methodology between analytical chemistry, environmental, and social sciences, it allows collaboration between different institutions. This approach is cost-effective, non-invasive, and

protects personal privacy, meaning the data cannot be associated with an individual, and personal privacy is not compromised.

Initial uses of WBE included analysis of illicit drugs [140] in municipal sewage. Promising results were demonstrated that allowed to extend this methodology to other groups of analytes, such as pharmaceuticals, alcohol and tobacco metabolites, pesticide exposure metabolites, and others. Several classes of food, stress, lifestyle, health, and population biomarkers are commonly used in the WBE approach [14]. A suitable biomarker can provide relevant information about lifestyle habits, health, and wellbeing of a population, but its selection is not an easy task as it should meet several specific requirements, such as stability in wastewater, specificity to the compound under investigation, and unique to human metabolism, thus ensuring that its presence only derives from human excretion and not from exogenous sources. Population biomarkers must have a low variance in the per capita daily excretion and must not be influenced by season, weather, and region. The main criteria for a compound to be used as a biomarker in WBE are its stability, specificity to human metabolism, applicability among different regions, and observed presence at acceptable detection levels[14,142]. The use of the WBE approach is also beneficial for pandemic outbreaks, for example, for COVID-19 surveillance in addition to diagnostic testing [143]. The WBE approach is widely applied to evaluate population lifestyle, including the use of illicit drugs, but it also can be applied to other substances, including alcohol, tobacco, caffeine, and others [14,144]. Not only the concentration of a target compound in wastewater could be determined by using this approach, but also consumption among the population can be estimated using one of two models commonly reported in the literature. One model relies on the quantitation of drug target residue concentrations in wastewater, wastewater flow rate, and population size [141]. Other model uses human-specific compounds such as cotinine or serotonin metabolite 5-hydroxy-indolic acid (5-HIAA) to evaluate population size [146]. Monitoring changes of concentrations of the target

analytes in WW samples over an extended period of time provides an opportunity to elucidate consumption changes among the population.

Several examples of WBE applications include the analysis of ethyl sulphate, which is one of the metabolites of ethanol and is used as a biomarker, allowing to evaluate the consumption of alcoholic beverages [145]. 5-HIAA is a metabolite of serotonin and could be effectively used as a population size biomarker, allowing correct estimations of population size based on the actual population size in a specific region, excluding the variations caused by the relocation of the population, seasonal differences, and tourism. Therefore, the consumption of various types of foods and drugs could be estimated more correctly by using normalization to the concentration of the population size biomarker instead of relying on statistical data [146]. Gabapentin is a pharmaceutical compound used for seizure and neuropathic pain treatment and is not metabolized in human organism [147]. Cotinine is one of the metabolites of nicotine and is used as a biomarker of tobacco consumption [148]. Cotinine could be also used as a population size biomarker, however, the seasonal and regional differences among different countries cause the additional variation of concentration, limiting the possibility of data comparison between regions. Caffeine is a neurostimulator drug that is widely consumed in various beverages [149]. Caffeine could be analyzed using the WBE approach either as a parent compound or as one of its metabolites, such as paraxanthine, 1-methylxanthine, 7-methylxanthine, and 1,7-dimethyluric acid [150]. Pharmaceutical compounds such as non-steroid anti-inflammatory drugs (NSAIDs) diclofenac and ibuprofen are crucial in maintaining health and improving the quality of life of the population. Both of those compounds are mostly metabolized by an organism and are being analyzed using the WBE approach as their non-metabolized form since the stability data of the compounds suggest suitability for analysis [151–153]. It is known that pharmaceutical drugs such as NSAIDs pose an environmental risk to ecosystems and living organisms[154–156], and wastewater treatment plants are not always capable of removing pharmaceuticals from WW [156,157].

The analysis of WW is challenging, considering the complexity of the matrix and the typically low concentrations of the analytes of interest in the sample. Therefore, analytical methods should provide the required sensitivity. Currently, the most common sample preparation techniques for WW analysis include SPE and evaporation to perform sample clean-up and pre-concentration [158,159]. The dilute-and-shoot approach is one of the possible sample preparation procedures for WW analysis that includes filtration of the samples as well as dilution with mobile phase or other solvent [160]. This approach brings several key benefits, such as reduced sample preparation time, reduced consumption of materials and lower analysis costs, low matrix effects, and high applicability. There is also the possibility to include multi-class analytes due to the more inclusive sample treatment (if any) since other sample treatment steps are typically more selective for a certain range of compounds. However, the drawback of this approach is that the sensitivity of a detector should be sufficient since the absence of clean-up results in higher background noise and coeluting matrix compounds. Both high-resolution and low-resolution mass spectrometry could be used with a dilute-and-shoot approach. The use of nano-LC in environmental sample analysis is not common in literature, however, it provides advantages over other types of chromatography. The use of nano-LC in environmental sample analysis has been limited so far; however, considering the advantages of this methodology, such as low matrix effects and improved sensitivity, it could provide better analytical performance compared to other types of liquid chromatography [15].

2. EXPERIMENTAL PART

2.1. Chemicals and materials

Formic acid (99%) was obtained from VWR International (Radnor, PA, USA). LC-MS grade ultra-pure water and acetonitrile (Merck, Germany) were used for the preparation of mobile phases. HPLC grade solvents (Merck, Germany) were used for sample extractions. Ammonium formate, sodium hydroxide, and 25% aqueous ammonia were obtained from Acros (Morris Plains, NJ, USA). High purity water (18.2 MΩ cm) was prepared using a Millipore Milli-Q purification system (Billerica, MA, USA).

All the mycotoxin standards were with purities ranging from 97.4 to 99.5% and assay uncertainties of 2–5%: Aflatoxin B_1 (AFB_1), deoxynivalenol (DON), deoxynivalenol-3-glucoside (D3G), fusarenon X (FUS X), nivalenol (NIV), ochratoxin A (OTA), T-2 toxin (T-2), zearalenone (ZEN) were procured from Biopure Romer Labs (Tulln, Austria). 15-acetyldeoxynivalenol (15-AcDON), 3-acetyldeoxynivalenol (3-AcDON), alternariol monomethyl ether (AME), enniatin B (ENN B), enniatin B_1,(ENN B_1), tentoxin (TEN) were purchased from Cayman Chemical (Ann Arbor, MI, USA) and 15-monoacetoxyscirpenol (15-MAS), aflatoxicol (AFL), altenuene (ALT), alternariol (AOH), altertoxin I (ATX I), fumonisin B_1 (FB_1), fumonisin B_2 (FB_2), fumonisin B_3 (FB_3), HT-2 toxin (HT-2), neosolaniol (NEO), ochratoxin B (OTB), T-2 toxin triol (T-2TRI) and T-2 tetraol (T-2TET) were purchased from Fermentek Ltd. (Jerusalem, Israel). Stock solutions of 1000 mg L^{-1} concentrations were prepared in non-aqueous solvents and stored in a freezer at −20°C temperature. Working standard solutions were prepared in 20% aqueous acetonitrile and stored frozen (−20°C temperature) in amber glass bottles.

Pyrrolizidine alkaloid standards (with purities ranging from 95% to 99% and uncertainty of assay of 5%) included echimidine, echimidine *N*-oxide, echinatine, echinatine *N*-oxide,

europine hydrochloride, europine *N*-oxide, heliosupine, heliosupine *N*-oxide, heliotrine, heliotrine *N*-oxide, indicine hydrochloride, indicine *N*-oxide, integerrimine, integerrimine *N*-oxide, intermedine, intermedine *N*-oxide, lasiocarpine, lasiocarpine *N*-oxide, lycopsamine, lycopsamine *N*-oxide, retrorsine, retrorsine *N*-oxide, senecionine, enecionine *N*-oxide, seneciphylline, seneciphylline *N*-oxide, senecivernine, senecivernine *N*-oxide, senkirkine, and usaramine (PhytoPlan, Germany). Stock solutions at 250 mg L^{-1} concentration and working standard solutions were prepared in 1:1 mixture of 50% aqueous acetonitrile and methanol. Some of the pure standards had poor solubility and were dissolved by acidifying the solvent with 0.4% of formic acid.

The standard of ibuprofen was obtained from Dr. Ehrenstorfer (Germany), while other standards including caffeine, cotinine, diclofenac sodium salt, ethyl sulphate sodium salt, gabapentin, and 5-HIAA were obtained from Sigma-Aldrich (Germany). The purity of the substances ranged from 98% to 99.6%. Tetrabutyl ammonium bromide (TBAB) (>98% purity) was obtained from Sigma-Aldrich (Germany). Stock solutions of the compounds at the concentrations of 1000 μg L^{-1} and 1 μg L^{-1} were prepared in LC-MS grade methanol. The standards were stored at – 20 °C temperature.

PFAS standards such as individual native standards in methanol, namely PFOA, PFNA, PFHxS and PFOS and their ^{13}C-labeled surrogates that served as internal standards were purchased from Cambridge Isotope Laboratories (CIL), Inc. (Andover, MA, USA). Stock solutions were prepared in methanol and were stored at -18°C temperature in amber colored glassware. Calibration solutions were prepared by serial dilution of stock solutions in methanol.

2.2. Samples

For the determination of mycotoxins 133 agricultural crop samples (110 grain cereals and 23 pulses) from the two research centers located in Stende and Priekuli towns of Latvia were provided by the Institute of Agricultural Resources and Economics. The samples were

harvested in 2019, and the cereals included rye (n = 6), triticale (n = 7), winter wheat (n = 21), summer wheat (n = 12), oat (n = 32) and barley (n = 31) varieties and pulses included broad beans (n = 8), peas (n = 8), and lupin beans (n = 7). The samples were crushed using disc type Laboratory mills 3303 (Perten Instruments AB., Huddinge, Sweden), homogenized and stored at –20°C temperature until analysis.

For the determination of pyrrolizidine alkaloids different foods of Latvian origin were analyzed, including tea (n = 15), honey (n = 40), herbal tinctures (n = 15), and milk (n = 10) samples were chosen due to their high consumption among the population and the high probability of finding pyrrolizidine alkaloids in these products. The samples were from Latvian market.

For the determination of biomarkers and pharmaceuticals untreated wastewater samples were collected from the wastewater treatment plants in several cities and towns of Latvia, including Jelgava, Liepaja, Valmiera, Ventspils, Jekabpils, Jurmala, Riga, Rezekne, Daugavpils, Salaspils, and Tukums. The samples were collected on Tuesday and Thursday from March 31 to April 28, 2022. In total, 116 samples were collected.

For the determination of perfluorinated compounds a multitude of food samples representing Latvian retail market were analyzed using the elaborated method, including fruits and vegetables (n = 30), grains, bread, and vegetable oils (n = 22), milk and dairy products (n = 21), eggs (n = 8), meat (n = 19), fish and seafood (n = 19). Sample collection was conducted during the period from January to September 2022. Samples were uniquely coded and transported to the laboratory at + 4°C temperature. Upon receiving, solid samples were thoroughly homogenized in a food blender (Kenwood FP101T, Kenwood Ltd, UK) and stored in polyethylene bags at –18°C temperature. Aliquots of sample homogenates of fruits, vegetables and berries were freeze-dried using a VirTis BenchTop K Series freeze dryer (SP Scientific, Warminster, PA, USA)) for 48 h prior to the analysis. Milk samples were homogenized prior to the analysis by vigorous mixing.

2.3. Determination of mycotoxins

2.3.1. Sample preparation

Five grams of each sample were weighed in 50 mL polypropylene tubes and were shaken after the addition of 10 mL of deionized water containing 2% formic acid to the tubes. Next, 10 mL of acetonitrile was added to the tubes, followed by shaking for 10 min in a programmable rotator. A mixture of QuEChERS salts, consisting of 4.0 g of anhydrous magnesium sulphate, 1.0 g of sodium chloride, 1.0 g of trisodium citrate and 0.5 g of disodium citrate were added to the tubes, followed by vigorous shaking for 3 min. The tubes were centrifuged (4,500 × g) at 15°C temperature for 10 min and 7 mL of the acetonitrile layer was transferred to 15 mL polypropylene tubes, which were then capped and stored in a freezer at −80°C temperature for 30 min. The tubes were then immediately centrifuged at 15°C temperature (4000 × g, 18 min). The samples were prepared by the addition of 47.5 µL of the supernatants and 2.5 µL of 20% acetonitrile or 500 µg L^{-1} of the standard mix (in the case of spiked extracts) by directly pipetting into 1950 µL of LC-MS water containing 0.1% formic acid and 0.1% acetonitrile (dilution factor of 40). The final solvent composition of the extracts was 2.5% aqueous acetonitrile and 0.1% formic acid. The diluted extracts were filtered directly into 2 mL crimp cap vials (0.22 µm pore size, PVDF).

A one-point post-extraction standard addition calibration was performed at 50 µg kg^{-1}. In the case of higher concentrations present in the sample, the standard addition was increased accordingly up to 2500 µg kg^{-1}, by decreasing the volume of sample extract with respect to the added standard solution. The decrease in volume of sample extract was compensated with an appropriate volume of LC-MS grade acetonitrile to maintain the composition of solution for injection at 2.5% acetonitrile, since the content of the sample extracts should precisely correspond to the initial gradient conditions.

2.3.2. Instrumental analysis

Chromatographic separation was carried out on an EASY-Spray PepMap nano-LC capillary column (150 × 0.075 mm) with 3 μm C18 bonded silica particles (Thermo Scientific, Waltham, MA, USA). Electrospray ionization was performed in the nano-electrospray ionization mode using the EASY-Spray ionization source. The analytical column was thermostated at 30°C temperature; the autosampler was thermostated at 5°C temperature; and injection volume was 1 μL. The following parameters were used for the ionization source: ion transfer capillary temperature 250°C; spray voltage ±2.5 kV. The mobile phases were 0.1% formic acid in ultra-pure water (A) and 0.1% formic acid in acetonitrile (B). The gradient was 0–50 min 2.5% B to 99% B; 50–59 min 99% B; 59–67 min 99% B to 2.5% B, 67–80 min 2.5% B. The flow rate was set to 225 nL min^{-1}.

A Q-Exactive Focus Orbitrap-HRMS (Thermo Fisher Scientific, Waltham, MA, USA) detection system was used in the PRM mode. Precursor ions were isolated using an isolation window of 0.4 m/z at the corresponding elution windows and fragmented at the average optimum collision energy of all identified fragments of the corresponding precursor ion. Fragments were detected simultaneously at a resolution of 70000. Ion injection time was set to 1000 ms. The list of analytes, their retention times and precursor ions are given in Annex 1.

2.4. Determination of pyrrolizidine alkaloids

2.4.1. Investigation of SPE procedure

In order to investigate the performance of a SPE procedure for the determination of PAs, an SPE procedure based on the Strata-X sorbent was used. 2.00 g of spiked and unspiked homogenized honey or tea samples were extracted in polypropylene tubes in 40 mL of 0.2% formic acid in deionized water for 30 min using a rotating shaker. The tubes were centrifuged at 4500 rpm for 15 min, 5 mL aliquots of the supernatant were adjusted to pH 7.5 ± 0.5 using aqueous 1 mol/L ammonium carbonate, transferred, and passed through pre-conditioned Strata-

X solid-phase extraction cartridges. The cartridges were then washed with 6 mL of 1% formic acid, 6 mL of deionized water, and eluted with 6 mL of methanol. The eluates were evaporated at 50 °C temperature and dissolved in 450 µL of deionized water containing 1% formic acid by applying vortex mixing, therefore the final dilution factor with this procedure was d = 1.8. The extracts were analyzed after filtration (0.22 µm pore size, PVDF).

2.4.2. Investigation of QuEChERS procedure

In order to investigate the performance of a QuEChERS-based extraction procedure with subsequent pre-concentration or dilution in combination with a conventional flow LC-MS analysis, 2.00 g of spiked and unspiked homogenized honey or tea samples were extracted in 20 mL of 50% acetonitrile containing 1% formic acid for 30 min, using an overhead shaker. A mixture of salts, consisting of 4.0 g of anhydrous magnesium sulphate, 1.0 g of sodium chloride, 1.0 g of trisodium citrate, and 0.5 g of disodium citrate, was added to the tubes and shaken vigorously for 3 min, then the tubes were centrifuged at 4500 rpm for 15 min. A 5 mL aliquot of the supernatant was subjected to freezing-out at −80 °C temperature for 30 min and 200 µL of the supernatant after centrifuging for 18 min at 4500 rpm at 15 °C temperature was evaporated at 50 °C temperature and dissolved in deionized water containing 1% formic acid by vortex mixing. The dry residues were reconstituted with the appropriate volumes of deionized water containing 1% formic acid to ensure the following dilution factors: d = 2 for tea and d = 0.4 for honey (for QuEChERS with pre-concentration); d = 40 for tea and honey (for QuEChERS with dilution). The extracts were analyzed after filtration (0.22 µm pore size, PVDF).

2.4.3. Sample preparation procedure

In order to analyze samples from the market, 2.00 g of spiked and unspiked homogenised honey or tea samples were extracted in 20 mL of 50% acetonitrile containing 1% formic acid

and 10 mL of milk samples were extracted in 10 mL of acetonitrile containing 2% formic acid and shaken for 30 min using an overhead shaker. A mixture of salts, consisting of 4.0 g of anhydrous magnesium sulphate, 1.0 g of sodium chloride, 1.0 g of trisodium citrate, and 0.5 g of disodium citrate was added to the tubes and shaken vigorously for 3 min, and the tubes were centrifuged at 4500 rpm for 15 min. A 5 mL aliquot of the supernatant was subjected to freezing-out at –80 °C temperature for 30 min and 200 µL of the supernatant after centrifuging for 18 min at 4500 rpm at 15 °C was evaporated at 50 °C temperature and dissolved in deionized water containing 1% formic acid by vortex mixing (300 µL for honey and milk samples, 1500 µL for tea samples). Herbal tinctures were evaporated directly due to their high ethanol content. Thus, 200 µL samples of spiked and unspiked homogenized herbal tinctures were evaporated at 50 °C temperature and dissolved in 300 µL of deionized water containing 1% formic acid by vortex mixing. The final dilution factor was d = 37.5 for tea, d = 7.5 for honey, d = 1.5 for milk and herbal tinctures. The final extracts were filtered (0.22 µm pore size, PVDF) and analyzed with nano-LC-MS.

A one-point standard addition calibration was performed by spiking another replicate at 4 µg kg^{-1} before extraction. In the case of higher concentrations in the sample a reanalysis was performed, and the standard addition was increased accordingly up to 40 µg kg^{-1}.

2.4.4. Instrumental analysis using conventional flow LC-MS method

The conventional flow electrospray ionization LC-MS analysis was performed using a Thermo Scientific Ultimate 3000 UHPLC system coupled to a Thermo Scientific TSQ Quantis mass spectrometer with Ion Max NG probe. The analytical column was a Kinetex (Phenomenex, Torrance, CA, USA) UHPLC column (100 × 3 mm) with 1.7 µm C18 bonded silica particles, and was thermostated at 50 °C; the autosampler was thermostated at 10 °C; the injection volume was 100 µL. The large injection volume was chosen as the reconstitution solvent was aqueous 1% formic acid, in which the PA analytes maintained high solubility, and

due to absence of organic solvents the early eluting peak separation was maintained. The following parameters were used with the ionization source: sheath gas: 50 arbitrary units; aux gas: 10 arbitrary units; sweep gas: 0.1 arbitrary units; probe heater temperature 400 °C; ion transfer capillary temperature 300 °C; spray voltage at +3.5 kV in the positive mode. The mobile phases were 0.1% formic acid in ultra-pure water (A) and 0.1% formic acid in acetonitrile (B). The gradient program was the following: 0-10 min 1-10% B; 10-15 min 10-15% B; 15-20 min 15-30% B; 20-21 min 30-99% B; 21-26 min 99% B; 26-32 min 1% B. The flow rate was 0.5 mL/min. Precursor ions and fragments were isolated by an isolation window of 0.7 m/z at the respective elution windows and fragmented at the optimum collision energy. A list of the analytes, precursor and fragment ions is given in the Annex 7.

2.4.5. Instrumental analysis using nano-LC method

Pyrrolizidine alkaloids were analyzed using a nano-LC chromatography system Thermo Scientific UltiMate 3000 RSLCnano coupled to a Thermo Scientific Orbitrap Focus mass spectrometer. To achieve the maximum chromatographic efficiency, a small volume sample loop was used (approximately 0.07 µL). The autosampler was programmed to perform an injection of 1 µL, thus resulting in additional washing of the sample loop. For the purpose of stabilizing the electrospray performance during the highly aqueous parts of the gradient and for avoiding the formation of droplets at the emitter tip, a post-column solvent was added with the secondary pump (80% LC-MS acetonitrile). High-pressure fittings were used to join the fluidics and the capillary column (nanoViper, IDEX MicroTight, and AB SCIEX SST mixing tee). Separation was carried out on a PepMap (Thermo Scientific, Waltham, MA, USA) capillary column (150 × 0.075 mm) with 3 µm C18 bonded silica particles. Electrospray ionization was performed in the nanoelectrospray ionization mode using the EASY-Spray ionization source and EASY-Spray transfer line (75 µm inner diameter and 50 cm length). The analytical column was thermostated at 50 °C temperature; the autosampler was thermostated at 10 °C temperature;

the actual injection volume was 70 nL. The small injection volume was necessary to separate early eluting PA analytes. In contrast to common nano-LC MS protocols, large injection volumes (for example – 1 µL) could not be applied to PA analytes due to their ionic and solubility properties. The following parameters were used with the ionization source: ion transfer capillary temperature 300 °C; spray voltage was set at +2.0 kV. The mobile phases were 1% formic acid in ultra-pure water (A) and 1% formic acid in acetonitrile (B), and the flow rate was 0.8 µL/min (both mobile phase and post-column solvent addition). The gradient program was the following: 0-22 min 1-11% B; 22-25 min 11-28% B; 25-30 min 28-80% B; 30-37 min 80- 99% B; 37-42 min 99% B; 42-45 min 1% B. The duration of injection preparation ensured sufficient time for return to the starting conditions. Precursor ions were isolated by an isolation window of 0.7 m/z at the respective elution windows, fragmented at the optimum collision energy, and detected simultaneously at 70 000 resolution. The ion injection time was set to 1000 ms and the automatic gain control (AGC) target was $1 \cdot 10^6$. A list of analytes, precursor and fragment ions are given in Annex 8.

2.4.6. The use of target ion screening for the determination of pyrrolizidine alkaloids

The aforementioned chromatography gradient for the analysis of pyrrolizidine alkaloids with nano-LC was scaled by extending the times in the gradient table by a factor of 4 and by reducing the flow rate by the same factor, thus the flow rate for screening was 0.2 µL min^{-1} (both mobile phase and post-column solvent addition). Additional equilibration time was added to the end of the analysis sequence to account for the large ratio of system volume to flow rate, thus ensuring sufficient equilibration when returning to the starting conditions for the next injection. A reagent blank injection was performed by using this procedure and ions with relative abundance over 0.075% from the averaged spectrum of the first half of the chromatogram were added to the method exclusion list in order to prevent them from triggering

dd-MS^2 (data dependent MS^2) scans for ions that do not originate from the samples or for ions arising from the background contamination. The scan mode was changed to Full MS with dd-MS^2 in discovery mode. The full scan resolution was 70000, with the scan range from 150 to 500 *m/z*, AGC target of $3 \cdot 10^6$ and the maximum IT of 500 ms. The dd-MS2 scan resolution was 17500, the isolation width was 0.7 *m/z*, and stepped collision energy was used at 10, 20, and 30 eV. The minimum AGC target was $1 \cdot 10^3$ and dynamic exclusion was set to 120 s. Centroid data was stored to reduce file size. These method parameters ensured that approximately 150 dd-MS^2 scans per peak could be performed, and together with dynamic exclusion and method exclusion list ensured that as many unique features as possible were interrogated by dd-MS^2 within a single run.

MS^2 spectra were extracted from the acquired raw data files with Raw Converter [161] and processed using a code written in VBA for Excel. The output consisted of precursor ion masses and scores calculated according to the Eq. (2.1). A window of 0.002 *m/z* was used in the processing to account for the dispersion of the measured accurate masses. The score represented the fraction of all signals in the spectrum that was due to the target ions. This approach was essentially similar to the NIST "reverse search", which ignores non-matching peaks, and does not penalize the score for peaks that are not found in the library spectrum [162].

$$Score = \frac{\sum Target\ ion\ signals}{\sum All\ ion\ signals} \tag{2.1}$$

A reagent blank was processed this way to establish a threshold score, then spiked samples (at 10 and 20 μg kg^{-1}) were analyzed and the data were processed. Two sets of target ions were compared – eight common fragment ions of pyrrolizidine alkaloids (94.0656, 120.0808, 136.0756, 138.0911, 150.0912, 156.1018, 168.1016, 172.0960 *m/z*), as well as one common fragment ion originating from the necine base substructure (94.0656 *m/z*). The results are given in Figure 3.5.

2.5. Determination of biomarkers and pharmaceuticals

2.5.1. Sample preparation

Wastewater samples were mixed and filtered through a polyvinylidene fluoride (PVDF, Phenomenex) syringe filter with pore size of 0.2 μm. The samples were then transferred into 2 mL Eppendorf tubes and centrifugated at 20000 rpm at 4 °C temperature. The samples were transferred into glass HPLC vials and aliquots of TBAB solution, ammonium acetate solution, and water were added. The final concentrations of TBAB and ammonium acetate in the vial was 11 and 10 mM, respectively, with the sample dilution factor equal to 5.

2.5.2. Instrumental analysis

The analysis of pharmaceuticals and biomarkers was performed using an UltiMate 3000 RSLCnano nano-LC (Thermo Scientific, Waltham, MA, USA) chromatography system coupled to an Orbitrap Focus mass spectrometer (Thermo Scientific, Waltham, MA, USA) equipped with a nanoflow EASY-Spray ionization source. Full loop injections of 70 nL using overfill mode requiring 1000 nL of sample were performed. The temperature inside the autosampler was set at 10 °C. The chromatographic separations were carried out using a Thermo Scientific PepMap capillary column (150 × 0.075 mm) packed with 3 μm C18 bonded silica particles. The mobile phase A consisted of a mixture of 10 mM ammonium acetate, 0.01% (v/v) acetic acid, and 1% (v/v) MeCN dissolved in LC-MS grade water, while the mobile phase B was LC-MS grade MeCN (B). The following gradient program at 500 nL min^{-1} flow rate was used for the separations: 0-1 min 5% B, 1-11 min 5-35% B, 11-13.5 min 35-80% B, 13.5-26 min 80% B, 26-27 min 80-5% B, and 27-45 min 5% B.

Q Exactive Focus Orbitrap mass spectrometer (Thermo Scientific, Waltham, MA, USA) equipped with an EASY-Spray nano-electrospray ionization source was used for the detection of analytes. Data acquisition was performed in full scan mode over the *m/z* range from 100 to 350 at a resolution of 70000. Fast polarity switching was used during the run to detect positively

and negatively charged analyte ions. The data acquisition parameters and the MS voltages were optimized during the method development experiments. The ion injection time (IT) was set at 300 ms. The ion transfer capillary temperature was 200 °C, RF lens level was 60, automatic gain control (AGC) target was $3 \cdot 10^6$. The spray voltage was set at +2.26 kV for positive and –1.70 kV for negative ionization mode. A list of analyte precursor ions is provided in the Annex 3.

2.6. Determination of PFAS

2.6.1. Sample preparation

The following sample aliquots of selected matrices were taken for the analysis: fruits and vegetables – 70 g; grains and bread – 10 g; milk – 15 g; fish, meat, and eggs – 2 g. In order to reduce the sample volume of fruits and vegetables, the weighted aliquots were freeze dried prior to sample extraction step. Portions of thoroughly homogenized samples were weighed in 50 mL PP tubes and spiked with 100 µL of internal standard solution in methanol containing ^{13}C-isotopically labelled standards (500 pg μL^{-1} of each surrogate). After equilibration for at least 30 min, acetonitrile (15 mL) and 0.2 M NaOH solution (1 mL) were added to each sample and the tubes were vigorously mixed before performing two extraction cycles using sonication (each cycle for 15 min). In order to remove some lipids and other highly molecular compounds the extracted samples were first centrifuged for 10 min at 3500 rpm, freeze-out at -80°C temperature for 30 min, and repeatedly centrifuged for 10 min at 4700 rpm. Immediately after centrifugation the organic extracts were decanted into 250 mL graduated glass volumetric flasks, diluted with water to 250 mL and 100 µL of formic acid was added. Clean-up of the samples was performed using SPE procedure with Strata-X-AW 33 µm 200 mg/3 mL (Phenomenex, Torrance, CA, USA) SPE cartridges with weak anion-exchange properties. The cartridges were previously pre-conditioned with 3 mL of 1% NH_4OH in MeOH, 3 mL of MeOH, and 3 mL of water. The cartridges were then washed with 1 mL of 2% formic acid in

water and 3 mL of MeOH, and after drying the columns for 30 min under vacuum, the analytes were eluted with 6 mL of 1% NH_4OH in MeOH into 15 mL glass tubes.

The eluates were evaporated at 30 °C temperature under a gentle stream of nitrogen and dissolved in 200 µL of LC-MS grade water/MeCN (75/25, v/v) with 5 mM ammonium formate by applying vortex mixing. After centrifugation for 10 min at 2000 rpm and 4 °C temperature the samples were transferred into 2 mL Eppendorf tube and repeatedly centrifuged at 20000 rpm and 4 °C temperature for 10 min. After centrifugation the final extracts were transferred into the chromatographic vials and immediately subjected to instrumental analysis.

2.6.2. Instrumental analysis

The analysis of PFAS was performed using an UltiMate 3000 RSLCnano nano-LC (Thermo Scientific, Waltham, MA, USA) chromatography system coupled to an Orbitrap Focus mass spectrometer (Thermo Scientific, Waltham, MA, USA) equipped with a nanoflow EASY-Spray ionization source. The chromatographic separations were carried out using a Thermo Scientific PepMap capillary column (150 × 0.075 mm) packed with 3 µm C_{18} bonded silica particles. The temperature inside the autosampler was set at 10 °C. Full loop injections of 1000 nL using overfill mode were performed. The mobile phase A consisted of 5 mM ammonium formate in LC-MS grade water, while the mobile phase B was 5 mM ammonium formate in LC-MS grade water/MeCN (95/5, v/v) (B). The following gradient program at 500 nL min^{-1} flow rate was used for the separations: 0-19.3 min from 25% B to 99% B, 19.3-28.3 99% B. The column was equilibrated for 10 min between runs with the composition corresponding to the initial gradient conditions.

Orbitrap-MS detection in parallel reaction monitoring (PRM) mode was used for quantitative determination of the selected compounds. The data acquisition parameters as well as the MS voltage were optimized during the method development experiments. Precursor ions were isolated by an isolation window of 0.7 *m/z* at the respective elution windows and fragments

were detected at 17500 resolution. The ion injection time was set to 50 ms and the automatic gain control (AGC) target was $1 \cdot 10^6$. The ion transfer capillary temperature was 200 °C, RF lens level was 60. The spray voltage was set at -2.0 kV for negative ionization mode. External calibration of the Orbitrap-MS system was performed weekly over the *m/z* range of 50 – 2000 according to the guidelines provided by the instrument manufacturer. The details of the optimized instrumental conditions and a list of analyte precursor ions and fragment ions is provided in the Annex 13.

3. RESULTS AND DISCUSSION

3.1. Determination of mycotoxins

3.1.1. Optimization of nano-LC setup and MS procedure

The chromatographic resolution for the separation of the mycotoxin analytes using the nano-LC method was evaluated for two different nano-LC-MS fluidic setups, as demonstrated in Figure 3.1. Instrumental setups with an Acclaim PepMap capillary column combined with an EASY-Spray transfer line and an emitter and an EASY-Spray capillary column with an integrated emitter were evaluated. Both setups were connected to the MS with the shortest possible capillaries and the chromatography system outlet located near the ion source. The capillary column and the EASY-Spray transfer line required a multitude of capillary connections, and the total length of capillaries necessary to perform the analysis resulted in significant peak broadening due to the increased system volume and thus overwhelming the MS^2 scanning capability with numerous coeluting peaks limiting the application range. The EASY-Spray capillary column with an integrated emitter offered superior separation and symmetrical and narrower peaks, enabling successful high-resolution MS^2 acquisition of many analytes.

Orbitrap MS was employed using PRM mode to ensure selectivity. No interferences were observed in the parallel reaction mode at a resolution of 70000. An ion injection time of 1000 ms was selected as a compromise between the co-elution and increased sensitivity due to the longer accumulation of ions in the ion trap. An ion injection time of <500 ms was found unfeasible due to droplet formation at the emitter tip during the highly aqueous part of the gradient. Droplet formation at the emitter tip with a highly aqueous mobile phase is a known problem using nanoflow electrospray ionization [163]. Since the droplets were transferred to the mass spectrometer at a low frequency, the gradient and flow rate was decreased accordingly to obtain a sufficient number of scans per peak. Four dilution factors of 100, 80, 40, and 20 were

tested. The lowest dilution factor for the sample extracts was optimized by injecting the standard solutions interlaced in the sequence with spiked sample extracts of decreasing dilution factors. The dilution factor of 40 was determined as optimal as it did not significantly affect the signals in the standard solutions.

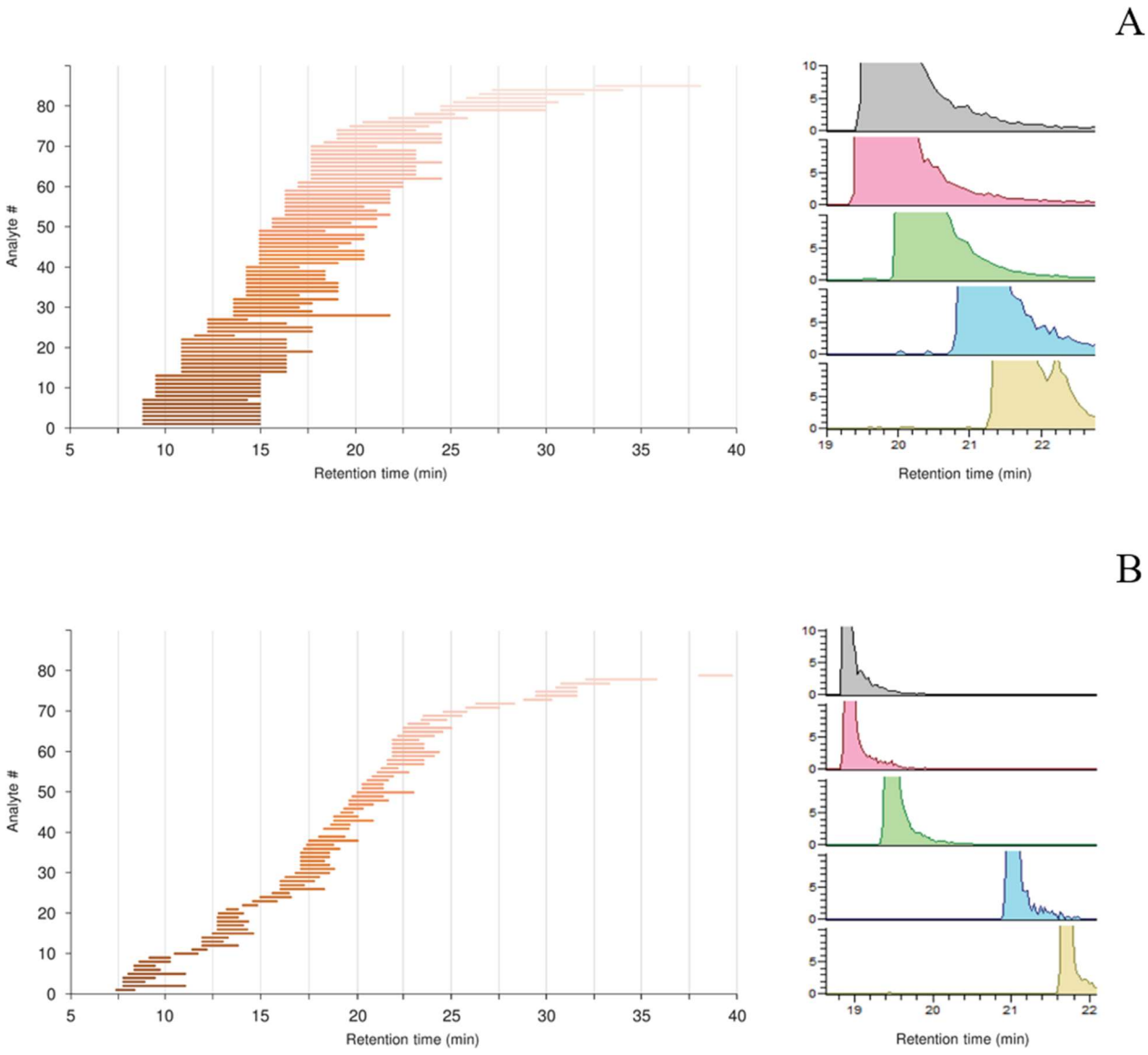

Figure 3.1. **Comparison of chromatographic resolution with tested instrumental configurations: (a) Acclaim PepMap capillary column combined with an EASY-Spray transfer line and an emitter and (b) EASY-Spray capillary column with an integrated emitter**

3.1.2. Method performance evaluation

For the quality analysis, in-house reference materials containing known concentrations of T-2 and HT-2 toxins were analyzed (barley and corn), and z-scores $|z| < 1.5$ were achieved, assuming a target standard deviation of 15%. For the determination of method trueness (recovery, R (%)), precision, and measurement uncertainty, a total of three replicates of six representative matrices (rye, oat, winter wheat, barley, beans, and peas) were spiked with 50 µg kg^{-1} of standard solutions and were analyzed over a three-day period. The trueness (recovery) was determined from the extraction efficiency (EEF) data according to Equation (3.1):

$$EEF = 100\,\% \cdot A_{spiked\ sample} / A_{spiked\ aliquot} \quad (3.1)$$

where $A_{spiked\ sample}/A_{spiked\ aliquot}$ is the ratio of analyte response from a blank matrix spiked prior to the extraction to the analyte response from a spiked extract aliquot from a sample that did not contain the analyte. Figure 3.2 demonstrates the EEF values for the analyzed compounds and corresponding logP values.

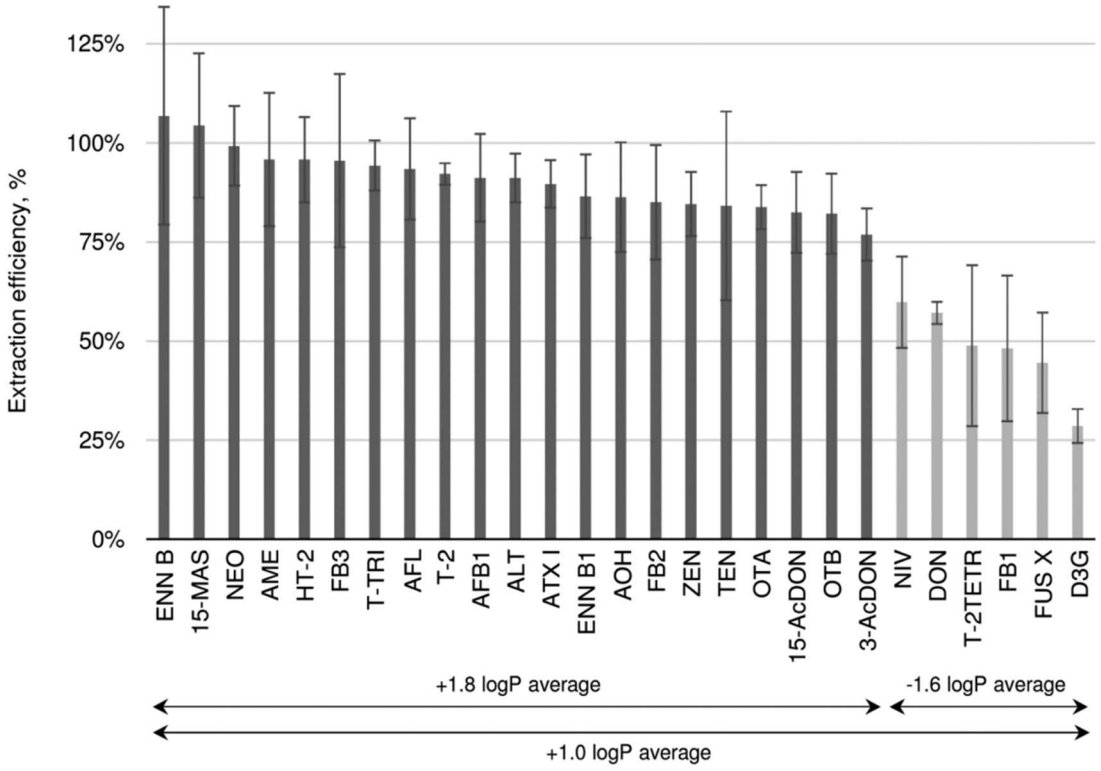

Figure 3.2. **Extraction efficiencies of the analyzed compounds using QuEChERS method**

The six mycotoxins, NIV, DON, D3G, and other *Fusarium* metabolites with a log P < 0 exhibited extraction efficiencies below 70%. Therefore, a correction for the extraction efficiency for these analytes was performed by applying standard addition [164]. The mean RSD values for most of the analytes were good, being 2.7–18%, except for ENN B, FB_3, T-2TETR, and TE, which had RSD values at or above 20%. The recovery rates calculated from the extraction data ranged between 77 and 104% and complied with the criterion established by the DG SANTE 2016/12089 guidelines [164].

The inter-day repeatability expressed as relative standard deviation (RSD) was calculated from the within-laboratory measurements. The expanded measurement uncertainties (U) were estimated according to Equation (3.2):

$$U = k \cdot \sqrt{RSD_{WR}^2 + RMS_{bias}^2 + u_{C_{ref}}{}^2} \quad (3.2)$$

where k = 2 (coverage factor at the 95% confidence interval), RSD_{WR} is the within-laboratory reproducibility, RMS_{bias} is the root mean squared bias, and uC_{ref} is the relative uncertainty of the certified value for the mycotoxin standard.

The individual values of the within-laboratory reproducibility and expanded uncertainty (U, %) are listed in Annex 2. Within these studies, the in-house reference materials (barley and corn) that contained known concentrations of T-2 and HT-2 toxins were analyzed. The average expanded measurement uncertainty was 38% and ranged between 17 and 61% for individual analytes. The high values of expanded uncertainty (>50%) determined in case of several mycotoxins can be associated with the matrix effects of grain and pulse varieties. Thus, to confirm this issue, the matrix effects were evaluated according to Equation (3.3):

$$ME = 100\,\% \cdot (A_{matrix}/A_{solvent} - 1) \quad (3.3)$$

where $A_{matrix}/A_{solvent}$ is the ratio of analyte response from spiked blank matrix to the analyte response from standard in solvent.

The determined matrix effects ranged between −36 and +26% for most of the analytes, except for AOH, AME, all ENNs and FBs, NIV, OTA, and OTB. For these samples, the ME was above 50%, indicating an elevated ionization enhancement effect (for example, the ME of ZEN was 60%), whereas FUS X presented a strong ionization suppression effect (ME was −60%). However, 14 analytes presented acceptable levels, e.g., AFB_1, AFL, T-2, TEN, and ATX I possessed moderate ionization enhancement with an ME that ranged between 5 and 26%. In contrast, the other type A (15-MAS, HT-2, T-2TRI, T-2TETR, and NEO) and type B (DON, D3G, 3-AcDON, and 15-AcDON) trichothecenes and ALT possessed a medium suppression effect with an ME that ranged between −36 and −13%.

The signal-to-noise (S/N) approach was used to estimate the limit of quantification (LOQ) using the chromatograms of spiked samples of six tested representative matrices. The LOQs were defined at levels resulting in S/N ≥ 10. The individual method performance indicators are summarized in Annex 2. The method sensitivity was evaluated from the calculated LOQ values, which ranged between 0.10 and 68 μg kg^{-1}. The sensitivity of the present method was sufficient for the quantification of the regulated and emerging mycotoxins and presented LOQs comparable to or slightly higher than those from the other recent studies for multi-mycotoxin analysis in cereals and pulse matrices [165,166]. The LOQs for OTA, T-2, HT-2, and 3-AcDON of the present method also coincided with the LOQ values reported in the literature [65].

3.1.3. The occurrence of mycotoxins in grain cereal and pulses harvested in Latvia

The developed nano-LC Orbitrap-MS method was applied to analyze the agricultural crop samples collected from the Stende and Priekuli Research centers in Latvia. The contamination with any of 23 different mycotoxins was present for 95% (n = 127) of the analyzed samples. Only one among the oat cereals, four among peas, and one lupin bean sample were mycotoxin-free according to the method's quantification levels. AFB_1, AFL, OTA, and FB_2 were absent in

the cereal and pulses samples. OTB, the dechlorinated OTA metabolite, and FB_3 both co-occurred in only one oat sample at concentrations of 0.34 and 0.27 μg kg^{-1}, respectively ranges of the concentration levels of the other 21 mycotoxins in cereals and legumes are presented in Figure 3.3.

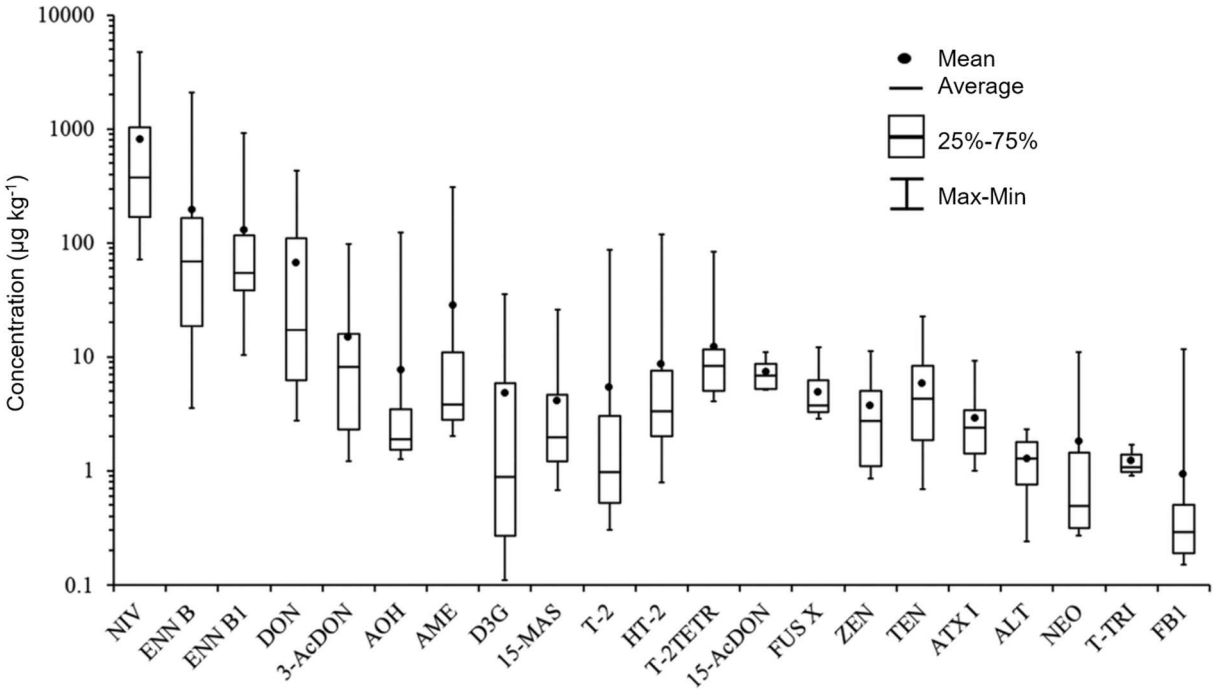

Figure 3.3. **The levels of mycotoxins in legume and cereal samples**

A comparison of the regulated mycotoxins indicated that the T-2 and HT-2 toxins co-occurred in 72% (n = 85) of the total 110 analyzed cereal samples and their individual concentrations were 0.30–7.6 μg kg^{-1} and 0.79–118 μg kg^{-1}, respectively. Winter wheat (18 samples from 21), barley (25 samples from 31), triticale (6 samples from 7), and rye (5 samples from 6) were the most contaminated with the T-2 and HT-2 toxins compared to oat (23 samples from 33) and summer wheat (6 samples from 12) varieties. The total concentration of T-2 and HT-2 levels in the cereals ranged between 1.1 and 205 μg kg^{-1}, with a mean value of 14 μg kg^{-1} and slightly exceeded the maximum limit of 200 μg kg^{-1}, as set by the Commission Recommendation 2013/165/EU for non-processed grains only in the case of one barley

sample [74]. Barley (20 samples from 31), oat (19 samples from 33) and winter wheat (12 samples from 21) cereals were mostly contaminated with DON compared to triticale (3 samples from 7), summer wheat (5 samples from 12) and rye (1 sample from 6) varieties The non-regulated modified DON derivatives (D3G, 3-AcDON, 15-AcDON and NIV) were mainly detected in all cereal varieties: barley (30 samples from 31), oat (32 samples from 33), winter wheat (18 samples from 21), summer wheat (9 samples from 12) and triticale (5 samples from 7), except for rye samples (1 sample from 6). While NIV was detected in 83% of the analyzed cereal samples, in concentrations ranging between 71 and 4780 μg kg^{-1}. Other class B trichothecenes detected were 15-AcDON, FUS X, 3-AcDON, and D3G in 4, 14, 24, and 58% of the analyzed cereals at concentrations below 50 μg kg^{-1}, taking expanded measurement uncertainty into account for one oat sample that contained 96 μg kg^{-1} of 3-AcDON. ZEN was detected in very low concentrations between 0.86 and 11 μg kg^{-1} in one triticale, three oat, and seven barley samples. FB_1 was determined at trace levels (0.15–1.6 μg kg^{-1}) in three barley, seven oat, and 10 winter wheat samples.

The emerging mycotoxins ENN B and ENN B_1 were frequently detected in all analyzed cereal varieties at individual concentrations of 3.5–2073 μg kg^{-1} and 10–922 μg kg^{-1}, respectively. Only one summer wheat, two rye, and two barley samples were tested positive for ENN concentrations above 1000 μg kg^{-1}. Among the pulse samples, only ENN B was determined at concentrations of 4.4–17 μg kg^{-1} in one bean and two lupin samples.

TEN was the most prevalent among *Alternaria* toxins determined in 80–100% of all analyzed cereal varieties at low concentrations of 0.72–23 μg kg^{-1}. TEN was the only mycotoxin determined at 0.69–3.8 μg kg^{-1} in peas (n = 8) and lupin beans (n = 5). AOH concentrations ranged between 1.3 and 125 μg kg^{-1} in oat (21 samples from 33), rye (5 samples from 6), winter wheat (2 samples from 21), and barley (7 samples from 31) varieties and were also determined in lupin beans (n = 4) in the range of 1.5–2.9 μg kg^{-1}. AME was mostly determined in oats (8 samples from 33) at concentrations of 2.52–28 μg kg^{-1}, except for the one

oat sample that simultaneously contained 307 μg kg^{-1} of AME and 125 μg kg^{-1} of AOH. ATX I was detected in trace levels (1.0 and 9.2 μg kg^{-1}) in 50% (n = 55) of the analyzed cereals and co-occurred with one lupin bean sample (3.3 μg kg^{-1}).

The results, particularly of the emerging toxins, were compared with previously reported results of determining mycotoxins in cereals in the European region. High levels of DON and ZEN contamination in grains from Poland, triticale being 100% contaminated with ZEN and DON and the sum of 3- and 15-AcDON and ENNs ranging between 8 and 3328 μg kg^{-1} [84]. In comparison, the ENN levels in Latvian cereals were lower than those determined in the Polish survey. The absence of OTA and aflatoxins in the cereal varieties was in good agreement with the results of the present study. A comparison of literature data for *Alternaria* toxins indicated good agreement with the overall prevalence of TEN, OTA, and AME, which were determined as the predominant contaminants in wheat samples [167].

Comparing pulse varieties, BEA and four ENNs were included among the 27 mycotoxins analyzed in legumes and other food matrices, and HT-2 as the most prevailing mycotoxin in legumes (56%) at concentrations between 4.0 and 7.8 μg kg^{-1} in grain and legume samples was reported [168]. A high prevalence (60%) of AOH (25–211 μg kg^{-1}) and AME (62–1153 μg kg^{-1}) in soybean samples from Argentina was reported [169]. However, studies on *Alternaria* toxins in other legume varieties are scarce, with the exception of a recent report from the European Food Safety Authority (EFSA), which indicated the high prevalence (>80%) of AOH, AME, and TEN in legumes, while only carob fruit and soy bean samples were included in the study [80]. Compared to these previous reports, the present study confirms the high prevalence of *Alternaria* mycotoxins in different grain legumes, especially of the lupin variety.

3.2. Determination of pyrrolizidine alkaloids

3.2.1. Evaluation of method performance and different sample preparation procedures

For the estimation of extraction efficiency and matrix effects, spiked samples and spiked extracts were prepared from two randomly selected blank samples of tea and honey matrices, as well as standard solutions and spiked blanks were prepared to an equal theoretical on-column mass for direct comparison according to Equations (3.1) and (3.3). The expanded measurement uncertainties at 95% confidence interval were estimated according to Equation (3.2). Pyrrolizidine alkaloids that could not be separated chromatographically were analyzed as the sum of coeluting analytes. Analytes were confirmed by a set of peaks from at least two different product ions. LOQ was determined experimentally as the average of individual values from three different blank samples based on peaks with S/N ≥ 10. For the estimation of measurement uncertainty, a total of 3 procedural replicate five-point calibration sets were analyzed for each representative matrix on at least two different days, and the reproducibility, trueness, and uncertainty were determined from the lowest calibration level. The average expanded measurement uncertainty was calculated using Equation (3.2), and it was 21% and the uncertainty for each representative matrix was the following: 18% for honey, 30% for tea, 20% for milk, and 17% for herbal tinctures.

The average extraction efficiency for all matrices obtained using the QuEChERS extraction procedure was 76 ± 30%, and 73 ± 15% using SPE. The average matrix effects and average peak height of all analytes are given in Figure 3.4. While the average matrix effect with dilution methods was low, the individual values varied widely; therefore, a standard addition calibration was needed for proper quantifications. Strong matrix effects were observed with the preconcentration methods and solid phase extraction. Taken together, the observations showed that the analysis of diluted extracts with nano-LC-MS is more sensitive than with conventional flow LC-MS used in this study. The median LOQ over all analytes was 0.33 μg kg^{-1} in honey

(0.05–2.5 µg kg^{-1}) and 3.6 µg kg^{-1} in tea (0.5–20 µg kg^{-1}), with conventional LC-MS, the LOQs were 6.0 µg kg^{-1} in honey (0.2–23 µg kg^{-1}) and 7.8 µg kg^{-1} in tea (0.8–44 µg kg^{-1}) for diluted QuEChERS samples. The data demonstrated that the sensitivity is comparable to or better than in methods from the literature (Table 1.3). The results of matrix effect estimation are given in Figure 3.4. The validation data is provided in Annex 9 to Annex 12. Most published methods use 50–150 mm long columns and particles in size < 3 µm. In this study, the median LOQ over all analytes was 0.33 µg kg^{-1} in honey (0.05–2.5 µg kg^{-1}), 3.6 µg kg^{-1} in tea (0.5–20 µg kg^{-1}), 3.3 µg kg^{-1} in herbal tinctures (0.3–10 µg kg^{-1}), and 0.32 µg kg^{-1} in milk (0.03–1.1 µg kg^{-1}). Chromatograms of the different matrices are provided in Annex 14.

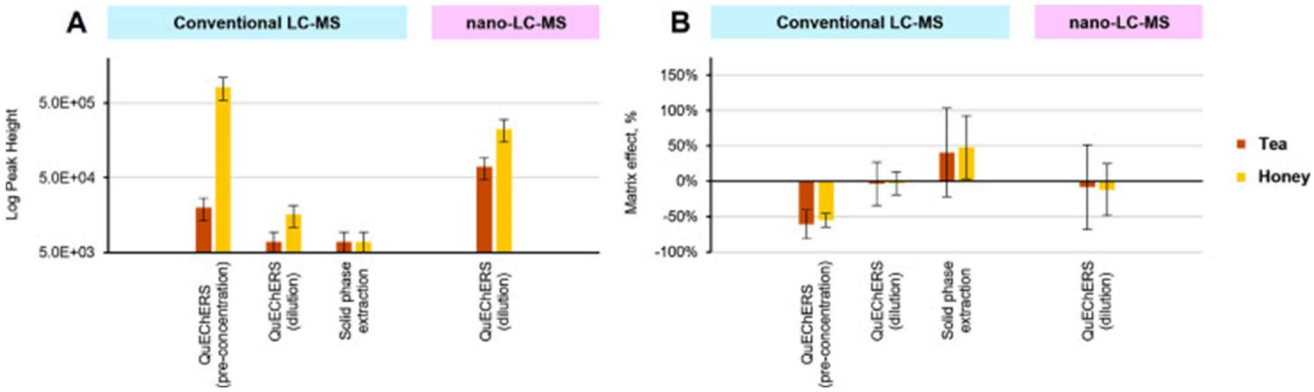

Figure 3.4. **Conventional LC-MS and nano-LC-MS average log peak height (A) and the comparison of average matrix effects (B) of all analytes. For conventional LC-MS, the solid phase extraction dilution factor was d=1.8; with QuEChERS and pre-concentration d=2 for tea and d=0.4 for honey; with QuEChERS and dilution d=40 for tea and honey. For nano-LC-MS, the dilution factor was d=37.5 for tea, and d=7.5 for honey**

The results demonstrated that standard stability might be limited at lower temperature. The literature data on the stability of PAs in stock solutions is rather limited. However, it is suggested that the standards are stable in methanol for at least a year at –20 °C [170]. In another study, the stability of analytes at different temperatures was evaluated, and the storage data at

–18 °C demonstrated that the stability is not ideal and loss of analytes by day 30 is about 30% from the initial, while some analytes remained the same or had some small losses [111], which is similar to this study where the loss is about 30–40%. In our study, the standards were dissolved in a 1:1 mixture of 50% aqueous acetonitrile and methanol, which could explain the difference in stability. Therefore, it can be concluded that the stability of analytes at –18 °C is good when methanol is used for dissolving the compounds, while if some other solvent or mixture is used, then the stability is reduced compared to pure methanol.

3.2.2. The occurrence of pyrrolizidine alkaloids in tea, honey, herbal tinctures, and milk from the Latvian market

To date, no studies have been performed on the occurrence of pyrrolizidine alkaloids in plants of Latvian origin. Some pyrrolizidine alkaloid-producing plants are widespread in Latvia, for example, chamomile and peppermint, which can produce high pyrrolizidine alkaloid levels, are widely grown in households, while coltsfoot, ragwort, and comfrey are widespread in the flora [106,171]. Thus, honey products and herbal tea products can be contaminated with pyrrolizidine alkaloids. The concentrations of pyrrolizidine alkaloids in food matrices are provided in Table 3.1.

Table 3.1

The total pyrrolizidine alkaloid concentrations measured in different foods of Latvian origin (the sum of 30 pyrrolizidine alkaloids is shown, including *N*-oxides)

Type of sample	N	Samples >LOQ, %	Minimum, μg kg^{-1}	Maximum, μg kg^{-1}	Mean, μg kg^{-1}
Herbal tea	15	47	5.8	215	71
Honey	40	33	0.14	74	9.4
Herbal tincture	15	0	–	–	–
Milk	10	0	–	–	–

Tea samples. 15 herbal tea samples were analyzed, five of which were plant mixtures that included not only different herbal plants, but also species like cloves and ginger root. Seven of the samples were found to contain pyrrolizidine alkaloids. In one sample of yarrow tea, the total pyrrolizidine alkaloid concentration was 215 μg/kg, which is the maximum limit according

to Commission Regulation (EU) 2020/2040[96] amending Regulation (EC) 1881/2006[11] on the maximum permissible levels of pyrrolizidine alkaloids. The average concentration for the positive samples was 71 μg kg^{-1}. The second highest concentration of 126 μg kg^{-1} was found in a branded product containing a complex mixture, including wormwood, yarrow, and cloves. Most of the detected pyrrolizidine alkaloids in the samples (97% of total concentration) were in the form of *N*-oxides. There is no information on whether yarrow plants produce pyrrolizidine alkaloids, therefore, the presence of these alkaloids may be due to contamination during harvesting. The levels of pyrrolizidine alkaloid contamination in herbal teas were consistent with other European studies [106].

Honey samples. A total of 40 honey samples originating from Latvia were purchased from the local market and analyzed. One third (33%) of the samples contained pyrrolizidine alkaloids, with an average concentration of 9.4 μg kg^{-1}. The highest level of pyrrolizidine alkaloids was found in summer season honey from forest flowers – 74 μg kg^{-1}. The concentrations of detected pyrrolizidine alkaloids in Latvian honey samples were also consistent with other European studies: 2.9 μg kg^{-1} reported in Poland [172], 6.1 - 15 μg kg^{-1} reported in Germany and Austria [106]. Similarly, as in the report from Poland [172], in this study, the percentage of positive samples was 32%, but this indicator of occurrence can change depending on the production years. The lycopsamine-type alkaloids, notably echimidine and lycopsamine, were the most prevalent, while senecionine-type alkaloids were detected significantly less frequently and at low concentrations. Other reports [95,173] provided similar findings, including the EFSA report 2016 [174]. Most of the analyzed honey samples were polyfloral, therefore it was not possible to evaluate the effect of flowering plant species on the concentration of alkaloids in honey.

Herbal tincture and milk samples. A total of 15 herbal tincture samples and 10 milk samples originating from Latvia were purchased from the local market and analyzed. The pyrrolizidine alkaloids were not detected in any of the samples.

3.2.3. Target ion screening approach

Preliminary experiments performed on analytical standards showed that pyrrolizidine alkaloids mainly produce common fragment ions upon collision-induced dissociation: 94.0656, 120.0808, 136.0756, 138.0911, 150.0912, 156.1018, 168.1016, and 172.0960 *m/z* (± 0.001 *m/z*). The exact fragments and abundance ratios depend on the structure of the alkaloid [175]. Fragment 94.0656 *m/z* could be of particular importance [103], as it may originate from all the tested analytical standards, particularly at higher collision energies, although with widely varying yields. Figure 3.5. provides a possible formation of this ion [176].

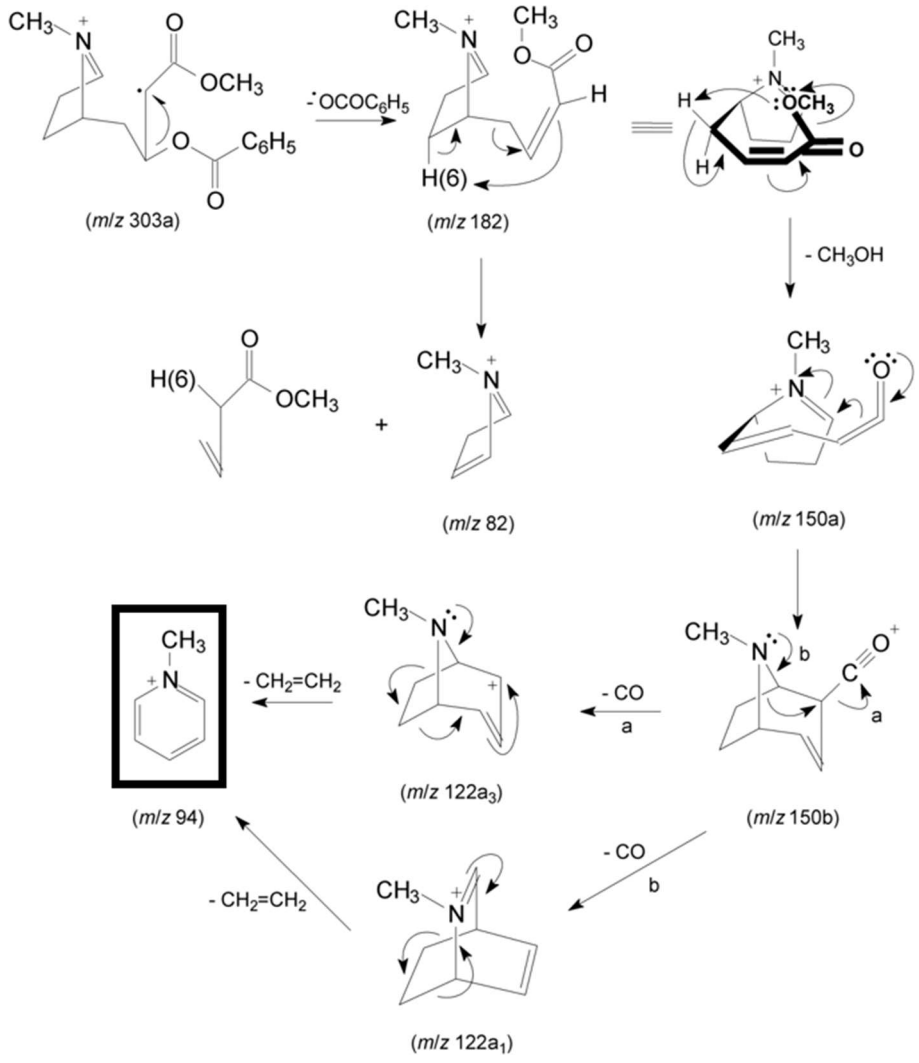

Figure 3.5. **Possible formation of the highly selective fragment 94.0656 *m/z*** [176]

Database searches were conducted to elucidate the most probable origins of the 94.0656 *m/z* fragment ion. It was found that the fragment ion signal 94.0656 ± 0.001 *m/z* corresponding

to $C_6H_8N^+$ (monoisotopic mass 94.0651 Da) can be obtained from molecules with such structural features as picoline, methylpyridine including *N*-methylpyridinium, aniline, 2,3,5,7a-tetrahydro-1H-pyrrolizine, pyrrolizidine, and tropane. The possible exact structures of the $C_6H_8N^+$ ion as a product ion from a tropane alkaloid have been proposed in the literature [176], where *N*-methylpyridinium structure was proposed. Figure 3.5. demonstrates the formation process of this specific ion. In silico models suggest that the structure of the $C_6H_8N^+$ ion as a product ion from a pyrrolizidine alkaloid could be 1-methyl-3-methylidene-3H-pyrrol-1-ium (heuristic prediction by Mass Frontier 7.0 in mzCloud database). It could be argued that the $C_6H_8N^+$ fragment ion is a highly selective target fragment ion for the detection and discovery of pyrrolizidine alkaloids and, possibly, tropane alkaloids, provided that the experimental chromatography and mass spectrometry setup has high-resolution and is optimal for broad MS^2 interrogation with narrow isolation, and provided that effective measures are taken to discern between the features originating from the sample and background contamination, as well as to perform fragmentation of the precursor ions optimally.

Furthermore, preliminary experiments in the all-ion fragmentation mode performed on extracts of several plants that do not produce alkaloids showed low baselines of chromatogram with no detected peaks, suggesting that the fragment 94.0656 *m/z* is rather uncommon. Therefore, the screening results were compared in the case of two sets of target fragments – all common fragment ions and the 94.0656 *m/z* fragment ion only. Also, two spiking levels were compared with respect to the detection rate of alkaloids in spiked samples. The results are demonstrated in Figure 3.6.

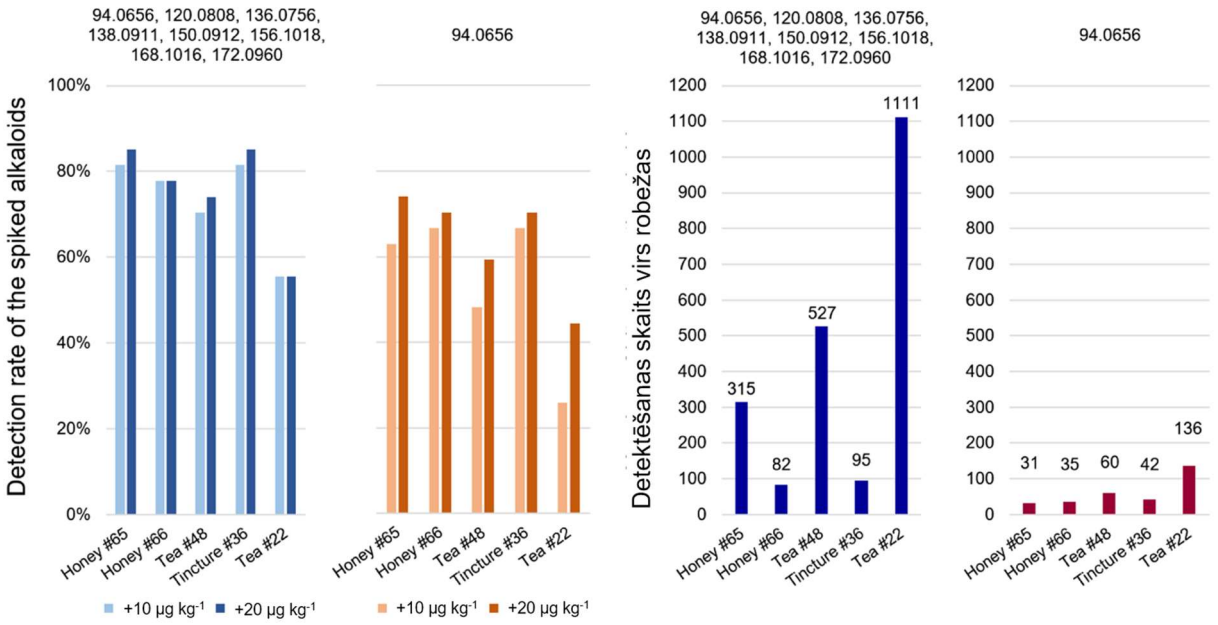

Figure 3.6. **Comparison of two different sets of target fragment ions for screening with respect to the detection rate of added alkaloids at two concentration levels (10 µg kg^{-1} and 20 µg kg^{-1}), and the number of hits above the threshold at 10 µg kg^{-1}**

The detection rate was approximately 20% higher if all common fragment ions were used as targets; however, in such a case, the number of hits above the threshold was about 10 times higher. The rate of detection for added alkaloids improved with increased spiking level, thus higher concentrations could be detected more reliably. The results given in Figure 3.5 correlate with the nature of samples – honey #65 and tea #48 were products that contained known pyrrolizidine alkaloids, and tea #22 was derived from *Calendula*, which could contain unknown or uncommon pyrrolizidine alkaloids, as shown recently [175], and the number of hits above the threshold in these samples was significantly higher, while honey #66 and herbal tincture #36 were not expected to contain any pyrrolizidine alkaloids or contaminated ingredients, and the number of hits above threshold in these samples was low. Reanalysis of the screening hits in high-resolution MS^2 with narrow precursor isolation is needed to confirm whether the observed fragment ions constitute a common chromatographic feature and to further analyze the spectral data in order to identify possible chemical structures of the precursor ion. Furthermore,

reanalysis with other detection techniques could provide additional structural information. Figure 3.7 illustrates the main advantage of the approach used in this study for trace contaminant detection in complex samples – after reanalysis of the hits exceeding threshold in high resolution with precursor isolation, easily interpretable chromatographic features were obtained for the detected spiked pyrrolizidine alkaloids, while the chromatographic features based on the precursors in full scan alone, even at the high resolution of 70000, were not useful for interpretation, due to the lack of selectivity.

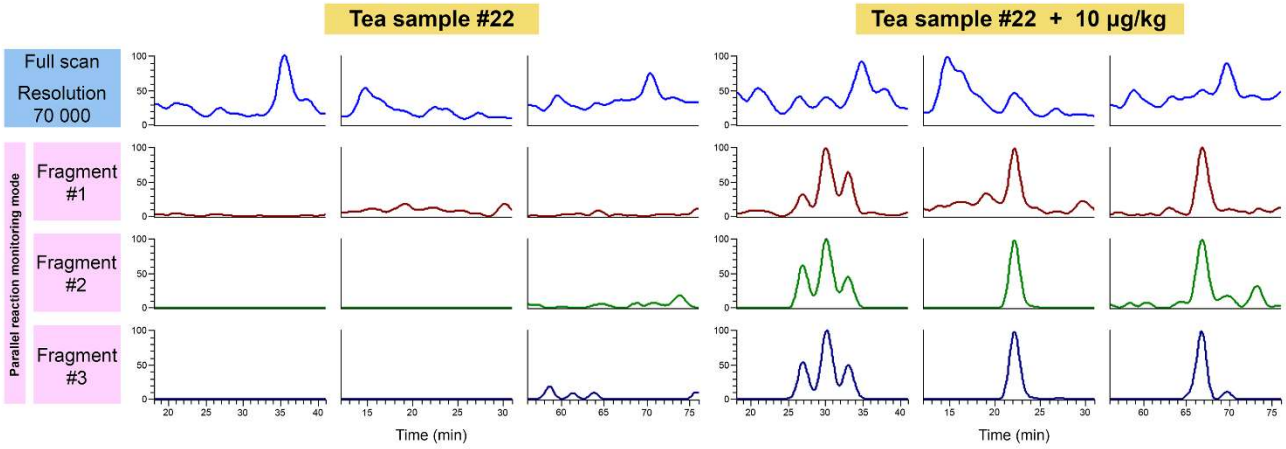

Figure 3.7. **Chromatographic features obtained by reanalysis of precursor ion hits above threshold in parallel reaction monitoring mode (PRM), compared to the precursor ion in full scan. The peaks in PRM mode are the following: echinatine *N*-oxide, 27 min; indicine *N*-oxide and intermedine *N*-oxide, 30 min; lycopsamine *N*-oxide, 33 min; europine, 22 min; seneciphylline *N*-oxide, 67 min**

The number of hits exceeding the threshold with the 94.0656 *m/z* target fragment ion was similar to the number of added alkaloids (30 different pyrrolizidine alkaloid standards were added) in samples where contamination was not expected. Tea samples #48 and #22, which were expected to contain alkaloids, showed a larger number of hits exceeding the threshold. Taken together, these findings show that the 94.0656 *m/z* fragment ion is a selective fragment ion for detection and discovery of pyrrolizidine alkaloids with high-resolution mass spectrometry.

3.3. Determination of biomarkers and pharmaceuticals

3.3.1. Method development and optimization of LC

Preliminary experiments using different solvents and mobile phase pH values demonstrated that the retention of highly polar acidic compounds (ethyl sulphate and 5-HIAA) was insufficient since the compounds were eluted at or near the void volume, indicating the possibility of interferences from matrix components and poor sensitivity. It is known that the addition of an ion-pair reagent into the mobile phase could improve chromatography of polar compounds on a C18 stationary phase; however, this may lead to serious contamination of the instrument due to poor volatility and tendency for the adsorption of such reagents. Thus, this approach was not considered in the current work. The other method was used, which was based on adding a large excess of an ion-pair reagent directly into the sample. After injection, the reagent is transferred onto a column together with the sample, providing the necessary interactions for analyte retention and leaving the column at a higher strength of the mobile phase at the end of the gradient. As a result, the analytes are retained longer in the column, reducing the possibility of co-elution with polar matrix components and thus mitigating the matrix effects [177]. Different types of ion-pair reagents are available based on the chemical structure and physical properties, such as the octanol-water partition coefficient (logP value) and solubility in the mobile phase. A commonly known ion-pair reagent TBAB was selected for method development due to its intermediate logP value (2.01) [178] among other reagents, providing the necessary increase of analyte retention while keeping acceptable retention time and retention window of the reagent itself. Optimization of the ion-pair reagent concentration was performed over the range of 1 to 15 mM, and optimal retention times for acidic analytes were achieved at 11 mM of TBAB added to the sample. The obtained chromatograms are provided in Figure 3.8.

The direct addition of TBAB into the samples led to a notable improvement of the retention time and signal intensity of 5-HIAA and ethyl sulphate peaks (see Figure 3.8). The retention time for 5-HIAA shifted from 3.8 to 8.7 min and the signal intensity increased about 6 times. The retention time of ethyl sulphate increased from 2.1 to 6.5 min while the signal intensity increased 9 times. Additionally, the symmetry of both peaks improved significantly. The signal intensity most probably increased due to the diminished content of interfering matrix compounds that usually elute in the column void volume. As expected, the retention times and signal intensities of other analytes did not change significantly except for diclofenac and ibuprofen. The latter two compounds were eluted at the tail portion of the ion-pair reagent, slightly suppressing the signal intensity of both analytes.

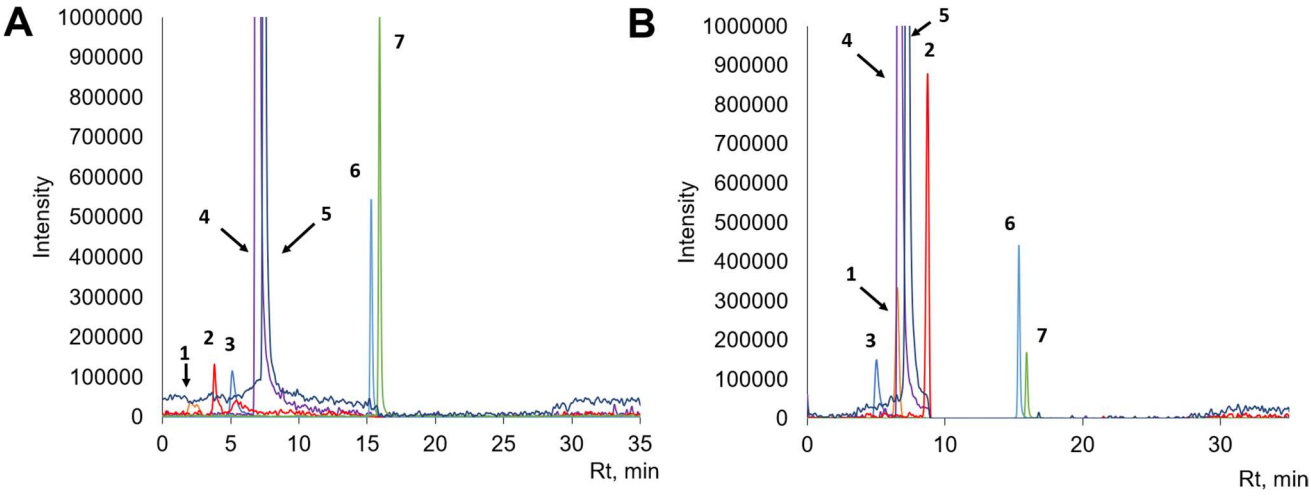

Figure 3.8. **Chromatograms of the analyzed pharmaceutical compounds and biomarkers (1 – ethyl sulphate, 2 – 5-HIAA, 3 – gabapentin, 4 – cotinine, 5 – caffeine, 6 – diclofenac, 7 - ibuprofen) without addition of TBAB reagent (A), with the in-sample addition of optimal concentration of 11 mM of TBAB (B)**

3.3.2. Optimization of the Orbitrap MS parameters

Preliminary experiments have demonstrated that the FS acquisition mode provided the most reliable results regarding sensitivity compared to the Selected Ion Monitoring (SIM) and PRM scanning modes. Despite some advantages of the SIM mode, including the improved

selectivity, which is beneficial for the analysis of complex matrices such as WW, other factors must also be considered, namely the possibility of performing a retrospective evaluation and identification of other analytes of interest that were not included in the original method [179–182]. Therefore, considering that the FS acquisition mode offers this possibility and WW could provide information on a wide range of chemical compounds, it was concluded that the FS mode is more suitable for the analysis. Despite the advantages of the full-range acquisition procedure, the selected methodology has limitations regarding the unequivocal identification of the compounds since no information about accurate mass for fragment/product ions is available.

The optimization of the MS voltages and scanning parameters has been carried out using neat standards. MS parameters were optimized during the preliminary experiments. An unstable electrospray was observed initially under gradient conditions with high aqueous content, which leads to decreased signal intensities and droplet formation at the emitter tip, affecting the sensitivity and applicability of the method. Several approaches to improve nano-electrospray stability have been described, such as post-column solvent addition [43,183], where a highly organic solvent is continuously added to the column eluate via a T-piece to reduce the aqueous phase content and facilitate electrospray, voltage regulation during analysis [44], and selection of the correct nano-ESI voltage. In this work, optimal nano-electrospray performance was achieved by manually selecting a suitable voltage in a range of 1.70 kV to 2.50 kV for both positive and negative modes under initial gradient conditions, and the optimal voltages that provided the most stable nano-electrospray were used. In addition, automatic gain control (AGC) and injection time (IT) were evaluated. AGC controls the number of ions entering the mass analyzer, and its values were investigated in a range from 5e4 to 3e6. IT limits the time for ions to accumulate in the C-trap and its values from 50 to 300 ms were investigated. However, considering the so-called “space charge effect”, when an incorrect combination of AGC and IT values is chosen, resulting in reduced mass precision [184–186], it was important to choose appropriate values. Therefore, a combination was selected that provided appropriate

mass precision and intensity. Another optimized parameter was the S-lens or the stacked-ring ion guide value. By changing the RF values of the S-lens, the focusing of the ions could be controlled to increase the number of ions entering the detector and thus improving the signal intensity and sensitivity. The value of the S-lens was optimized in a range from 10 to 100 in increments of 10. The final optimized value of 60 was selected as it provided the best signal intensities for all compounds analyzed.

3.3.3. Method performance evaluation

The results of method validation have been summarized in Annex 5. Trueness, repeatability, and reproducibility of the method were determined using a wastewater sample with standard addition method using two-day validation approach at 10 and 50 µg L^{-1} (n = 6 for each) levels. Trueness was estimated at two levels according to Equation 3.4:

$$Trueness = \frac{C_{sp,average}}{C_{sp}} \cdot 100\% \quad (3.4)$$

where $C_{sp,average}$ is the average calculated concentration of the spike determined from repeated measurements (n = 6) at two spiking levels (C_{sp}) of 10 and 50 µg L^{-1}, respectively.

The matrix effects (ME) were estimated by comparison of the slopes of the calibration curves obtained for neat standard solutions (a_{std}) and a wastewater sample spiked with standards ($a_{std\ addition}$) at comparable concentrations. The following Equation (3.5) was used for calculations:

$$ME = \frac{a_{std\ addition}}{a_{std}} \cdot 100\% \quad (3.5)$$

Since the presence of biomarkers and pharmaceuticals in wastewater samples is inevitable, LOQ estimation was based on a standard addition method taking into account the signal-to-noise ratio (S/N) according to Equation (3.6) [187]:

$$LOQ = \frac{10 \cdot C}{S/N} \quad (3.6)$$

where C is the concentration of analyte in the sample according to the standard addition method, S/N – signal to noise ratio of the analyte obtained without the addition of standard.

The expanded measurement uncertainty of the method (95% confidence interval) for each analyte was calculated based on the reproducibility using Equation (3.7), since the method including recovery could not be applied due to the fact that the sample preparation procedure did not involve such steps as evaporation or SPE, therefore an alternative formula was used:

$$U_c = k \cdot RSD_{WR} \quad (3.7)$$

where k = 2 is a coverage factor at the 95% confidence interval and RSD_{WR} is reproducibility.

Quantitative analysis of the analytes was performed using a five-point calibration curve in a range of 0.5 – 50 μg L^{-1}. The analyzed compounds were confirmed based on the retention time (±0.1 min), S/N ≥ 10, and by two ions with mass deviation <5 ppm. Quality control samples with the standard addition at the level of 10 μg L^{-1} were included in batches to evaluate the recovery of the analytes. The mass deviations of the diagnostic ions are provided in Annex 4.

It is evident that the proposed method performed well in terms of accuracy, precision, and other validation parameters for the analytes of interest. Compared to other methods found in the literature (see Table 3.2), the proposed procedure can be characterized by similar or lower LOQ values (0.005 – 0.3 μg L^{-1}) as well as by negligible matrix effects (70-111%). Since the proposed method does not require any sample preparation (i.e., LLE or SPE) except for dilution and filtration, the loss of analytes has been significantly reduced. Finally, one of the main advantages of this method is the demonstrated applicability to analytes of different polarity, including the ionic compound ethyl sulphate within one run.

Table 3.2

Comparison between the previously published methods and this work

Analytes	Instrumentation	Main sample preparation steps	Analytical column	Injection volume	LOQ, μg L^{-1}	Matrix effects, %	Reference
Several biomarkers and pharmaceuticals	Nano-LC Orbitrap MS	Dilute-and-shoot method, addition of TBAB	PepMap C18 150 × 0.075 mm, 3 μm	70 nL	0.005 - 0.3	70 - 111%	This study
Biomarkers and pharmaceuticals	UHPLC QqQ MS	Dilute-and-shoot method	1D: Kinetex C18, 50 mm × 3 mm, 1.7 μm, 2D: Synergy Max-RP, 150 × 3 mm, 4 μm	10 μL	1 - 5	ND	188
	UHPLC QqQ MS	SPE, evaporation			0.1 - 50	ND	
Diclofenac and ibuprofen	UHPLC QqQ MS	Liquid-phase microextraction	Luna Phenyl-Hexyl, 150 mm × 2.0 mm, 3 μm	90 μL	0.14 - 0.25	94.4	189
Ethyl sulphate	UHPLC QqQ MS	Dilute-and-shoot method	Synergi Fusion-RP, 150 mm × 4.6 mm, 4 μm	100 μL	0.3	21 - 25	177
	UHPLC ToF MS				0.6	61 - 72	
5-HIAA	UHPLC QqQ MS	LLE, derivatization	Kinetex PFP, 100 mm × 2.1 mm, 1.7 μm	1 μL	1	ND	190

3.3.4. The occurrence of biomarkers and pharmaceuticals in wastewater

Untreated wastewater samples were collected from the wastewater treatment plants in several cities and towns of Latvia, including Jelgava, Liepaja, Valmiera, Ventspils, Jekabpils, Jurmala, Riga, Rezekne, Daugavpils, Salaspils, and Tukums. Annex 6 demonstrates a map of Latvia demonstrating the locations of the cities. The samples were collected on Tuesday and Thursday from March 31 to April 28, 2022. In total, 116 samples were collected and analyzed using the developed method. All of the samples contained the analyzed biomarkers and pharmaceuticals. The obtained concentrations with comparison to literature data from the same region are provided in Table 3.3. A good agreement was observed with the literature data,

indicating the applicability of the proposed analytical methodology in determining the selected biomarkers.

Table 3.3

Comparison to literature data

Compound	Concentration range, µg L^{-1} [this work]	Median concentration, µg L^{-1} [this work]	Concentration range from literature, µg L^{-1} [188]
Gabapentin	9.6 - 71.9	20	7.3 - 50.2
Cotinine	2.7 - 10.3	4.6	2.4 - 10.1
Ethyl sulphate	4.5 - 83.7	25	13.1 - 43.6
Caffeine	19.9 - 162	58	23.8 - 156
5-HIAA	0.4 - 20.2	7.6	4.9 - 17.7
Diclofenac	0.6 - 7.4	3.8	0.6 - 2.7
Ibuprofen	6.6 - 36.4	12	7.3 - 25.4

3.4. Determination of PFAS

3.4.1. Control of background contamination

The analysis of PFAS at trace levels is challenging due to the presence of these contaminants in the environment [191–194]. Therefore, additional measures were taken to reduce the possible background contamination originating from the instrumentation and other sources during the method development and application to real sample analysis. Extensive washing of critical parts of the instrument was performed, including the autosampler port and capillaries. As a result, the presence of analytes of interest was not detected during the analysis of standard solutions in methanol containing only internal standards at concentrations equivalent to those in the final extracts of real samples. The procedures for eliminating the possible contamination by washing the glassware with organic solvents and by other procedures were evaluated by analyzing the procedural blanks that were included in the protocol regularly. Procedural blanks were prepared in each analytical sequence to assess the possible contamination during the sample treatment, and some presence of PFOA and PFOS was detected. These levels were also considered, setting the respective m-LOQs that were agreed as the lowest validation level for

all tested matrices. The results from real samples were corrected by subtracting the PFAS content of the procedural blanks analyzed in the respective sample sequence.

3.4.2. Selection of the nano-LC fluidics setup

Despite numerous advantages of implementation of the nano-LC methodology, still one of the issues is the availability of different types of commercially available stationary phases used in analytical columns, and applications are represented mainly by reversed stationary phase C18 (RP-C18) columns [15,195]. Recent literature data demonstrated that the C18 stationary phases are widely used for the analysis of PFAS [138,196,197]; therefore, this study focused on implementation of C18 phases in two different instrumental nano-LC fluidics setups. Two different setups were tested, namely an EASY-Spray C18 capillary column with the integrated emitter and thermostat and an Acclaim PepMap C18 capillary column connected with an EASY-Spray microflow transfer line. Taking into consideration that the efficiency of chromatographic separation in nano-LC relies on the presence of dead volume in the setup, lengths of capillaries or any additional connections, even in the case of zero dead volume, could produce inferior quality of separation and broadening of chromatographic peaks. This effect is also prominent in other conventional types of liquid chromatography; however, with the scale of nano-LC, this effect is substantially more pronounced [69]. The comparison between the two instrumental setups is provided in Figure 3.9.

Preliminary experiments have demonstrated acceptable chromatographic separation and optimal peak shapes by applying the EASY-Spray column with an integrated emitter, while the Acclaim PepMap column with microflow transfer line and emitter showed less effective chromatography, and Figure 3.10. demonstrates the comparison between the two setups.

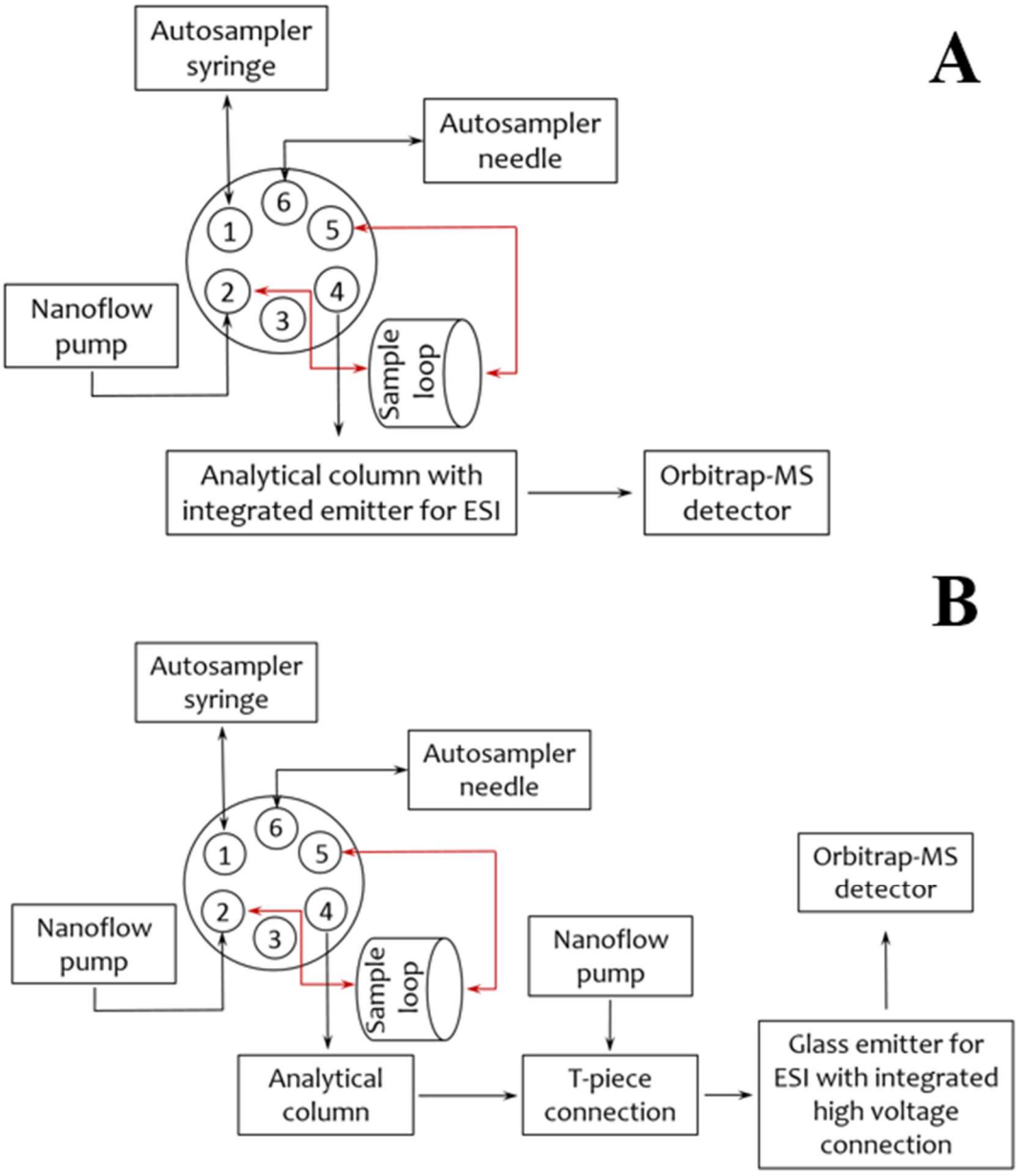

Figure 3.9. **Two setups EASY-Spray C18 capillary column with the integrated emitter and thermostat (A), and an Acclaim PepMap C18 capillary column connected with an EASY-Spray microflow transfer line (B)**

The Acclaim PepMap setup contained additional connections and capillaries; therefore, a zero-dead-volume EASY-Spray column should provide less peak broadening due to the increased length of the fluidics system and imperfections between the capillary connections. Figure 3.10. confirms this hypothesis since the peak asymmetry and peak broadening were observed with the Acclaim PepMap column setup.

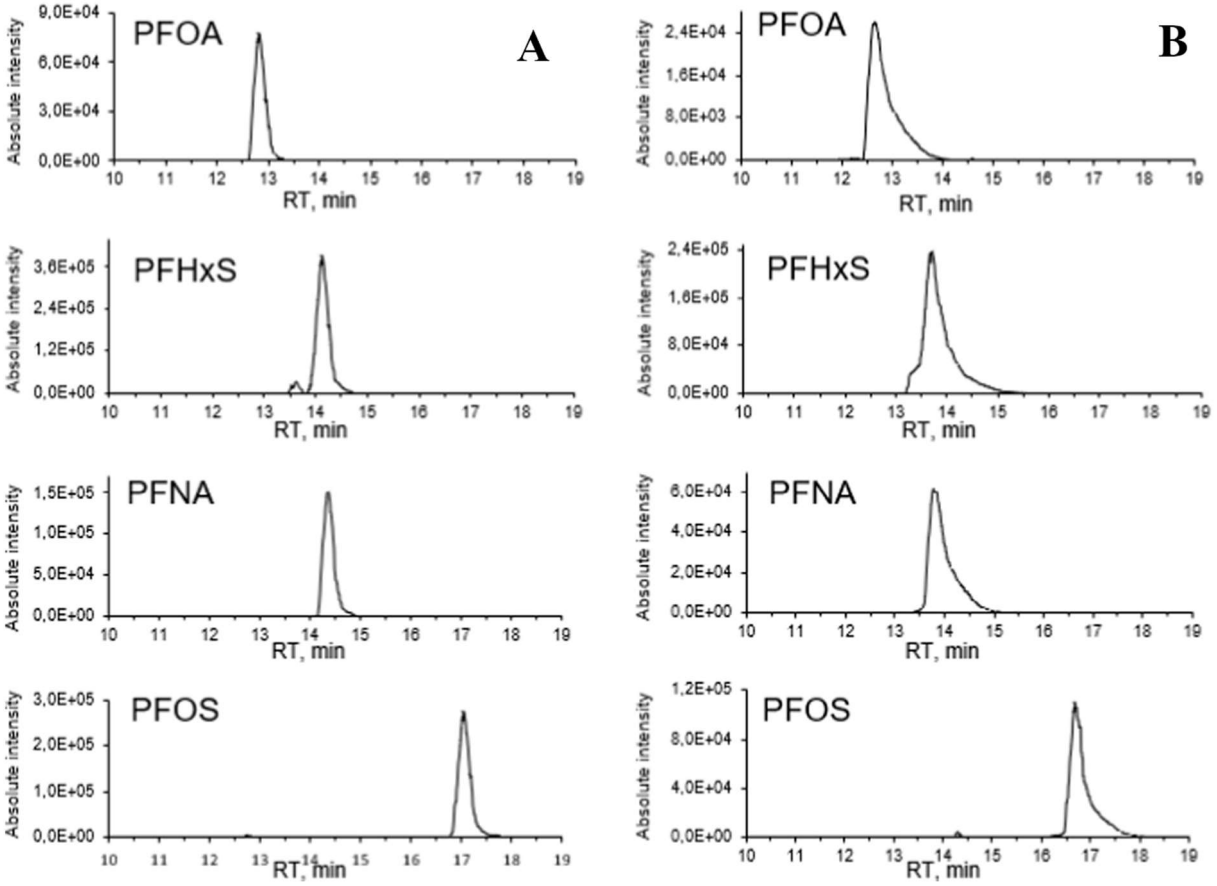

Figure 3.10. **The comparison between two setups EASY-Spray C18 capillary column with the integrated emitter and thermostat (A), and an Acclaim PepMap C18 capillary column connected with an EASY-Spray microflow transfer line (B)**

3.4.3. Method performance evaluation

The method performance was evaluated considering recently developed Guidance Document on Analytical Parameters for the Determination of Per- and Polyfluoroalkyl Substances (PFAS) in Food and Feed [198]. Several parameters were evaluated to assess analytical performance, including LOQ, linearity, matrix effects, recovery, and RSD. Validation was performed using real samples of the appropriate matrix groups. The results of spiking experiments were corrected by considering the concentrations of blank samples. A minimum of five batches of different matrices representing one matrix group (e.g., meat and seafood or milk and milk products) were spiked at three concentration levels (1 x targeted LOQ, 5 x

targeted LOQ, and 25 x targeted LOQ) and analyzed in the frame of two separate analytical sequences on two different days. The recovery and within-laboratory reproducibility for each fortification level were examined. The method LOQs (*m*-LOQs) were set as the lowest validated level of individual PFAS for each matrix group. The lowest recommended validation levels for different matrix groups are overviewed elsewhere [198,199] and take into consideration the recent toxicological findings with regards to selected PFAS and recently established TWI.

Assessment of instrumental sensitivity (instrumental LOD and LOQ (*i*-LOD and *i*-LOQ)) relying on the S/N ratio as a criterion in the case of Orbitrap-MS could be problematic since the HRMS typically provides low background noise. Therefore, in the first approximation, the *i*-LOD values were assessed by injecting 0.8 pg of each analyte on the column, considering the dynamic range of the detector and signals above the intensity of 1×10^4 for reliable detection. The *i*-LODs were calculated by extrapolating concentrations corresponding to the intensities of 1×10^4 from the intensities observed by the on-column injection. The *i*-LOQs were defined as 3 × *i*-LOD, and for the most intensive PRM transitions were equal to 0.05 pg for PFOA, 0.04 pg for PFNA, 0.03 pg for PFHxS, and 0.02 pg for PFOS, respectively.

Sufficient linearity over the concentration range of 0.5 – 1000 pg μL^{-1} was observed for individual PFAS with correlation coefficients (R^2) of ≥ 0.995 and residual values less than 20 %. Due to the ubiquity of some PFAS in blank matrices, applying solvent-matched calibration solutions for quantitative purposes was considered preferable. No significant differences in the calibration curves obtained by matrix-matched and solvent-matched linearity experiments were observed since the difference in slope values was 1–3% depending on the individual PFAS. Therefore, a six-point solvent-matched calibration solution set covering the concentration range of 0.5–100 pg μL^{-1} was used for routine samples in each sample sequence.

The results of the spiking experiments show that the mean recovery values for target analytes ranged from 83 to 118%, while the within-laboratory reproducibility in terms of RSDs were in the range of 7–18%. The validation data is provided in Annex 14. Additionally, to verify

method performance, the analysis of materials that underwent interlaboratory testing within the framework of proficiency tests (PTs) to determine PFAS in food organized by the European Union Reference Laboratory for Halogenated POPs (Freiburg, Germany) was conducted. The results were in good agreement with the provided consensus values, as shown in Figure 11. Four PT materials representing three matrices were analyzed by the developed method: wheat flour, pork liver, and liquid whole egg.

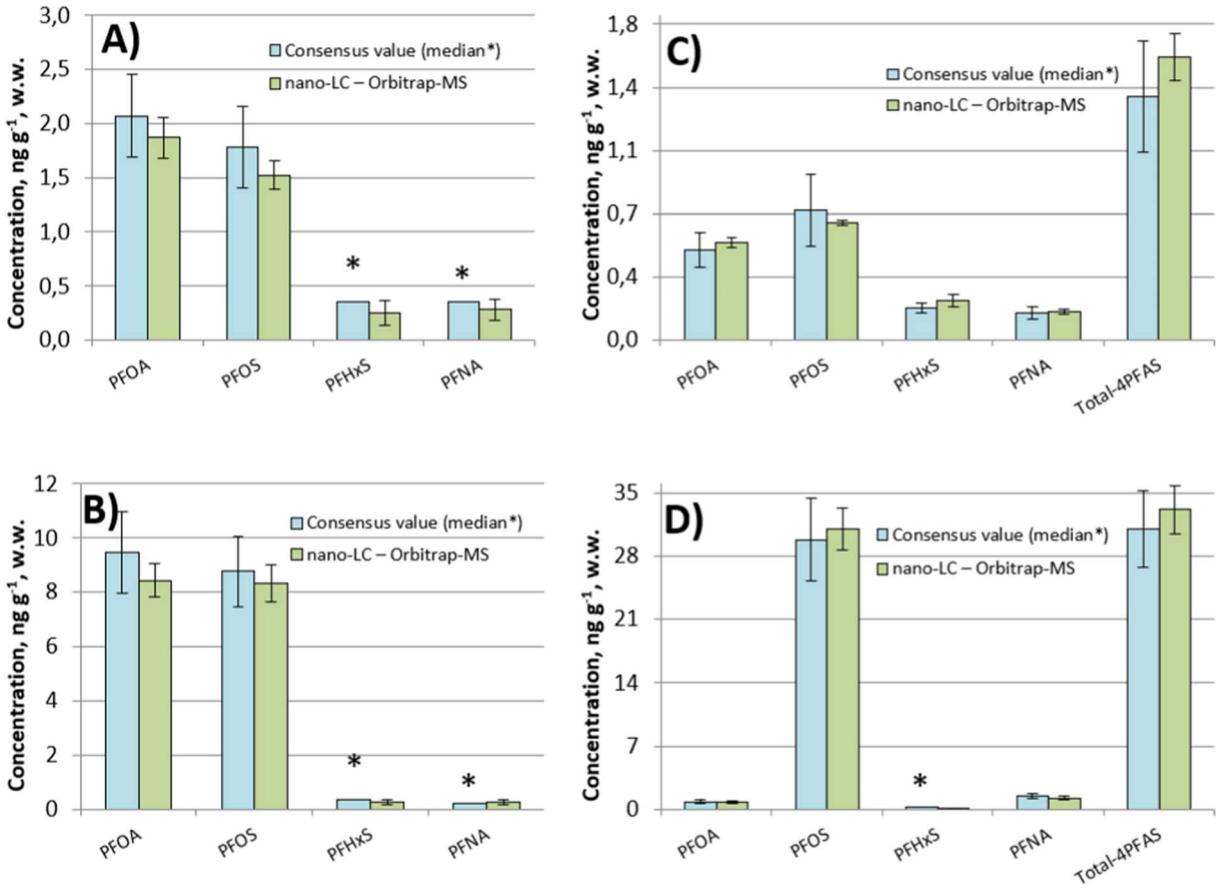

Figure 3.11. **Method performance evaluation in the analysis of EURL-PT reference materials: A) Wheat Flour 2019 (1903-WFA-063); B) Wheat Flour 2019 (1903-WFB-038); C) Liquid Whole Egg 2021 (2102-LWE-006/010); D) Pork Liver 2022 (2201-PL-168)**

The accuracy calculated as a percentage of the measured concentration versus the consensus value (when consensus values were not available, the median value was taken) was in the range of 85–124%, with RSDs from 3 to 17%. The observed analytical performance characteristics demonstrate that the developed method could be used for both monitoring

purposes and compliance testing of maximum levels for selected food groups considering the requirements of Regulation (EU) 2022/1428[200], provisions of Recommendation (EU) 2022/1431[201], and the Guidance Document on Analytical Parameters for the Determination of Per- and Polyfluoroalkyl Substances (PFAS) in Food and Feed [198].

Matrix effects are major factors affecting the sensitivity of the LC-MS determination since the effects of signal suppression or enhancement are caused by the matrix components. To evaluate the matrix effects observed by applying the different matrix concentration factors for each type of food, different weights of sample aliquots of each matrix type (n = 3) were treated according to the sample preparation protocol, the final extracts were reconstituted in the initial gradient conditions, and isotopically labelled internal standard solution (500 pg μL^{-1} for each PFAS) was added followed by the instrumental analysis, and concentrations were calculated by the means of external calibration. The isotopically labelled standards were used for the experiment due to the unavailability of PFAS-free representative matrices and taking into consideration the similarities in chemical properties and structure, resulting in analogous interactions compared to the native standards in the presence of matrix components. The matrix concentration factor was evaluated in the range from 1 to 10 (e.g., the sample aliquots from 0.20 to 2.0 g were taken for analysis with the final extract volume of 200 µL) for all analyzed food groups, except for fruits and vegetables. Since the water content in most of fruit and vegetable matrices is high (up to 95%), and the proposed LOQ values by the regulatory bodies were low, the effect of the matrix concentration factor was evaluated in the range from 5 to 50 (e.g., sample aliquots from 1.0 to 10 g for the final volume of 200 µL). Figure 3.12 demonstrates the matrix effects with various matrix concentration factors.

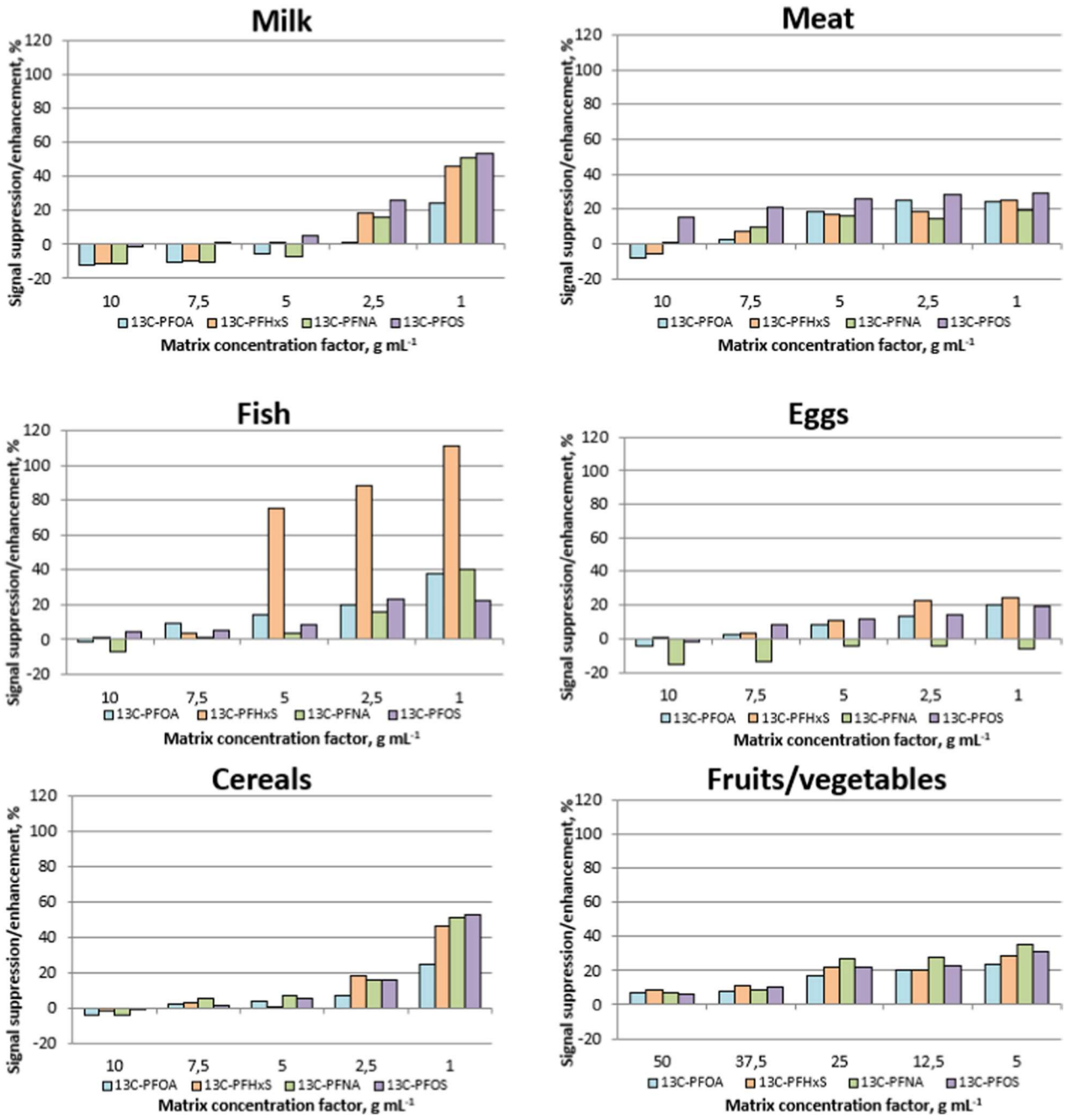

Figure 3.12. **The evaluation of matrix effect for analyzed matrices by applying different matrix concentration factors**

As demonstrated in Figure 3.12, both signal suppression and enhancement could be observed for different matrix groups depending on the matrix concentration factor. Signal suppression was more pronounced with increasing the applied concentration factor, reaching suppression for some PFAS up to 15% in some matrices (e.g., eggs and milk) and more, while the signal enhancement was observed for almost all compounds in the matrix concentration

factor range from 1 to 5 with exception of fruit and vegetable group for which signal enhancement was observed in the concentration factor range up to 50. The differences in the observed effects of the matrix concentration factors could be explained by the complexity of the analyzed sample extract composition since some of the matrix components tend to suppress the ionization of analytes, while others enhance the ionization. The result of this competition is not proportionally dependent on the matrix component concentration in the extract. Therefore, the applied matrix concentration factor should be carefully optimized during the method development since higher pre-concentration factors could facilitate the undesirable signal suppression and possible overloading or damaging of the nano-LC column, while excessive dilution of the sample aliquot could not provide the required LOQs even considering signal enhancement effect.

The observed performance characteristics of the method demonstrated that, generally, it could be used for both monitoring purposes and compliance testing of maximum levels for selected food groups according to the requirements.

3.4.4. The occurrence of PFAS in food

The developed nano-LC Orbitrap-MS method was applied to the analysis of real food samples representing Latvian retail market. The occurrence of perfluorinated compounds in a variety of samples was investigated, including fruits and vegetables (n = 30), grains, bread, and vegetable oils (n = 22), milk and dairy products (n = 21), eggs (n = 8), meat (n = 19), fish and seafood (n = 19). In total, 119 food samples representing the most consumed food groups were analyzed. The summary of the observed concentrations of four priority PFAS is presented in Table 3.4. While a detailed interpretation of the observed data is outside the scope of the present work, some generalization of the results would be appropriate.

The observed occurrence of four priority PFAS in different food groups (concentrations expressed on a w.w. basis and given in ng g^{-1})

Compound	Min[a] - max	Median[a]	Mean[a]	Detection frequency[b], %	Detected concentration range below the m-LOQ[c]
Fruits, vegetables and fungi (*n* = 30)					
PFOA	<0.002–0.005	<0.002	<0.002	20	0.0004–0.0007
PFHxS	<0.001–0.002	<0.001	<0.001	7	ND
PFNA	<0.001	<0.001	<0.001	0	ND
PFOS	<0.001	<0.001	<0.001	0	ND
Total 4 PFAS (lowerbound)	<0.001–0.005	<0.001	<0.001	–	–
Grains, bread and vegetable oils (*n* = 22)					
PFOA	<0.015	<0.015	<0.015	50	0.001–0.005
PFHxS	<0.01	<0.01	<0.01	0	ND
PFNA	<0.01–0.05	<0.01	<0.01	46	0.003–0.004
PFOS	<0.01–0.01	<0.01	<0.01	5	ND
Total 4 PFAS (lowerbound)	<0.01–0.05	<0.01	<0.01	–	–
Milk and dairy products (*n* = 21)					
PFOA	<0.01–0.01	<0.01	<0.01	43	0.001–0.002
PFHxS	<0.01–0.03	<0.01	0.01	33	ND
PFNA	<0.01–0.01	<0.01	<0.01	10	0.003
PFOS	<0.01–0.05	<0.01	<0.01	24	0.001–0.003
Total 4 PFAS (lowerbound)	<0.01–0.10	<0.01	0.01	–	–
Eggs (*n* = 8)					
PFOA	<0.30	<0.30	<0.30	25	0.003
PFHxS	<0.30	<0.30	<0.30	100	0.004–0.06
PFNA	<0.30	<0.30	<0.30	0	ND
PFOS	<0.30	<0.30	<0.30	38	0.005–0.03
Total 4 PFAS (lowerbound)	<0.30	<0.30	<0.30	–	–
Meat (*n* = 19)					
PFOA	<0.10	<0.10	<0.10	16	0.001–0.004
PFHxS	<0.10–0.20	<0.10	0.10	63	0.004–0.01
PFNA	<0.10	<0.10	<0.10	0	ND
PFOS	<0.10–0.16	<0.10	<0.10	47	0.01–0.03
Total 4 PFAS (lowerbound)	<0.10–0.20	0.10	0.10	–	–

Fish and seafood (n = 19)					
PFOA	<0.10–6.6	0.27	0.86	68	ND
PFHxS	0.10–0.25	0.10	<0.10	100	0.02–0.05
PFNA	<0.10–0.54	<0.10	<0.10	21	0.03
PFOS	0.20–5.7	1.2	2.2	100	ND
Total 4 PFAS (lowerbound)	0.17–12.4	2.0	3.2	–	–

[a] – only concentrations above or equal to *m*-LOQ are considered.
[b] – including results below the *m*-LOQ.
[c] – indicative values.

All analyzed foods showed the presence of PFAS, although the detection frequency and relative distribution varied depending on the specific PFAS representative and the type of food. While the main focus of the developed method was intended for compliance testing of four priority PFAS in food at the maximum permissible levels according to the recently adopted legislation and guidelines, reporting the occurrence of these chemicals below the established *m*-LOQs could also be of interest for monitoring purposes and the creation of datasets relevant to possible toxicological reevaluation of PFAS in the future. Therefore, an overview of this information is also presented. Food products of plant origin were less contaminated with the selected PFAS, generally showing concentrations below the *m*-LOQ, while products of animal origin showed a more pronounced presence of these contaminants. As expected, fish and seafood showed the highest concentrations of PFAS, revealing the presence of the most studied PFAS representatives PFOA and PFOS in all samples from this food group. Generally, the prevalence of sulfonic acids over carboxylic acids was observed for samples of animal origin, which was in agreement with the different bioaccumulative properties of these PFAS classes [202]. By summarizing the observed occurrence of four priority PFAS in the analyzed food groups, it can be concluded that the contamination levels and patterns were generally similar to those found in recent studies from different European countries [121].

CONCLUSIONS

The literature review performed in the initial stages of this work provided an overview of the wide range of recent applications of nano-LC methods for determining chemical contaminants, such as antibiotics, veterinary drugs, pesticides, and mycotoxins in food and environment. Sample preparation procedures and analytical performance were proposed and compared with other types of liquid chromatography. The literature review has demonstrated that, despite some application-specific drawbacks, nano-LC methods offer considerable improvements in analytical performance, such as sensitivity and low matrix effects, as well as low solvent consumption and reduced sample preparation steps.

Different instrumental nano-LC setups were evaluated, and an EASY-Spray column with an integrated emitter and thermostat provided better symmetry of the peaks compared to the Acclaim PepMap column with a microflow transfer line and emitter. Additionally, the setup with post-column solvent addition has shown significant improvement of nanoelectrospray stability during the aqueous part of a gradient and was applied to determine pyrrolizidine alkaloids.

The following developed nano-LC Orbitrap MS methods have demonstrated low matrix effects and great sensitivity, ensuring reliable and effective determination of different analytes in various matrices providing improvements over other liquid chromatography techniques:

1. The developed nano-LC method for the analysis of 27 multi-class mycotoxins in grain cereals and legumes demonstrated sufficient trueness and precision for the analysis of most analytes. The consumption of mobile phase was significantly reduced compared to that for conventional methods. The method was successfully applied to the analysis of a total of 133 samples of nine crop varieties harvested in Latvia, and 99% of the analyzed cereals (n = 109) and 78% of the pulses (n = 18) contained 1 to 16 of the 27 analyzed mycotoxins, including four *Alternaria* toxins and the regulated mycotoxins (DON, ZEN, sum of T2 and

HT-2 toxins and F1) were found prevalent in the analyzed grain samples at concentrations far below their maximum tolerable levels, and high distributions of enniatins and *Alternaria* toxins were observed.

2. A nano-LC-MS method was developed for the determination of pyrrolizidine alkaloids in tea, honey, herbal tinctures, and milk samples. Various sample preparation procedures were evaluated. A QuEChERS procedure with sample dilution achieved negligible matrix effects compared to the same procedure using a pre-concentration step or an SPE procedure. The nano-LC MS method demonstrated superior sensitivity compared to a conventional flow LC-MS. Various food products available on the Latvian market were analyzed employing the developed method, including samples of tea (n = 15), honey (n = 40), herbal tinctures (n = 15), and milk (n = 10). The occurrence of pyrrolizidine alkaloids was at low levels, far below the maximum limit set by Commission Regulation (EU) 2020/2040, except for one herbal tea sample. The screening analysis included MS^2 screening for fragment ions commonly produced by pyrrolizidine alkaloids during collision-induced dissociation. It is proposed that the $C_6H_8N^+$ fragment ion could be used as a highly selective target fragment ion for the detection and discovery of pyrrolizidine alkaloids using high-resolution mass spectrometry.
3. A novel nano-LC Orbitrap MS method has been developed for the determination of several pharmaceuticals and biomarkers in wastewater samples. WW samples from several cities and towns of Latvia, including Jelgava, Liepaja, Valmiera, Ventspils, Jekabpils, Jurmala, Riga, Rezekne, Daugavpils, Salaspils, and Tukums (in total n = 116). All of the samples contained the analyzed biomarkers and pharmaceuticals. It has been demonstrated that the dilute-and-shoot approach can be successfully applied for wastewater matrices, avoiding tedious sample clean-up procedures like LLE or SPE and providing greater accuracy and simplicity of the method. The direct in-sample addition of TBAB as an ion-pair reagent allowed the separation of ionic and less polar analytes within one run using a single C18

nano-LC column. The presence of TBAB in the samples significantly improved the retention and signal intensity of ethyl sulphate and 5-HIAA. Overall, the proposed procedure provided low LOQ values (0.005 – 0.3 μg L^{-1}) as well as negligible matrix effects for most of the analytes of interest. A basis for further monitoring program has been prepared to evaluate the consumption patterns of pharmaceuticals and lifestyle of a population among different cities in Latvia during an extended period, as well as for extending the method to a broader scope of analytes and sample matrices.

4. The developed nano-LC Orbitrap-MS method for the quantitative analysis of four priority PFAS (PFOA, PFNA, PFHxS, and PFOS) in food products generally met the performance criteria stated in Commission Regulation (EU) 2022/1428, Commission Recommendation (EU) 2022/1431, as well as the Guidance document on analytical parameters for the determination of per- and polyfluoroalkyl substances (PFAS) in food and feed. Therefore, this method can be applied for monitoring and compliance testing of PFAS in food. The method was applied to the analysis of real samples, including fruits and vegetables (n = 30), grains, bread, and vegetable oils (n = 22), milk and dairy products (n = 21), eggs (n = 8), meat (n = 19), fish and seafood (n = 19). The presence of PFAS in food products was generally at low levels except for fish samples, which contained PFAS at higher levels.

ACKNOWLEDGMENTS

I want to express my deepest gratitude to my scientific supervisor, professor, *Dr. Chem.* Vadims Bartkevics, for his inspiration, continuous support, patience, and invaluable guidance.

I want to express my sincere gratitude to *Dr. chem.* Iveta Pugajeva, for inspiration, understanding, and support throughout the process of creating this work.

I want to thank my colleagues from the Institute of Food Safety, Animal Health and Environment "BIOR" and co-authors of scientific publications for their dedication, valuable discussions, and assistance. Special thanks to *Dr. Chem.* Mārtiņš Jansons for cooperation, for his time and efforts.

I want to express my sincere gratitude to professor, *Dr. Sc. Math.* Sharif E. Guseynov and *Dr. Biol.* Jekaterina V. Aleksejeva and their family for valuable discussions, inspiration, interest, and support during the development of this thesis.

Finally, I would like to thank my family and friends for their support, encouragement, and patience over the past few years throughout my studies.

A part of the research was funded by the Ministry of Economics, project "State research project in the field of biomedicine, medical technologies, and pharmacy", project No. VPP-EM-BIOMEDICĪNA-2022/1-0001.

REFERENCE

(1) Sui, Q.; Cao, X.; Lu, S.; Zhao, W.; Qiu, Z.; Yu, G. Occurrence, Sources and Fate of Pharmaceuticals and Personal Care Products in the Groundwater: A Review. *Emerging Contaminants* **2015**, *1* (1), 14–24. https://doi.org/10.1016/j.emcon.2015.07.001.

(2) Gunther, F. A.; Whitacre, D. M.; Albert, L. A.; Hutzinger, O.; Knaak, J. B.; Mayer, F. L.; Morgan, D. P.; Park, D. L.; Tjeerdema, R. S.; de Voogt, P.; Yang, R. S. H.; Gerba, C. P.; Giesy, J.; Stevens, J. T.; Ware, G.; Monteiro, S. C.; Boxall, A. B. A. Occurrence and Fate of Human Pharmaceuticals in the Environment. In *Reviews of Environmental Contamination and Toxicology*; Springer New York: New York, NY, 2010; Vol. 202, pp 53–154. https://doi.org/10.1007/978-1-4419-1157-5_2.

(3) Gross, B.; Montgomery-Brown, J.; Naumann, A.; Reinhard, M. Occurrence and Fate of Pharmaceuticals and Alkylphenol Ethoxylate Metabolites in an Effluent-Dominated River and Wetland. *Environmental Toxicology and Chemistry* **2004**, *23* (9), 2074–2083. https://doi.org/10.1897/03-606.

(4) Occurrence and Toxicity of Antibiotics in the Aquatic Environment: A Review. *Chemosphere* **2020**, *251*, 126351. https://doi.org/10.1016/j.chemosphere.2020.126351.

(5) Kotthoff, M.; Müller, J.; Jürling, H.; Schlummer, M.; Fiedler, D. Perfluoroalkyl and Polyfluoroalkyl Substances in Consumer Products. *Environ Sci Pollut Res Int* **2015**, *22* (19), 14546–14559. https://doi.org/10.1007/s11356-015-4202-7.

(6) Banzhaf, S.; Filipovic, M.; Lewis, J.; Sparrenbom, C. J.; Barthel, R. A Review of Contamination of Surface-, Ground-, and Drinking Water in Sweden by Perfluoroalkyl and Polyfluoroalkyl Substances (PFASs). *Ambio* **2017**, *46* (3), 335–346. https://doi.org/10.1007/s13280-016-0848-8.

(7) Haukås, M.; Berger, U.; Hop, H.; Gulliksen, B.; Gabrielsen, G. W. Bioaccumulation of Per- and Polyfluorinated Alkyl Substances (PFAS) in Selected Species from the Barents Sea

Food Web. *Environmental Pollution* **2007**, *148* (1), 360–371. https://doi.org/10.1016/j.envpol.2006.09.021.

(8) Abrunhosa, L.; Morales, H.; Soares, C.; Calado, T.; Vila-Chã, A. S.; Pereira, M.; Venâncio, A. A Review of Mycotoxins in Food and Feed Products in Portugal and Estimation of Probable Daily Intakes. *Crit Rev Food Sci Nutr* **2016**, *56* (2), 249–265. https://doi.org/10.1080/10408398.2012.720619.

(9) Brugnerotto, P.; Seraglio, S. K. T.; Schulz, M.; Gonzaga, L. V.; Fett, R.; Costa, A. C. O. Pyrrolizidine Alkaloids and Beehive Products: A Review. *Food Chemistry* **2021**, *342*, 128384. https://doi.org/10.1016/j.foodchem.2020.128384.

(10) Tsagkaris, A. S.; Prusova, N.; Dzuman, Z.; Pulkrabova, J.; Hajslova, J. Regulated and Non-Regulated Mycotoxin Detection in Cereal Matrices Using an Ultra-High-Performance Liquid Chromatography High-Resolution Mass Spectrometry (UHPLC-HRMS) Method. *Toxins (Basel)* **2021**, *13* (11), 783. https://doi.org/10.3390/toxins13110783.

(11) *Commission Regulation (EC) No 1881/2006 of 19 December 2006 Setting Maximum Levels for Certain Contaminants in Foodstuffs (Text with EEA Relevance)Text with EEA Relevance*; 2022. http://data.europa.eu/eli/reg/2006/1881/2022-07-01/eng (accessed 2022-09-24).

(12) *EUR-Lex - 32013L0039 - EN - EUR-Lex*. https://eur-lex.europa.eu/eli/dir/2013/39/oj/?locale=en (accessed 2022-09-25).

(13) Deloitte; Directorate-General for Environment (European Commission); INERIS; Milieu Ltd; Kümmerer, K. *Options for a Strategic Approach to Pharmaceuticals in the Environment: Final Report*; Publications Office of the European Union: LU, 2019.

(14) Gracia-Lor, E.; Castiglioni, S.; Bade, R.; Been, F.; Castrignanò, E.; Covaci, A.; González-Mariño, I.; Hapeshi, E.; Kasprzyk-Hordern, B.; Kinyua, J.; Lai, F. Y.; Letzel, T.; Lopardo, L.; Meyer, M. R.; O'Brien, J.; Ramin, P.; Rousis, N. I.; Rydevik, A.; Ryu, Y.; Santos, M. M.; Senta, I.; Thomaidis, N. S.; Veloutsou, S.; Yang, Z.; Zuccato, E.; Bijlsma,

L. Measuring Biomarkers in Wastewater as a New Source of Epidemiological Information: Current State and Future Perspectives. *Environment International* **2017**, *99*, 131–150. https://doi.org/10.1016/j.envint.2016.12.016.

(15) Fedorenko, D.; Bartkevics, V. Recent Applications of Nano-Liquid Chromatography in Food Safety and Environmental Monitoring: A Review. *Critical Reviews in Analytical Chemistry* **2021**, *0* (0), 1–25. https://doi.org/10.1080/10408347.2021.1938968.

(16) Fanali, S. An Overview to Nano-Scale Analytical Techniques: Nano-Liquid Chromatography and Capillary Electrochromatography. *Electrophoresis* **2017**, *38* (15), 1822–1829. https://doi.org/10.1002/elps.201600573.

(17) Novotny, M. Microcolumns in Liquid Chromatography. *Anal. Chem.* **1981**, *53* (12), 1294A-1308A. https://doi.org/10.1021/ac00235a001.

(18) Karlsson, K. E.; Novotny, M. Separation Efficiency of Slurry-Packed Liquid Chromatography Microcolumns with Very Small Inner Diameters. *Anal. Chem.* **1988**, *60* (17), 1662–1665. https://doi.org/10.1021/ac00168a006.

(19) Knox, J. H. Theoretical Aspects of LC with Packed and Open Small-Bore Columns. *J Chromatogr Sci* **1980**, *18* (9), 453–461. https://doi.org/10.1093/chromsci/18.9.453.

(20) Kinetic Optimization of Straight Open-Tubular Liquid Chromatography. *Journal of Chromatography A* **1979**, *186*, 405–418. https://doi.org/10.1016/S0021-9673(00)95263-4.

(21) Yandamuri, N. Comparative Study of New Trends in HPLC: A Review. *International Journal of Pharmaceutical Sciences Review and Research* **2013**, *23*.

(22) Chervet, J. P.; Ursem, M.; Salzmann, J. P. Instrumental Requirements for Nanoscale Liquid Chromatography. *Anal. Chem.* **1996**, *68* (9), 1507–1512. https://doi.org/10.1021/ac9508964.

(23) Alcántara-Durán, J.; Moreno-González, D.; Gilbert-López, B.; Molina-Díaz, A.; García-Reyes, J. F. Matrix-Effect Free Multi-Residue Analysis of Veterinary Drugs in Food Samples of Animal Origin by Nanoflow Liquid Chromatography High Resolution Mass

Spectrometry. *Food Chemistry* **2018**, *245*, 29–38. https://doi.org/10.1016/j.foodchem.2017.10.083.

(24) Moreno-González, D.; Pérez-Ortega, P.; Gilbert-López, B.; Molina-Díaz, A.; García-Reyes, J. F.; Fernández-Alba, A. R. Evaluation of Nanoflow Liquid Chromatography High Resolution Mass Spectrometry for Pesticide Residue Analysis in Food. *Journal of Chromatography A* **2017**, *1512*, 78–87. https://doi.org/10.1016/j.chroma.2017.07.019.

(25) Moreno-González, D.; Alcántara-Durán, J.; Addona, S. M.; Beneito-Cambra, M. Multi-Residue Pesticide Analysis in Virgin Olive Oil by Nanoflow Liquid Chromatography High Resolution Mass Spectrometry. *Journal of Chromatography A* **2018**, *1562*, 27–35. https://doi.org/10.1016/j.chroma.2018.05.053.

(26) Moreno-González, D.; Cutillas, V.; Hernando, M. D.; Alcántara-Durán, J.; García-Reyes, J. F.; Molina-Díaz, A. Quantitative Determination of Pesticide Residues in Specific Parts of Bee Specimens by Nanoflow Liquid Chromatography High Resolution Mass Spectrometry. *Science of The Total Environment* **2020**, *715*, 137005. https://doi.org/10.1016/j.scitotenv.2020.137005.

(27) Berlioz-Barbier, A.; Buleté, A.; Faburé, J.; Garric, J.; Cren-Olivé, C.; Vulliet, E. Multi-Residue Analysis of Emerging Pollutants in Benthic Invertebrates by Modified Micro-Quick-Easy-Cheap-Efficient-Rugged-Safe Extraction and Nanoliquid Chromatography-Nanospray-Tandem Mass Spectrometry Analysis. *J Chromatogr A* **2014**, *1367*, 16–32. https://doi.org/10.1016/j.chroma.2014.09.044.

(28) Wilson, S. R.; Vehus, T.; Berg, H. S.; Lundanes, E. Nano-LC in Proteomics: Recent Advances and Approaches. *Bioanalysis* **2015**, *7* (14), 1799–1815. https://doi.org/10.4155/bio.15.92.

(29) Gama, M. R.; Collins, C. H.; Bottoli, C. B. G. Nano-Liquid Chromatography in Pharmaceutical and Biomedical Research. *J Chromatogr Sci* **2013**, *51* (7), 694–703. https://doi.org/10.1093/chromsci/bmt023.

(30) Šesták, J.; Moravcová, D.; Kahle, V. Instrument Platforms for Nano Liquid Chromatography. *Journal of Chromatography A* **2015**, *1421*, 2–17. https://doi.org/10.1016/j.chroma.2015.07.090.

(31) Szumski, M.; Buszewski, B. State of the Art in Miniaturized Separation Techniques. *Critical Reviews in Analytical Chemistry* **2002**, *32* (1), 1–46. https://doi.org/10.1080/10408340290765434.

(32) Vissers, J. P. C.; Claessens, H. A.; Cramers, C. A. Microcolumn Liquid Chromatography: Instrumentation, Detection and Applications. *Journal of Chromatography A* **1997**, *779* (1), 1–28. https://doi.org/10.1016/S0021-9673(97)00422-6.

(33) Schmidt, A.; Karas, M.; Dülcks, T. Effect of Different Solution Flow Rates on Analyte Ion Signals in Nano-ESI MS, or: When Does ESI Turn into Nano-ESI? *Journal of the American Society for Mass Spectrometry* **2003**, *14* (5), 492–500. https://doi.org/10.1016/S1044-0305(03)00128-4.

(34) Rigano, F.; Tranchida, P. Q.; Dugo, P.; Mondello, L. High-Performance Liquid Chromatography Combined with Electron Ionization Mass Spectrometry: A Review. *TrAC Trends in Analytical Chemistry* **2019**, *118*, 112–122. https://doi.org/10.1016/j.trac.2019.05.032.

(35) El-Faramawy, A.; Siu, K. W. M.; Thomson, B. A. Efficiency of Nano-Electrospray Ionization. *Journal of the American Society for Mass Spectrometry* **2005**, *16* (10), 1702–1707. https://doi.org/10.1016/j.jasms.2005.06.011.

(36) *From Analytical to Nano-Flow LC-MS: High Robustness and Sensitivity to Answer Complex Biological Questions*; 2017. http://tools.thermofisher.com/content/sfs/brochures/PP-72444-Analytical-Nano-Flow-LC-MS-MSB2017-PP72444-EN.pdf.

(37) Fast-Liquid Chromatography Using Columns of Different Internal Diameters Packed with Sub-2 Mm Silica Particles. *Journal of Chromatography A* **2012**, *1228*, 213–220. https://doi.org/10.1016/j.chroma.2011.05.053.

(38) Yandamuri, N. Advanced Study of Nano Liquid Chromatography and Its Application-A Review. *World Journal of Pharmaceutical Research*.

(39) Fanali, C.; Dugo, L.; Dugo, P.; Mondello, L. Capillary-Liquid Chromatography (CLC) and Nano-LC in Food Analysis. *TrAC Trends in Analytical Chemistry* **2013**, *52*, 226–238. https://doi.org/10.1016/j.trac.2013.05.021.

(40) D'Orazio, G.; Fanali, S. Combination of Two Different Stationary Phases for On-Line Pre-Concentration and Separation of Basic Drugs by Using Nano-Liquid Chromatography. *Journal of Chromatography A* **2013**, *1285*, 118–123. https://doi.org/10.1016/j.chroma.2013.02.035.

(41) *Handbook of Advanced Chromatography /Mass Spectrometry Techniques*; Elsevier, 2017. https://doi.org/10.1016/C2016-0-01418-3.

(42) Reinholds, I.; Jansons, M.; Fedorenko, D.; Pugajeva, I.; Zute, S.; Bartkiene, E.; Bartkevics, V. Mycotoxins in Cereals and Pulses Harvested in Latvia by NanoLC-Orbitrap MS. *Food Additives & Contaminants: Part B* **2021**, *14* (2), 115–123. https://doi.org/10.1080/19393210.2021.1892204.

(43) Jansons, M.; Fedorenko, D.; Pavlenko, R.; Berzina, Z.; Bartkevics, V. Nanoflow Liquid Chromatography Mass Spectrometry Method for Quantitative Analysis and Target Ion Screening of Pyrrolizidine Alkaloids in Honey, Tea, Herbal Tinctures, and Milk. *Journal of Chromatography A* **2022**, *1676*, 463269. https://doi.org/10.1016/j.chroma.2022.463269.

(44) Marginean, I.; Kelly, R. T.; Moore, R. J.; Prior, D. C.; LaMarche, B. L.; Tang, K.; Smith, R. D. Selection of the Optimum Electrospray Voltage for Gradient Elution LC-MS Measurements. *J. Am. Soc. Mass Spectrom.* **2009**, *20* (4), 682–688. https://doi.org/10.1016/j.jasms.2008.12.004.

(45) *The Thermo Scientific Capillary-Flow LC-MS Solutions*; 2022. https://assets.thermofisher.com/TFS-Assets/CMD/Reference-Materials/pp-72314-capillary-flow-lc-ms-solutions-pp72314-en.pdf.

(46) Liu, H.-Y.; Lin, S.-L.; Chan, S.-A.; Lin, T.-Y.; Fuh, M.-R. Microfluidic Chip-Based Nano-Liquid Chromatography Tandem Mass Spectrometry for Quantification of Aflatoxins in Peanut Products. *Talanta* **2013**, *113*, 76–81. https://doi.org/10.1016/j.talanta.2013.03.053.

(47) Oedit, A.; Vulto, P.; Ramautar, R.; Lindenburg, P. W.; Hankemeier, T. Lab-on-a-Chip Hyphenation with Mass Spectrometry: Strategies for Bioanalytical Applications. *Current Opinion in Biotechnology* **2015**, *31*, 79–85. https://doi.org/10.1016/j.copbio.2014.08.009.

(48) Vasconcelos Soares Maciel, E.; de Toffoli, A. L.; Sobieski, E.; Domingues Nazário, C. E.; Lanças, F. M. Miniaturized Liquid Chromatography Focusing on Analytical Columns and Mass Spectrometry: A Review. *Analytica Chimica Acta* **2020**, *1103*, 11–31. https://doi.org/10.1016/j.aca.2019.12.064.

(49) Desmet, G.; Eeltink, S. Fundamentals for LC Miniaturization. *Anal. Chem.* **2013**, *85* (2), 543–556. https://doi.org/10.1021/ac303317c.

(50) Eikel, D.; Henion, J. Liquid Extraction Surface Analysis (LESA) of Food Surfaces Employing Chip-Based Nano-Electrospray Mass Spectrometry. *Rapid Communications in Mass Spectrometry* **2011**, *25* (16), 2345–2354. https://doi.org/10.1002/rcm.5107.

(51) Sainiemi, L.; Nissilä, T.; Kostiainen, R.; Franssila, S.; Ketola, R. A. A Microfabricated Micropillar Liquid Chromatographic Chip Monolithically Integrated with an Electrospray Ionization Tip. *Lab Chip* **2011**, *12* (2), 325–332. https://doi.org/10.1039/C1LC20874H.

(52) Xie, X.; Tolley, L. T.; Truong, T. X.; Tolley, H. D.; Farnsworth, P. B.; Lee, M. L. Dual-Wavelength Light-Emitting Diode-Based Ultraviolet Absorption Detector for Nano-Flow Capillary Liquid Chromatography. *Journal of Chromatography A* **2017**, *1523*, 242–247. https://doi.org/10.1016/j.chroma.2017.07.097.

(53) Hsieh, S.-H.; Huang, H.-Y.; Lee, S. Determination of Eight Penicillin Antibiotics in Pharmaceuticals, Milk and Porcine Tissues by Nano-Liquid Chromatography. *Journal of Chromatography A* **2009**, *1216* (43), 7186–7194. https://doi.org/10.1016/j.chroma.2009.05.080.

(54) Fanali, C.; Asensio-Ramos, M.; D'Orazio, G.; Hernández-Borges, J.; Rocco, A.; Fanali, S. Chapter 9 - Nano-Liquid Chromatographic Separations. In *Handbook of Advanced Chromatography/Mass Spectrometry Techniques*; Holčapek, M., Byrdwell, Wm. C., Eds.; AOCS Press, 2017; pp 309–363. https://doi.org/10.1016/B978-0-12-811732-3.00009-1.

(55) Vehus, T.; Saeterdal, K. E.; Krauss, S.; Lundanes, E.; Wilson, S. Comparison of Commercial Nano LC Columns for Fast, Targeted Proteomics of Cancer Cells. **2015**. https://doi.org/10.6084/m9.figshare.1418241.

(56) Cappiello, A.; Famiglini, G.; Palma, P.; Pierini, E.; Termopoli, V.; Trufelli, H. Overcoming Matrix Effects in Liquid Chromatography−Mass Spectrometry. *Anal. Chem.* **2008**, *80* (23), 9343–9348. https://doi.org/10.1021/ac8018312.

(57) Matrix-Effect Free Quantitative Liquid Chromatography Mass Spectrometry Analysis in Complex Matrices Using Nanoflow Liquid Chromatography with Integrated Emitter Tip and High Dilution Factors. *Journal of Chromatography A* **2017**, *1519*, 110–120. https://doi.org/10.1016/j.chroma.2017.09.006.

(58) Aydoğan, C.; Rassi, Z. E. MWCNT Based Monolith for the Analysis of Antibiotics and Pesticides in Milk and Honey by Integrated Nano-Liquid Chromatography-High Resolution Orbitrap Mass Spectrometry. *Anal. Methods* **2018**, *11* (1), 21–28. https://doi.org/10.1039/C8AY02173B.

(59) Contreras, M. del M.; Arráez-Román, D.; Fernández-Gutiérrez, A.; Segura-Carretero, A. Nano-Liquid Chromatography Coupled to Time-of-Flight Mass Spectrometry for Phenolic Profiling: A Case Study in Cranberry Syrups. *Talanta* **2015**, *132*, 929–938. https://doi.org/10.1016/j.talanta.2014.10.049.

(60) D'Orazio, G.; Rocchi, S.; Fanali, S. Nano-Liquid Chromatography Coupled with Mass Spectrometry: Separation of Sulfonamides Employing Non-Porous Core–Shell Particles. *Journal of Chromatography A* **2012**, *1255*, 277–285. https://doi.org/10.1016/j.chroma.2012.03.032.

(61) Mirabelli, M. F.; Wolf, J.-C.; Zenobi, R. Pesticide Analysis at Ppt Concentration Levels: Coupling Nano-Liquid Chromatography with Dielectric Barrier Discharge Ionization-Mass Spectrometry. *Anal Bioanal Chem* **2016**, *408* (13), 3425–3434. https://doi.org/10.1007/s00216-016-9419-x.

(62) Berlioz-Barbier, A.; Baudot, R.; Wiest, L.; Gust, M.; Garric, J.; Cren-Olivé, C.; Buleté, A. MicroQuEChERS–Nanoliquid Chromatography–Nanospray–Tandem Mass Spectrometry for the Detection and Quantification of Trace Pharmaceuticals in Benthic Invertebrates. *Talanta* **2015**, *132*, 796–802. https://doi.org/10.1016/j.talanta.2014.10.030.

(63) *Quality of wastewater in the El Paso, Texas region — Analysis of pharmaceuticals and personal care products using high performance liquid chromatography tandem mass spectrometry - ProQuest*. https://search.proquest.com/docview/916754906/?pq-origsite=primo (accessed 2019-11-04).

(64) Wilson, S. R.; Malerod, H.; Holm, A.; Molander, P.; Lundanes, E.; Greibrokk, T. On-Line SPE--Nano-LC--Nanospray-MS for Rapid and Sensitive Determination of Perfluorooctanoic Acid and Perfluorooctane Sulfonate in River Water. *Journal of Chromatographic Science* **2007**, *45* (3), 146–152. https://doi.org/10.1093/chromsci/45.3.146.

(65) Alcántara-Durán, J.; Moreno-González, D.; García-Reyes, J. F.; Molina-Díaz, A. Use of a Modified QuEChERS Method for the Determination of Mycotoxin Residues in Edible Nuts by Nano Flow Liquid Chromatography High Resolution Mass Spectrometry. *Food Chemistry* **2019**, *279*, 144–149. https://doi.org/10.1016/j.foodchem.2018.11.149.

(66) Asensio-Ramos, M.; D'Orazio, G.; Hernandez-Borges, J.; Rocco, A.; Fanali, S. Multi-Walled Carbon Nanotubes–Dispersive Solid-Phase Extraction Combined with Nano-Liquid Chromatography for the Analysis of Pesticides in Water Samples. *Anal Bioanal Chem* **2011**, *400* (4), 1113–1123. https://doi.org/10.1007/s00216-011-4885-7.

(67) Moreno-González, D.; Alcántara-Durán, J.; Gilbert-López, B.; Beneito-Cambra, M.; Cutillas, V. M.; Rajski, Ł.; Molina-Díaz, A.; García-Reyes, J. F. Sensitive Detection of Neonicotinoid Insecticides and Other Selected Pesticides in Pollen and Nectar Using Nanoflow Liquid Chromatography Orbitrap Tandem Mass Spectrometry. *J AOAC Int* **2018**, *101* (2), 367–373. https://doi.org/10.5740/jaoacint.17-0412.

(68) Separation of Organophosphorus Pesticides by Using Nano-Liquid Chromatography. *Journal of Chromatography A* **2009**, *1216* (18), 3970–3976. https://doi.org/10.1016/j.chroma.2009.03.005.

(69) Noga, M.; Sucharski, F.; Suder, P.; Silberring, J. A Practical Guide to Nano-LC Troubleshooting. *Journal of Separation Science* **2007**, *30* (14), 2179–2189. https://doi.org/10.1002/jssc.200700225.

(70) Lehotay, S. J.; Chen, Y. Hits and Misses in Research Trends to Monitor Contaminants in Foods. *Anal Bioanal Chem* **2018**, *410* (22), 5331–5351. https://doi.org/10.1007/s00216-018-1195-3.

(71) Xia, R.; Schaafsma, A. w.; Wu, F.; Hooker, D. c. Impact of the Improvements in Fusarium Head Blight and Agronomic Management on Economics of Winter Wheat. *World Mycotoxin Journal* **2020**, *13* (3), 423–439. https://doi.org/10.3920/WMJ2019.2518.

(72) Awuchi, C. G.; Ondari, E. N.; Nwozo, S.; Odongo, G. A.; Eseoghene, I. J.; Twinomuhwezi, H.; Ogbonna, C. U.; Upadhyay, A. K.; Adeleye, A. O.; Okpala, C. O. R. Mycotoxins' Toxicological Mechanisms Involving Humans, Livestock and Their Associated Health Concerns: A Review. *Toxins (Basel)* **2022**, *14* (3), 167. https://doi.org/10.3390/toxins14030167.

(73) Claeys, L.; Romano, C.; De Ruyck, K.; Wilson, H.; Fervers, B.; Korenjak, M.; Zavadil, J.; Gunter, M. J.; De Saeger, S.; De Boevre, M.; Huybrechts, I. Mycotoxin Exposure and Human Cancer Risk: A Systematic Review of Epidemiological Studies. *Comprehensive Reviews in Food Science and Food Safety* **2020**, *19* (4), 1449–1464. https://doi.org/10.1111/1541-4337.12567.

(74) *2013/165/EU: Commission Recommendation of 27 March 2013 on the Presence of T-2 and HT-2 Toxin in Cereals and Cereal Products Text with EEA Relevance*; 2013; Vol. 091. http://data.europa.eu/eli/reco/2013/165/oj/eng (accessed 2022-09-26).

(75) Pleadin, J.; Vasilj, V.; Kudumija, N.; Petrović, D.; Vilušić, M.; Škrivanko, M. Survey of T-2/HT-2 Toxins in Unprocessed Cereals, Food and Feed Coming from Croatia and Bosnia & Herzegovina. *Food Chemistry* **2017**, *224*, 153–159. https://doi.org/10.1016/j.foodchem.2016.12.063.

(76) Chen, P.; Xiang, B.; Shi, H.; Yu, P.; Song, Y.; Li, S. Recent Advances on Type A Trichothecenes in Food and Feed: Analysis, Prevalence, Toxicity, and Decontamination Techniques. *Food Control* **2020**, *118*, 107371. https://doi.org/10.1016/j.foodcont.2020.107371.

(77) Haque, M. A.; Wang, Y.; Shen, Z.; Li, X.; Saleemi, M. K.; He, C. Mycotoxin Contamination and Control Strategy in Human, Domestic Animal and Poultry: A Review. *Microbial Pathogenesis* **2020**, *142*, 104095. https://doi.org/10.1016/j.micpath.2020.104095.

(78) Żelechowski, M.; Olszewski, J.; Kulik, T. A Preliminary Survey of Cultured Fusaria from Symptomatic Legume Grains in North-Eastern Poland. *Toxins (Basel)* **2019**, *11* (10), 569. https://doi.org/10.3390/toxins11100569.

(79) Holanda, D. M.; Kim, S. W. Efficacy of Mycotoxin Detoxifiers on Health and Growth of Newly-Weaned Pigs under Chronic Dietary Challenge of Deoxynivalenol. *Toxins (Basel)* **2020**, *12* (5), 311. https://doi.org/10.3390/toxins12050311.

(80) *Dietary exposure assessment to Alternaria toxins in the European population | EFSA*. https://www.efsa.europa.eu/en/efsajournal/pub/4654 (accessed 2022-09-26).

(81) Orlando, B.; Grignon, G.; Vitry, C.; Kashefifard, K.; Valade, R. Fusarium Species and Enniatin Mycotoxins in Wheat, Durum Wheat, Triticale and Barley Harvested in France. *Mycotoxin Res* **2019**, *35* (4), 369–380. https://doi.org/10.1007/s12550-019-00363-x.

(82) Gotthardt, M.; Asam, S.; Gunkel, K.; Moghaddam, A. F.; Baumann, E.; Kietz, R.; Rychlik, M. Quantitation of Six Alternaria Toxins in Infant Foods Applying Stable Isotope Labeled Standards. *Front Microbiol* **2019**, *10*, 109. https://doi.org/10.3389/fmicb.2019.00109.

(83) Malachová, A.; Stránská, M.; Václavíková, M.; Elliott, C. T.; Black, C.; Meneely, J.; Hajšlová, J.; Ezekiel, C. N.; Schuhmacher, R.; Krska, R. Advanced LC–MS-Based Methods to Study the Co-Occurrence and Metabolization of Multiple Mycotoxins in Cereals and Cereal-Based Food. *Anal Bioanal Chem* **2018**, *410* (3), 801–825. https://doi.org/10.1007/s00216-017-0750-7.

(84) Bryła, M.; Waśkiewicz, A.; Podolska, G.; Szymczyk, K.; Jędrzejczak, R.; Damaziak, K.; Sułek, A. Occurrence of 26 Mycotoxins in the Grain of Cereals Cultivated in Poland. *Toxins* **2016**, *8* (6), 160. https://doi.org/10.3390/toxins8060160.

(85) Mousavi Khaneghah, A.; Fakhri, Y.; Gahruie, H. H.; Niakousari, M.; Sant'Ana, A. S. Mycotoxins in Cereal-Based Products during 24 Years (1983–2017): A Global Systematic Review. *Trends in Food Science & Technology* **2019**, *91*, 95–105. https://doi.org/10.1016/j.tifs.2019.06.007.

(86) Righetti, L.; Paglia, G.; Galaverna, G.; Dall'Asta, C. Recent Advances and Future Challenges in Modified Mycotoxin Analysis: Why HRMS Has Become a Key Instrument in Food Contaminant Research. *Toxins* **2016**, *8* (12), 361. https://doi.org/10.3390/toxins8120361.

(87) Seremet, O. C.; Olaru, O. T.; Gutu, C. M.; Nitulescu, G. M.; Ilie, M.; Negres, S.; Zbarcea, C. E.; Purdel, C. N.; Spandidos, D. A.; Tsatsakis, A. M.; Coleman, M. D.; Margina, D. M. Toxicity of Plant Extracts Containing Pyrrolizidine Alkaloids Using Alternative Invertebrate Models. *Molecular Medicine Reports* **2018**, *17* (6), 7757–7763. https://doi.org/10.3892/mmr.2018.8795.

(88) Geburek, I.; Preiss-Weigert, A.; Lahrssen-Wiederholt, M.; Schrenk, D.; These, A. In Vitro Metabolism of Pyrrolizidine Alkaloids – Metabolic Degradation and GSH Conjugate Formation of Different Structure Types. *Food and Chemical Toxicology* **2020**, *135*, 110868. https://doi.org/10.1016/j.fct.2019.110868.

(89) Casado, N.; Morante-Zarcero, S.; Sierra, I. The Concerning Food Safety Issue of Pyrrolizidine Alkaloids: An Overview. *Trends in Food Science & Technology* **2022**, *120*, 123–139. https://doi.org/10.1016/j.tifs.2022.01.007.

(90) Castells, E.; Mulder, P. P. J.; Pérez-Trujillo, M. Diversity of Pyrrolizidine Alkaloids in Native and Invasive Senecio Pterophorus (Asteraceae): Implications for Toxicity. *Phytochemistry* **2014**, *108*, 137–146. https://doi.org/10.1016/j.phytochem.2014.09.006.

(91) Kaltner, F.; Rychlik, M.; Gareis, M.; Gottschalk, C. Occurrence and Risk Assessment of Pyrrolizidine Alkaloids in Spices and Culinary Herbs from Various Geographical Origins. *Toxins* **2020**, *12* (3), 155. https://doi.org/10.3390/toxins12030155.

(92) Selmar, D.; Wittke, C.; Beck-von Wolffersdorff, I.; Klier, B.; Lewerenz, L.; Kleinwächter, M.; Nowak, M. Transfer of Pyrrolizidine Alkaloids between Living Plants: A Disregarded Source of Contaminations. *Environmental Pollution* **2019**, *248*, 456–461. https://doi.org/10.1016/j.envpol.2019.02.026.

(93) Hoogenboom, L. a. P.; Mulder, P. P. J.; Zeilmaker, M. J.; van den Top, H. J.; Remmelink, G. J.; Brandon, E. F. A.; Klijnstra, M.; Meijer, G. a. L.; Schothorst, R.; Van Egmond, H. P. Carry-over of Pyrrolizidine Alkaloids from Feed to Milk in Dairy Cows.

Food Addit Contam Part A Chem Anal Control Expo Risk Assess **2011**, *28* (3), 359–372. https://doi.org/10.1080/19440049.2010.547521.

(94) Mulder, P. P. J.; de Witte, S. L.; Stoopen, G. M.; van der Meulen, J.; van Wikselaar, P. G.; Gruys, E.; Groot, M. J.; Hoogenboom, R. L. A. P. Transfer of Pyrrolizidine Alkaloids from Various Herbs to Eggs and Meat in Laying Hens. *Food Additives & Contaminants: Part A* **2016**, *33* (12), 1826–1839. https://doi.org/10.1080/19440049.2016.1241430.

(95) Huybrechts, B.; Callebaut, A. Pyrrolizidine Alkaloids in Food and Feed on the Belgian Market. *Food Addit Contam Part A Chem Anal Control Expo Risk Assess* **2015**, *32* (11), 1939–1951. https://doi.org/10.1080/19440049.2015.1086821.

(96) *Commission Regulation (EU) 2020/2040 of 11 December 2020 Amending Regulation (EC) No 1881/2006 as Regards Maximum Levels of Pyrrolizidine Alkaloids in Certain Foodstuffs (Text with EEA Relevance)*; 2020; Vol. 420. http://data.europa.eu/eli/reg/2020/2040/oj/eng (accessed 2022-09-26).

(97) Dusemund, B.; Nowak, N.; Sommerfeld, C.; Lindtner, O.; Schäfer, B.; Lampen, A. Risk Assessment of Pyrrolizidine Alkaloids in Food of Plant and Animal Origin. *Food and Chemical Toxicology* **2018**, *115*, 63–72. https://doi.org/10.1016/j.fct.2018.03.005.

(98) Chen, T.; Mei, N.; Fu, P. P. Genotoxicity of Pyrrolizidine Alkaloids. *Journal of Applied Toxicology* **2010**, *30* (3), 183–196. https://doi.org/10.1002/jat.1504.

(99) Ma, C.; Liu, Y.; Zhu, L.; Ji, H.; Song, X.; Guo, H.; Yi, T. Determination and Regulation of Hepatotoxic Pyrrolizidine Alkaloids in Food: A Critical Review of Recent Research. *Food and Chemical Toxicology* **2018**, *119*, 50–60. https://doi.org/10.1016/j.fct.2018.05.037.

(100) Crews, C.; Berthiller, F.; Krska, R. Update on Analytical Methods for Toxic Pyrrolizidine Alkaloids. *Anal Bioanal Chem* **2010**, *396* (1), 327–338. https://doi.org/10.1007/s00216-009-3092-2.

(101) *Straightforward Determination of Pyrrolizidine Alkaloids in Honey through Simplified Methanol Extraction (QuPPE) and LC-MS/MS Modes | ACS Omega*. https://pubs.acs.org/doi/full/10.1021/acsomega.9b03538 (accessed 2022-09-26).

(102) Zhang, W.; Huai, W.; Zhang, Y.; Shen, J.; Tang, X.; Xie, X.; Wang, K.; Fan, H. Ultra-Performance Liquid Chromatography Hyphenated with Quadrupole-Orbitrap Mass Spectrometry for Simultaneous Determination of Necine-Core-Structure Pyrrolizidine Alkaloids in Crotalaria Sessiliflora L. without All Corresponding Standards. *Phytochemical Analysis* **2017**, *28* (5), 365–373. https://doi.org/10.1002/pca.2683.

(103) Avula, B.; Sagi, S.; Wang, Y.-H.; Zweigenbaum, J.; Wang, M.; Khan, I. A. Characterization and Screening of Pyrrolizidine Alkaloids and N-Oxides from Botanicals and Dietary Supplements Using UHPLC-High Resolution Mass Spectrometry. *Food Chemistry* **2015**, *178*, 136–148. https://doi.org/10.1016/j.foodchem.2015.01.053.

(104) Griffin, C. T.; Danaher, M.; Elliott, C. T.; Glenn Kennedy, D.; Furey, A. Detection of Pyrrolizidine Alkaloids in Commercial Honey Using Liquid Chromatography–Ion Trap Mass Spectrometry. *Food Chemistry* **2013**, *136* (3), 1577–1583. https://doi.org/10.1016/j.foodchem.2012.02.112.

(105) Martinello, M.; Cristofoli, C.; Gallina, A.; Mutinelli, F. Easy and Rapid Method for the Quantitative Determination of Pyrrolizidine Alkaloids in Honey by Ultra Performance Liquid Chromatography-Mass Spectrometry: An Evaluation in Commercial Honey. *Food Control* **2014**, *37*, 146–152. https://doi.org/10.1016/j.foodcont.2013.09.037.

(106) Bodi, D.; Ronczka, S.; Gottschalk, C.; Behr, N.; Skibba, A.; Wagner, M.; Lahrssen-Wiederholt, M.; Preiss-Weigert, A.; These, A. Determination of Pyrrolizidine Alkaloids in Tea, Herbal Drugs and Honey. *Food Addit Contam Part A Chem Anal Control Expo Risk Assess* **2014**, *31* (11), 1886–1895. https://doi.org/10.1080/19440049.2014.964337.

(107) Picron, J.-F.; Herman, M.; Van Hoeck, E.; Goscinny, S. Analytical Strategies for the Determination of Pyrrolizidine Alkaloids in Plant Based Food and Examination of the

Transfer Rate during the Infusion Process. *Food Chemistry* **2018**, *266*, 514–523. https://doi.org/10.1016/j.foodchem.2018.06.055.

(108) Dübecke, A.; Beckh, G.; Lüllmann, C. Pyrrolizidine Alkaloids in Honey and Bee Pollen. *Food Addit Contam Part A Chem Anal Control Expo Risk Assess* **2011**, *28* (3), 348–358. https://doi.org/10.1080/19440049.2010.541594.

(109) *Survey of pyrrolizidine alkaloids in teas and herbal teas on the Swiss market using HPLC-MS/MS | SpringerLink*. https://link.springer.com/article/10.1007/s00216-014-8142-8 (accessed 2022-09-26).

(110) Bolechová, M.; Čáslavský, J.; Pospíchalová, M.; Kosubová, P. UPLC–MS/MS Method for Determination of Selected Pyrrolizidine Alkaloids in Feed. *Food Chemistry* **2015**, *170*, 265–270. https://doi.org/10.1016/j.foodchem.2014.08.072.

(111) Kowalczyk, E.; Kwiatek, K. Use of a New LC-MS Method for The Determination of Pyrrolizidine Alkaloids in Feeds. *J Vet Res* **2018**, *62* (2), 183–191. https://doi.org/10.2478/jvetres-2018-0028.

(112) Sixto, A.; Niell, S.; Heinzen, H. Straightforward Determination of Pyrrolizidine Alkaloids in Honey through Simplified Methanol Extraction (QuPPE) and LC-MS/MS Modes. *ACS Omega* **2019**, *4* (27), 22632–22637. https://doi.org/10.1021/acsomega.9b03538.

(113) Schulz, M.; Meins, J.; Diemert, S.; Zagermann-Muncke, P.; Goebel, R.; Schrenk, D.; Schubert-Zsilavecz, M.; Abdel-Tawab, M. Detection of Pyrrolizidine Alkaloids in German Licensed Herbal Medicinal Teas. *Phytomedicine* **2015**, *22* (6), 648–656. https://doi.org/10.1016/j.phymed.2015.03.020.

(114) Birru, R. L.; Liang, H.-W.; Farooq, F.; Bedi, M.; Feghali, M.; Haggerty, C. L.; Mendez, D. D.; Catov, J. M.; Ng, C. A.; Adibi, J. J. A Pathway Level Analysis of PFAS Exposure and Risk of Gestational Diabetes Mellitus. *Environmental Health* **2021**, *20* (1), 63. https://doi.org/10.1186/s12940-021-00740-z.

(115) Li, F.; Duan, J.; Tian, S.; Ji, H.; Zhu, Y.; Wei, Z.; Zhao, D. Short-Chain per- and Polyfluoroalkyl Substances in Aquatic Systems: Occurrence, Impacts and Treatment. *Chemical Engineering Journal* **2020**, *380*, 122506. https://doi.org/10.1016/j.cej.2019.122506.

(116) Sunderland, E. M.; Hu, X. C.; Dassuncao, C.; Tokranov, A. K.; Wagner, C. C.; Allen, J. G. A Review of the Pathways of Human Exposure to Poly- and Perfluoroalkyl Substances (PFASs) and Present Understanding of Health Effects. *J Expo Sci Environ Epidemiol* **2019**, *29* (2), 131–147. https://doi.org/10.1038/s41370-018-0094-1.

(117) Faithfull, N. s.; Weers, J. g. Perfluorocarbon Compounds. *Vox Sanguinis* **1998**, *74* (S2), 243–248. https://doi.org/10.1111/j.1423-0410.1998.tb05426.x.

(118) Wang, Z.; Cousins, I. T.; Scheringer, M.; Hungerbuehler, K. Hazard Assessment of Fluorinated Alternatives to Long-Chain Perfluoroalkyl Acids (PFAAs) and Their Precursors: Status Quo, Ongoing Challenges and Possible Solutions. *Environment International* **2015**, *75*, 172–179. https://doi.org/10.1016/j.envint.2014.11.013.

(119) Wang, Z.; Cousins, I. T.; Scheringer, M.; Buck, R. C.; Hungerbühler, K. Global Emission Inventories for C4–C14 Perfluoroalkyl Carboxylic Acid (PFCA) Homologues from 1951 to 2030, Part I: Production and Emissions from Quantifiable Sources. *Environment International* **2014**, *70*, 62–75. https://doi.org/10.1016/j.envint.2014.04.013.

(120) Gyllenhammar, I.; Berger, U.; Sundström, M.; McCleaf, P.; Eurén, K.; Eriksson, S.; Ahlgren, S.; Lignell, S.; Aune, M.; Kotova, N.; Glynn, A. Influence of Contaminated Drinking Water on Perfluoroalkyl Acid Levels in Human Serum – A Case Study from Uppsala, Sweden. *Environmental Research* **2015**, *140*, 673–683. https://doi.org/10.1016/j.envres.2015.05.019.

(121) Pasecnaja, E.; Bartkevics, V.; Zacs, D. Occurrence of Selected Per- and Polyfluorinated Alkyl Substances (PFASs) in Food Available on the European Market – A Review on

Levels and Human Exposure Assessment. *Chemosphere* **2022**, *287*, 132378. https://doi.org/10.1016/j.chemosphere.2021.132378.

(122) Crone, B. C.; Speth, T. F.; Wahman, D. G.; Smith, S. J.; Abulikemu, G.; Kleiner, E. J.; Pressman, J. G. Occurrence of Per- and Polyfluoroalkyl Substances (PFAS) in Source Water and Their Treatment in Drinking Water. *Crit Rev Environ Sci Technol* **2019**, *49* (24), 2359–2396. https://doi.org/10.1080/10643389.2019.1614848.

(123) Rankin, K.; Lee, H.; Tseng, P. J.; Mabury, S. A. Investigating the Biodegradability of a Fluorotelomer-Based Acrylate Polymer in a Soil–Plant Microcosm by Indirect and Direct Analysis. *Environ. Sci. Technol.* **2014**, *48* (21), 12783–12790. https://doi.org/10.1021/es502986w.

(124) Houde, M.; De Silva, A. O.; Muir, D. C. G.; Letcher, R. J. Monitoring of Perfluorinated Compounds in Aquatic Biota: An Updated Review. *Environ. Sci. Technol.* **2011**, *45* (19), 7962–7973. https://doi.org/10.1021/es104326w.

(125) Dickman, R. A.; Aga, D. S. A Review of Recent Studies on Toxicity, Sequestration, and Degradation of per- and Polyfluoroalkyl Substances (PFAS). *Journal of Hazardous Materials* **2022**, *436*, 129120. https://doi.org/10.1016/j.jhazmat.2022.129120.

(126) Conder, J. M.; Hoke, R. A.; Wolf, W. de; Russell, M. H.; Buck, R. C. Are PFCAs Bioaccumulative? A Critical Review and Comparison with Regulatory Criteria and Persistent Lipophilic Compounds. *Environ. Sci. Technol.* **2008**, *42* (4), 995–1003. https://doi.org/10.1021/es070895g.

(127) Haug, L. S.; Huber, S.; Becher, G.; Thomsen, C. Characterisation of Human Exposure Pathways to Perfluorinated Compounds — Comparing Exposure Estimates with Biomarkers of Exposure. *Environment International* **2011**, *37* (4), 687–693. https://doi.org/10.1016/j.envint.2011.01.011.

(128) Chambers, W. S.; Hopkins, J. G.; Richards, S. M. A Review of Per- and Polyfluorinated Alkyl Substance Impairment of Reproduction. *Frontiers in Toxicology* **2021**, *3*.

(129) Conti, A.; Strazzeri, C.; Rhoden, K. J. Perfluorooctane Sulfonic Acid, a Persistent Organic Pollutant, Inhibits Iodide Accumulation by Thyroid Follicular Cells in Vitro. *Molecular and Cellular Endocrinology* **2020**, *515*, 110922. https://doi.org/10.1016/j.mce.2020.110922.

(130) Buckalew, A. R.; Wang, J.; Murr, A. S.; Deisenroth, C.; Stewart, W. M.; Stoker, T. E.; Laws, S. C. Evaluation of Potential Sodium-Iodide Symporter (NIS) Inhibitors Using a Secondary Fischer Rat Thyroid Follicular Cell (FRTL-5) Radioactive Iodide Uptake (RAIU) Assay. *Arch Toxicol* **2020**, *94* (3), 873–885. https://doi.org/10.1007/s00204-020-02664-y.

(131) Rappazzo, K. M.; Coffman, E.; Hines, E. P. Exposure to Perfluorinated Alkyl Substances and Health Outcomes in Children: A Systematic Review of the Epidemiologic Literature. *Int J Environ Res Public Health* **2017**, *14* (7), 691. https://doi.org/10.3390/ijerph14070691.

(132) Averina, M.; Brox, J.; Huber, S.; Furberg, A.-S. Exposure to Perfluoroalkyl Substances (PFAS) and Dyslipidemia, Hypertension and Obesity in Adolescents. The Fit Futures Study. *Environmental Research* **2021**, *195*, 110740. https://doi.org/10.1016/j.envres.2021.110740.

(133) *Perfluorooctane sulfonate (PFOS), perfluorooctanoic acid (PFOA) and their salts Scientific Opinion of the Panel on Contaminants in the Food chain [1] | EFSA*. https://www.efsa.europa.eu/en/efsajournal/pub/653 (accessed 2022-09-27).

(134) Fenton, S. E.; Ducatman, A.; Boobis, A.; DeWitt, J. C.; Lau, C.; Ng, C.; Smith, J. S.; Roberts, S. M. Per- and Polyfluoroalkyl Substance Toxicity and Human Health Review: Current State of Knowledge and Strategies for Informing Future Research. *Environmental Toxicology and Chemistry* **2021**, *40* (3), 606–630. https://doi.org/10.1002/etc.4890.

(135) Chain (CONTAM), E. P. on C. in the F.; Knutsen, H. K.; Alexander, J.; Barregård, L.; Bignami, M.; Brüschweiler, B.; Ceccatelli, S.; Cottrill, B.; Dinovi, M.; Edler, L.; Grasl-

Kraupp, B.; Hogstrand, C.; Hoogenboom, L. (Ron); Nebbia, C. S.; Oswald, I. P.; Petersen, A.; Rose, M.; Roudot, A.-C.; Vleminckx, C.; Vollmer, G.; Wallace, H.; Bodin, L.; Cravedi, J.-P.; Halldorsson, T. I.; Haug, L. S.; Johansson, N.; van Loveren, H.; Gergelova, P.; Mackay, K.; Levorato, S.; van Manen, M.; Schwerdtle, T. Risk to Human Health Related to the Presence of Perfluorooctane Sulfonic Acid and Perfluorooctanoic Acid in Food. *EFSA Journal* **2018**, *16* (12), e05194. https://doi.org/10.2903/j.efsa.2018.5194.

(136) *Risk to human health related to the presence of perfluoroalkyl substances in food | EFSA*. https://www.efsa.europa.eu/en/efsajournal/pub/6223 (accessed 2022-09-27).

(137) Winchell, L. J.; Wells, M. J. M.; Ross, J. J.; Fonoll, X.; Norton, J. W.; Kuplicki, S.; Khan, M.; Bell, K. Y. Analyses of Per- and Polyfluoroalkyl Substances (PFAS) through the Urban Water Cycle: Toward Achieving an Integrated Analytical Workflow across Aqueous, Solid, and Gaseous Matrices in Water and Wastewater Treatment. *Science of The Total Environment* **2021**, *774*, 145257. https://doi.org/10.1016/j.scitotenv.2021.145257.

(138) Di Giorgi, A.; La Maida, N.; Taoussi, O.; Pichini, S.; Busardò, F. P.; Tini, A.; Di Trana, A. Analysis of Perfluoroalkyl Substances (PFAS) in Conventional and Unconventional Matrices: Clinical Outcomes. *Journal of Pharmaceutical and Biomedical Analysis Open* **2023**, *1*, 100002. https://doi.org/10.1016/j.jpbao.2023.100002.

(139) Kaufmann, A.; Butcher, P.; Maden, K.; Walker, S.; Widmer, M. Simplifying Nontargeted Analysis of PFAS in Complex Food Matrixes. *Journal of AOAC INTERNATIONAL* **2022**, *105* (5), 1280–1287. https://doi.org/10.1093/jaoacint/qsac071.

(140) Daughton, C. G. Illicit Drugs in Municipal Sewage. In *Pharmaceuticals and Care Products in the Environment*; ACS Symposium Series; American Chemical Society, 2001; Vol. 791, pp 348–364. https://doi.org/10.1021/bk-2001-0791.ch020.

(141) Zuccato, E.; Chiabrando, C.; Castiglioni, S.; Bagnati, R.; Fanelli, R. Estimating Community Drug Abuse by Wastewater Analysis. *Environmental Health Perspectives* **2008**, *116* (8), 1027–1032. https://doi.org/10.1289/ehp.11022.

(142) Choi, P. M.; Bowes, D. A.; O'Brien, J. W.; Li, J.; Halden, R. U.; Jiang, G.; Thomas, K. V.; Mueller, J. F. Do Food and Stress Biomarkers Work for Wastewater-Based Epidemiology? A Critical Evaluation. *Science of The Total Environment* **2020**, *736*, 139654. https://doi.org/10.1016/j.scitotenv.2020.139654.

(143) Shah, S.; Gwee, S. X. W.; Ng, J. Q. X.; Lau, N.; Koh, J.; Pang, J. Wastewater Surveillance to Infer COVID-19 Transmission: A Systematic Review. *Science of The Total Environment* **2022**, *804*, 150060. https://doi.org/10.1016/j.scitotenv.2021.150060.

(144) Vitale, D.; Morales Suárez-Varela, M.; Picó, Y. Wastewater-Based Epidemiology, a Tool to Bridge Biomarkers of Exposure, Contaminants, and Human Health. *Current Opinion in Environmental Science & Health* **2021**, *20*, 100229. https://doi.org/10.1016/j.coesh.2021.100229.

(145) Helander, A.; Beck, O. Ethyl Sulfate: A Metabolite of Ethanol in Humans and a Potential Biomarker of Acute Alcohol Intake. *Journal of Analytical Toxicology* **2005**, *29* (5), 270–274. https://doi.org/10.1093/jat/29.5.270.

(146) Rico, M.; Andrés-Costa, M. J.; Picó, Y. Estimating Population Size in Wastewater-Based Epidemiology. Valencia Metropolitan Area as a Case Study. *Journal of Hazardous Materials* **2017**, *323*, 156–165. https://doi.org/10.1016/j.jhazmat.2016.05.079.

(147) Ra, J.; Yoom, H.; Son, H.; Lee, Y. Occurrence and Transformation of Gabapentin in Urban Water Quality Engineering: Rapid Formation of Nitrile from Amine during Drinking Water Chlorination. *Water Research* **2020**, *184*, 116123. https://doi.org/10.1016/j.watres.2020.116123.

(148) Castiglioni, S.; Senta, I.; Borsotti, A.; Davoli, E.; Zuccato, E. A Novel Approach for Monitoring Tobacco Use in Local Communities by Wastewater Analysis. *Tob Control* **2015**, *24* (1), 38–42. https://doi.org/10.1136/tobaccocontrol-2014-051553.

(149) Gracia-Lor, E.; Rousis, N. I.; Zuccato, E.; Castiglioni, S. Monitoring Caffeine and Nicotine Use in a Nationwide Study in Italy Using Wastewater-Based Epidemiology.

Science of The Total Environment **2020**, *747*, 141331. https://doi.org/10.1016/j.scitotenv.2020.141331.

(150) Choi, P. M.; Tscharke, B. J.; Donner, E.; O'Brien, J. W.; Grant, S. C.; Kaserzon, S. L.; Mackie, R.; O'Malley, E.; Crosbie, N. D.; Thomas, K. V.; Mueller, J. F. Wastewater-Based Epidemiology Biomarkers: Past, Present and Future. *TrAC Trends in Analytical Chemistry* **2018**, *105*, 453–469. https://doi.org/10.1016/j.trac.2018.06.004.

(151) Ahmed, F.; Li, J.; O'Brien, J. W.; Tscharke, B. J.; Samanipour, S.; Thai, P. K.; Yuan, Z.; Mueller, J. F.; Thomas, K. V. In-Sewer Stability of Selected Analgesics and Their Metabolites. *Water Research* **2021**, *204*, 117647. https://doi.org/10.1016/j.watres.2021.117647.

(152) Tang, W. The Metabolism of Diclofenac--Enzymology and Toxicology Perspectives. *Curr Drug Metab* **2003**, *4* (4), 319–329. https://doi.org/10.2174/1389200033489398.

(153) Mazaleuskaya, L. L.; Theken, K. N.; Gong, L.; Thorn, C. F.; FitzGerald, G. A.; Altman, R. B.; Klein, T. E. PharmGKB Summary: Ibuprofen Pathways. *Pharmacogenet Genomics* **2015**, *25* (2), 96–106. https://doi.org/10.1097/FPC.0000000000000113.

(154) Di Lorenzo, T.; Cifoni, M.; Baratti, M.; Pieraccini, G.; Di Marzio, W. D.; Galassi, D. M. P. Four Scenarios of Environmental Risk of Diclofenac in European Groundwater Ecosystems. *Environmental Pollution* **2021**, *287*, 117315. https://doi.org/10.1016/j.envpol.2021.117315.

(155) Jia, Y.; Khanal, S. K.; Yin, L.; Sun, L.; Lu, H. Influence of Ibuprofen and Its Biotransformation Products on Different Biological Sludge Systems and Ecosystem. *Environment International* **2021**, *146*, 106265. https://doi.org/10.1016/j.envint.2020.106265.

(156) Li, Y.; Niu, X.; Yao, C.; Yang, W.; Lu, G. Distribution, Removal, and Risk Assessment of Pharmaceuticals and Their Metabolites in Five Sewage Plants. *Int J Environ Res Public Health* **2019**, *16* (23), E4729. https://doi.org/10.3390/ijerph16234729.

(157) Angeles, L. F.; Mullen, R. A.; Huang, I. J.; Wilson, C.; Khunjar, W.; Sirotkin, H. I.; McElroy, A. E.; Aga, D. S. Assessing Pharmaceutical Removal and Reduction in Toxicity Provided by Advanced Wastewater Treatment Systems. *Environ. Sci.: Water Res. Technol.* **2019**, *6* (1), 62–77. https://doi.org/10.1039/C9EW00559E.

(158) Duan, L.; Zhang, Y.; Wang, B.; Yu, G.; Gao, J.; Cagnetta, G.; Huang, C.; Zhai, N. Wastewater Surveillance for 168 Pharmaceuticals and Metabolites in a WWTP: Occurrence, Temporal Variations and Feasibility of Metabolic Biomarkers for Intake Estimation. *Water Research* **2022**, *216*, 118321. https://doi.org/10.1016/j.watres.2022.118321.

(159) Fatta, D.; Achilleos, A.; Nikolaou, A.; Meriç, S. Analytical Methods for Tracing Pharmaceutical Residues in Water and Wastewater. *TrAC Trends in Analytical Chemistry* **2007**, *26* (6), 515–533. https://doi.org/10.1016/j.trac.2007.02.001.

(160) Greer, B.; Chevallier, O.; Quinn, B.; Botana, L. M.; Elliott, C. T. Redefining Dilute and Shoot: The Evolution of the Technique and Its Application in the Analysis of Foods and Biological Matrices by Liquid Chromatography Mass Spectrometry. *TrAC Trends in Analytical Chemistry* **2021**, *141*, 116284. https://doi.org/10.1016/j.trac.2021.116284.

(161) He, L.; Diedrich, J.; Chu, Y.-Y.; Yates, J. R. Extracting Accurate Precursor Information for Tandem Mass Spectra by RawConverter. *Anal Chem* **2015**, *87* (22), 11361–11367. https://doi.org/10.1021/acs.analchem.5b02721.

(162) Kind, T.; Tsugawa, H.; Cajka, T.; Ma, Y.; Lai, Z.; Mehta, S. S.; Wohlgemuth, G.; Barupal, D. K.; Showalter, M. R.; Arita, M.; Fiehn, O. Identification of Small Molecules Using Accurate Mass MS/MS Search. *Mass Spectrom Rev* **2018**, *37* (4), 513–532. https://doi.org/10.1002/mas.21535.

(163) Schneider, B. B.; Guo, X.; Fell, L. M.; Covey, T. R. Stable Gradient Nanoflow LC-MS. *Journal of the American Society for Mass Spectrometry* **2005**, *16* (9), 1545–1551. https://doi.org/10.1016/j.jasms.2005.05.004.

(164) *European Commission. Guidance Document on Identification of Mycotoxins in Food and Feed, SANTE/12089 /2016*. https://food.ec.europa.eu/system/files/2017-05/cs_contaminants_sampling_guid-doc-ident-mycotoxins.pdf.

(165) Rausch, A.-K.; Brockmeyer, R.; Schwerdtle, T. Development and Validation of a QuEChERS-Based Liquid Chromatography Tandem Mass Spectrometry Multi-Method for the Determination of 38 Native and Modified Mycotoxins in Cereals. *J. Agric. Food Chem.* **2020**, *68* (16), 4657–4669. https://doi.org/10.1021/acs.jafc.9b07491.

(166) Kunz, B. M.; Wanko, F.; Kemmlein, S.; Bahlmann, A.; Rohn, S.; Maul, R. Development of a Rapid Multi-Mycotoxin LC-MS/MS Stable Isotope Dilution Analysis for Grain Legumes and Its Application on 66 Market Samples. *Food Control* **2020**, *109*, 106949. https://doi.org/10.1016/j.foodcont.2019.106949.

(167) Fraeyman, S.; Croubels, S.; Devreese, M.; Antonissen, G. Emerging Fusarium and Alternaria Mycotoxins: Occurrence, Toxicity and Toxicokinetics. *Toxins (Basel)* **2017**, *9* (7), 228. https://doi.org/10.3390/toxins9070228.

(168) Carballo, D.; Moltó, J. C.; Berrada, H.; Ferrer, E. Presence of Mycotoxins in Ready-to-Eat Food and Subsequent Risk Assessment. *Food and Chemical Toxicology* **2018**, *121*, 558–565. https://doi.org/10.1016/j.fct.2018.09.054.

(169) Oviedo, M. S.; Barros, G. G.; Chulze, S. N.; Ramirez, M. L. Natural Occurrence of Alternariol and Alternariol Monomethyl Ether in Soya Beans. *Mycotoxin Res* **2012**, *28* (3), 169–174. https://doi.org/10.1007/s12550-012-0132-0.

(170) Willocx, M.; Van der Beeten, I.; Asselman, P.; Delgat, L.; Baert, W.; Janssens, S. B.; Leliaert, F.; Picron, J.-F.; Vanhee, C. Sorting out the Plants Responsible for a Contamination with Pyrrolizidine Alkaloids in Spice Seeds by Means of LC-MS/MS and DNA Barcoding: Proof of Principle with Cumin and Anise Spice Seeds. *Food Chemistry: Molecular Sciences* **2022**, *4*, 100070. https://doi.org/10.1016/j.fochms.2021.100070.

(171) *Jēkaba krustaine - Senecio jacobaea L. - Augi - Latvijas daba*. https://www.latvijasdaba.lv/augi/senecio-jacobaea-l/ (accessed 2022-09-26).

(172) Kowalczyk, E.; Kwiatek, K. Pyrrolizidine Alkaloids in Honey: Determination with Liquid Chromatography-Mass Spectrometry Method. *J Vet Res* **2018**, *62* (2), 173–181. https://doi.org/10.2478/jvetres-2018-0027.

(173) Martinello, M.; Borin, A.; Stella, R.; Bovo, D.; Biancotto, G.; Gallina, A.; Mutinelli, F. Development and Validation of a QuEChERS Method Coupled to Liquid Chromatography and High Resolution Mass Spectrometry to Determine Pyrrolizidine and Tropane Alkaloids in Honey. *Food Chemistry* **2017**, *234*, 295–302. https://doi.org/10.1016/j.foodchem.2017.04.186.

(174) *Dietary exposure assessment to pyrrolizidine alkaloids in the European population - - 2016 - EFSA Journal - Wiley Online Library*. https://efsa.onlinelibrary.wiley.com/doi/full/10.2903/j.efsa.2016.4572 (accessed 2022-09-26).

(175) These, A.; Bodi, D.; Ronczka, S.; Lahrssen-Wiederholt, M.; Preiss-Weigert, A. Structural Screening by Multiple Reaction Monitoring as a New Approach for Tandem Mass Spectrometry: Presented for the Determination of Pyrrolizidine Alkaloids in Plants. *Anal Bioanal Chem* **2013**, *405* (29), 9375–9383. https://doi.org/10.1007/s00216-013-7365-4.

(176) *The Mass Spectrum of Cocaine: Deuterium Labeling and MS/MS Studies (Microgram Journal 2010;7(1):16-41)*. https://www.dea.gov/documents/2010/2010-01/2010-01-01/mass-spectrum-cocaine-deuterium-labeling-and-msms-studies (accessed 2022-09-26).

(177) Rodríguez-Álvarez, T.; Rodil, R.; Cela, R.; Quintana, J. B. Ion-Pair Reversed-Phase Liquid Chromatography–Quadrupole-Time-of-Flight and Triple-Quadrupole–Mass Spectrometry Determination of Ethyl Sulfate in Wastewater for Alcohol Consumption

Tracing. *Journal of Chromatography A* **2014**, *1328*, 35–42. https://doi.org/10.1016/j.chroma.2013.12.076.

(178) *Tetrabutylammonium bromide*. https://www.chemsrc.com/en/cas/1643-19-2_329726.html (accessed 2022-08-19).

(179) Hernández, F.; Ibáñez, M.; Gracia-Lor, E.; Sancho, J. V. Retrospective LC-QTOF-MS Analysis Searching for Pharmaceutical Metabolites in Urban Wastewater. *Journal of Separation Science* **2011**, *34* (24), 3517–3526. https://doi.org/10.1002/jssc.201100540.

(180) Kaufmann, A.; Arrizabalaga-Larrañaga, A.; Blokland, M. H.; Sterk, S. S. Potential and Limitation of Retrospective HRMS Based Data Analysis: "Have Meat-Producing Animals Been Exposed to Illegal Growth Promotors Such as SARMs?" *Food Control* **2023**, *147*, 109611. https://doi.org/10.1016/j.foodcont.2023.109611.

(181) Günthardt, B. F.; Wettstein, F. E.; Hollender, J.; Singer, H.; Härri, J.; Scheringer, M.; Hungerbühler, K.; Bucheli, T. D. Retrospective HRMS Screening and Dedicated Target Analysis Reveal a Wide Exposure to Pyrrolizidine Alkaloids in Small Streams. *Environ. Sci. Technol.* **2021**, *55* (2), 1036–1044. https://doi.org/10.1021/acs.est.0c06411.

(182) Alygizakis, N. A.; Samanipour, S.; Hollender, J.; Ibáñez, M.; Kaserzon, S.; Kokkali, V.; van Leerdam, J. A.; Mueller, J. F.; Pijnappels, M.; Reid, M. J.; Schymanski, E. L.; Slobodnik, J.; Thomaidis, N. S.; Thomas, K. V. Exploring the Potential of a Global Emerging Contaminant Early Warning Network through the Use of Retrospective Suspect Screening with High-Resolution Mass Spectrometry. *Environ. Sci. Technol.* **2018**, *52* (9), 5135–5144. https://doi.org/10.1021/acs.est.8b00365.

(183) Nguyen-Khuong, T.; Pralow, A.; Reichl, U.; Rapp, E. Improvement of Electrospray Stability in Negative Ion Mode for Nano-PGC-LC-MS Glycoanalysis via Post-Column Make-up Flow. *Glycoconj J* **2018**, *35* (6), 499–509. https://doi.org/10.1007/s10719-018-9848-1.

(184) Kalli, A.; Smith, G. T.; Sweredoski, M. J.; Hess, S. Evaluation and Optimization of Mass Spectrometric Settings during Data-Dependent Acquisition Mode: Focus on LTQ-Orbitrap Mass Analyzers. *J Proteome Res* **2013**, *12* (7), 3071–3086. https://doi.org/10.1021/pr3011588.

(185) Kalli, A.; Hess, S. Effect of Mass Spectrometric Parameters on Peptide and Protein Identification Rates for Shotgun Proteomic Experiments on an LTQ-Orbitrap Mass Analyzer. *Proteomics* **2012**, *12* (1), 21–31. https://doi.org/10.1002/pmic.201100464.

(186) Hohenester, U. M.; Barbier Saint-Hilaire, P.; Fenaille, F.; Cole, R. B. Investigation of Space Charge Effects and Ion Trapping Capacity on Direct Introduction Ultra-High-Resolution Mass Spectrometry Workflows for Metabolomics. *Journal of Mass Spectrometry* **2020**, *55* (10), e4613. https://doi.org/10.1002/jms.4613.

(187) Hasegawa, K.; Minakata, K.; Suzuki, M.; Suzuki, O. The Standard Addition Method and Its Validation in Forensic Toxicology. *Forensic Toxicol* **2021**, *39* (2), 311–333. https://doi.org/10.1007/s11419-021-00585-8.

(188) Pugajeva, I.; Ikkere, L. E.; Jansons, M.; Perkons, I.; Sukajeva, V.; Bartkevics, V. Two-Dimensional Liquid Chromatography - Mass Spectrometry as an Effective Tool for Assessing a Wide Range of Pharmaceuticals and Biomarkers in Wastewater-Based Epidemiology Studies. *Journal of Pharmaceutical and Biomedical Analysis* **2021**, *205*, 114295. https://doi.org/10.1016/j.jpba.2021.114295.

(189) Quintana, J. B.; Rodil, R.; Reemtsma, T. Suitability of Hollow Fibre Liquid-Phase Microextraction for the Determination of Acidic Pharmaceuticals in Wastewater by Liquid Chromatography–Electrospray Tandem Mass Spectrometry without Matrix Effects. *Journal of Chromatography A* **2004**, *1061* (1), 19–26. https://doi.org/10.1016/j.chroma.2004.10.090.

(190) Pandopulos, A. J.; Gerber, C.; Tscharke, B. J.; O'Brien, J.; White, J. M.; Bade, R. A Sensitive Analytical Method for the Measurement of Neurotransmitter Metabolites as

Potential Population Biomarkers in Wastewater. *Journal of Chromatography A* **2020**, *1612*, 460623. https://doi.org/10.1016/j.chroma.2019.460623.

(191) Zacs, D.; Bartkevics, V. Trace Determination of Perfluorooctane Sulfonate and Perfluorooctanoic Acid in Environmental Samples (Surface Water, Wastewater, Biota, Sediments, and Sewage Sludge) Using Liquid Chromatography – Orbitrap Mass Spectrometry. *Journal of Chromatography A* **2016**, *1473*, 109–121. https://doi.org/10.1016/j.chroma.2016.10.060.

(192) Kelly, B. C.; Ikonomou, M. G.; Blair, J. D.; Surridge, B.; Hoover, D.; Grace, R.; Gobas, F. A. P. C. Perfluoroalkyl Contaminants in an Arctic Marine Food Web: Trophic Magnification and Wildlife Exposure. *Environ. Sci. Technol.* **2009**, *43* (11), 4037–4043. https://doi.org/10.1021/es9003894.

(193) Taniyasu, S.; Kannan, K.; So, M. K.; Gulkowska, A.; Sinclair, E.; Okazawa, T.; Yamashita, N. Analysis of Fluorotelomer Alcohols, Fluorotelomer Acids, and Short- and Long-Chain Perfluorinated Acids in Water and Biota. *Journal of Chromatography A* **2005**, *1093* (1), 89–97. https://doi.org/10.1016/j.chroma.2005.07.053.

(194) Capriotti, A. L.; Cavaliere, C.; Cavazzini, A.; Foglia, P.; Laganà, A.; Piovesana, S.; Samperi, R. High Performance Liquid Chromatography Tandem Mass Spectrometry Determination of Perfluorinated Acids in Cow Milk. *Journal of Chromatography A* **2013**, *1319*, 72–79. https://doi.org/10.1016/j.chroma.2013.10.029.

(195) Wilson, S. R.; Olsen, C.; Lundanes, E. Nano Liquid Chromatography Columns. *Analyst* **2019**, *144* (24), 7090–7104. https://doi.org/10.1039/C9AN01473J.

(196) Al Amin, Md.; Sobhani, Z.; Liu, Y.; Dharmaraja, R.; Chadalavada, S.; Naidu, R.; Chalker, J. M.; Fang, C. Recent Advances in the Analysis of Per- and Polyfluoroalkyl Substances (PFAS)—A Review. *Environmental Technology & Innovation* **2020**, *19*, 100879. https://doi.org/10.1016/j.eti.2020.100879.

(197) Weiss, J. M.; van der Veen, I.; de Boer, J.; van Leeuwen, S. P. J.; Cofino, W.; Crum, S. Analytical Improvements Shown over Four Interlaboratory Studies of Perfluoroalkyl Substances in Environmental and Food Samples. *TrAC Trends in Analytical Chemistry* **2013**, *43*, 204–216. https://doi.org/10.1016/j.trac.2012.10.005.

(198) Guidance Document on Analytical Parameters for the Determination of Per- and Polyfluoroalkyl Substances (PFAS) in Food and Feed. Version 1.2. https://food.ec.europa.eu/system/files/2022-05/cs_contaminants_sampling_guid-doc-analyt-para_0.pdf (accessed 2022-09-24).

(199) Joint Research Centre (European Commission); Robouch, P.; Stroka, J.; Haedrich, J.; Schaechtele, A.; Wenzl, T. *Guidance Document on the Estimation of LOD and LOQ for Measurements in the Field of Contaminants in Feed and Food*; Publications Office of the European Union: LU, 2016.

(200) *EUR-Lex - 32022R1428 - EN - EUR-Lex*. https://eur-lex.europa.eu/eli/reg_impl/2022/1428/oj (accessed 2022-09-24).

(201) *Commission Recommendation (EU) 2022/1431 of 24 August 2022 on the Monitoring of Perfluoroalkyl Substances in Food*; 2022; Vol. 221. http://data.europa.eu/eli/reco/2022/1431/oj/eng (accessed 2022-09-24).

(202) Zabaleta, I.; Bizkarguenaga, E.; Prieto, A.; Ortiz-Zarragoitia, M.; Fernández, L. A.; Zuloaga, O. Simultaneous Determination of Perfluorinated Compounds and Their Potential Precursors in Mussel Tissue and Fish Muscle Tissue and Liver Samples by Liquid Chromatography–Electrospray-Tandem Mass Spectrometry. *Journal of Chromatography A* **2015**, *1387*, 13–23. https://doi.org/10.1016/j.chroma.2015.01.089.

ANNEXES

Annex 1

Instrumental parameters of the nano-LC-MS method for the determination of multi-class mycotoxins in grain cereals and legumes

Analyte	RT (min)	Precursor ion (*m/z*)	Polarity	CE (eV)
T-2TETR	15.4	343.1398	Negative	10
NIV	15.9	357.1190	Negative	10
D3G	17.5	503.1769	Negative	15
DON	18.0	341.1241	Negative	20
FUS X	20.6	355.1387	Positive	20
NEO	21.7	400.1965	Positive	20
15-AcDON	23.7	339.1438	Positive	10
3-AcDON	24.2	339.1438	Positive	10
15-MAS	24.7	342.1910	Positive	10
FB_1	25.6	722.3957	Positive	40
FB_3	27.1	706.4008	Positive	40
T-2TRI	27.6	400.2329	Positive	15
FB_2	28.1	706.4008	Positive	35
ALT	28.2	293.1019	Positive	15
AFB_1	29.5	313.0706	Positive	30
HT-2	30.9	442.2434	Positive	10
TEN	31.2	415.2339	Positive	25
AFL	31.5	315.0863	Positive	25
ATX I	31.6	351.0873	Negative	35
AOH	33.4	257.0454	Negative	30
OTB	35.0	370.1285	Positive	20
T-2	35.9	484.2540	Positive	15
OTA	38.5	402.0749	Negative	20
ZEN	38.6	317.1393	Negative	25
AME	40.1	271.0611	Negative	30
ENN B	50.6	657.4432	Positive	15
ENN B_1	52.3	671.4589	Positive	15

Analytical performance parameters of the nano-LC-MS method for the determination of multi-class mycotoxins in grain cereals and legumes

Analyte	LOQ ($\mu g\ kg^{-1}$)	Recovery (%) (mean, n = 18)	RSD (%) (mean, n = 18)	RMS_{bias} (%)	U (%)
15-MAS	0.64	104	18	4.3	37
15-AcDON	2.9	82	10	18	41
3-AcDON	0.70	77	6.6	23	48
AFL	4.5	93	13	6.5	29
AFB_1	0.24	91	11	8.8	28
ALT	0.21	91	6.2	8.8	22
AOH	1.3	86	14	14	39
AME	1.9	96	17	4.2	35
ATX I	0.98	90	6.0	1.0	24
DON	2.7	57	2.8	9.4	20
D3G	0.10	29	4.3	12	25
ENN B	2.3	107	27	6.9	57
ENN B_1	14	87	11	13	34
FB_1	0.15	48	18	19	52
FB_2	3.0	85	14	15	42
FB_3	0.26	96	21	4.4	45
FUS X	2.8	44	13	25	56
HT-2	0.79	96	11	4.2	23
NEO	0.26	99	10	1.0	20
NIV	68	60	11	28	61
OTA	0.53	84	5.6	16	34
OTB	0.13	82	10	18	41
T-2TETR	3.9	49	20	32	76
T-2	0.28	92	2.7	7.8	17
T-2TRI	0.78	94	6.3	5.6	17
TEN	0.62	84	24	16	57
ZEN	0.65	85	8.1	15	35

List of analyzed biomarkers and pharmaceuticals and precursor ions used for detection in Full scan mode

Compound	Ionization mode	Molecular ion type	Quantifier ion (*m/z*)	Ionization mode	Molecular ion type	Qualifier ion (*m/z*)
Caffeine	Positive	$[M+H]^+$	195.0876	Positive	$[M+Na]^+$	217.0696
Cotinine	Positive	$[M+H]^+$	177.1022	Positive	$[M+H]^+$	178.1056
Diclofenac	Negative	$[M-H]^-$	294.0094	Positive	$[M+H]^+$	296.0240
Ethylsulfate	Negative	$[M-H]^-$	124.9914	Negative	$[M]^{-\bullet}$	125.9987
Gabapentin	Positive	$[M+H]^+$	172.1332	Negative	$[M-H]^-$	170.1187
5-HIAA	Positive	$[M+H]^+$	192.0655	Negative	$[M-H]^-$	190.0510
Ibuprofen	Negative	$[M-H]^-$	205.1234	Negative	$[M-HCOOH]^-$	159.1179*

* - in-source fragmentation

List of analyzed compounds, ions and mass deviation in Full scan mode

Compound	Theoretical mass (*m/z*)	Experimental mass (*m/z*)	Δ (*ppm)*
Caffeine	195.0876	195.0869	-3.6
	217.0696	217.0687	-4.1
Cotinine	177.1022	177.1016	-3.4
	178.1056	178.1048	-4.5
Diclofenac	294.0094	294.0093	-0.3
	296.0240	296.0229	-3.7
Ethylsulfate	124.9914	124.9920	4.8
	125.9987	125.9985	-1.6
Gabapentin	172.1332	172.1325	-4.1
	170.1187	170.1178	-5.3
5-HIAA	192.0655	192.0647	-4.2
	190.0510	190.0501	-4.7
Ibuprofen	205.1234	205.1225	-4.4
	159.1179	159.1171	-5.0

Validation data for the determination of biomarkers and pharmaceuticals

Compound	Linear range, µg L^{-1}	LOQ, µg L^{-1}	Trueness, % at 10 µg L^{-1} (*n* = 12)	Trueness, % at 50 µg L^{-1} (*n* = 12)	RSD, % at 10 µg L^{-1} (*n* = 6)	RSD, % at 50 µg L^{-1} (*n* = 6)	RSD_{wr}, % at 10 µg L^{-1} (*n* = 12)	RSD_{wr}, % at 50 µg L^{-1} (*n* = 12)	U, % at 10 µg L^{-1} (*k* = 2)	U, % at 50 µg L^{-1} (*k* = 2)	ME, %
Caffeine	0.5 – 100	0.17	104	101	4.1	3.7	5.5	5.8	11	12	70
Cotinine	0.5 – 100	0.005	102	94	4.3	5.5	4.4	5.8	8.9	12	104
Diclofenac	0.5 – 100	0.03	97	96	5.6	4.9	5.4	5.3	11	11	111
Ethyl sulfate	0.5 – 100	0.3	97	95	7.9	8.5	6.3	7.7	13	15	86
Gabapentin	0.5 – 100	0.08	99	96	6.2	5.8	5.5	5.5	11	11	100
5-HIAA	0.5 – 100	0.11	99	95	9.8	9.3	8.3	8.4	17	17	83
Ibuprofen	0.5 – 100	0.05	102	98	5.5	4.7	4.6	5.3	9.2	11	100

The wastewater treatment plant on the map of Latvia

List of analytes, precursor and fragment ions in positive ionization mode for the determination of pyrrolizidine alkaloids using conventional flow LC-MS (quantifier ions in bold, qualifier ions in italic)

Compound	Retention Time (min)	Acquisition window (min)	Precursor (*m/z*)	Product (*m/z*)	Collision Energy (V)	Min Dwell Time (ms)
Intermedine	7.0	1.0 - 13.0	300.2	**94.0**	27.3	4.233
Intermedine	7.0	1.0 - 13.0	300.2	*138.1*	20.2	4.233
Intermedine	7.0	1.0 - 13.0	300.2	*156.2*	31.1	4.233
Indicine	7.4	1.4 - 13.4	300.2	**94.0**	28.2	4.233
Indicine	7.4	1.4 - 13.4	300.2	*138.0*	21.0	4.233
Indicine	7.4	1.4 - 13.4	300.2	*156.1*	30.3	4.233
Lycopsamine	7.4	1.4 - 13.4	300.2	**94.1**	27.9	4.233
Lycopsamine	7.4	1.4 - 13.4	300.2	*138.0*	20.9	4.233
Lycopsamine	7.4	1.4 - 13.4	300.2	*156.0*	30.6	4.233
Echinatine	7.6	1.6 - 13.6	300.2	*94.0*	36.7	4.233
Echinatine	7.6	1.6 - 13.6	300.2	*120.0*	31.1	4.233
Echinatine	7.6	1.6 - 13.6	300.2	**138.0**	22.9	4.233
Echinatine	7.6	1.6 - 13.6	300.2	*156.1*	28.2	4.233
Europine	7.6	3.6 - 11.6	330.2	*120.1*	40.3	4.355
Europine	7.6	3.6 - 11.6	330.2	**138.1**	24.1	4.355
Europine	7.6	3.6 - 11.6	330.2	*156.1*	33.1	4.355
Europine	7.6	3.6 - 11.6	330.2	*254.1*	20.6	4.355
Europine *N*-oxide	8.2	4.2 - 12.2	346.2	*111.0*	46.3	4.233
Europine *N*-oxide	8.2	4.2 - 12.2	346.2	**171.9**	32.3	4.233
Europine *N*-oxide	8.2	4.2 - 12.2	346.2	*256.2*	24.9	4.233
Europine *N*-oxide	8.2	4.2 - 12.2	346.2	*328.1*	24.4	4.233
Echinatine *N*-oxide	8.3	4.3 - 12.3	316.2	*94.0*	39.3	4.233
Echinatine *N*-oxide	8.3	4.3 - 12.3	316.2	**111.0**	40.6	4.233
Echinatine *N*-oxide	8.3	4.3 - 12.3	316.2	*155.2*	29.8	4.233
Echinatine *N*-oxide	8.3	4.3 - 12.3	316.2	*172.2*	30.0	4.233
Intermedine *N*-oxide	8.7	4.7 - 12.7	316.2	**94.0**	39.8	4.233
Intermedine *N*-oxide	8.7	4.7 - 12.7	316.2	*138.0*	28.5	4.233
Intermedine *N*-oxide	8.7	4.7 - 12.7	316.2	*172.0*	28.3	4.233
Indicine *N*-oxide	8.8	4.8 - 12.8	316.2	*80.0*	53.7	4.233
Indicine *N*-oxide	8.8	4.8 - 12.8	316.2	**94.0**	41.9	4.233
Indicine *N*-oxide	8.8	4.8 - 12.8	316.2	*111.0*	43.5	4.233
Indicine *N*-oxide	8.8	4.8 - 12.8	316.2	*138.1*	29.3	4.233
Indicine *N*-oxide	8.8	4.8 - 12.8	316.2	*172.1*	29.1	4.233
Lycopsamine *N*-oxide	9.1	5.1 - 13.1	316.2	**93.9**	34.5	4.233
Lycopsamine *N*-oxide	9.1	5.1 - 13.1	316.2	*138.0*	30.0	4.233
Lycopsamine *N*-oxide	9.1	5.1 - 13.1	316.2	*172.0*	26.4	4.233
Usaramine	10.7	7.7 - 13.7	352.2	**120.0**	30.8	4.233
Usaramine	10.7	7.7 - 13.7	352.2	*276.3*	30.0	4.233
Usaramine	10.7	7.7 - 13.7	352.2	*324.2*	28.2	4.233
Retrorsine *N*-oxide	11.3	7.3 - 15.3	368.2	**93.9**	54.0	4.233
Retrorsine *N*-oxide	11.3	7.3 - 15.3	368.2	*118.0*	32.7	4.233
Retrorsine N-oxide	11.3	7.3 - 15.3	368.2	*120.0*	35.7	4.233

Retrorsine N-oxide	11.3	7.3 - 15.3	368.2	*136.1*	37.9	4.233
Retrorsine N-oxide	11.3	7.3 - 15.3	368.2	*220.1*	28.9	4.233
Retrorsine	11.0	8.0 - 14.0	352.2	**94.0**	46.8	4.233
Retrorsine	11.0	8.0 - 14.0	352.2	*120.1*	30.9	4.233
Retrorsine	11.0	8.0 - 14.0	352.2	*138.0*	31.1	4.233
Heliotrine	11.7	7.7 - 15.7	314.2	**94.0**	35.4	4.233
Heliotrine	11.7	7.7 - 15.7	314.2	*96.0*	30.1	4.233
Heliotrine	11.7	7.7 - 15.7	314.2	*120.1*	34.2	4.233
Heliotrine	11.7	7.7 - 15.7	314.2	*138.1*	22.7	4.233
Heliotrine	11.7	7.7 - 15.7	314.2	*156.1*	29.7	4.233
Heliotrine *N*-oxide	12.5	8.5 - 16.5	330.2	*79.9*	52.1	4.993
Heliotrine *N*-oxide	12.5	8.5 - 16.5	330.2	*94.1*	43.9	4.993
Heliotrine *N*-oxide	12.5	8.5 - 16.5	330.2	**110.9**	41.1	4.993
Heliotrine *N*-oxide	12.5	8.5 - 16.5	330.2	*172.1*	29.0	4.993
Seneciphylline	12.1	9.1 - 15.1	334.2	*90.9*	45.7	4.993
Seneciphylline	12.1	9.1 - 15.1	334.2	*94.0*	36.3	4.993
Seneciphylline	12.1	9.1 - 15.1	334.2	*120.0*	28.5	4.993
Seneciphylline	12.1	9.1 - 15.1	334.2	**138.0**	29.9	4.993
Seneciphylline	12.1	9.1 - 15.1	334.2	*306.2*	27.1	4.993
Seneciphylline *N*-oxide	13.0	10.0 - 16.0	350.2	*94.0*	40.3	4.993
Seneciphylline *N*-oxide	13.0	10.0 - 16.0	350.2	*118.0*	32.0	4.993
Seneciphylline *N*-oxide	13.0	10.0 - 16.0	350.2	*120.0*	34.8	4.993
Seneciphylline *N*-oxide	13.0	10.0 - 16.0	350.2	**136.0**	32.9	4.993
Integerrimine	14.2	10.2 - 18.2	336.2	**94.0**	38.3	4.993
Integerrimine	14.2	10.2 - 18.2	336.2	*120.0*	28.9	4.993
Integerrimine	14.2	10.2 - 18.2	336.2	*137.9*	32.1	4.993
Integerrimine	14.2	10.2 - 18.2	336.2	*307.9*	26.9	4.993
Senecivernine	14.4	10.4 - 18.4	336.2	*120.0*	34.8	4.993
Senecivernine	14.4	10.4 - 18.4	336.2	**138.2**	32.2	4.993
Senecivernine	14.4	10.4 - 18.4	336.2	*308.1*	27.1	4.993
Senecionine	14.6	10.6 - 18.6	336.2	*94.0*	38.1	4.993
Senecionine	14.6	10.6 - 18.6	336.2	*120.1*	32.2	4.993
Senecionine	14.6	10.6 - 18.6	336.2	**138.1**	30.2	4.993
Senecionine	14.6	10.6 - 18.6	336.2	*308.0*	26.5	4.993
Senecivernine *N*-oxide	14.8	10.8 - 18.8	352.2	**94.0**	44.1	4.993
Senecivernine *N*-oxide	14.8	10.8 - 18.8	352.2	*95.1*	32.6	4.993
Senecivernine *N*-oxide	14.8	10.8 - 18.8	352.2	*118.0*	34.7	4.993
Senecivernine *N*-oxide	14.8	10.8 - 18.8	352.2	*120.1*	38.5	4.993
Integerrimine *N*-oxide	14.9	10.9 - 18.9	352.2	**94.0**	40.9	4.993
Integerrimine *N*-oxide	14.9	10.9 - 18.9	352.2	*118.1*	33.3	4.993
Integerrimine *N*-oxide	14.9	10.9 - 18.9	352.2	*120.2*	38.2	4.993
Integerrimine *N*-oxide	14.9	10.9 - 18.9	352.2	*136.0*	34.8	4.993
Senecionine *N*-oxide	15.3	11.3 - 19.3	352.2	**94.3**	46.2	5.035
Senecionine *N*-oxide	15.3	11.3 - 19.3	352.2	*118.1*	32.6	5.035
Senecionine *N*-oxide	15.3	11.3 - 19.3	352.2	*120.1*	35.4	5.035
Senecionine *N*-oxide	15.3	11.3 - 19.3	352.2	*136.0*	36.2	5.035
Senecionine *N*-oxide	15.3	11.3 - 19.3	352.2	*138.1*	30.4	5.035
Senkirkine	16.5	12.5 - 20.5	366.2	*70.1*	43.9	5.466

Senkirkine	16.5	12.5 - 20.5	366.2	*150.1*	29.8	5.466
Senkirkine	16.5	12.5 - 20.5	366.2	*153.0*	27.2	5.466
Senkirkine	16.5	12.5 - 20.5	366.2	**168.2**	31.3	5.466
Heliosupine	16.6	12.6 - 20.6	398.2	**120.0**	30.1	5.466
Heliosupine	16.6	12.6 - 20.6	398.2	*220.1*	19.9	5.466
Heliosupine	16.6	12.6 - 20.6	398.2	*336.1*	19.0	5.466
Echimidine *N*-oxide	16.6	12.6 - 20.6	414.2	**254.0**	33.2	5.466
Echimidine *N*-oxide	16.6	12.6 - 20.6	414.2	*352.2*	26.9	5.466
Echimidine *N*-oxide	16.6	12.6 - 20.6	414.2	*395.9*	25.9	5.466
Echimidine	16.9	12.9 - 20.9	398.2	*83.0*	27.3	5.466
Echimidine	16.9	12.9 - 20.9	398.2	**119.9**	25.8	5.466
Echimidine	16.9	12.9 - 20.9	398.2	*336.2*	17.5	5.466
Heliosupine *N*-oxide	17.9	13.9 - 21.9	414.2	**254.2**	31.7	5.466
Heliosupine *N*-oxide	17.9	13.9 - 21.9	414.2	*396.2*	24.7	5.466
Lasiocarpine	19.3	16.3 - 22.3	412.2	**120.0**	29.8	13.051
Lasiocarpine	19.3	16.3 - 22.3	412.2	*219.8*	20.0	13.051
Lasiocarpine	19.3	16.3 - 22.3	412.2	*336.2*	19.1	13.051
Lasiocarpine *N*-oxide	20.2	17.2 - 23.2	428.2	*94.0*	45.5	20.317
Lasiocarpine *N*-oxide	20.2	17.2 - 23.2	428.2	**254.1**	30.8	20.317
Lasiocarpine *N*-oxide	20.2	17.2 - 23.2	428.2	*352.2*	24.4	20.317
Lasiocarpine *N*-oxide	20.2	17.2 - 23.2	428.2	*410.2*	23.6	20.317

List of analytes, precursor, and fragment ions in positive ionization mode for the determination of pyrrolizidine alkaloids using nano-LC-MS (quantifier ions in bold, qualifier ions in italic)

Mass [*m/z*]	Acquisition window [min]	CE	Comment	Fragments [*m/z*]
300.18050	4.0 - 8.5	30	Intermedine	**94.0656**; *138.0911*
300.18050	4.0 - 8.5	30	Indicine	**94.0656**; *138.0911*
300.18050	4.0 - 8.5	30	Echinatine	**94.0656**; *120.0808*
300.18050	4.0 - 8.5	30	Lycopsamine	**94.0656**; *138.0911*
330.19110	5.6 - 8.6	30	Europine	**120.0808**; *138.0911*
346.18600	7.8 - 10.0	30	Europine N-oxide	**111.0682**; *172.0966*
316.17550	7.5 - 11.6	30	Echinatine N-oxide	**94.0656**; *111.0682*
316.17550	7.5 - 11.6	30	Indicine N-oxide	**80.0501**; *94.0656*
316.17550	7.5 - 11.6	30	Intermedine N-oxide	**94.0656**; *138.0911*
316.17550	7.5 - 11.6	30	Lycopsamine N-oxide	**94.0656**; *138.0911*
352.17550	13.3 - 15.1	30	Retrorsine	**120.0808**; *91.0548*
352.17550	13.3 - 15.1	30	Usaramine	**120.0808**; *276.1587*
314.19620	13.8 - 15.6	30	Heliotrine	**94.0656**; *120.0808*
368.17040	14.2 - 15.4	50	Retrorsine N-oxide	**94.0656**; *118.0653*
334.16490	14.6 - 16.6	30	Seneciphylline	**120.0808;** *91.0548*
330.19110	15.4 - 17.0	30	Heliotrine N-oxide	**120.0808**; *94.0656*
350.15980	16.2 - 18.1	30	Seneciphylline N-oxide	**118.0653**; *94.0656*
336.18050	18.1 - 20.8	35	Integerrimine	**94.0656**; *120.0808*
336.18050	18.1 - 20.8	35	Senecivernine	**138.0911**; *120.0808*
336.18050	18.1 - 20.8	35	Senecionine	**94.0656**; *120.0808*
352.17550	19.2 - 20.6	30	Senecivernine N-oxide	**94.0656**; *118.0653*
352.17550	20.4 - 22.3	50	Integerrimine N-oxide	**94.0656**; *118.0653*
352.17550	20.4 - 22.3	50	Senecionine N-oxide	**94.06563**; *118.0653*
414.21220	23.2 - 26.5	30	Echimidine N-oxide	**254.1382**; *352.1751*
414.21220	23.2 - 26.5	30	Heliosupine N-oxide	**254.1382**; *396.2014*
366.19110	23.3 - 25.0	30	Senkirkine	**150.0912;** *70.0659*
398.21730	23.4 - 25.1	30	Heliosupine	**120.0808**; *220.133*
398.21730	23.4 - 25.1	30	Echimidine	**120.0808;** *83.0497*
412.23300	25.6 - 26.5	30	Lasiocarpine	**120.0808**; *220.133*
428.22790	26.5 - 27.4	30	Lasiocarpine N-oxide	**254.1382**; *94.0656*

Nano-LC-MS method validation results for tea matrix. Five-point calibration sets were analyzed for each representative matrix on at least two different days. Trueness, RSD and uncertainty determined from lowest calibration level

Compound	ME, %	LOQ, µg kg^{-1}	Concentration range, µg kg^{-1}	r	RSD, %	Trueness, %	Uncertainty, %
Echimidine	-2.7%	0.6	0.6–40	0.996	17%	-3.8%	8.7%
Echimidine N-oxide	41%	1.9	1.9–40	0.87	46%	-19%	47%
Echinatine	56%	2.9	2.9–40	0.997	18%	-5.9%	27%
Echinatine N-oxide	97%	5.8	5.8–40	0.994	17%	-14%	25%
Europine	22%	2.6	2.6–40	0.97	27%	-2.4%	46%
Europine N-oxide	-4.9%	7.5	7.5–40	0.999	9.2%	-14%	24%
Heliosupine	-4.6%	0.75	0.75–40	0.995	16%	-1.9%	29%
Heliosupine N-oxide	-99%	3.4	3.4–40	0.90	41%	8.9%	50%
Heliotrine	20%	0.95	0.95–40	0.992	11%	-4.6%	20%
Heliotrine N-oxide	-12%	2.3	2.3–40	0.994	10%	-6.9%	20%
Integerrimine	-15%	4.6	4.6–40	0.99	24%	-17%	34%
Integerrimine N-oxide	-97%	20	20–40	0.993	13%	12%	20%
Intermedine	83%	5.5	5.5–40	0.97	27%	18%	24%
Lasiocarpine	-16%	2.1	2.1–40	0.990	19%	1.8%	31%
Lasiocarpine N-oxide	20%	0.52	0.52–40	0.91	35%	-10%	37%
Lycopsamine N-oxide	-84%	0.85	0.85–40	0.992	13%	-8.9%	20%
Retrorsine & Usaramine	-99%	1.8	1.8–40	0.986	18%	4.7%	36%
Retrorsine N-oxide	32%	4.4	4.4–40	0.989	14%	-7.4%	36%
Senecionine	5.3%	13	13–40	0.998	13%	-8.7%	17%
Senecionine N-oxide	66%	7.5	7.5–40	0.98	23%	13%	38%
Seneciphylline	-91%	4.5	4.5–40	0.96	32%	-6.1%	29%
Seneciphylline N-oxide	41%	3.6	3.6–40	0.997	8.0%	-4.1%	21%
Senecivernine	37%	5.7	5.7–40	0.990	13%	-13%	20%
Senecivernine N-oxide	-80%	8.4	8.4–40	0.98	20%	14%	46%
Senkirkine	-56%	11	11–40	0.985	21%	-5.7%	43%
Indicine & Lycopsamine	9.3%	1.2	1.2–40	0.93	37%	-5.7%	43%
Indicine N-oxide & Intermedine N-oxide	-89%	3.7	3.7–40	0.989	10%	-4.3%	16%

Nano-LC-MS method validation results for honey matrix. Five-point calibration sets were analyzed for each representative matrix on at least two different days. Trueness, RSD and uncertainty determined from lowest calibration level

Compound	ME, %	LOQ, µg kg^{-1}	Concentration range, µg kg^{-1}	r	RSD, %	Trueness, %	Uncertainty, %
Echimidine	-52%	0.095	0.095–40	0.98	19%	-13%	19%
Echimidine N-oxide	-30%	0.33	0.33–40	0.98	24%	-16%	24%
Echinatine	16%	1.2	1.2–40	0.97	28%	-13%	28%
Echinatine N-oxide	-30%	1.1	1.1–40	0.98	20%	-13%	20%
Europine	14%	0.29	0.29–40	0.993	22%	-8.0%	22%
Europine N-oxide	-43%	0.57	0.57–40	0.95	32%	-15%	32%
Heliosupine	18%	0.088	0.088–40	0.991	18%	-13%	18%
Heliosupine N-oxide	36%	0.36	0.36–40	0.96	28%	-8.2%	28%
Heliotrine	-17%	0.1	0.1–40	0.999	6.6%	-2.4%	6.6%
Heliotrine N-oxide	-78%	0.33	0.33–40	0.997	14%	-13%	14%
Integerrimine	-53%	0.4	0.4–40	0.988	17%	-8.4%	17%
Integerrimine N-oxide	-27%	0.25	0.25–40	0.991	6.5%	-0.7%	6.5%
Intermedine	24%	0.66	0.66–40	0.999	12%	1.4%	12%
Lasiocarpine	-14%	0.15	0.15–40	0.98	25%	-10%	25%
Lasiocarpine N-oxide	-13%	0.05	0.05–40	0.996	10%	-7.1%	10%
Lycopsamine N-oxide	8.0%	0.13	0.13–40	0.991	14%	5.0%	14%
Retrorsine & Usaramine	50%	0.15	0.15–40	0.993	20%	-7.2%	20%
Retrorsine N-oxide	-23%	0.85	0.85–40	0.991	17%	-11%	17%
Senecionine	-7.2%	2.5	2.5–40	0.986	19%	-5.6%	19%
Senecionine N-oxide	-83%	0.2	0.2–40	0.990	6.2%	0.1%	6.2%
Seneciphylline	-72%	0.62	0.62–40	0.998	10%	-2.8%	10%
Seneciphylline N-oxide	29%	0.35	0.35–40	0.993	16%	-5.0%	16%
Senecivernine	-47%	1.1	1.1–40	0.98	22%	4.5%	22%
Senecivernine N-oxide	18%	0.27	0.27–40	0.992	20%	7.0%	20%
Senkirkine	21%	1.3	1.3–40	0.97	30%	9.2%	30%
Indicine & Lycopsamine	2.1%	0.11	0.11–40	0.993	20%	-14%	20%
Indicine N-oxide & Intermedine N-oxide	32%	0.89	0.89–40	0.989	8.1%	-5.8%	8.1%

Nano-LC-MS method validation results for herbal tincture matrix. Five-point calibration sets were analyzed for each representative matrix on at least two different days. Trueness, RSD and uncertainty determined from lowest calibration level

Compound	ME, %	LOQ, µg kg^{-1}	Concentration range, µg kg^{-1}	r	RSD, %	Trueness, %	Uncertainty, %
Echimidine	14%	8	8–40	0.95	33%	-5.6%	33%
Echimidine N-oxide	3.2%	0.58	0.58–40	0.990	15%	3.7%	15%
Echinatine	5.3%	0.8	0.8–40	0.986	21%	4.2%	21%
Echinatine N-oxide	46%	3.3	3.3–40	0.999	11%	-3.0%	11%
Europine	3.1%	0.4	0.4–40	0.999	12%	1.7%	12%
Europine N-oxide	8.3%	8.8	8.8–40	0.9999	9.0%	-3.0%	9.0%
Heliosupine	10%	10	10–40	0.97	28%	1.3%	28%
Heliosupine N-oxide	-50%	1.8	1.8–40	0.994	6.8%	0.3%	6.8%
Heliotrine	-4.2%	0.32	0.32–40	0.991	8.3%	2.0%	8.3%
Heliotrine N-oxide	-36%	10	10–40	0.94	34%	1.6%	34%
Integerrimine	-75%	0.29	0.29–40	0.98	23%	3.8%	23%
Integerrimine N-oxide	-96%	3	3–40	0.993	10%	0.2%	10%
Intermedine	-8.6%	9	9–40	0.994	10%	-0.8%	10%
Lasiocarpine	3.1%	6.6	6.6–40	0.990	20%	3.3%	20%
Lasiocarpine N-oxide	4.8%	6	6–40	0.95	35%	7.6%	35%
Lycopsamine N-oxide	-83%	4.1	4.1–40	0.998	7.2%	-1.3%	7.2%
Retrorsine & Usaramine	-42%	5.4	5.4–40	0.95	32%	9.0%	32%
Retrorsine N-oxide	6.6%	2.5	2.5–40	0.998	8.3%	3.3%	8.3%
Senecionine	3.5%	5.5	5.5–40	0.992	15%	5.7%	15%
Senecionine N-oxide	0.6%	3	3–40	0.988	17%	-1.3%	17%
Seneciphylline	-93%	8	8–40	0.97	28%	10%	28%
Seneciphylline N-oxide	28%	8	8–40	0.996	17%	-2.1%	17%
Senecivernine	2.8%	3.3	3.3–40	0.986	21%	11%	21%
Senecivernine N-oxide	-16%	3	3–40	0.990	13%	0.9%	13%
Senkirkine	-24%	8	8–40	0.992	9.0%	-1.9%	9.0%
Indicine & Lycopsamine	4.6%	0.41	0.41–40	0.991	8.9%	-0.7%	8.9%
Indicine N-oxide & Intermedine N-oxide	-37%	1.4	1.4–40	0.988	16%	3.2%	16%

Nano-LC-MS method validation results for milk matrix. Five-point calibration sets were analyzed for each representative matrix on at least two different days. Trueness, RSD and uncertainty determined from lowest calibration level

Compound	ME, %	LOQ, µg kg^{-1}	Concentration range, µg kg^{-1}	r	RSD, %	Trueness, %	Uncertainty, %
Echimidine	-19%	0.092	0.092–40	0.996	17%	4.1%	17%
Echimidine N-oxide	9.4%	0.32	0.32–40	0.86	46%	15%	46%
Echinatine	-2.4%	0.66	0.66–40	0.993	18%	-12%	18%
Echinatine N-oxide	-14%	1.1	1.1–40	0.995	17%	-0.1%	17%
Europine	-0.7%	0.25	0.25–40	0.97	27%	-17%	27%
Europine N-oxide	-0.4%	0.54	0.54–40	0.999	9.2%	-8.1%	9.2%
Heliosupine	-2.8%	0.097	0.097–40	0.98	16%	14%	16%
Heliosupine N-oxide	-12%	0.33	0.33–40	0.88	41%	-4.8%	41%
Heliotrine	5.8%	0.14	0.14–40	0.98	11%	-6.0%	11%
Heliotrine N-oxide	13%	0.33	0.33–40	0.994	10%	-2.7%	10%
Integerrimine	27%	0.5	0.5–40	0.98	24%	-5.8%	24%
Integerrimine N-oxide	3.2%	0.23	0.23–40	0.994	13%	-0.7%	13%
Intermedine	-4.7%	0.74	0.74–40	0.96	27%	6.2%	27%
Lasiocarpine	0.1%	0.25	0.25–40	0.992	19%	-11%	19%
Lasiocarpine N-oxide	5.9%	0.027	0.027–40	0.94	35%	-29%	35%
Lycopsamine N-oxide	-0.9%	0.1	0.1–40	0.990	13%	8.3%	13%
Retrorsine & Usaramine	-6.0%	0.14	0.14–40	0.98	18%	-8.9%	18%
Retrorsine N-oxide	4.4%	0.77	0.77–40	0.98	14%	0.5%	14%
Senecionine	1.1%	1.1	1.1–40	0.9998	13%	-6.6%	13%
Senecionine N-oxide	-23%	0.21	0.21–40	0.97	23%	-8.1%	23%
Seneciphylline	-13%	0.37	0.37–40	0.93	32%	-28%	32%
Seneciphylline N-oxide	-14%	0.29	0.29–40	0.999	8.0%	-5.1%	8.0%
Senecivernine	3.3%	0.57	0.57–40	0.97	13%	-4.7%	13%
Senecivernine N-oxide	-2.4%	0.29	0.29–40	0.989	20%	-5.6%	20%
Senkirkine	-1.1%	0.49	0.49–40	0.97	21%	12%	21%
Indicine & Lycopsamine	-0.7%	0.5	0.5–40	0.93	37%	38%	37%
Indicine N-oxide & Intermedine N-oxide	-13%	0.22	0.22–40	0.98	10%	-4.1%	10%

A list of analyte precursor ions and fragment ions for the determination of PFAS

Compound	Retention Time (min)	Precursors (*m/z*)	Products (*m/z*)	Collision Energy (V)
PFHxS	14.1	398.9	79.9537*	50
			98.9516	
PFOA	12.8	413.0	368.9668*	10
			168.9883	20
PFNA	14.3	463.0	418.9626*	10
			218.9795	20
PFOS	17.0	498.9	79.9558*	60
			98.9542	
$^{13}C_6$-PFHxS	14.1	405.0	98.9515	50
$^{13}C_8$-PFOS	17.0	507.0	79.9536	60
$^{13}C_8$-PFOA	12.7	421.0	171.9937	20
$^{13}C_5$-PFNA	14.3	472.0	426.9881	10

* - quantifier ion

Validation results of the nano-LC – nano-ESI – Orbitrap-MS method for different food groups (the spiking concentrations are given on a wet weight (w.w.) basis)

Food group	Meat and seafood		Milk and dairy products		Eggs		Fruits and vegetables		Grains and bread	
	Spike 0.1 ng g^{-1} w.w.		Spike 0.01 ng g^{-1} w.w.		Spike 0.3 ng g^{-1} w.w.		Spike 0.001 ng g^{-1} w.w.		Spike 0.01 ng g^{-1} w.w.	
Compound	Recovery (n=10), %	RSD (n=10), %	Recovery (n=10), %	RSD (n=10), %	Recovery (n=10), %	RSD (n=10), %	Recovery (n=10), %	RSD (n=10), %	Recovery (n=10), %	RSD (n=10), %
PFOA	107	9	112	16	103	11	108	17	87	17
PFHxS	112	12	115	13	109	12	118	18	108	9
PFNA	97	17	103	15	90	17	87	16	85	16
PFOS	107	14	103	16	111	15	109	17	104	17
	Spike 0.5 ng g^{-1} w.w.		Spike 0.05 ng g^{-1} w.w.		Spike 1.5 ng g^{-1} w.w.		Spike 0.005 ng g^{-1} w.w.		Spike 0.05 ng^{-1} w.w.	
Compound	Recovery (n=10), %	RSD (n=10), %	Recovery (n=10), %	RSD (n=10), %	Recovery (n=10), %	RSD (n=10), %	Recovery (n=10), %	RSD (n=10), %	Recovery (n=10), %	RSD (n=10), %
PFOA	109	12	107	15	98	9	82	14	83	14
PFHxS	98	14	108	16	107	8	101	9	99	16
PFNA	92	8	98	12	83	14	96	17	91	18
PFOS	109	17	106	13	96	8	117	17	91	12
	Spike 2.5 ng g^{-1} w.w.		Spike 0.25 ng g^{-1} w.w.		Spike 7.5 ng g^{-1} w.w.		Spike 0.025 ng g^{-1} w.w.		Spike 0.25 ng^{-1} w.w.	
Compound	Recovery (n=10), %	RSD (n=10), %	Recovery (n=10), %	RSD (n=10), %	Recovery (n=10), %	RSD (n=10), %	Recovery (n=10), %	RSD (n=10), %	Recovery (n=10), %	RSD (n=10), %
PFOA	103	9	107	11	102	7	116	14	97	16
PFHxS	108	17	111	12	109	16	113	13	98	9
PFNA	95	11	98	13	91	17	84	15	88	10
PFOS	110	16	115	12	107	13	112	8	83	12

PUBLICATIONS

Application of nano-LC – nano-ESI – Orbitrap-MS for trace determination of four priority PFAS in food products considering recently established tolerable weekly intake (TWI) limits

Zacs, D.; **Fedorenko, D.**; Pasecnaja, E.; Bartkevics, V. *Analytica Chimica Acta*[1] **2023**, 341027.

[1] *Peer reviewed journal, imprint of Elsevier (IF= 6.911 (2022)), ISSN: 1873-4324*

Analytica Chimica Acta 1251 (2023) 341027

Contents lists available at ScienceDirect

Analytica Chimica Acta

journal homepage: www.elsevier.com/locate/aca

Application of nano-LC – nano-ESI – Orbitrap-MS for trace determination of four priority PFAS in food products considering recently established tolerable weekly intake (TWI) limits

Dzintars Zacs *, Denis Fedorenko, Elina Pasecnaja, Vadims Bartkevics

Institute of Food Safety, Animal Health and Environment "BIOR", Lejupes Iela 3, Riga, LV-1076, Latvia

HIGHLIGHTS

- Ultra trace determination of four priority PFAS in foods is presented.
- Nanoscale LC – Orbitrap-MS is an efficient tool for analysis of PFAS.
- AcCeptable performance characteristics were obtained for all target PFAS.
- Recoveries between 83 and 118% and repeatability between 7 and 18% were obtained.
- Method met the criteria stated in EU 2022/1428 and EU 2022/1431.

GRAPHICAL ABSTRACT

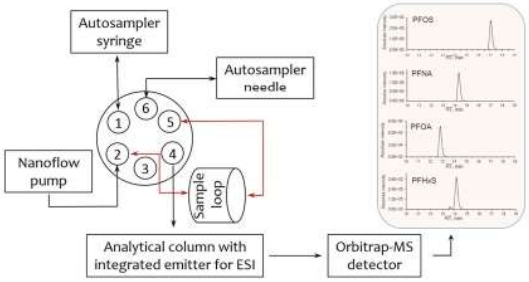

ARTICLE INFO

Handling Editor: Dr. L. Liang

Keywords:
Nanoscale liquid chromatography
Orbitrap mass spectrometry
Per- and polyfluoroalkyl substances (PFAS)
Tolerable weekly intake
Food products

ABSTRACT

An analytical method was developed and validated for the analysis of four priority perfluoroalkyl substances (PFAS), namely, perfluorooctanoic acid (PFOA), perfluorononanoic acid (PFNA), perfluorohexanesulfonic acid (PFHxS), and perfluorooctanesulfonate (PFOS) in food products using nanoscale liquid chromatography (nano-LC) coupled with nanoscale electrospray ionization (nano-ESI) and Orbitrap mass spectrometry (Orbitrap-MS) detection. The efficiency of two different nano-LC setups for chromatographic separation of selected PFAS was evaluated. The optimal LC separation of analytes was achieved using a reversed phase C18 (RP-C18) nano bore column with an integrated emitter. The effect of matrix concentration factor on signal suppression/enhancement was evaluated for different matrices. The method validation indicated analyte recoveries in the range 83–118% and within-laboratory reproducibility from 7 to 18%, while reanalysis of the materials from proficiency tests (PTs) showed that the accuracy of the obtained concentrations ranged from 85 to 124% of the provided consensus values. The method limits of quantification (m-LOQs) were set as first validation levels ranging from 0.001 to 0.3 ng g^{-1} sample depending on the type of the food group. The observed method performance characteristics met the criteria stated in Commission Regulation (EU) 2022/1428, Commission Recommendation (EU) 2022/1431, as well as Guidance Document on Analytical Parameters for the Determination of Per- and Polyfluoroalkyl Substances (PFAS) in Food and Feed with regards to the compliance testing of PFAS maximum levels (MLs) and monitoring purposes. The elaborated method was applied for the analysis of selected priority PFAS in different food groups collected from the Latvian retail market.

* Corresponding author.
E-mail address: dzintars.zacs@bior.lv (D. Zacs).

https://doi.org/10.1016/j.aca.2023.341027
Received 1 December 2022; Received in revised form 15 February 2023; Accepted 26 February 2023
Available online 2 March 2023

1. Introduction

During the past decades, a number of per- and polyfluorinated compounds (PFAS) have been commercially produced and extensively used for many industrial purposes and consumer-related applications (e.g., textiles, firefighting foams, food packaging) [1]. According to recent studies, more than 5000 PFAS substances have been identified [2], while about 7300 tons of various PFAS have been released into the environment over the last 60 years according to conservative estimates [3]. Due to the high stability of fluorine-carbon bonds in their structures, these compounds are known to resist degradation and metabolism, whereas their bioaccumulative properties [4] have resulted in ubiquitous presence in various biological and environmental media, including those from remote areas as well as in food products and human tissues [1,5]. Dietary exposure has been recognized as one of the essential pathways of PFAS exposure for humans [6–8] and since some PFAS representatives exhibit potential adverse health effects in humans, control of these chemicals in food is of great relevance. Historically, perfluorooctane sulfonic acid (PFOS) and perfluorooctanoic acid (PFOA) have been the most studied PFAS representatives [9–11]. In 2008, the European Food Safety Authority (EFSA) established a tolerable daily intake (TDI) of 150 ng kg^{-1} body weight (b.w.) day^{-1} for PFOS and 1500 ng kg^{-1} b.w. day^{-1} for PFOA, respectively [12]. The TDI levels were derived in 2008 from the occurence data available at that time, which were rather limited and the intake levels were based on a subchronic study in *Cynomolgus* monkeys. By evaluating recent toxicological studies, including possible human health impacts and the newest occurrence data, EFSA derived separate tolerable weekly intakes (TWI) for PFOS and PFOA and dramatically decreased the recommended intake limits [13,14]. The recommended TWI limits were reduced as follows: by a factor of 81 for PFOS (from 1050 ng kg^{-1} bw.wk^{-1} to 13 ng kg^{-1} bw.wk^{-1}) and by a factor of 1750 for PFOA (from 10500 ng kg^{-1} bw.wk^{-1} to 6 ng kg^{-1} bw.wk^{-1}) [13]. Thereafter, in 2020, EFSA Panel on Contaminants in the Food Chain (CONTAM Panel) addressed the risk assessment for other PFAS and reviewed the risk assessment of the previous Opinion by applying a mixture approach. Based on several similar effects in animals, toxicokinetics, the observed levels in human blood, as well as occurrence data, two additional compounds apart from PFOA and PFOS were included in the PFAS priority list, namely, perfluorononanoic acid (PFNA) and perfluorohexane sulfonic acid (PFHxS). Thereafter, the CONTAM Panel established TWI of 4.4 ng kg^{-1} b.w.wk^{-1} for the sum of selected four PFAS [15]. Considering the updated TWI limits, it could be concluded that there is a strong need to control ultra-trace levels of selected PFAS in food products while special attention should be paid to matrices with high relative proportion in the food basket (e.g., milk, fruits and vegetables). In order to promote data collection relevant to the newly proposed TWI limits, Commission conceptually endorsed amendment of Regulation (EC) No 1881/2006 [16] regarding the maximum levels (MLs) for PFAS in certain foodstuffs, while addressing the respective criteria for analytical method performance in Regulation (EU) 2022/1428 [17] and Recommendation (EU) 2022/1431 [18]. According to newly established legislation, method limits of quantification (m-LOQs) for certain food groups should be reduced down to few pg g^{-1} on product basis.

The currently applied PFAS analysis methods rely on liquid chromatography coupled with mass spectrometry (LC-MS). Even though the detection limits of these methods are in the sub-ppb range [19], generally they are far too high to allow meaningful exposure assessment considering the recently proposed TWI values [13,15]. Typically, high performance or ultra-high performance chromatography (HPLC or UHPLC) is used for separation, while selective detection is ensured by applying tandem MS (MS/MS) or high resolution MS (HRMS) systems equipped with electrospray ionization (ESI) sources [19]. However, it is well known that the analytical performance of LC-ESI-MS based methods at ultra-trace levels could be substantially affected by ion suppression phenomena when complex objects, such as food products are analyzed [20]. In order to overcome analytical difficulties related to matrix effects, the technical advantages of nanoscale LC (nano-LC) techniques coupled with nano-ESI and MS detection have become commercially available in recent years [21,22]. Nano-LC coupled with nano-ESI and MS is a well-established miniaturized analytical technique in food analysis.Nano-LC-MS offers improved separation of analytes with unprecedented sensitivity and specificity, which far exceed those for conventional LC-MS. This instrumental solution ensures higher tolerance to signal suppression effects by using of nano-LC columns (e.g., 75–500 μm i.d. and 10–15 cm long) for which the flow rates of nL min^{-1} are typically applied [23]. The significant reduction of the ESI flow rate leads to increased ionization and transfer efficiency while nano-ESI results not only in enhanced concentration sensitivity but also provides better resistance to ionization suppression effects over conventional LC-ESI conducted at higher flow rates. Besides improved sensitivity, higher signal-to-noise (S/N), and lower LOQs, nano-LC-MS also significantly decreases solvent consumption, which reduces costs and emerges as an environmentally friendly alternative to available separation methods. Taking into account the great potential of nano-LC coupled with nano-ESI and HRMS, this technique may support the development of highly sensitive and efficient analytical methods that will enable the monitoring of PFAS at trace levels in food products and will support the strategic tools for reducing PFAS human dietary intake below the established TWI [15]. Since there is no comprehensive information available regarding the analytical capabilities of nanoscale LC techniques in PFAS analysis, the principal aim of this study was to propose a new analytical method for quantitative determination of four priority PFAS (PFOA, PFNA, PFHxS, and PFOS) in food products using nano-LC coupled with nano-ESI and Orbitrap-MS, with a special emphasis on achieving the method sensitivity required to control the human dietary intake of selected PFAS.

2. Experimental

2.1. Chemicals and materials

Standard methanolic solutions of the individual native analytes, namely, PFOA, PFNA, PFHxS, and PFOS and their ^{13}C-labeled surrogates which were used as internal standards were purchased from Cambridge Isotope Laboratories, Inc. (Andover, MA, USA). Stock solutions were prepared in methanol and were stored at −18 °C. HPLC grade methanol and acetonitrile were purchased from Sigma-Aldrich Chemie GmbH (Buchs, Switzerland). Ammonium formate, formic acid, sodium hydroxide, as well as 25% aqueous ammonia were obtained from Acros (Morris Plains, NJ, USA). High purity water (18.2 MΩ cm) was prepared using a Millipore Milli-Q purification system (Billerica, MA, USA). Calibration solution sets were prepared by serial dilution of stock solutions in methanol. For the pre-concentration and clean-up steps, Strata-X-AW 33 μm 200 mg/3 mL (Phenomenex, Torrance, CA, USA) SPE cartridges with weak anion-exchange sorbent were used.

2.2. Samples

A multitude of food samples representing products available on the Latvian retail market were analyzed using the elaborated method. Sample collection was conducted during the period from January to September 2022. The samples were coded and transported to the laboratory at +4 °C. Upon receiving, the solid samples were homogenized in a food blender (Kenwood FP101T, Kenwood Ltd., UK). The homogenates were packed into polyethylene bags and stored at −18 °C. Aliquots of sample homogenates obtained from samples of fruits, vegetables, and berries were freeze-dried using a Beta 2–8 LSCplus freeze dryer (Martin Christ GmbH, Osterode am Harz, Germany) for 48 h prior to the analysis. Milk samples were homogenized prior to the analysis by vigorous mixing. Organic extracts of the samples were analyzed on the day of sample preparation.

2.3. Sample extraction and clean-up

2.3.1. Control of background contamination

In order to reduce the possible background contamination originating from instrumentation, the capillaries and tubes of the LC system were replaced wherever possible with spare parts made of HDPE, PEEK or metal. As a result of these measures, the analysis of standard solutions containing only isotopically labeled surrogates at concentrations equivalent to those in the final extracts of real samples did not show the presence of native analytes. Nevertheless, despite the attempts to completely eliminate any possible background artifacts by washing the glassware with organic solvents, procedural blanks that were included in each sample sequence frequently indicated the presence of PFOA and PFOS and these levels were also considered setting the respective m-LOQs that were agreed as a lowest validation level for all tested matrices. The results from real samples were corrected by subtracting the PFAS content of the procedural blanks analyzed in respective sample sequence.

2.3.2. Sample extraction

The following sample aliquots of selected matrices were taken for the analysis: fruits and vegetables – 70 g; grains and bread – 10 g; milk and dairy products – 15 g; fish, meat, and eggs – 2 g. In order to reduce the sample volume of fruits and vegetables, the weighed aliquots were freeze-dried prior to the sample extraction step. Portions of homogenized samples were weighed in 50 mL PP tubes (in case of fruits and vegetables sample aliquot was equally distributed over two PP tubes) and spiked with 100 μL of methanolic solution containing ^{13}C-isotopically labeled PFAS (20 pg μL^{-1} of each surrogate). After equilibration for 30 min, acetonitrile (15 mL) and 0.2 M NaOH solution (1 mL) were added to each sample and the tubes were vigorously mixed before performing two extraction cycles using sonication (each cycle for 15 min). In order to remove the bulk of lipids and other high molecular mass compounds, the extracted samples were first centrifuged for 10 min at 3500 rpm, frozen out at −80 °C for 30 min, and again centrifuged for 10 min at 4700 rpm. Immediately after centrifugation, the organic extracts were decanted into a 250 mL graduated glass volumetric flask, diluted with reagent grade water to 250 mL and 100 μL of formic acid was added to each sample. The samples were applied at a flow rate of ~5 mL min^{-1} on the top of Strata-X-AW 33 μm 200 mg/3 mL SPE cartridges that were provisionally conditioned with 3 mL of 1% NH_4OH in MeOH, 3 mL of MeOH, and 3 mL of reagent grade water. After the sample loading, the columns were washed with 2% formic acid (1 mL) and MeOH (3 mL), dried for 30 min under vacuum, and the analytes were eluted with 6 mL of 1% NH_4OH in MeOH to a 10 mL glass vial. The eluted extracts were concentrated to dryness under a stream of nitrogen at 30 °C, reconstituted in 200 μL of the initial mobile phase of the nano-LC system, vortexed for 30 s and centrifuged at 3500 rpm for 10 min. After centrifugation, the extracts were transferred into a 2.5 mL PP tube and centrifuged again at 20 000 rpm for 10 min (4 °C) in order to remove dispersed solid particles from the extracts. The supernatants after the centrifugation were transferred into chromatographic vials and immediately subjected to instrumental analysis.

2.4. Nano-LC – nano-ESI – Orbitrap-MS analysis

The instrumental analysis was performed using an UltiMate 3000 RSLCnano system coupled to a Orbitrap Focus mass spectrometer (Thermo Scientific, Bremen, Germany). The chromatographic separation was performed on an EASY-Spray PepMap™ (Thermo Scientific, Waltham, MA, USA) nano-LC capillary column (150 × 0.075 mm, 3 μm particle size) with an integrated emitter. The column temperature was kept at 25 °C and the mobile phase was composed of (A) 5 mM ammonium formate in LC-MS grade water and (B) 5 mM ammonium formate in 95% LC-MS grade acetonitrile with 5% LC-MS grade water. The mobile phase flow rate was held constant at 500 nL min^{-1}. The gradient began at the initial composition (A/B) of 75:25 (v/v), which was linearly ramped to A/B ratio of 1:99 (v/v) over a 19.3 min period, where it was held for 9.0 min before returning to the initial conditions over 0.5 min. The column was equilibrated with the initial A/B ratio of 75:25 (v/v) for 10.0 min between the runs. A 1000 nL sample loop was used and the injection volume of 1000 nL in a loop overfill option was applied both for the standard solutions and the sample extracts. The mass spectra were recorded in negative ion mode. Orbitrap-MS detection in parallel reaction monitoring (PRM) mode was used for quantitative determination of the selected PFAS using the two most abundant transitions for the analyzed compounds and one transition for the respective ^{13}C-labeled surrogate. The width of the ion extraction window was 5 × 10^{-6} amu (5 ppm). External calibration of the Orbitrap-MS system was performed weekly over the *m/z* range of 50–2000 according to the guidelines of the instrument manufacturer. The details of the optimized instrumental conditions are summarized in Table 1.

2.5. Quality assurance/quality control

Analyte identification was based on their retention times and isotopic peak ratios of the monitored ion transitions. The acceptable deviation of the isotope ratio of two monitored transitions (target/confirmation) was set as 30% of the average value obtained for the calibration standards from same sequence. Six-point calibration curves over the concentration range of 0.5–100 pg μL^{-1} were used for the quantitation of analytes in each analytical sequence. At the end of the analytical sequence the calibration middle point was analyzed to check the system performance and the validity of calibration setting the acceptable calculated concentration within ±20% of the theoretical value. Quantitation was carried out based on isotope dilution with ^{13}C-labeled surrogates and internal standardization. To control the suitability of the obtained results for quantification, the chromatographic peak areas of ^{13}C-labeled internal standards were checked for each sample. Quantification was performed only in case if ample showing

Table 1
The optimized instrumental nano-LC – nano-ESI – Orbitrap-MS analysis conditions (negative ionization mode) for the determination of selected PFAS.

<!–Col Count:2–>Nano-ESI conditions					
Capillary temperature				200 °C	
Spray voltage				2.0 kV	
S-lens radio frequency				60 arbitrary units	
Orbitrap-MS conditions					
Maximum injection time				50 ms	
Automatic gain control (AGC target)				1 × 10^6	
Detection mode				PRM	
MS resolution				17.5 K (FWHM)	
Default charge state				1	
Microscans				1	
Component	RT, min	Quant. trace, (*m/z* → *m/z*)	HCD, %	Qual. trace, (*m/z* → *m/z*)	HCD, %
PFOA	12.8	413.0 → 368.9668	10	413.0 → 168.9883	20
PFHxS	14.1	398.9 → 79.9537	50	398.9 → 98.9516	50
PFNA	14.3	463.0 → 418.9626	10	463.0 → 218.9795	20
PFOS	17.0	498.9 → 79.9558	60	498.9 → 98.9542	50
$^{13}C_8$-PFOA (ISTD)	12.8	421.0 → 171.9937	20	–	–
$^{13}C_6$-PFHxS (ISTD)	14.1	405.0 → 98.9515	50	–	–
$^{13}C_5$-PFNA (ISTD)	14.3	472.0 → 426.9881	10	–	–
$^{13}C_8$-PFOS (ISTD)	17.0	507.0 → 79.9536	60	–	–

Analyte and surrogate retention time, transitions, and the higher-energy collisional dissociation (HCD) energy values.

peak areas of internal standards ≥30% of the mean peak areas of the ^{13}C-labeled surrogates obtained from a six-point calibration curve. In order to evaluate the ongoing recovery of target analytes, spiked samples and materials of previous proficiency tests (PT) were included in the QC protocol on routine basis and were also included in each sample sequence. Procedural blanks with added internal standards were analyzed in each sample sequence and were prepared without matrix by using only the reagents from the analytical protocol and were taken through all steps of the analytical procedure. Each sample sequence consisted of maximum twelve samples including one procedural blank, one QC sample and ten food samples, and was limited by the design of the manifold used for the SPE procedure.

3. Results and discussion

3.1. Selection of the nano-LC setup

The variety of commercially available columns for nano-LC applications is currently very limited, while the majority of common commercially available nano-LC columns are packed with C18 stationary phase (RP-C18) [24]. Considering that RP-C18 is one of the most efficient and the most frequently used stationary phases in the analysis of PFAS under HPLC and UHPLC conditions [19,25], two different RP-C18 based nano-LC fluidics setups available from Thermo Scientific were tested: 1) *Acclaim PepMap* C18 capillary column with connected *EASY-Spray* transfer line and 2) *EASY-Spray* C18 capillary column with an integrated emitter. Fig. 1 illustrates the principal schemes of both nano-LC setups. The ionization processes implemented in nano-LC analysis have a similar physical basis to common LC-MS instrumentation where the most critical performance criterion is the ionization efficiency of analyte molecules. While capillaries with applied voltage are used in regular LC-MS systems, efficient electrospray under the nano-LC-MS conditions can be achieved with nano-spray emitters that feature miniaturized capillaries. It should be considered that the efficiency of chromatographic separation in nano-LC is critically affected by the presence of dead volume nodes in the setup. Any additional lengths of capillaries and any added connections, even in the case of zero dead volume, produce inferior quality of separation and broadening of chromatographic peaks. Acceptable chromatographic separation and optimal peak shapes were observed when employing *EASY-Spray* column with an integrated emitter, while *Acclaim PepMap* column with a connected transfer line and emitter showed less effective separation (Fig. 1). Along with the solvent composition of the injected extract, the initial gradient conditions and the dilution of extracts were found to significantly influence the quality of separation and detection. It should be noted that, in order to achieve effective chromatography, the final

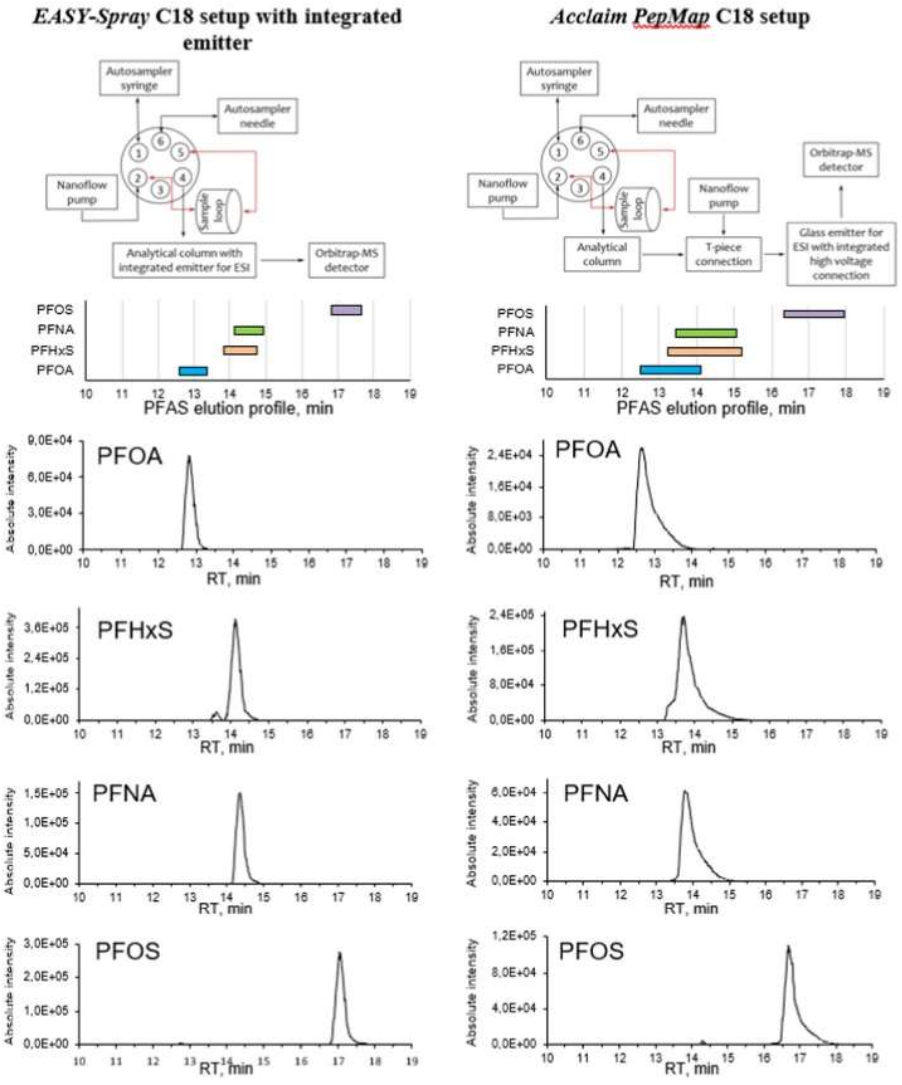

Fig. 1. The principal schemes of two nano-LC-MS sets and the observed chromatograms of selected PFAS.

extracts of real food samples were reconstituted in the initial mobile phase containing a relatively high proportion of water. In this case, residual amounts of high molecular mass matrix components remained in the sample extracts after clean-up. While these residues were poorly soluble in aqueous solvent mixtures, they could precipitate during the storage of the final extracts and bind analytes from the liquid phase, especially considering the strong affinity of PFAS to protein-rich media [26]. This could considerably affect the method sensitivity, therefore immediate instrumental analysis of reconstituted final sample extracts is strongly advised. It should be also noted that the application of centrifugal or syringe disk filters for the removal of dispersed solid particles from the sample extracts should be carefully evaluated due to the potential of some filter materials to adsorb PFAS, resulting in additional method uncertainties and sensitivity losses. The experimental results regarding the adsorption of selected PFAS by some filters are presented in Fig. S1. It was concluded that the available centrifugal filters had a significant adsorption potential for selected PFAS, while the application of syringe disk filters was hindered by the relatively small volumes of sample extracts. Therefore, filtration of sample extracts was avoided and centrifugation at 20 000 rpm for 10 min (4 °C) for the removal of solid particles was chosen.

Overloading the column with matrix extract should be avoided in the selected nano-LC-MS setup with integrated emitter since the contamination of column and emitter significantly reduce the electrospray efficiency and result in the formation of mobile phase droplets on the tip of the emitter. If system contamination occurs and the electrospray performance is affected, the setup can be recovered by flushing with voltage applied and washing the emitter tip with pure isopropanol. Switching between polarities during the flushing enhances the regeneration by diffusion of isopropanol along the emitter away from the ion source, resulting in an additional controlled wash of the emitter tip. Fig. S2 represents the mobile phase beading at the tip of the emitter and normal emitter operation during the applied electrospray voltage and eluent flow.

3.1.1. Selecting the operating mode of Orbitrap-MS instrument

The Orbitrap-MS instrument supports different detection modes both for the molecular ions or product ions produced while using the tandem-MS option. The efficiency of three different detection modes were provisionally evaluated: Full-MS (full scan) over the specified m/z range, targeted-SIM (t-SIM), and the PRM, which provided MS/MS experiments. Considering the efficiency of the additional m/z isolation step when t-SIM and PRM modes were applied, reducing of the undesirable background from the obtained ion current was expected, providing better sensitivity and selectivity compared to the Full-MS mode. An additional benefit of the PRM mode was the possibility of MS/MS option that ensured a complementary element of selectivity. Taking into account that the current method was developed for the monitoring of target PFAS components and there was no requirement for scanning modes, the application of the PRM mode with MS resolving power of 17.5 K (FWHM) was chosen as the most favorable option in terms of sensitivity and selectivity.

3.1.2. Optimization of Nano-ESI and Orbitrap-MS parameters in the PRM mode

In order to ensure effective ion transmission in the Orbitrap-MS system after ejecting from the nano-ESI source, S-lens ion optics (the so-called stacked-ring ion guide) should be carefully optimized. It was found that effective transfer of the analyte fragments could be achieved in the radiofrequency level range of 50–70, with the optimal value of 60. Effective performance of the Orbitrap-MS detection could be achieved by paying special attention to "automatic gain control (AGC)", which controls the number of ions transferred to the analyzer and the "maximum injection time" parameter, which limits the ion accumulation time in the C-trap prior to HRMS analysis. Theoretically optimal sensitivity and scan rate of Orbitrap-MS analyzer can be achieved by targeting high ion count (e.g., 1×10^6) and short accumulation time (<50 ms). A combination of these cross-linked parameters [27,28] should be critically optimized in order to avoid the "space charging" effect in the Orbitrap and obtaining the highest possible scan rate. Incorrect setting of these parameters will result to two terminal scenarios (i) if the relatively high ion count (e.g., 1×10^6): is selected for the increasing of sensitivity requiring a long accumulation time (e.g., >300 ms), it could reduce the scanning speed of the system, thus affecting the instrumental reproducibility; (ii) if the injection frequency of ion flux controlled by the "maximum injection time" will be too short (e.g., <50 ms) in combination with insufficient filling of the Orbitrap analyzer with ions, this will degrade both the sensitivity (due to the decreasing of analyte ions in the trap) and instrumental response reproducibility (due to the total ion current (TIC) variations). It was concluded that the optimal scan rate and sensitivity under the selected nanoscale LC conditions could be achieved by keeping the AGC target at 1×10^6 ions and limiting the maximum injection time to 50 ms. HCD energies were further optimized for the analytes in order to achieve the maximal instrumental response for the specific transitions during the MS/MS recording. The MS/MS spectra of selected PFAS were in agreement with previously reported fragmentation patterns [29,30] revealing dominant product fragments $[SO3]^-$ and $[FSO3]^-$ for sulfonates and $[CxF2x+1]^-$ for carboxylates, respectively. The ion transitions used for the determination of selected PFAS are listed in Table 1.

3.2. Selection of SPE cartridge, signal suppression/enhancement effect, matrix concentration factor

In our previous study, we compared the efficiency of different SPE cartridges in the analysis of PFAS in complex matrices [31]. Based on this knowledge, Strata-X-AW 33 μm 200 mg/3 mL SPE cartridges were selected in the current study as the best compromise in terms of the matrix removal potential, recovery performance, and cost.

One of the most important factors that can affect the sensitivity of LC-MS analysis is the effect of signal suppression/enhancement caused by matrix components and, therefore, the matrix concentration/dilution factor (expressed in grams of sample per milliliter of the final volume of the sample extract). In order to evaluate the signal suppression/enhancement effect observed by applying different matrix concentration factors for each food group, different sample weights of each matrix type ($n = 3$) were treated according to the sample preparation protocol (Section 2.3.2). The final extracts were reconstituted in 200 μL of ^{13}C-labeled internal standard solution (c = 10 pg μL^{-1} for each PFAS) before the instrumental analysis and the concentrations were calculated by applying external calibration method versus ^{13}C-labeled surrogate standard solution of equal concentration (i.e., 10 pg μL^{-1} for each PFAS). Such an approach was chosen due to the unavailability of PFAS-free representative matrices and taking into consideration that ^{13}C-labeled surrogates behaved analogously to the native analytes in the presence of matrix components. For all the examined food groups except the fruits/vegetables group, the matrix concentration factor was evaluated in the range from 1 to 10 (e.g., with the final extract volume of 200 μL, sample aliquots from 0.20 to 2.0 g were taken for the analysis). Since the water content in fruit and vegetable matrices was typically quite high (up to 95%), while the proposed LOQ values were rather low (0.005–0.015 pg g^{-1} w.w., depending on the component), the effect of matrix concentration factor was evaluated in the range from 5 to 50 (e.g., a sample intake from 1.0 to 10 g for the final volume of 200 μL). As shown in Fig. 2, depending on the matrix concentration factor, both signal suppression and enhancement could be observed for different matrix types. Signal suppression was more pronounced upon increasing the applied concentration factor, reaching a suppression of up to 15% for some PFAS in certain matrices (e.g., eggs and milk). Signal enhancement was expressed for almost all compounds in the matrix concentration factor range from 1 to 5, except for the fruit and vegetable group, for which signal enhancement was observed over the concentration factor

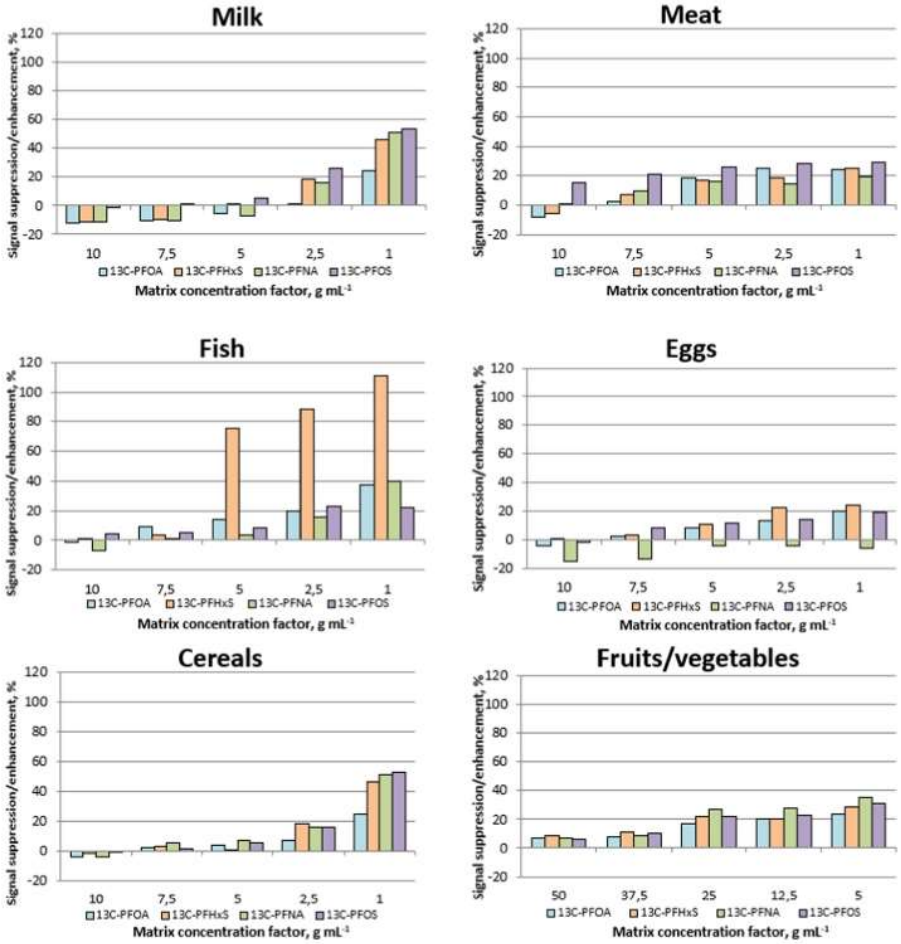

Fig. 2. The effect of applied matrix concentration factor on the signal suppression/enhancement.

range up to 50. These differences in the observed effect of matrix concentration could be explained with the complexity of the analyzed sample extracts where some of matrix components tend to suppress ionization of analytes, while others enhance the ionization, resulting in non-linear dependence of ionization on matrix component concentration in the analyzed sample extracts. Therefore, the applied matrix concentration factor should be carefully optimized during method development, since an excessive sample aliquot taken for the analysis will cause undesirable signal suppression and possible overloading or damage to the LC column, while extreme dilution of sample aliquot will not allow to reach the required ultra-low LOQs, even considering the signal enhancement effect.

While the conventional sample preparation procedure for food products based on the extraction and isolation of PFAS components using SPE has been proven to be efficient in the analysis of most food matrices, freezing the sample extract at −80 °C before the SPE procedure can be beneficial. A freeze-out step at low temperature ensures additional removal of co-extracted fats and other components that have limited solubility in acetonitrile, reducing the possible instrumental background and improving the detection of analytes of interest while significantly increasing the lifetime of the nano bore column. No significant signal suppression/enhancement effects were observed by inclusion of the freeze-out step in the sample preparation procedure, but interfering background matrix signals could be reduced in some cases (Fig. S3), proving that the freezing of acetonitrile sample extract prior to SPE procedure can result in better method selectivity.

3.3. Validation

Method validation was based on the provisions of the recently developed Guidance Document on Analytical Parameters for the Determination of Per- and Polyfluoroalkyl Substances (PFAS) in Food and Feed [32]. Validation was performed using real samples of the appropriate matrix groups. The results of spiking experiments were corrected by taking into account the concentrations of blank samples. A minimum of five batches of different matrices representing one product group (e.g., meat and seafood or milk and dairy products) were spiked at three concentration levels (1 × targeted m-LOQ, 5 × targeted m-LOQ, and 25 × targeted m-LOQ) and analyzed in two separate analytical sequences. The validation scheme is summarized in Table S1. The apparent recovery and within-laboratory reproducibility were examined for each fortification level. The m-LOQs were set as the lowest validated level of individual PFAS for each product group. The lowest recommended validation levels for different product groups have been reviewed elsewhere [18,32], taking into account the recent toxicological findings regarding selected PFAS and the recently established TWI values.

An objective assessment of instrumental LOD and LOQ (i-LOD and i-LOQ) relying on the S/N ratio as a criterion in the case of target *m/z* fragment extraction from the Orbitrap-MS raw data within 5 ppm of the theoretical values is not appropriate in many cases due to the typical absence of any background noise on the observed chromatograms [33,34]. Therefore, in the first approximation, the i-LOD values were assessed from injecting 0.8 pg of each analyte on the column, considering the dynamic range of the Orbitrap-MS and taking into account that

only signals above the intensity of 1×10^4 could be used for reliable detection. The i-LODs were calculated by the extrapolation of concentrations corresponding to the intensities of 1×10^4 from the intensities observed by on-column injection. The i-LOQs were defined as 3 × i-LOD and for the most intensive PRM transitions were equal to 0.05 pg for PFOA, 0.04 pg for PFNA, 0.03 pg for PFHxS, and 0.02 pg for PFOS.

A linearity over the concentration range of 0.5–1000 pg μL^{-1} was observed for selected PFAS with correlation coefficients ≥0.995 and residual values of less than 20%. Due to the ubiquity of some PFAS in blank matrices and procedural blanks, the use of solvent-matched calibration solution is likely preferable for quantitation. There were no significant differences in the calibration curves obtained by matrix-matched and solvent-matched linearity experiments (the difference of slope values was 1–3% depending on the individual PFAS), therefore six-point solvent-matched calibration solution set covering the concentration range of 0.5–100 pg μL^{-1} was used for routine samples in each sample sequence.

Procedural blanks were prepared in each analytical sequence to assess the contamination present during the sample treatment. It was concluded that PFOA and PFOS were frequently present as background contamination, while PFNA and PFHxS were not detected. The levels of this background contamination in procedural blanks over the period of method development are summarized in Table S2 and were considered setting the m-LOQs. As it could be seen, the achievement of recommended m-LOQs could be obstructed for some matrices (e.g. fruits and vegetables) due to the ubiquitous presence of PFOA in procedural blanks.

The results of the spiking experiments show that the mean apparent recovery values for target analytes ranged from 83 to 118%, while the within-laboratory reproducibility expressed as RSDs was in the range of 7–18% (Table 2). The data derived from the analyses of materials that underwent interlaboratory testing within the framework of proficiency tests (PTs) for the determination of PFAS in food organized by the European Union Reference Laboratory for Halogenated POPs (Freiburg, Germany) were in a good agreement with the provided consensus values (Fig. 3). Four PT materials representing three matrices were analyzed by the developed method: wheat flour, pork liver, and liquid whole egg. The accuracy calculated as a percentage of the measured concentration versus the consensus value (when consensus values were not available the median value was taken) was in the range of 85–124%, with RSDs from 3 to 17%. The observed performance characteristics of the method demonstrated that generally it could be used for both monitoring purposes and compliance testing of maximum levels for selected food groups according to the requirements of Regulation (EU) 2022/1428 [17], provisions of Recommendation (EU) 2022/1431 [18], and the Guidance Document on Analytical Parameters for the Determination of Per- and Polyfluoroalkyl Substances (PFAS) in Food and Feed [32].

3.4. Application to real samples

The developed analytical method was applied for the testing of 119 food samples representing the most consumed food groups such as milk and dairy products, meat, eggs, fish and seafood, fruits and vegetables, as well as bread and cereals. The summary of the observed concentrations of selected PFAS is presented in Table 3. While detailed interpretation of the observed data is outside the scope of the present work, some generalization of the results would be appropriate. All analyzed foods showed the presence of PFAS, although the frequency of detection and the relative distribution varied depending on the specific PFAS representative and the type of food. While the main focus of the developed method was intended for compliance testing of four priority PFAS in food at the maximum permissible levels according to the recently adopted legislation and guidelines, reporting the occurrence of these chemicals below the established m-LOQs could be also of interest for monitoring purposes and for the creation of datasets relevant to possible toxicological reevaluation of PFAS in the future. Therefore, an overview of this information is also presented. Food products of plant origin was less contaminated with the selected PFAS, generally showing concentrations below the m-LOQ, while products of animal origin showed more pronounced presence of these contaminants. As expected, fish and

Table 2
Validation results of the nano-LC – nano-ESI – Orbitrap-MS method for different food groups (the spiking concentrations are given on a wet weight (w.w.) basis).

Food group	Meat and seafood		Milk and dairy products		Eggs		Fruits and vegetables		Grains and bread	
1st validation level (target LOQ)										
Compound	Spike 0.1 ng g^{-1} w.w.		Spike 0.01 ng g^{-1} w.w.		Spike 0.3 ng g^{-1} w.w.		Spike 0.001[a] ng g^{-1} w.w.		Spike 0.01[b] ng g^{-1} w.w.	
	Recovery (n = 10), %	RSD (n = 10), %	Recovery (n = 10), %	RSD (n = 10), %	Recovery (n = 10), %	RSD (n = 10), %	Recovery (n = 10), %	RSD (n = 10), %	Recovery (n = 10), %	RSD (n = 10), %
PFOA	107	9	112	16	103	11	108	17	87	17
PFHxS	112	12	115	13	109	12	118	18	108	9
PFNA	97	17	103	15	90	17	87	16	85	16
PFOS	107	14	103	16	111	15	109	17	104	17
2nd validation level (target LOQ × 5)										
Compound	Spike 0.5 ng g^{-1} w.w.		Spike 0.05 ng g^{-1} w.w.		Spike 1.5 ng g^{-1} w.w.		Spike 0.005 ng g^{-1} w.w.		Spike 0.05 ng^{-1} w.w.	
	Recovery (n = 10), %	RSD (n = 10), %	Recovery (n = 10), %	RSD (n = 10), %	Recovery (n = 10), %	RSD (n = 10), %	Recovery (n = 10), %	RSD (n = 10), %	Recovery (n = 10), %	RSD (n = 10), %
PFOA	109	12	107	15	98	9	82	14	83	14
PFHxS	98	14	108	16	107	8	101	9	99	16
PFNA	92	8	98	12	83	14	96	17	91	18
PFOS	109	17	106	13	96	8	117	17	91	12
3rd validation level (target LOQ × 25)										
Compound	Spike 2.5 ng g^{-1} w.w.		Spike 0.25 ng g^{-1} w.w.		Spike 7.5 ng g^{-1} w.w.		Spike 0.025 ng g^{-1} w.w.		Spike 0.25 ng^{-1} w.w.	
	Recovery (n = 10), %	RSD (n = 10), %	Recovery (n = 10), %	RSD (n = 10), %	Recovery (n = 10), %	RSD (n = 10), %	Recovery (n = 10), %	RSD (n = 10), %	Recovery (n = 10), %	RSD (n = 10), %
PFOA	103	9	107	11	102	7	116	14	97	16
PFHxS	108	17	111	12	109	16	113	13	98	9
PFNA	95	11	98	13	91	17	84	15	88	10
PFOS	110	16	115	12	107	13	112	8	83	12

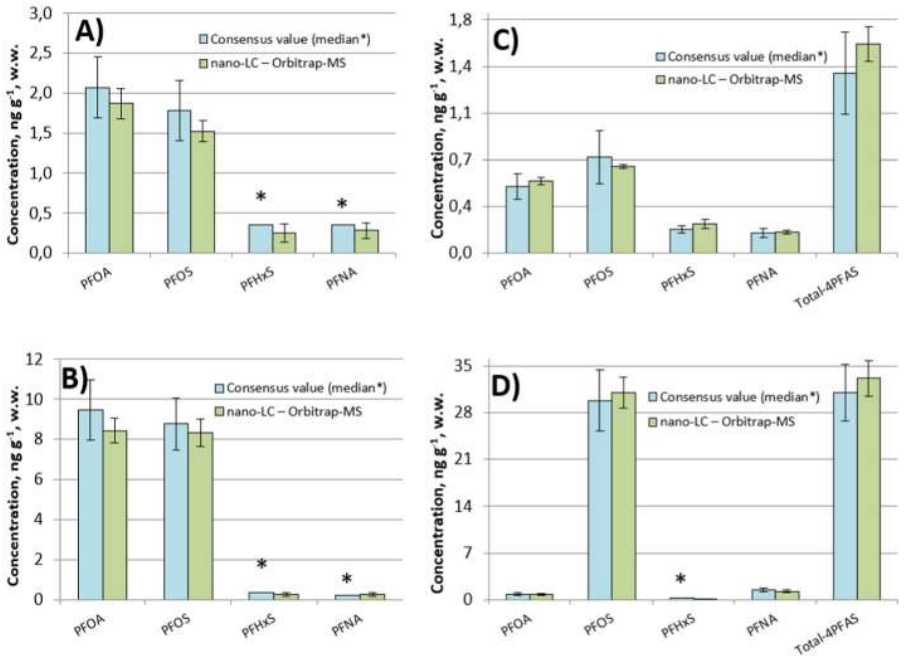

Fig. 3. Method performance in the analysis of EURL-PT reference materials: A) Wheat Flour 2019 (1903-WFA-063); B) Wheat Flour 2019 (1903-WFB-038); C) Liquid Whole Egg 2021 (2102-LWE-006/010); D) Pork Liver 2022 (2201-PL-168).

Table 3
The observed occurrence of four priority PFAS in different food groups (concentrations expressed on a w.w. basis and given in ng g^{-1}).

Compound	Min[a] - max	Median[a]	Mean[a]	Detection frequency[b], %	Detected concentration range below the m-LOQ[c]
Fruits, vegetables and fungi (n = 30)					
PFOA	<0.002–0.005	<0.002	<0.002	20	0.0004–0.0007
PFHxS	<0.001–0.002	<0.001	<0.001	7	ND
PFNA	<0.001	<0.001	<0.001	0	ND
PFOS	<0.001	<0.001	<0.001	0	ND
Total 4 PFAS (lowerbound)	<0.001–0.005	<0.001	<0.001	–	–
Grains, bread and vegetable oils (n = 22)					
PFOA	<0.015	<0.015	<0.015	50	0.001–0.005
PFHxS	<0.01	<0.01	<0.01	0	ND
PFNA	<0.01–0.05	<0.01	<0.01	46	0.003–0.004
PFOS	<0.01–0.01	<0.01	<0.01	5	ND
Total 4 PFAS (lowerbound)	<0.01–0.05	<0.01	<0.01	–	–
Milk and dairy products (n = 21)					
PFOA	<0.01–0.01	<0.01	<0.01	43	0.001–0.002
PFHxS	<0.01–0.03	<0.01	0.01	33	ND
PFNA	<0.01–0.01	<0.01	<0.01	10	0.003
PFOS	<0.01–0.05	<0.01	<0.01	24	0.001–0.003
Total 4 PFAS (lowerbound)	<0.01–0.10	<0.01	0.01	–	–
Eggs (n = 8)					
PFOA	<0.30	<0.30	<0.30	25	0.003
PFHxS	<0.30	<0.30	<0.30	100	0.004–0.06
PFNA	<0.30	<0.30	<0.30	0	ND
PFOS	<0.30	<0.30	<0.30	38	0.005–0.03
Total 4 PFAS (lowerbound)	<0.30	<0.30	<0.30	–	–
Meat (n = 19)					
PFOA	<0.10	<0.10	<0.10	16	0.001–0.004
PFHxS	<0.10–0.20	<0.10	0.10	63	0.004–0.01
PFNA	<0.10	<0.10	<0.10	0	ND
PFOS	<0.10–0.16	<0.10	<0.10	47	0.01–0.03
Total 4 PFAS (lowerbound)	<0.10–0.20	0.10	0.10	–	–
Fish and seafood (n = 19)					
PFOA	<0.10–6.6	0.27	0.86	68	ND
PFHxS	0.10–0.25	0.10	<0.10	100	0.02–0.05
PFNA	<0.10–0.54	<0.10	<0.10	21	0.03
PFOS	0.20–5.7	1.2	2.2	100	ND
Total 4 PFAS (lowerbound)	0.17–12.4	2.0	3.2	–	–

[a] – only concentrations above or equal to m-LOQ are considered.
[b] – including results below the m-LOQ.
[c] – indicative values.

seafood showed the highest concentrations of PFAS, revealing the presence of the most studied PFAS representatives PFOA and PFOS in all samples from this food group. Generally, the prevalence of sulfonic acids over carboxylic acids was observed for samples of animal origin, which was in agreement with the different bioaccumulative properties of these PFAS classes [35]. By summarizing the observed occurrence of four priority PFAS in the analyzed food groups it can be concluded that the contamination levels and patterns were generally similar to those found in recent studies from different European countries [36].

4. Conclusions

This work represents method development for the trace determination of four priority PFAS in a wide range of food product groups using nano-LC – nano-ESI – Orbitrap-MS techniques. Sample preparation conditions, chromatographic separation of the selected PFAS, as well as their detection were optimized during the method development. The extensively validated methodology was found to be selective, sensitive, and readily applicable to a wide range of food products. Additional confidence was gained by the analysis of PT materials. The observed method performance generally met the criteria stated in Commission Regulation (EU) 2022/1428, Commission Recommendation (EU) 2022/1431, as well as the Guidance Document on Analytical Parameters for the Determination of Per- and Polyfluoroalkyl Substances (PFAS) in Food and Feed. Therefore, this method can be applied as an effective tool for monitoring and compliance testing of PFAS MLs in food. The elaborated method was applied for the analysis of selected four priority PFAS in different food groups collected from the Latvian retail market, providing the first data on the occurrence of these contaminants in the Baltic states and creating the opportunity to perform preliminary risk assessment and to inform regulatory bodies.

CRediT authorship contribution statement

Dzintars Zacs: Methodology, Formal analysis, Data curation, Writing – review & editing. **Denis Fedorenko:** Methodology, Formal analysis, Data curation, Writing – review & editing. **Elina Pasecnaja:** Methodology, Formal analysis, Data curation, Writing – review & editing. **Vadims Bartkevics:** Conceptualization, Methodology, Funding acquisition, Formal analysis, Data curation, Writing – original draft, Writing – review & editing.

Declaration of competing interest

The authors declare that they have no known competing financial interests or personal relationships that could have appeared to influence the work reported in this paper.

Data availability

Data will be made available on request.

Appendix A. Supplementary data

Supplementary data to this article can be found online at https://doi.org/10.1016/j.aca.2023.341027.

References

[1] P. De Voogt, M. Saez, Analytical chemistry of perfluoroalkylated substance, Trends Anal. Chem. 25 (2006) 326–342, https://doi.org/10.1016/j.trac.2005.10.008.

[2] Y. Liu, L.A. D'Agostino, Q. Guangbo, J. Guibin, J.W. Martin, High-resolution mass spectrometry (HRMS) methods for nontarget discovery and characterization of poly- and per-fluoroalkyl substances (PFASs) in environmental and human samples, Trends Anal. Chem. 121 (2019), 115420, https://doi.org/10.1016/j.trac.2019.02.021.

[3] M. Villagrasa, M.L. De Alda, D. Barcelo, Environmental analysis of fluorinated alkyl substances by liquid chromatography–(tandem) mass spectrometry: a review, Anal. Bioanal. Chem. 386 (2006) 953–972, https://doi.org/10.1007/s00216-006-0471-9.

[4] B. Jurado-Sanchez, E. Ballesteros, M. Gallego, Semiautomated solid-phase extraction followed by derivatisation and gas chromatography–mass spectrometry for determination of perfluoroalkyl acids in water, J. Chromatogr. A 1318 (2013) 65–71, https://doi.org/10.1016/j.chroma.2013.10.034.

[5] C.M. Butt, U. Berger, R. Bossi, G.T. Tomy, Review: levels and trends of poly- and perfluorinated compounds in the arctic environment, Sci. Total Environ. 408 (2010) 2936–2965, https://doi.org/10.1016/j.scitotenv.2010.03.015.

[6] I. Ericson, R. Marti-Cid, M. Nadal, B. Van Bavel, G. Lindstrom, J.L. Domingo, Human exposure to perfluorinated chemicals through the diet: intake of perfluorinated compounds in foods from the Catalan (Spain) market, J. Agric. Food Chem. 56 (2008) 1787–1794, https://doi.org/10.1021/jf0732408.

[7] L.S. Haug, S. Salihovic, I.E. Jogsten, C. Thomsen, B. van Bavel, G. Lindstrom, G. Becher, Levels in food and beverages and daily intake of perfluorinated compounds in Norway, Chemosphere 80 (2010) 1137–1143, https://doi.org/10.1016/j.chemosphere.2010.06.023.

[8] R. Vestergren, U. Berger, A. Glynn, I.T. Cousins, Dietary exposure to perfluoroalkyl acids for the Swedish population in 1999, 2005 and 2010, Environ. Int. 49 (2012) 120–127, https://doi.org/10.1016/j.envint.2012.08.016.

[9] R.C. Buck, J. Franklin, U. Berger, J.M. Conder, I.T. Cousins, P. De Voogt, A. A. Jensen, K. Kannan, S.A. Mabury, S.P. Van Leeuwen, Perfluoroalkyl and polyfluoroalkyl substances in the environment: terminology, classification, and origins, Integrated Environ. Assess. Manag. 7 (2011) 513–541, https://doi.org/10.1002/ieam.258.

[10] C. Lau, K. Anitole, C. Hodes, D. Lai, A. Pfahles-Hutchens, J. Seed, Perfluoroalkyl acids: a Review of monitoring and toxicological findings, Toxicol. Sci. 99 (2007) 366–394, https://doi.org/10.1093/toxsci/kfm128.

[11] A.G. Paul, K.C. Jones, A.J. Sweetman, A first global production, emission, and environmental inventory for perfluorooctane sulfonate, Environ. Sci. Technol. 43 (2009) 386–392, https://doi.org/10.1021/es802216n.

[12] EFSA, European Food Safety Authority, Perfluorooctane sulfonate (PFOS), perfluorooctanoic acid (PFOA) and their salts Scientific Opinion of the Panel on Contaminants in the Food chain, EFSA J. 6 (2008) 653, https://doi.org/10.2903/j.efsa.2008.653.

[13] EFSA, European Food Safety Authority, Risk to human health related to the presence of perfluorooctane sulfonic acid and perfluorooctanoic acid in food, EFSA J. 16 (5194) (2018) 284, https://doi.org/10.2903/j.efsa.2018.5194.

[14] S.E. Fenton, A. Ducatman, A. Boobis, J.C. DeWitt, C. Lau, C. Ng, J.S. Smith, S. M. Roberts, Per- and polyfluoroalkyl substance toxicity and human health review: current state of knowledge and strategies for informing future research, Environ. Toxicol. Chem. 40 (2021) 606–630, https://doi.org/10.1002/etc.4890.

[15] EFSA, European Food Safety Authority, Risk to human health related to the presence of perfluoroalkyl substances in food, EFSA J. 18 (6223) (2020) 391, https://doi.org/10.2903/j.efsa.2020.6223.

[16] European Commission, Commission regulation (EC) No 1881/2006 of 19 december 2006 setting maximum levels for certain contaminants in foodstufs, OJ L 364 20 (2006) 12.

[17] European Commission, Commission Implementing Regulation (EU) 2022/1428 of 24 August 2022 laying down methods of sampling and analysis for the control of perfluoroalkyl substances in certain foodstuffs, OJ L 221 (2022) 66–73.

[18] European Commission, Commission Recommendation (EU) 2022/1431 of 24 August 2022 on the monitoring of perfluoroalkyl substances in food, OJ L 221 (2022) 105–109.

[19] Md Al Amin, Z. Sobhani, Y. Liu, R. Dharmaraja, S. Chadalavada, R. Naidu, J. M. Chalker, C. Fang, Recent advances in the analysis of per- and polyfluoroalkyl substances (PFAS) – a review, Environ. Technol. Innovat. 19 (2020), 100879, https://doi.org/10.1016/j.eti.2020.100879.

[20] H. Trufelli, P. Palma, G. Famiglini, A. Cappiello, An overview of matrix effects in liquid chromatography-mass spectrometry, Mass Spectrom. Rev. 30 (2011) 491–509, https://doi.org/10.1002/mas.20298.

[21] D. Fedorenko, V. Bartkevics, Recent applications of nano-liquid chromatography in food safety and environmental monitoring: a review, Crit. Rev. Anal. Chem. (2021) 1–25, https://doi.org/10.1080/10408347.2021.1938968, 0.

[22] Y. Saito, K. Jinno, T. Greibrokk, Capillary columns in liquid chromatography: between conventional columns and microchips, J. Separ. Sci. 27 (2004) 1379–1390, https://doi.org/10.1002/jssc.200401902.

[23] C. Aydogan, Nanoscale separations based on LC and CE for food analysis: a review, Trends Anal. Chem. 121 (2019), 115693, https://doi.org/10.1016/j.trac.2019.115693.

[24] S.R. Wilson, C. Olsen, E. Lundanes, Nano liquid chromatography columns, Analyst 144 (2019) 7090–7104, https://doi.org/10.1039/c9an01473j.

[25] J.M. Weiss, I. Van der Veen, S.P.J. Van Leeuwen, W. Cofino, S. Crum, J. De Boer, Analytical improvements shown over four interlaboratory studies of perfluoroalkyl substances in environmental and food samples, Trends Anal. Chem. 43 (2013) 204–216, https://doi.org/10.1016/j.trac.2012.10.005.

[26] B.C. Kelly, M.G. Ikonomou, J.D. Blair, B. Surridge, D. Hoover, R. Grace, F.A.P. C. Gobas, Perfluoroalkyl contaminants in an arctic marine food web: trophic magnification and wildlife exposure, Environ. Sci. Technol. 43 (2009) 4037–4043, https://doi.org/10.1021/es9003894.

[27] A. Kalli, G.T. Smith, M.J. Sweredoski, S. Hess, Evaluation and optimization of mass spectrometric settings during data-dependent acquisition mode: focus on LTQ-Orbitrap mass analyzers, J. Proteome Res. 12 (2013) 3071–3086, https://doi.org/10.1021/pr3011588.

[28] G. Munoz, S.V. Duy, H. Budzinski, P. Labadie, J. Liu, S. Sauve, Quantitative analysis of poly- and perfluoroalkyl compounds in water matrices using high

resolution mass spectrometry: optimization for a laser diode thermal desorption method, Anal. Chim. Acta 881 (2015) 98–106, https://doi.org/10.1016/j.aca.2015.04.015.

[29] R. Guo, Q. Zhou, Y. Cai, G. Jiang, Determination of perfluorooctanesulfonate and perfluorooctanoic acid in sewage sludge samples using liquid chromatography/quadrupole time-of-flight mass spectrometry, Talanta 75 (2008) 1394–1399, https://doi.org/10.1016/j.talanta.2008.01.052.

[30] T.J. Hensema, B.J.A. Berendsen, S.P.J. Van Leeuwen, Non-targeted identification of per- and polyfluoroalkyl substances at trace level in surface water using fragment ion flagging, Chemosphere 265 (2021), 128599, https://doi.org/10.1016/j.chemosphere.2020.128599.

[31] D. Zacs, V. Bartkevics, Trace determination of perfluorooctane sulfonate and perfluorooctanoic acid in environmental samples (surface water, wastewater, biota, sediments, and sewage sludge) using liquid chromatography–Orbitrap mass spectrometry, J. Chromatogr. A 1473 (2016) 109–121, https://doi.org/10.1016/j.chroma.2016.10.060.

[32] EURL for halogenated POPs in feed and food, Guidance Document on Analytical Parameters for the Determination of Per- and Polyfluoroalkyl Substances (PFAS) in Food and Feed, 2022 version 1.2 of 11 May 2022. Available online under, https://eurl-pops.eu/core-working-groups#_pfas.

[33] A. Thomas, H. Geyer, W. Schanzer, C. Crone, M. Kellmann, T. Moehring, M. Thevis, Sensitive determination of prohibited drugs in dried blood spots (DBS) for doping controls by means of a benchtop quadrupole/Orbitrap mass spectrometer, Anal. Bioanal. Chem. 403 (2012) 1279–1289, https://doi.org/10.1007/s00216-011-5655-2.

[34] S.M. Lehner, N.K.N. Neumann, M. Sulyok, M. Lemmens, R. Krska, R. Schuhmacher, Evaluation of LC-high-resolution FT-Orbitrap MS for the quantification of selected mycotoxins and the simultaneous screening of fungal metabolites in food, Food Addit. Contam. 28 (2011) 1457–1468, https://doi.org/10.1080/19440049.2011.599340.

[35] I. Zabaleta, E. Bizkarguenaga, A. Prieto, M. Ortiz-Zarragoitia, L.A. Fernandez, O. Zuloaga, Simultaneous determination of perfluorinated compounds and their potential precursors in mussel tissue and fish muscle tissue and liver samples by liquid chromatography–electrospray-tandem mass spectrometry, J. Chromatogr. A 1387 (2015) 13–23, https://doi.org/10.1016/j.chroma.2015.01.089.

[36] E. Pasecnaja, V. Bartkevics, D. Zacs, Occurrence of selected per-and polyfluorinated alkyl substances (PFASs) in food available on the European market–A review on levels and human exposure assessment, Chemosphere 287 (2022), 132378, https://doi.org/10.1016/j.chemosphere.2021.132378.

Dilute-and-shoot approach for determination of several biomarkers and pharmaceuticals in wastewater using nanoflow liquid chromatography – Orbitrap mass spectrometry

Fedorenko, D.; Podjava, A.; Prikulis, A.; Bartkevics, V. *Journal of Separation Science*[2] **2023**, 46:2201002.

[2] *Peer reviewed journal, imprint of John Wiley & Sons (IF= 3.614 (2022)), ISSN: 1615-9314*

Received: 6 December 2022 | Revised: 16 March 2023 | Accepted: 19 March 2023

DOI: 10.1002/jssc.202201002

JOURNAL OF SEPARATION SCIENCE

RESEARCH ARTICLE

Dilute-and-shoot approach for determination of several biomarkers and pharmaceuticals in wastewater using nanoflow liquid chromatography – Orbitrap mass spectrometry

Deniss Fedorenko[1,2] | **Antons Podjava**[1,2] | **Arvis Prikulis**[1,2] | **Vadims Bartkevics**[1,2]

[1]Institute of Food Safety, Animal Health, and Environment "BIOR", Riga, Latvia

[2]Faculty of Chemistry, University of Latvia, Riga, Latvia

Correspondence
Deniss Fedorenko, Postal address: Lejupes iela 3, Riga, LV-1076, Latvia.
Email: deniss.fedorenko@bior.lv

A new method for quantitative analysis of several biomarkers and pharmaceutical compounds in wastewater has been developed employing nanoflow liquid chromatography with Orbitrap mass spectrometry. An easy dilute-and-shoot approach has been used for sample preparation with a dilution factor of 5. Improved retention of ionic and highly polar compounds has been achieved by the addition of tetrabutylammonium bromide as an ion pair reagent into the final diluted sample. The new nanoflow liquid chromatography method has demonstrated low matrix effects (70%–111%), high sensitivity in terms of limits of quantification (0.005 to 0.3 μg/L), low injection volume (70 nl) and solvent consumption, and the ability to analyze diverse polar and ionic analytes within one run using a single reversed-phase nanoflow liquid chromatography column. Wastewater samples (n = 116) from the wastewater treatment plants of different cities in Latvia were analyzed using the developed method. The observed concentrations of biomarkers were in line with the literature data.

KEYWORDS
biomarkers, ion-pair reagent, nanoflow liquid chromatography, Orbitrap mass spectrometry, wastewater

1 | INTRODUCTION

The analysis of metabolites and pharmaceutical compounds in wastewater (WW) provides a comprehensive view of the well-being and lifestyle habits of a population. The elucidation of changes in these characteristics forms the basis of the WW-based epidemiology approach (WBE). There are different classes of food, stress, lifestyle, health, and population biomarkers [1] commonly used in WBE. The main criteria for a compound to be used as a biomarker in WBE are its stability, specificity to human metabolism, applicability among different regions, and observed presence at acceptable detection levels [1, 2]. The use of the WBE approach is also beneficial for pandemic outbreaks, for example, for coronavirus disease 2019 surveillance in addition to diagnostic testing [3]. Several population and lifestyle biomarkers, such as 5-hydroxy-indolic acid (5-HIAA) [4], ethyl sulfate [5], cotinine [6], gabapentin [7], caffeine [8], as well as non-steroidal anti-inflammatory drugs such as diclofenac and ibuprofen

Article Related Abbreviations: 5-HIAA, 5-hydroxy-indolic acid; AGC, automatic gain control; FS, full scan; IT, ion injection time; MEs, matrix effects; nano-LC, nanoflow liquid chromatography; PVDF, polyvinylidene fluoride; TBAB, tetrabutylammonium bromide; WBE, wastewater-based epidemiology approach; WW, wastewater.

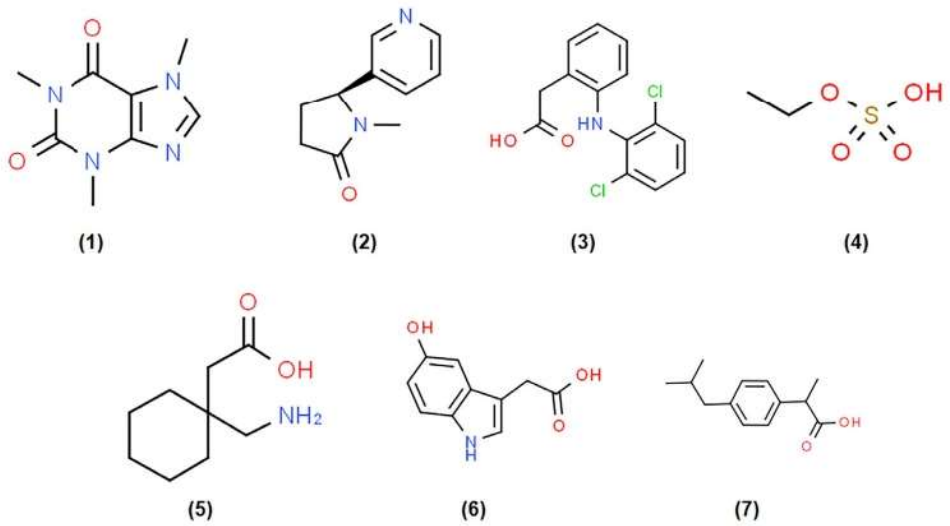

FIGURE 1 The chemical structures of pharmaceuticals and biomarkers analyzed in this study: caffeine (1), cotinine (2), diclofenac (3), ethyl sulfate (4), gabapentin (5), 5-hydroxy-indolic acid (5-HIAA) (6), ibuprofen (7).

[9–11], provide information on consumption habits and allow the estimation of population size.

The analysis of WW is challenging because of the complexity of the matrix and the typically low concentrations of the analytes of interest in the sample. Currently, the most common sample preparation techniques for WW analysis include SPE and evaporation to perform sample clean-up and pre-concentration [12–14]. The dilute-and-shoot approach is one of the possible sample preparation procedures that include filtration of the samples as well as dilution with mobile phase or other solvents [15]. This approach brings several key benefits, such as reduced sample preparation time, reduced consumption of materials and lower analysis costs, low matrix effects (MEs), and applicability. There is also the possibility to include multiclass analytes due to the more inclusive sample treatment (if any) since other sample treatment steps are typically more selective for a certain range of compounds. The use of nanoflow LC (nano-LC) in environmental sample analysis has been limited so far, however, it may provide several important advantages over other types of chromatography [16]. Typically, the use of nano-LC reduces the number of sample preparation steps and decreases MEs while simultaneously improving the sensitivity due to the reduced inner diameter of the analytical column and lower chromatographic dilution [17–19].

In this study, a new nano-LC Orbitrap MS method was developed for the quantitative determination of pharmaceuticals, population, and lifestyle biomarkers in WW. The main advantages of the method include good sensitivity and a simple and fast sample preparation procedure. Additionally, the use of nano-LC combined with Orbitrap MS for WW sample analysis is rather limited in the literature. Taking into account that the use of in-sample addition of ion-pair reagent in order to improve the retention of highly polar compounds in nano-LC has not been published in the literature to date, we demonstrate that this approach combined with the dilute-and-shoot methodology can be very efficient for quantitative analysis of pharmaceuticals and biomarkers in WW.

2 | MATERIALS AND METHODS

2.1 | Materials, reagents, and samples

LC-MS grade ACN and water were obtained from Merck (Darmstadt, Germany), and formic acid (99%)—from VWR International (Radnor, PA, USA). LC-MS grade water was used for preparing the solution of tetrabutylammonium bromide (TBAB), for the dilution of WW samples, and for the preparation of mobile phases. The standard of ibuprofen was obtained from Dr. Ehrenstorfer (Germany), while other standards including caffeine, cotinine, diclofenac sodium salt, ethyl sulfate sodium salt, gabapentin, and 5-HIAA were obtained from Sigma-Aldrich (Germany). The purity of the substances ranged from 98% to 99.6%. TBAB (> 98% purity) was obtained from Sigma-Aldrich (Germany). The chemical structures of the compounds from the ChemSpider database are presented in Figure 1. Stock solutions of the compounds at the concentrations of 1000 and 1 μg/L were prepared in LC-MS grade methanol. The standards were stored at −20°C temperature. The WW samples were obtained from WW treatment plants in various cities and towns of Latvia, including Jelgava, Liepaja, Valmiera, Ventspils, Jekabpils, Jurmala, Riga, Rezekne, Daugavpils, Salaspils, and Tukums.

2.2 | Sample preparation procedure using the dilute-and-shoot approach

Wastewater samples were mixed and filtered through a polyvinylidene fluoride (PVDF, Phenomenex) syringe filter with a pore size of 0.2 μm. The samples were then transferred into 2 ml Eppendorf tubes and centrifugated at 20 000 rpm at 4°C temperature. The samples were transferred into glass HPLC vials and aliquots of TBAB solution, ammonium acetate solution, and water were added. The final concentrations of TBAB and ammonium acetate in the vial were 11 and 10 mM, respectively, with the sample dilution factor equal to 5.

2.3 | Nano-LC Orbitrap MS instrumental parameters for the analysis of biomarkers and pharmaceuticals in WW

The analysis of pharmaceuticals and biomarkers was performed using an UltiMate 3000 RSLCnano nano-LC (Thermo Scientific, Waltham, MA, USA) chromatography system coupled to an Orbitrap Focus mass spectrometer (Thermo Scientific) equipped with a nanoflow EASY-Spray ionization source. Full loop injections of 70 nl using overfill mode requiring 1000 nl of the sample were performed. The temperature inside the autosampler was set at 10°C. The chromatographic separations were carried out using a Thermo Scientific PepMap capillary column (150 × 0.075 mm) packed with 3 μm C_{18} bonded silica particles. The mobile phase A consisted of a mixture of 10 mM ammonium acetate, 0.01% (v/v) acetic acid, and 1% (v/v) MeCN dissolved in LC-MS grade water, while the mobile phase B was LC-MS grade MeCN (B). The following gradient program at 500 nl min^{-1} flow rate was used for the separations: 0–1 min 5% B, 1–11 min 5%–35% B, 11–13.5 min 35%–80% B, 13.5–26 min 80% B, 26–27 min 80%–5% B, and 27–45 min 5% B.

Q Exactive Focus Orbitrap mass spectrometer (Thermo Scientific) equipped with an EASY-Spray nano-ESI source was used for the detection of analytes. Data acquisition was performed in full scan mode over the *m/z* range from 100 to 350 at a resolution of 70 000. Fast polarity switching was used during the run to detect positively and negatively charged analyte ions. The data acquisition parameters and the MS voltages were optimized during the method development experiments. The ion injection time (IT) was set at 300 ms. The ion transfer capillary temperature was 200°C, the RF lens level was 60, automatic gain control (AGC) target was 3×10^6. The spray voltage was set at +2.26 kV for positive and −1.70 kV for negative ionization mode. A list of analyte precursor ions is provided in Table S1.

2.4 | Analytical parameters of the developed method

Trueness, repeatability, and reproducibility of the method were determined using a WW sample with a standard addition method using a 2-day validation approach at 10 and 50 μg/L ($n = 6$ for each) levels. Validation results are presented in Table S2. Trueness was estimated at two levels according to Equation (1).

$$Trueness = \frac{C_{sp,average}}{C_{sp}} \cdot 100\% \quad (1)$$

where $C_{sp,average}$ is the average calculated concentration of the spike determined from repeated measurements ($n = 6$) at two spiking levels (C_{sp}) of 10 and 50 μg/L, respectively.

The MEs were estimated by comparison of the slopes of the calibration curves obtained for neat standard solutions (a_{std}) and a WW sample spiked with standards ($a_{std\ addition}$) at comparable concentrations. The following Equation (2) was used for calculations:

$$ME = \frac{a_{std\ addition}}{a_{std}} \cdot 100\% \quad (2)$$

Since the presence of biomarkers and pharmaceuticals in WW samples is inevitable, LOQ estimation was based on a standard addition method taking into account the S/N according to Equation (3) [20]:

$$LOQ = \frac{10 \cdot C}{S/N} \quad (3)$$

where C is the concentration of analyte in the sample according to the standard addition method and S/N is the signal-to-noise ratio of the analyte obtained without the addition of standard.

The expanded measurement uncertainty of the method (95% confidence interval) for each analyte was calculated based on the reproducibility using Equation (4) since the method including recovery could not be applied due to the fact that the sample preparation procedure did not involve such steps as evaporation or SPE, therefore an alternative formula was used:

$$U_c = k \cdot RSD_{WR} \quad (4)$$

where k = 2 is a coverage factor at the 95% confidence interval and RSD_{WR} is reproducibility.

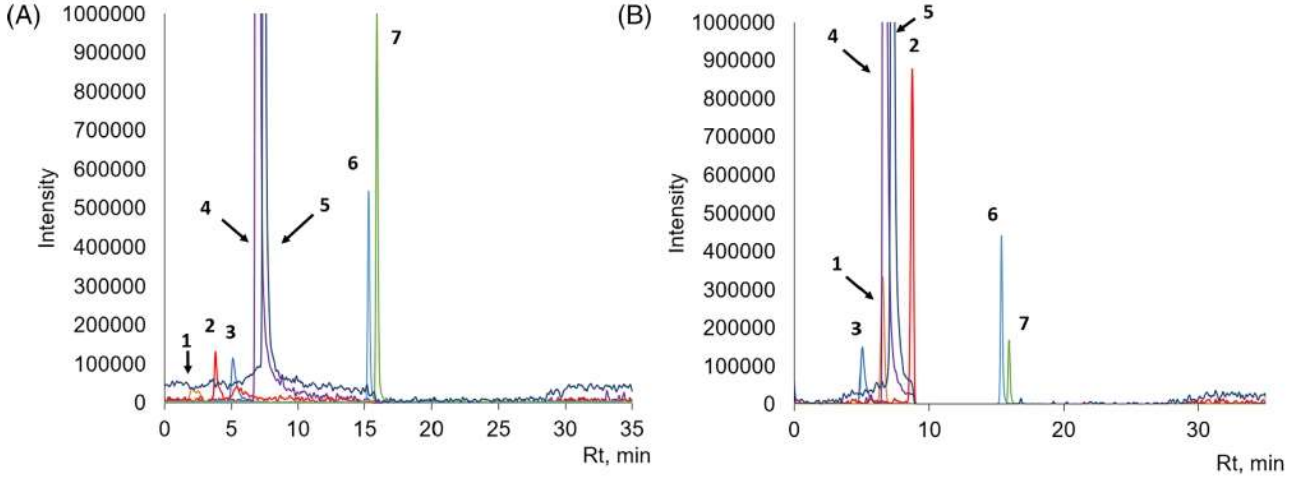

FIGURE 2 Chromatograms of the analyzed pharmaceutical compounds and biomarkers (1 – ethyl sulfate, 2 – 5-hydroxy-indolic acid [5-HIAA], 3 – gabapentin, 4 – cotinine, 5 – caffeine, 6 – diclofenac, and 7 - ibuprofen) without the addition of tetrabutylammonium bromide (TBAB) reagent (A), with the addition of optimal concentration of 11 mM of TBAB (B), and the peak of the reagent at the concentration of 11 mM.

2.5 | Quality assurance and identification of analytes

Quantitative analysis of the analytes was performed using a 5-point calibration curve in a range of 0.5–50 μg/L. The analyzed compounds were confirmed based on the retention time (± 0.1 min), S/N ≥ 10, and by two ions with mass deviation < 5 ppm. Quality control samples with the standard addition at the level of 10 μg/L were included in batches to evaluate the recovery of the analytes. The chromatograms are shown in Figure S1, and the mass deviations of the diagnostic ions are provided in Table S3.

3 | RESULTS AND DISCUSSION

3.1 | Method development and optimization of LC

Preliminary method development experiments using different solvents and mobile phase pH values demonstrated that the retention of highly polar acidic compounds (ethyl sulfate and 5-HIAA) was insufficient for real sample analysis. The compounds were eluted at or near the void volume, indicating the possibility of interference and poor sensitivity of the method due to the early elution of matrix components. In order to improve the retention of highly polar acidic compounds in RP-HPLC, two approaches can be used. The first approach is based on the addition of an ion-pair reagent into the mobile phase, which may lead to serious contamination of the instrument due to poor volatility and the tendency for the adsorption of such reagents. Thus, this approach was not considered in the current work. The other method is based on adding a large excess of an ion-pair reagent directly into the sample. After injection, the reagent is transferred onto a column together with the sample, providing the necessary interactions for analyte retention and leaving the column at a higher strength of the mobile phase at the end of the gradient. As a result, the analytes are retained longer in the column, reducing the possibility of co-elution with polar matrix components and mitigating the MEs [21]. Different types of ion-pair reagents are available based on the chemical structure and physical properties, such as the octanol-water partition coefficient (log *P* value) and solubility in the mobile phase. A commonly known ion-pair reagent TBAB was selected for method development due to its intermediate log *P* value (2.01) [22] among other reagents, providing the necessary increase of analyte retention while keeping acceptable retention time and retention window of the reagent itself. Optimization of the ion-pair reagent concentration was performed over the range of 1–15 mM and optimal retention times for acidic analytes were achieved at 11 mM of TBAB added to the sample. The obtained chromatograms are provided in Figure 2.

The direct addition of TBAB into the samples led to a notable improvement in the retention time and signal intensity of 5-HIAA and ethyl sulfate peaks (see Figure 1). The retention time for 5-HIAA shifted from 3.8 to 8.7 min and the signal intensity increased about six times. The retention time of ethyl sulfate increased from 2.1 to 6.5 min while the signal intensity increased 9 times. Additionally, the symmetry of both peaks improved significantly. The signal intensity most probably increased due to the diminished content of interfering matrix compounds that usually elute in the column void volume. As expected,

the retention times and signal intensities of other analytes did not change significantly except for diclofenac and ibuprofen. The latter two compounds were eluted at the tail portion of the ion-pair reagent, slightly suppressing the signal intensity of both analytes.

Additionally, the possibility of adsorption of analytes on a PVDF filter was investigated. A standard solution with a concentration of 10 μg/L was prepared and filtered with a PVDF syringe filter and compared with values obtained without filtration. As a result, no losses of analytes due to adsorption on a filter were observed, and the comparison is shown in Figure S2.

3.2 | Optimisation of the Orbitrap MS parameters

Preliminary experiments have demonstrated that the full scan (FS) acquisition mode provided the most reliable results in terms of sensitivity compared to the selected ion monitoring and parallel reaction monitoring scanning modes. Despite some advantages of the selected ion monitoring mode, including the improved selectivity, which is beneficial for the analysis of complex matrices such as WW, other factors must also be considered, namely the possibility of performing a retrospective evaluation and identification of other analytes of interest that were not included in the original method [23–26]. Therefore, considering that the FS acquisition mode offers this possibility and WW could provide information on a wide range of chemical compounds, it was concluded that the FS mode is more suitable for the analysis. Despite the advantages of the full-range acquisition procedure, the selected methodology has limitations regarding the unequivocal identification of the compounds since no information about accurate mass for fragment/product ions is available.

The optimization of the MS voltages and scanning parameters has been carried out using neat standards. Several crucial MS parameters were optimized during the preliminary experiments. Achieving stability of the nano-electrospray under gradient conditions with high aqueous content was especially challenging. An unstable electrospray leads to decreased signal intensities and droplet formation at the emitter tip, which affects the sensitivity and applicability of the method. Several approaches to improve nano-electrospray stability have been described, such as post-column solvent addition [27, 28], where a highly organic solvent is continuously added to the column eluate via a T-piece to reduce the aqueous phase content and facilitate electrospray, voltage regulation during analysis [29], and selection of the correct nano-ESI voltage. In this work, optimal nano-electrospray performance was achieved by manually selecting a suitable voltage in a range of 1.70–2.50 kV for both positive and negative modes under initial gradient conditions, and the optimal voltages that provided the most stable nano-electrospray were used. In addition, AGC and IT were evaluated. AGC controls the number of ions entering the mass analyzer and its values were investigated in a range from 5e4 to 3e6. IT limits the time for ions to accumulate in the C-trap and its values from 50 to 300 ms were investigated. However, considering the so-called "space charge effect", when an incorrect combination of AGC and IT values is chosen, resulting in reduced mass precision [30–32], it was important to choose appropriate values. Therefore, a combination was selected that provided appropriate mass precision and intensity. Another optimized parameter was the S-lens or the stacked-ring ion guide value. By changing the RF values of the S-lens, the focusing of the ions could be controlled to increase the number of ions entering the detector and thus improving the signal intensity and sensitivity. The value of the S-lens was optimized in a range from 10 to 100 in increments of 10. The final optimized value of 60 was selected as it provided the best signal intensities for all compounds analyzed.

3.3 | Method performance

The results of method validation have been summarised in Table S2. It is evident that the proposed method performed well in terms of accuracy, precision, and other validation parameters for the analytes of interest. Compared to other methods found in the literature (see Table 1), the proposed procedure can be characterized by similar or lower LOQ values (0.005–0.3 μg/L) as well as by negligible MEs (70%–111%). Since the proposed method does not require any sample preparation (i.e., liquid-liquid extraction or SPE) except for dilution and filtration, the loss of analytes has been significantly reduced. Finally, one of the main advantages of this method is the demonstrated applicability to analytes of different polarity, including the ionic compound ethyl sulfate within one run.

3.4 | Real sample analysis

Untreated WW samples were collected from the WW treatment plants in several cities and towns of Latvia, including Jelgava, Liepaja, Valmiera, Ventspils, Jekabpils, Jurmala, Riga, Rezekne, Daugavpils, Salaspils, and Tukums. The samples were collected on Tuesday and Thursday from March 31 to April 28, 2022. In total, 116 samples were collected and analyzed using the developed method. All of the samples contained the analyzed biomarkers and pharmaceuticals. The obtained concentrations with comparison

TABLE 1 Comparison between the previously published methods and this work

Analytes	Instrumentation	Main sample preparation steps	Analytical column	Injection volume	LOQ, µg/L	Matrix effects, %	Reference
Several biomarkers and pharmaceuticals	Nano-LC Orbitrap MS	Dilute-and-shoot method, the addition of TBAB	PepMap C18 150 × 0.075 mm, 3 µm	70 nl	0.005–0.3	70%–111%	This study
Biomarkers and pharmaceuticals	UHPLC QqQ MS	Dilute-and-shoot method	1D: Kinetex C18, 50 mm × 3 mm, 1.7 µm, 2D: Synergy Max-RP, 150 × 3 mm, 4 µm	10 µl	1–5	ND	[33]
	UHPLC QqQ MS	SPE, evaporation			0.1–50	ND	
Diclofenac and ibuprofen	UHPLC QqQ MS	Liquid-phase microextraction	Luna Phenyl-Hexyl, 150 mm × 2.0 mm, 3 µm	90 µl	0.14–0.25	94.4	[34]
Ethyl sulfate	UHPLC QqQ MS	Dilute-and-shoot method	Synergi Fusion-RP, 150 mm × 4.6 mm, 4 µm	100 µl	0.3	21–25	[21]
	UHPLC ToF MS				0.6	61–72	
5-HIAA	UHPLC QqQ MS	LLE, derivatization	Kinetex PFP, 100 mm × 2.1 mm, 1.7 µm	1 µl	1	ND	[35]

Abbreviations: 5-HIAA, 5-hydroxy-indolic acid; LLE, liquid-liquid extraction; ND, no data; TBAB, tetrabutylammonium bromide.

TABLE 2 Comparison to literature data

Compound	Concentration range, µg/L [this work]	Median concentration, µg/L [this work]	Concentration ranges from literature, µg/L [21]
Gabapentin	9.6–71.9	20	7.3–50.2
Cotinine	2.7–10.3	4.6	2.4–10.1
Ethyl sulfate	4.5–83.7	25	13.1–43.6
Caffeine	19.9–162	58	23.8–156
5-HIAA	0.4–20.2	7.6	4.9–17.7
Diclofenac	0.6–7.4	3.8	0.6–2.7
Ibuprofen	6.6–36.4	12	7.3–25.4

Abbreviation: 5-HIAA, 5-hydroxy-indolic acid.

to literature data from the same region are provided in Table 2. A good agreement was observed with the literature data, indicating the applicability of the proposed analytical methodology in determining the selected biomarkers.

4 | CONCLUDING REMARKS

A novel nano-LC Orbitrap MS method has been developed for the determination of several pharmaceuticals and biomarkers in WW samples. It has been demonstrated that the dilute-and-shoot approach can be successfully applied for WW matrices avoiding tedious sample clean-up procedures like liquid-liquid extraction or SPE and providing greater accuracy and simplicity of the method. The direct in-sample addition of TBAB as an ion-pair reagent allowed the separation of ionic and less polar analytes within one run using a single RP nano-LC column. The presence of TBAB in the samples significantly improved the retention and signal intensity of ethyl sulfate and 5-HIAA. Overall,

the proposed procedure provided low LOQ values (0.005–0.3 μg/L) as well as negligible MEs (70%–111%) for most of the analytes of interest.

ACKNOWLEDGMENTS

This research is funded by the Ministry of Economics, project "State research project in the field of biomedicine, medical technologies, and pharmacy", project No. VPP-EM-BIOMEDICĪNA-2022/1-0001.

CONFLICT OF INTEREST STATEMENT

The authors declare no conflict of interest.

DATA AVAILABILITY STATEMENT

The data that support the findings of this study are available from the corresponding author upon reasonable request.

ORCID

Deniss Fedorenko https://orcid.org/0000-0001-7577-6864
Antons Podjava https://orcid.org/0000-0003-1807-9848
Arvis Prikulis https://orcid.org/0000-0002-6936-6276
Vadims Bartkevics https://orcid.org/0000-0002-6193-7409

REFERENCES

1. Gracia-Lor E, Castiglioni S, Bade R, Been F, Castrignanò E, Covaci A, et al. Measuring biomarkers in wastewater as a new source of epidemiological information: current state and future perspectives. Environ Int. 2017;99:131–50.
2. Choi PM, Bowes DA, O'Brien JW, Li J, Halden RU, Jiang G, et al. Do food and stress biomarkers work for wastewater-based epidemiology? A critical evaluation. Sci Total Environ. 2020;736:139654.
3. Shah S, Gwee SXW, Ng JQX, Lau N, Koh J, Pang J. Wastewater surveillance to infer COVID-19 transmission: a systematic review. Sci Total Environ. 2022;804:150060.
4. Rico M, Andrés-Costa MJ, Picó Y. Estimating population size in wastewater-based epidemiology. Valencia metropolitan area as a case study. J Hazard Mater. 2017;323:156–65.
5. Helander A, Beck O. Ethyl sulfate: a metabolite of ethanol in humans and a potential biomarker of acute alcohol intake. J Anal Toxicol. 2005;29:270–4.
6. Castiglioni S, Senta I, Borsotti A, Davoli E, Zuccato E. A novel approach for monitoring tobacco use in local communities by wastewater analysis. Tob Control. 2015;24:38–42.
7. Ra J, Yoom H, Son H, Lee Y. Occurrence and transformation of gabapentin in urban water quality engineering: Rapid formation of nitrile from amine during drinking water chlorination. Water Res. 2020;184:116123.
8. Gracia-Lor E, Rousis NI, Zuccato E, Castiglioni S. Monitoring caffeine and nicotine use in a nationwide study in Italy using wastewater-based epidemiology. Sci Total Environ. 2020;747:141331.
9. Ahmed F, Li J, O'Brien JW, Tscharke BJ, Samanipour S, Thai PK. In-sewer stability of selected analgesics and their metabolites. Water Res. 2021;204:117647.
10. Tang W. The metabolism of diclofenac–enzymology and toxicology perspectives. Curr Drug Metab. 2003;4:319–29.
11. Mazaleuskaya LL, Theken KN, Gong L, Thorn CF, FitzGerald GA, Altman RB, et al. PharmGKB summary: ibuprofen pathways. Pharmacogenet. Genomics. 2015;25:96–106.
12. Duan L, Zhang Y, Wang B, Yu G, Gao J, Cagnetta G, et al. Wastewater surveillance for 168 pharmaceuticals and metabolites in a WWTP: Occurrence, temporal variations and feasibility of metabolic biomarkers for intake estimation. Water Res. 2022;216:118321.
13. Fatta D, Achilleos A, Nikolaou A, Meriç S. Analytical methods for tracing pharmaceutical residues in water and wastewater. TrAC, Trends Anal Chem. 2007;26:515–33.
14. Mutavdžić Pavlović D, Babić S, Dolar D, Ašperger D, Košutić K, Horvat AJM, et al. Development and optimization of the SPE procedure for determination of pharmaceuticals in water samples by HPLC-diode array detection. J Sep Sci. 2010;33:258–67.
15. Greer B, Chevallier O, Quinn B, Botana LM, Elliott CT. Redefining dilute and shoot: The evolution of the technique and its application in the analysis of foods and biological matrices by liquid chromatography mass spectrometry. TrAC, Trends Anal Chem. 2021;141:116284.
16. Fedorenko D, Bartkevics V. Recent applications of nano-liquid chromatography in food safety and environmental monitoring: a review. Crit Rev Anal Chem. 2021;0:1–25.
17. Szumski M, Buszewski B. State of the art in miniaturized separation techniques. Crit Rev Anal Chem. 2002;32:1–46.
18. Alcántara-Durán J, Moreno-González D, Gilbert-López B, Molina-Díaz A, García-Reyes JF. Matrix-effect free multiresidue analysis of veterinary drugs in food samples of animal origin by nanoflow liquid chromatography high resolution mass spectrometry. Food Chem. 2018;245:29–38.
19. Langford JB, Lurie IS. Use of micro, capillary, and nano liquid chromatography for forensic analysis. J Sep Sci. 2022;45:38–50.
20. Hasegawa K, Minakata K, Suzuki M, Suzuki O. The standard addition method and its validation in forensic toxicology. Forensic Toxicol. 2021;39:311–33.
21. Rodríguez-Álvarez T, Rodil R, Cela R, Quintana JB. Ion-pair reversed-phase liquid chromatography–quadrupole-time-of-flight and triple-quadrupole–mass spectrometry determination of ethyl sulfate in wastewater for alcohol consumption tracing. J Chromatogr A. 2014;1328:35–42.
22. Tetrabutylammonium bromide. https://www.chemsrc.com/en/cas/1643-19-2_329726.html Accessed: August 19, 2022
23. Hernández F, Ibáñez M, Gracia-Lor E, Sancho JV. Retrospective LC-QTOF-MS analysis searching for pharmaceutical metabolites in urban wastewater. J Sep Sci. 2011;34:3517–26.
24. Kaufmann A, Arrizabalaga-Larrañaga A, Blokland MH, Sterk SS. Potential and limitation of retrospective HRMS based data analysis: "Have meat-producing animals been exposed to illegal growth promotors such as SARMs?" Food Control. 2023;147:109611.
25. Günthardt BF, Wettstein FE, Hollender J, Singer H, Härri J, Scheringer M, et al. Retrospective HRMS Screening and Dedicated Target Analysis Reveal a Wide Exposure to Pyrrolizidine

Alkaloids in Small Streams. Environ Sci Technol. 2021;55:1036–44.
26. Alygizakis NA, Samanipour S, Hollender J, Ibáñez M, Kaserzon S, Kokkali V, et al. Exploring the potential of a global emerging contaminant early warning network through the use of retrospective suspect screening with high-resolution mass spectrometry. Environ Sci Technol. 2018;52:5135–44.
27. Jansons M, Fedorenko D, Pavlenko R, Berzina Z, Bartkevics V. Nanoflow liquid chromatography mass spectrometry method for quantitative analysis and target ion screening of pyrrolizidine alkaloids in honey, tea, herbal tinctures, and milk. J Chromatogr A. 2022;1676:463269.
28. Nguyen-Khuong T, Pralow A, Reichl U, Rapp E. Improvement of electrospray stability in negative ion mode for nano-PGC-LC-MS glycoanalysis via post-column make-up flow. Glycoconj J. 2018;35:499–509.
29. Marginean I, Kelly RT, Moore RJ, Prior DC, LaMarche BL, Tang K, et al. Selection of the optimum electrospray voltage for gradient elution LC-MS measurements. J Am Soc Mass Spectrom. 2009;20:682–8.
30. Kalli A, Smith GT, Sweredoski MJ, Hess S. Evaluation and optimization of mass spectrometric settings during data-dependent acquisition mode: focus on LTQ-orbitrap mass analyzers. J Proteome Res. 2013;12:3071–86.
31. Kalli A, Hess S. Effect of mass spectrometric parameters on peptide and protein identification rates for shotgun proteomic experiments on an LTQ-orbitrap mass analyzer. Proteomics. 2012;12;21–31.
32. Hohenester UM, Barbier Saint-Hilaire P, Fenaille F, Cole RB. Investigation of space charge effects and ion trapping capacity on direct introduction ultra-high-resolution mass spectrometry workflows for metabolomics. J. Mass Spectrom. 2020;55:e4613.
33. Pugajeva I, Ikkere LE, Jansons M, Perkons I, Sukajeva V, Bartkevics V, Two-dimensional liquid chromatography - mass spectrometry as an effective tool for assessing a wide range of pharmaceuticals and biomarkers in wastewater-based epidemiology studies. J Pharm Biomed Anal. 2021, 205, 114295.
34. Quintana JB, Rodil R, Reemtsma T, Suitability of hollow fibre liquid-phase microextraction for the determination of acidic pharmaceuticals in wastewater by liquid chromatography–electrospray tandem mass spectrometry without matrix effects. J Chromatogr A 2004, 1061, 19–26.
35. Pandopulos AJ, Gerber C, Tscharke BJ, O'Brien J, White JM, Bade R, A sensitive analytical method for the measurement of neurotransmitter metabolites as potential population biomarkers in wastewater. J Chromatogr A 2020, 1612, 460623.

SUPPORTING INFORMATION

Additional supporting information can be found online in the Supporting Information section at the end of this article.

How to cite this article: Fedorenko D, Podjava A, Prikulis A, Bartkevics V. Dilute-and-shoot approach for determination of several biomarkers and pharmaceuticals in wastewater using nanoflow liquid chromatography – Orbitrap mass spectrometry. J Sep Sci. 2023;2201002. https://doi.org/10.1002/jssc.202201002

Nanoflow Liquid Chromatography Mass Spectrometry Method for Quantitative Analysis and Target Ion Screening of Pyrrolizidine Alkaloids in Honey, Tea, Herbal Tinctures, and Milk

Jansons, M.; **Fedorenko, D.**; Pavlenko, R.; Berzina, Z.; Bartkevics, V. *Journal of Chromatography A*[3] **2022**, *1676*, 463269.

[3] *Peer reviewed journal, imprint of Elsevier (IF=4.601 (2022)), ISSN: 0021-9673*

Journal of Chromatography A 1676 (2022) 463269

Contents lists available at ScienceDirect

Journal of Chromatography A

journal homepage: www.elsevier.com/locate/chroma

Nanoflow liquid chromatography mass spectrometry method for quantitative analysis and target ion screening of pyrrolizidine alkaloids in honey, tea, herbal tinctures, and milk

Martins Jansons[a,*], Deniss Fedorenko[a,b], Romans Pavlenko[a,b], Zane Berzina[a,b], Vadims Bartkevics[a,b]

[a] Animal Health and Environment "BIOR", Institute of Food Safety, Lejupes iela 3, Riga, LV 1076, Latvia
[b] Faculty of Chemistry, University of Latvia, Jelgavas iela 1, Riga, LV 1004, Latvia

ARTICLE INFO

Article history:
Received 28 May 2021
Revised 19 June 2022
Accepted 20 June 2022
Available online 21 June 2022

Keywords:
Pyrrolizidine alkaloids
Honey
Tea
Nano-LC-MS
Target ion screening

ABSTRACT

A method for the determination of pyrrolizidine alkaloids in tea, honey, herbal tinctures, and milk samples was developed by employing nano-LC-MS with high-resolution Orbitrap mass spectrometry. Quantitation was performed using the available analytical standards, and a MS^2 target ion screening approach was developed using fragment ions that were specific for pyrrolizidine alkaloids under collision-induced dissociation. Proof of concept was delivered for the screening approach, proposing that the $C_6H_8N^+$ fragment ion is a highly selective fragment ion for the detection of potential pyrrolizidine alkaloids. The elaborated quantitation was applied for the occurrence study of pyrrolizidine alkaloids in food products available on the Latvian market, including samples of tea ($n = 15$), honey ($n = 40$), herbal tinctures ($n = 15$), and milk ($n = 10$). The median LOQ over all analytes was 0.33 μg kg^{-1} in honey, 3.6 μg kg^{-1} in tea, 3.3 μg kg^{-1} in herbal tinctures, and 0.32 μg kg^{-1} in milk. The herbal tinctures samples and milk samples did not contain pyrrolizidine alkaloids above LOQ values. Analytes were detected in 33% of honey and 47% of tea samples. Most common were echimidine, intermedine, and enchinatine *N*-oxide. Pyrrolizidine alkaloids in tea samples were mainly *N*-oxides, with the highest total concentration being 215 μg kg^{-1} among the samples, exceeding the maximum limit of 200 μg kg^{-1} set by Commission Regulation (EU) 2020/2040. In honey samples, lycopsamine-type alkaloids were detected most frequently, with the highest total concentration equal to 74 μg kg^{-1}. Advantages of the developed nano-LC-MS methods included increased sensitivity in comparison with conventional flow LC-MS, low solvent consumption typical with nano-LC and the novel use of a selective common target ion for detection and discovery of potential pyrrolizidine alkaloids using high resolution mass spectrometry.

1. Introduction

Pyrrolizidine alkaloids (PA) are a widespread class of hepatotoxic heterocyclic organic compounds found in flora (notably, in the *Fabaceae*, *Boraginaceae*, and *Asteraceae* plant families), and have been shown to have genotoxic and carcinogenic effects [1]. PAs can be classified according to their chemical structure, by the characteristic part of the structure referred to as necine base [1,2], which may be 1,2-saturated or 1,2-unsaturated (often referred to as dehydropyrrolizidine alkaloids). The necine base nitrogen may be oxidised, in which case the compound is referred to as pyrrolizidine alkaloid *N*-oxide [1,3]. More than 150 pyrrolizidine alkaloids, varying in toxicological potency, have been identified in *Senecio* spp. Pyrrolizidine alkaloids are synthesised in the roots of plants as *N*-oxides and transported to the rest of the plant, accumulating in the flowers, stems, and leaves [4], and serve as plant defence agents against herbivores [5]. The alkaloid *N*-oxides from plants are converted into free bases when ingested orally and are reduced, therefore, the *N*-oxides are similar in toxicity to the free base PAs. The highest concentrations of PAs in most *Senecio* spp. are in the seeds, flowers, and buds [4].

Clinically, acute PA toxicosis in animals is attributable to acute liver failure: anorexia, depression, icterus, and ascites. No effective treatment has been developed and the affected animals rarely recover [4]. Possible health risks to humans due to the occurrence of pyrrolizidine alkaloids have received an increasing recognition. Some widely consumed foods, for example, herbs, cereals, milk, meat, eggs, honey, pollen, and products thereof, may contain PAs

* Corresponding author.
E-mail address: martins.jansons@bior.lv (M. Jansons).

https://doi.org/10.1016/j.chroma.2022.463269
0021-9673/

Table 1
Brief overview of methods reported in scientific literature for determination of pyrrolizidine alkaloids in different matrices.

Method	Mass spectrometry	Samples	Analytical column	Extraction procedure and clean-up	LOQ	Refs.
HPLC	Ion trap	Honey	Hypersil Gold C18, 3 µm, 150 × 2.1 mm	Acidic extraction with 50 mM sulfuric acid in H_2O, Strata-X-C SPE, filtering	0.045 - 0.10 µg kg^{-1}	[9]
UHPLC	Single quadrupole	Honey	Ascentis Express C8, 2.7 µm, 150 × 5 mm	Acidic extraction with 50 mM sulfuric acid in H_2O, use of Zn dust, QuEChERS salts, dSPE	0.081 - 4.35 µg kg^{-1}	[10]
UHPLC	Triple quadrupole	Tea, honey	Hypersil Gold C18, 1.9 µm, 150 × 2.1 mm	Honey: acidic extraction with 50 mM sulfuric acid in H_2O, HF Bond Elut LRC-SCX SPE, filtering Tea: acidic extraction with 50 mM sulfuric acid in H_2O, C18 SPE, filtering	1.7 - 6.4 µg kg^{-1} (tea), 0.18 - 0.62 µg kg^{-1} (honey)	[11]
UHPLC	Triple quadrupole	Salads, herbs, tea	Acquity BEH C18, 1.7 µm, 100 × 2.1 mm	Dry plants: 0.1% FA in MeOH, Envi-Carb SPE Infusions: boiling water, basification, C18 SPE	0.1 - 1 µg kg^{-1}	[12]
UHPLC	Triple quadrupole	Honey, pollen	Hypersil Gold C18, 1.9 µm, 50 × 2.1 mm	Acidic extraction with 50 mM sulfuric acid in H_2O, use of Zn dust, QuEChERS salts, dSPE	1 - 3 µg kg^{-1}	[13]
UHPLC	Triple quadrupole	Tea	Kinetex pentafluorophenyl, 1.7 µm, 50 × 2.1 mm	Boiling water, basification, EXtrelut NT1 column	1 - 5 µg L^{-1}	[14]
UHPLC	Triple quadrupole	Feed	Acquity BEH C18, 1.7 µm, 50 × 2.1 mm	0.1% FA in ACN/H_2O 50/50 (v/v), $MgSO_4$ and NaCl, filtering	5 µg kg^{-1}	[15]
HPLC	Single quadrupole	Feed	Gemini NX-C18, 3 µm, 150 × 4.6 mm	Acidic extraction with 50 mM sulfuric acid in H_2O, filtering, use of Zn dust, Strata SCX SPE, filtering	5 µg kg^{-1}	[16]
HPLC	Triple quadrupole	Honey	ZORBAX Eclipse XDB C18, 3 µm, 150 × 4.6 mm	1. ACN/H_2O 50/50 (v/v), $MgSO_4$ and NaCl, filtering; 2. 0.1% FA in MeOH/H_2O 50/50 (v/v), filtering	8.6 - 18 µg kg^{-1}	[17]
UHPLC	Triple quadrupole	Tea	Hypersil Gold C18, 1.9 µm, 150 × 2.1 mm	Acidic extraction with 50 mM sulfuric acid in H_2O, glass syringe filter, C18 SPE	10 µg kg^{-1}	[18]

and their *N*-oxides at trace levels. While insufficient to cause acute poisoning, the occurrence may exceed toxicologically safe levels, depending on the season and the severity of contamination [6]. The Federal Institute for Risk Assessment (BfR) of Germany has, according to their available data, recommended that the human dietary exposure to 1,2-unsaturated pyrrolizidine alkaloids should be kept below 0.007 µg kg^{-1} body weight per day. There is a need for more research and data on analytical methods and the occurrence of PAs in food and feed, because no standardised procedures have been developed that could be used in food control for the analysis of pyrrolizidine alkaloids [7]. Several hundred pyrrolizidine alkaloids have been identified to date, but only around 30 are readily available as analytical standards [8]. Due to the chemical diversity of PAs and the limited availability of analytical standards, reliable screening methods would be of great interest and would find practical applications in risk assessment.

The analysis of pyrrolizidine alkaloids in food matrices is challenging, considering the complexity of the matrices, similarity of chemical structure of closely related compounds, as well as availability of analytical standards. To date, several approaches for analysis and quantitation of this type of analytes have been used. The comparison between limits of quantification and extraction procedures of the methods presented in scientific literature is provided in Table 1. Most published methods use UHPLC with 50–150 mm long columns and particles in size < 3 µm, and sample preparation procedures include extraction with acidified water or methanol, as well as different types of SPE.

Different methods for determination of PAs are available, such as UV–vis spectrometry, thin-layer chromatography, nuclear magnetic resonance, GC–MS,

LC-MS, and immunology-based methods [19], as well as capillary electophoresis, and enzyme linked immunosorbent assay (ELISA). LC-MS methods are the most common in determination of PAs, since they provide more reliable data, are selective and sensitive, and sample preparation is simplified in comparison with LC-UV methods or GC–MS methods. Additionally, electrospray ionisation (ESI) common with LC-MS analyses provide better sensitivity due to easily ionisable nitrogen atoms in the chemical structure of PAs, thus being analysed mainly in positive ionisation mode [20]. In comparison to GC–MS, no thermal dergadation of *N*-oxides is present in LC-MS analysis, making it sutable not only for free bases, but also for *N*-oxide form [17]. Taking into account the fact, that the variety of PAs is significant, but the availability of analytical standards for each individul compound is rather limited, several different approaches have been used in order to analyse pyrrolizidine alkaloids.

The quantitation of the alkaloids can be performed using a single available standard; therefore, the obtained concentrations are only estimations [20]. Different types of PAs produce characteristic mass spectras, such as: retronecine-type PAs have common ion at *m/z* 94, 120, 138, otonecine-type PAs – at *m/z* 150, 168, platynecine-type – at *m/z* 122, 140, and other fragments [20–22]. Based on the fact, that structurally the PAs could have common structural elements, and under fragmentation process in collision cell in MS different compounds could provide fragments with the same *m/z*, therefore the signal could indicate the presence of a PA compound, that does not have available analytical standard. This non-targeted approach for analysis and quantitation is based on characteristic target ions and fragmentation patterns, and it allows to perform analysis without analytical standards [19,21,22].

In this study, a nano-LC-MS method was developed and applied for the determination of pyrrolizidine alkaloids in foods from the Latvian market, as well as a risk assessment was performed. Additionally, a proof of concept was delivered for MS^2 target ion screening of pyrrolizidine alkaloids using high-resolution Orbitrap mass spectrometry. This study demonstrates applicability of the nano-LC method in the analysis of pyrrolizidine alkaloids in foods using quantitative method, featuring post-column solvent addition and small sample loop for improved chromatography of polar compounds, as well as the applicability of novel use of MS^2 target ion

screening approach. To date, no nano-LC-MS method for determination of pyrrolizidine alkaloids in foods has been published in literature. To the best of our knowledge, post-column solvent addition for electrospray stability at highly aqueous part of a gradient of a chromatographic run and a small sample loop is not a common instrumental setup in nano-LC analysis with published methods, and no such setup has been implemented in food analysis using nano-LC technique, while it clearly demonstrates advantages in stabilizing electrospray and allowing to successfully improve resolution for the aqueous part during gradient separation.

2. Materials and methods

2.1. Materials and reagents

Formic acid (99%) was obtained from VWR International (Radnor, PA, USA). LC-MS grade ultra-pure water and acetonitrile (Merck, Germany) were used for the preparation of mobile phases. HPLC grade solvents (Merck, Germany) were used for sample extractions. Pyrrolizidine alkaloid standards (with purities ranging from 95% to 99% and uncertainty of assay of 5%) included echimidine, echimidine *N*-oxide, echinatine, echinatine *N*-oxide, europine hydrochloride, europine *N*-oxide, heliosupine, heliosupine *N*-oxide, heliotrine, heliotrine *N*-oxide, indicine hydrochloride, indicine *N*-oxide, integerrimine, integerrimine *N*-oxide, intermedine, intermedine *N*-oxide, lasiocarpine, lasiocarpine *N*-oxide, lycopsamine, lycopsamine *N*-oxide, retrorsine, retrorsine *N*-oxide, senecionine, senecionine *N*-oxide, seneciphylline, seneciphylline *N*-oxide, senecivernine, senecivernine *N*-oxide, senkirkine, and usaramine (PhytoPlan, Germany). Chemical structures of the compounds given in Fig. S1 in Supplementary materials. Stock solutions at 250 mg/L concentration and working standard solutions were prepared in 1:1 mixture of 50% aqueous acetonitrile and methanol. Some of the pure standards had poor solubility and were dissolved by acidifying the solvent with 0.4% of formic acid.

The stability of mixed working standard solution prepared in 50% aqueous methanol acidified with 0.005% of formic acid was investigated at -18 °C, +4 °C, and +30 °C (see Fig. 1). Individual stability data for each compound has been provided in Supplementary materials (Table S4). Considering the obtained stability data, all stock solutions and working standard solutions were stored at +4 °C.

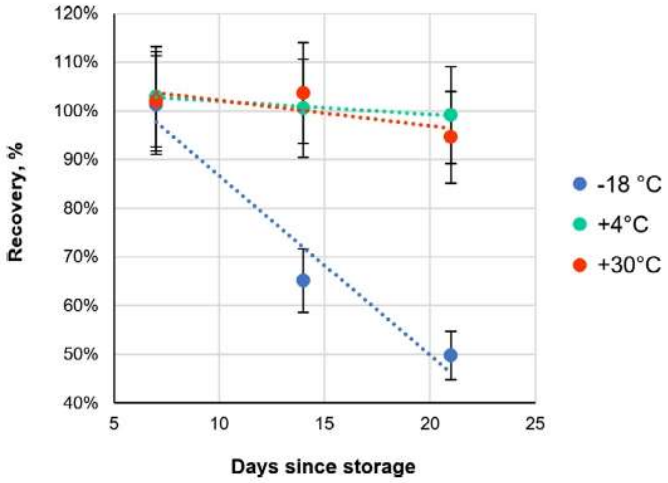

Fig. 1. Stability of diluted pyrrolizidine alkaloid standard mix solutions in 50% aqueous methanol acidified to 0.005% with formic acid, at −18 °C, +4 °C, and +30 °C.

2.2. Investigating the performance of SPE procedure and QuEChERS procedure

2.2.1. SPE procedure

In order to investigate the performance of a solid-phase extraction (SPE) procedure based on the *Strata-X* sorbent, 2.00 g of spiked and unspiked homogenised honey or tea samples were extracted in polypropylene tubes in 40 mL of 0.2% formic acid in deionised water for 30 min using a rotating shaker. The tubes were centrifuged at 4500 rpm for 15 min, 5 mL aliquots of the supernatant were adjusted to pH 7.5 ± 0.5 using aqueous 1 mol/L ammonium carbonate, transferred, and passed through pre-conditioned Strata-X solid-phase extraction cartridges. The cartridges were then washed with 6 mL of 1% formic acid, 6 mL of deionised water, and eluted with 6 mL of methanol. The eluates were evaporated at 50 °C and dissolved in 450 µL of deionised water containing 1% formic acid by applying vortex mixing, therefore the final dilution factor with this procedure was $d = 1.8$. The extracts were analysed after filtration (0.22 µm pore size, PVDF).

2.2.2. QuEChERS procedure

In order to investigate the performance of a QuEChERS-based extraction procedure with subsequent pre-concentration or dilution in combination with a conventional flow LC-MS analysis, 2.00 g of spiked and unspiked homogenised honey or tea samples were extracted in 20 mL of 50% acetonitrile containing 1% formic acid for 30 min, using an overhead shaker. A mixture of salts, consisting of 4.0 g of anhydrous magnesium sulphate, 1.0 g of sodium chloride, 1.0 g of trisodium citrate, and 0.5 g of disodium citrate, was added to the tubes and shaken vigorously for 3 min, then the tubes were centrifuged at 4500 rpm for 15 min. A 5 mL aliquot of the supernatant was subjected to freezing-out at −80 °C for 30 min and 200 µL of the supernatant after centrifuging for 18 min at 4500 rpm at 15 °C was evaporated at 50 °C and dissolved in deionised water containing 1% formic acid by vortex mixing. The dry residues were reconstituted with the appropriate volumes of deionised water containing 1% formic acid to ensure the following dilution factors: $d = 2$ for tea and $d = 0.4$ for honey (for QuEChERS with pre-concentration); $d = 40$ for tea and honey (for QuEChERS with dilution). The extracts were analysed after filtration (0.22 µm pore size, PVDF). In order to investigate the performance of QuEChERS-based extraction procedure in combination with nano-LC-MS, the procedure was as described in Section 2.3.

2.3. Sample preparation for the quantitative analysis of pyrrolizidine alkaloids in samples from the market

Several products (tea, honey, herbal tinctures, and milk) were chosen for this study due to their high consumption among the population and the high probability of finding pyrrolizidine alkaloids in these products. Standard addition approach was used for quantifying the content of PAs in samples. The products were of Latvian origin and were obtained from Latvian market.

In order to analyse samples from the market, 2.00 g of spiked and unspiked homogenised honey or tea samples were extracted in 20 mL of 50% acetonitrile containing 1% formic acid and 10 mL of milk samples were extracted in 10 mL of acetonitrile containing 2% formic acid, and shaken for 30 min using an overhead shaker. A mixture of salts, consisting of 4.0 g of anhydrous magnesium sulphate, 1.0 g of sodium chloride, 1.0 g of trisodium citrate, and 0.5 g of disodium citrate was added to the tubes and shaken vigorously for 3 min, and the tubes were centrifuged at 4500 rpm for 15 min. A 5 mL aliquot of the supernatant was subjected to freezing-out at −80 °C for 30 min and 200 µL of the supernatant after centrifuging for 18 min at 4500 rpm at 15 °C was evaporated at 50 °C and dissolved in deionised water containing 1% formic acid by vortex

mixing (300 µL for honey and milk samples, 1500 µL for tea samples). Herbal tinctures were evaporated directly due to their high ethanol content. Thus, 200 µL samples of spiked and unspiked homogenised herbal tinctures were evaporated at 50 °C and dissolved in 300 µL of deionised water containing 1% formic acid by vortex mixing. The final dilution factor was $d = 37.5$ for tea, $d = 7.5$ for honey, $d = 1.5$ for milk and herbal tinctures. The final extracts were filtered (0.22 µm pore size, PVDF) and analysed with nano-LC-MS.

2.4. Instrumental parameters for conventional flow LC-MS method used for comparison with nano-LC-MS

The conventional flow electrospray ionisation LC-MS analysis was done using a Thermo Scientific Ultimate 3000 UHPLC system coupled to a Thermo Scientific TSQ Quantis mass spectrometer with Ion Max NG probe. The analytical column was a Kinetex™ (Phenomenex, Torrance, CA, USA) UHPLC column (100 × 3 mm) with 1.7 µm C18 bonded silica particles, and was thermostated at 50 °C; the autosampler was thermostated at 10 °C; the injection volume was 100 µL. The large injection volume was chosen as the reconstitution solvent was aqueous 1% formic acid, in which the PA analytes maintained high solubility, and due to absence of organic solvents the early eluting peak separation was maintained. The following parameters were used with the ionisation source: sheath gas: 50 arbitrary units; aux gas: 10 arbitrary units; sweep gas: 0.1 arbitrary units; probe heater temperature 400 °C; ion transfer capillary temperature 300 °C; spray voltage at +3.5 kV in the positive mode. The mobile phases were 0.1% formic acid in ultra-pure water (A) and 0.1% formic acid in acetonitrile (B). The gradient programme was the following: 0-10 min 1-10% B; 10-15 min 10-15% B; 15-20 min 15-30% B; 20-21 min 30-99% B; 21-26 min 99% B; 26-32 min 1% B. The flow rate was 0.5 mL/min. Precursor ions and fragments were isolated by an isolation window of 0.7 *m/z* at the respective elution windows and fragmented at the optimum collision energy. A list of the analytes, precursor and fragment ions is given in the Supplementary Table S1.

2.5. Instrumental parameters for the quantitative analysis of pyrrolizidine alkaloids with nano-LC-MS

Pyrrolizidine alkaloids were analysed using a nano-LC chromatography system Thermo Scientific UltiMate 3000 RSLCnano coupled to a Thermo Scientific Orbitrap Focus mass spectrometer. To achieve the maximum chromatographic efficiency, a small volume sample loop was used (approximately 0.07 µL). The autosampler was programmed to perform an injection of 1 µL, thus resulting in additional washing of the sample loop. For the purpose of stabilising the electrospray performance during the highly aqueous parts of the gradient and for avoiding the formation of droplets at the emitter tip, a post-column solvent was added with the secondary pump (80% LC-MS acetonitrile). High-pressure fittings were used to join the fluidics and the capillary column (nanoViper™, IDEX MicroTight®, and AB SCIEX SST mixing tee). Separation was carried out on a PepMap™ (Thermo Scientific, Waltham, MA, USA) capillary column (150 × 0.075 mm) with 3 µm C_{18} bonded silica particles. Electrospray ionisation was performed in the nano-electrospray ionisation mode using the EASY-Spray™ ionisation source and EASY-Spray™ transfer line (75 µm inner diameter and 50 cm length). The analytical column was thermostated at 50 °C; the autosampler was thermostated at 10 °C; the actual injection volume was 70 nL. The small injection volume was necessary to separate early eluting PA analytes. In contrast to common nano-LC-MS protocols, large injection volumes (for example – 1 µL) could not be applied to PA analytes due to their ionic and solubility properties. The following parameters were used with the ionisation source: ion transfer capillary temperature 300 °C; spray voltage was set at +2.0 kV. The mobile phases were 1% formic acid in ultra-pure water (A) and 1% formic acid in acetonitrile (B), and the flow rate was 0.8 µL/min (both mobile phase and post-column solvent addition). The gradient program was the following: 0-22 min 1-11% B; 22-25 min 11-28% B; 25-30 min 28-80% B; 30-37 min 80-99% B; 37-42 min 99% B; 42-45 min 1% B. The duration of injection preparation ensured sufficient time for return to the starting conditions. Precursor ions were isolated by an isolation window of 0.7 *m/z* at the respective elution windows, fragmented at the optimum collision energy, and detected simultaneously at 70 000 resolution. The ion injection time was set to 1000 ms and the automatic gain control (AGC) target was $1 \cdot 10^6$. A list of analytes, precursor and fragment ions are given in the Supplementary Table S2.

2.6. Nano-LC-MS procedure for target ion screening of pyrrolizidine alkaloids

The aforementioned chromatography gradient for the analysis of pyrrolizidine alkaloids with nano-LC was scaled by extending the times in the gradient table by a factor of 4 and by reducing the flow rate by the same factor, thus the flow rate for screening was 0.2 µL/min (both mobile phase and post-column solvent addition). Additional equilibration time was added to the end of the analysis sequence to account for the large ratio of system volume to flow rate, thus ensuring sufficient equilibration when returning to the starting conditions for the next injection. A reagent blank injection was performed by using this procedure and ions with relative abundance over 0.075% from the averaged spectrum of the first half of the chromatogram were added to the method exclusion list in order to prevent them from triggering dd-MS^2 (data dependent MS^2) scans for ions that do not originate from the samples or for ions arising from the background contamination. The scan mode was changed to Full MS with dd-MS^2 in discovery mode. The full scan resolution was 70 000, with the scan range from 150 to 500 *m/z*, AGC target of $3 \cdot 10^6$ and the maximum IT of 500 ms. The dd-MS^2 scan resolution was 17 500, the isolation width was 0.7 *m/z*, and stepped collision energy was used at 10, 20, and 30 eV. The minimum AGC target was $1 \cdot 10^3$ and dynamic exclusion was set to 120 s. Centroid data was stored to reduce file size. These method parameters ensured that approximately 150 dd-MS^2 scans per peak could be performed, and together with dynamic exclusion and method exclusion list should ensure that as many unique features as possible are interrogated by dd-MS^2 within a single run.

MS^2 spectra were extracted from the acquired raw data files with Raw Converter [23] and processed using a code written in VBA for Excel. The output consisted of precursor ion masses and scores calculated according to the Eq. (1). A window of 0.002 *m/z* was used in the processing to account for the dispersion of the measured accurate masses. The score represented the fraction of all signals in the spectrum that was due to the target ions. This approach was essentially similar to the NIST "reverse search", which ignores non-matching peaks, and does not penalise the score for peaks that are not found in the library spectrum [24].

$$Score = \sum target\ ion\ signals \ / \ \sum all\ ion\ signals \quad (1)$$

A reagent blank was processed this way to establish a threshold score, then spiked samples (at 10 and 20 µg kg^{-1}) were analysed and the data were processed. Two sets of target ions were compared – 8 common fragment ions of pyrrolizidine alkaloids (94.0656, 120.0808, 136.0756, 138.0911, 150.0912, 156.1018, 168.1016, 172.0960 *m/z*), as well as 1 common fragment ion originating from the necine base substructure (94.0656 *m/z*). The results are given in Fig. 3.

2.7. Calculations

For the estimation of extraction efficiency and matrix effects, spiked samples and spiked extracts were prepared from two randomly selected blank samples of tea and honey matrices, as well as standard solutions and spiked blanks were prepared to an equal theoretical on-column mass for direct comparison according to Eqs. (2) and (3). The extraction efficiency was estimated according to the Eq. (2):

$$EEF = 100\% \cdot A_{spiked\ sample}/A_{spiked\ aliquot} \quad (2)$$

where $A_{spiked\ sample}/A_{spiked\ aliquot}$ is the ratio of analyte response from a blank matrix spiked prior to the extraction to the analyte response from a spiked extract aliquot from a sample not containing the analyte.

The matrix effect was estimated according to the Eq. (3):

$$ME = 100\% \cdot \left(A_{spiked\ aliquot}/A_{spiked\ solvent} - 1\right) \quad (3)$$

where $A_{spiked\ aliquot}/A_{spiked\ solvent}$ is the ratio of analyte response from a spiked blank matrix extract aliquot to the analyte response from standard in the solvent.

The expanded measurement uncertainties at 95% confidence interval were estimated according to the Eq. (4):

$$U = k \cdot \sqrt{RSD_{WR}^2 + RMS_{bias}^2 + u_{C_{ref}}{}^2} \quad (4)$$

where k is the coverage factor, RSD_{WR} is the within-laboratory reproducibility, RMS_{bias} is the root-mean-squared bias, and u_{Cref} is the relative uncertainty of the value for the standard. The combination of RMS_{bias} and u_{Cref} was expressed as trueness in the Supplementary material (Table S6).

2.8. Calibration and quality assurance

A one-point standard addition calibration was performed by spiking another replicate at 4 µg kg^{-1} before extraction. In the case of higher concentrations in the sample a reanalysis was performed, and the standard addition was increased accordingly up to 40 µg kg^{-1}. Pyrrolizidine alkaloids that could not be separated chromatographically were analysed as the sum of coeluting analytes. Analytes were confirmed by a set of peaks from at least two different product ions. LOQ was determined experimentally as the average of individual values from three different blank samples based on peaks with S/$N \geq 10$. For the estimation of measurement uncertainty, a total of 3 procedural replicate five-point calibration sets were analysed for each representative matrix on at least two different days, and the reproducibility, trueness and uncertainty were determined from lowest calibration level. The average expanded measurement uncertainty was 21%, and the uncertainty for each representative matrix was the following: 18% for honey, 30% for tea, 20% for milk, and 17% for herbal tinctures. The validation results of the nano-LC-MS method are given in Supplementary materials (Table S6).

3. Results and discussion

3.1. Evaluation of matrix effects and sensitivity for different sample preparation procedures and standard stability evaluation

The average extraction efficiency for all matrices obtained by using the QuEChERS extraction procedure was 76 ± 30%, and 73 ± 15% by using SPE. The average matrix effects and average peak height of all analytes are given in Fig. 2, and the individual peak heights and matrix effects are given in Supplementary materials (Table S5). While the average matrix effect with dilution methods was low, the individual values varied widely, therefore a standard addition calibration was needed for proper quantifications. Strong matrix effects were observed with the preconcentration methods and solid phase extraction. Taken together, the observations show that the analysis of diluted extracts with nano-LC-MS is more sensitive than with conventional flow LC-MS used in our study. The median LOQ over all analytes was 0.33 µg kg^{-1} in honey (0.05–2.5 µg kg^{-1}) and 3.6 µg kg^{-1} in tea (0.5–20 µg kg^{-1}), with conventional LC-MS the LOQs were 6.0 µg kg^{-1} in honey (0.2–23 µg kg^{-1}) and 7.8 µg kg^{-1} in tea (0.8–44 µg kg^{-1}) for diluted QuEChERS samples. The results of matrix effect estimation are given in Fig. 2. The estimated limits of the quantification method are given in the Supplementary Table S3, together with the quantified concentrations of pyrrolizidine alkaloids. Most published methods use at 50–150 mm long columns and particles in size < 3 µm. In this study the median LOQ over all analytes was 0.33 µg kg^{-1} in honey (0.05–2.5 µg kg^{-1}), 3.6 µg kg^{-1} in tea (0.5–20 µg kg^{-1}), 3.3 µg kg^{-1} in herbal tinctures (0.3–10 µg kg^{-1}), and 0.32 µg kg^{-1} in milk (0.03–1.1 µg kg^{-1}). The data demonstrates that in this study the sensitivity is comparable or better than in methods from the literature (Table 1).

Our results demonstrated that standard stability might be limited at lower temperature (see Fig. 1). The literature data on stability of PAs in stock solutions is rather limited. However, it is suggested that the standards are stable in methanol for at least a year at −20 °C [25]. In other study, the stability of analytes at different temperatures was evaluated, and the storage data at −18 °C demonstrated that the stability is not ideal and loss of analytes by

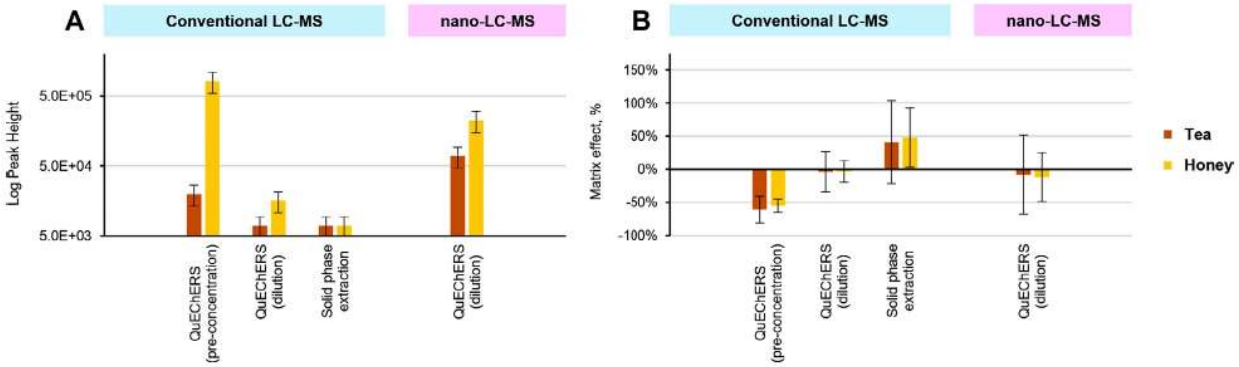

Fig. 2. Conventional LC-MS and nano-LC-MS average log peak height (A) and the comparison of average matrix effects (B) of all analytes. For conventional LC-MS, the solid phase extraction dilution factor was $d = 1.8$; with QuEChERS and pre-concentration $d = 2$ for tea and $d = 0.4$ for honey; with QuEChERS and dilution $d = 40$ for tea and honey. For nano-LC-MS, the dilution factor was $d = 37.5$ for tea, and $d = 7.5$ for honey. These dilution factors represent the highest amount of matrix reasonable to be injected without encountering immediate instrumental problems or deterioration of separation quality. These dilution factors were established empirically.

the day 30 is about 30% from the initial, while some analytes remained the same or had some small losses [26], which is similar to this study where the loss is about 30–40%. In our study the standards were dissolved in a 1:1 mixture of 50% aqueous acetonitrile and methanol, which could explain the difference in stability. Therefore, it can be concluded, that the stability of analytes at −18 °C is good when methanol is used for dissolving the compounds, while if some other solvent or mixture is used, then the stability is reduced in comparison to pure methanol.

3.2. The occurrence of pyrrolizidine alkaloids in tea, honey, herbal tinctures, and milk in Latvia and the assessment of risk to consumers

To date, no studies have been performed on the occurrence of pyrrolizidine alkaloids in plants of Latvian origin. Some pyrrolizidine alkaloid producing plants are widespread in Latvia, for example, camomile and peppermint, which can produce high pyrrolizidine alkaloid levels, are widely grown in households, while coltsfoot, ragwort, and comfrey are widespread in the flora [27,28]. Thus, honey products and herbal tea products can be contaminated with pyrrolizidine alkaloids.

3.2.1. Tea samples

15 herbal tea samples were analysed, five of which were plant mixtures that included not only different herbal plants, but also species like cloves and ginger root. Seven of the samples were found to contain pyrrolizidine alkaloids. In one sample of yarrow tea, the total pyrrolizidine alkaloid concentration was 215 µg/kg, which is the maximum limit according to Commission Regulation (EU) 2020/2040 amending Regulation (EC) 1881/2006 on the maximum permissible levels of pyrrolizidine alkaloids. The average concentration for the positive samples was 71 µg kg^{-1}. The second highest concentration of 126 µg kg^{-1} was found in a branded product containing a complex mixture, including wormwood, yarrow, and cloves. Most of the detected pyrrolizidine alkaloids in the samples (97% of total concentration) were in the form of *N*-oxides. There is no information on whether yarrow plants produce pyrrolizidine alkaloids, therefore, the presence of these alkaloids may be due to contamination during harvesting. The levels of pyrrolizidine alkaloid contamination in herbal teas were consistent with other European studies [27].

Due to the fact that the bioavailability of pyrrolizidine alkaloids and their *N*-oxides depend on their extraction into the liquid phase during the infusion of tea, it was interesting to investigate the correlation between the content of each pyrrolizidine alkaloid and its *N*-oxide in dry tea and the concentration of these compounds in the hot tea obtained via infusion process. Two additional tea samples (fennel and anise) were chosen, containing the highest natural contamination with pyrrolizidine alkaloids. The concentrations in three parallel tea infusions prepared by following the instructions on tea package were determined and compared with the concentration off pyrrolizidine alkaloids in the dry product. The data obtained are shown in the Supplementary Fig. S2. The obtained data showed that the total number of alkaloids extracted with the different treatments was comparable. While inhomogeneity of distribution of PAs in a sample and measurement uncertainty could explain variance in quantitative assessment, however, the infusion extracts had overall greater concentrations than QuEChERS extracts, which could be explained by prolonged extraction at higher temperature. A stability experiment at elevated temperature was previously performed with solutions of analyte standards, which confirmed that the temperature up to 100 °C did not cause degradation of the analytes. For risk assessment procedures, the amount of extracted pyrrolizidine alkaloids in tea infusions could be equated to the amount in a dry product.

3.2.2. Honey samples

A total of 40 honey samples originating from Latvia were purchased from the local market and analysed. One third (33%) of the samples contained pyrrolizidine alkaloids, with an average concentration of 9.4 µg kg^{-1}. The highest level of pyrrolizidine alkaloids was found in summer season honey from forest flowers – 74 µg kg^{-1}. The concentrations of detected pyrrolizidine alkaloids in Latvian honey samples were also consistent with other European studies: 2.9 µg kg^{-1} reported in Poland [5], 6.1 - 15 µg kg^{-1} reported in Germany and Austria [27]. Similarly, as in the report from Poland [5], in this study the percentage of positive samples was 32%, but this indicator of occurrence can change depending on the production years. The lycopsamine-type alkaloids, notably echimidine and lycopsamine, were the most prevalent, while senecionine-type alkaloids were detected significantly less frequently and at low concentrations. Other reports [29,30] gave similar findings, including the EFSA report 2016 [31]. Most of the analysed honey samples were polyfloral, therefore it was not possible to evaluate the effect of flowering plant species on the concentration of alkaloids in honey.

In an EFSA report from 2017 [32], the CONTAM Panel reported a $BMDL_{10}$ of 237 µg kg^{-1} per day (the lower confidence limit on the benchmark dose associated with 10% response) based on the carcinogenicity of riddelliine in rats with the MOE (margin of exposure) of 10,000. Based on the long term consumption data, the most frequent consumers of honey were adults and adolescents, with an average consumption of 15.6 g per day and 11.4 g per day, respectively, while typical consumption by children was up to 10 g per day [33]. Considering the average adult weight of 70 kg and an average child weight of 15 kg, adults can have a maximum daily intake of pyrrolizidine alkaloids at $(237 \cdot 70\text{kg} / 10{,}000) = 1.65$ µg, and children – 0.35 µg. The maximum concentration in honey should, therefore, not exceed (1.65 µg / 0.0156 kg) = 105 µg kg^{-1} for adults, and 35 µg kg^{-1} for children. among the analysed samples, only one exceeded the recommended limit for children. Other positive samples had relatively low concentrations of pyrrolizidine alkaloids (0.14 - 11.6 µg kg^{-1}), therefore there is essentially no risk to children unless the typical daily consumption would be exceeded at least 3-fold. The consumption data were retrieved from the Food Consumption Data section of EFSA database.

3.2.3. Herbal tincture and milk samples

A total of 15 herbal tincture samples and 10 milk samples originating from Latvia were purchased from the local market and analysed. The pyrrolizidine alkaloids were not detected in any of the samples.

3.3. Results and conclusions from target ion screening workflow

Preliminary experiments performed on analytical standards showed that pyrrolizidine alkaloids mainly produce common fragment ions upon collision-induced dissociation: 94.0656, 120.0808, 136.0756, 138.0911, 150.0912, 156.1018, 168.1016, and 172.0960 *m/z* (± 0.001 *m/z*). The exact fragments and abundance ratios depend on the structure of the alkaloid [34]. Fragment 94.0656 *m/z* could be of particular importance [35], as it may originate from all the tested analytical standards, particularly at higher collision energies, although with widely varying yields. Furthermore, preliminary experiments in the all-ion fragmentation mode performed on extracts of several plants that do not produce alkaloids showed low baselines of chromatogram with no detected peaks, suggesting that the fragment 94.0656 *m/z* is rather uncommon. Therefore, the screening results were compared in the case of two sets of target fragments – all common fragment ions and the 94.0656 *m/z* fragment ion only. Also, two spiking levels were compared with

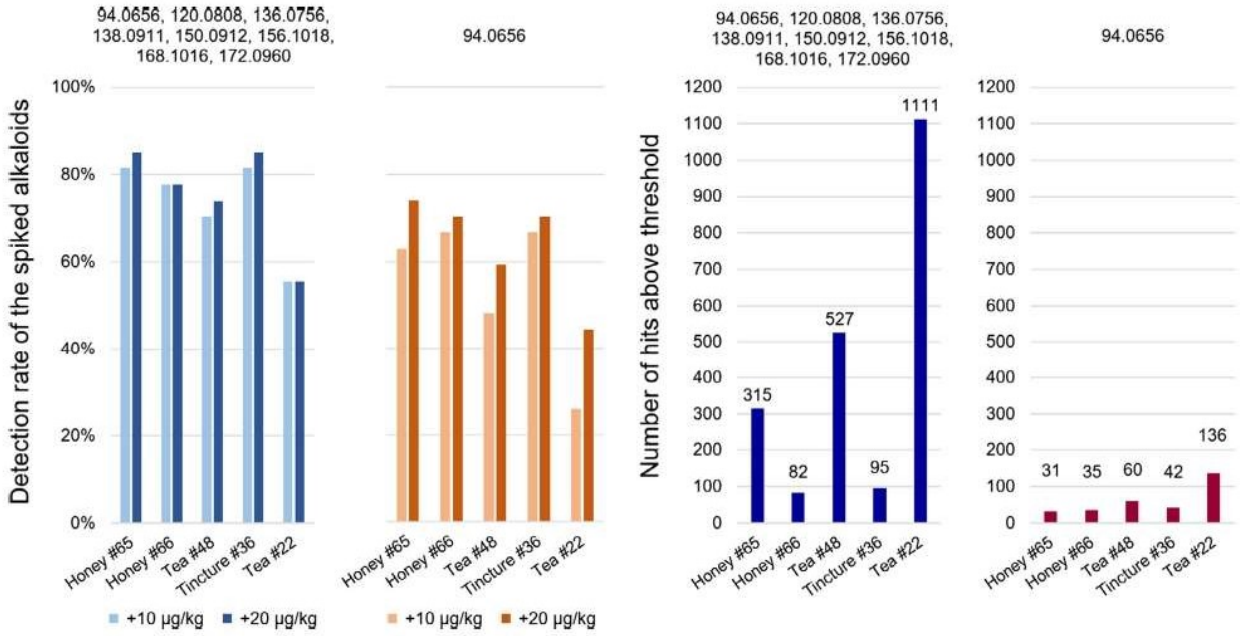

Fig. 3. Comparison of two different sets of target fragment ions for screening with respect to the detection rate of added alkaloids at two concentration levels – 10 µg kg^{-1} and 20 µg kg^{-1}, and the number of hits above the threshold at 10 µg kg^{-1}.

respect to the detection rate of alkaloids in spiked samples. The results are given in Fig. 3. The detection rate was approximately 20% higher if all common fragment ions were used as targets, however, in such a case the number of hits above the threshold were about 10 times higher. The rate of detection for added alkaloids improved with increased spiking level, thus higher concentrations could be detected more reliably. The results given in Fig. 3 correlate with the nature of samples – honey #65 and tea #48 were products that contained known pyrrolizidine alkaloids, and tea #22 was derived from *Calendula*, which could contain unknown or uncommon pyrrolizidine alkaloids, as shown recently [34], and the number of hits above the threshold in these samples was significantly higher, while honey #66 and herbal tincture #36 were not expected to contain any pyrrolizidine alkaloids or contaminated ingredients, and the number of hits above threshold in these samples was low. Reanalysis of the screening hits in high resolution MS^2 with narrow precursor isolation is needed to confirm whether the observed fragment ions constitute a common chromatographic feature and to further analyse the spectral data in order to identify possible chemical structures of the precursor ion. Furthermore, reanalysis with other detection techniques could provide additional structural information. Fig. 4 illustrates the main advantage of the approach used in this study for trace contaminant detection in complex samples – after reanalysis of the hits exceeding threshold in high resolution with precursor isolation, easily interpretable chromatographic features were obtained for the detected spiked pyrrolizidine alkaloids, while the chromatographic features based on the precursors in full scan alone, even at the high resolution of 70 000, were not useful for interpretation, due to the lack of selectivity. The number of hits exceeding the threshold with the 94.0656 *m/z* target fragment ion was similar to the number of added alkaloids (30 different pyrrolizidine alkaloid standards were added) in samples where contamination was not expected. Tea samples #48 and #22, which were expected to contain alkaloids, showed a larger number of hits exceeding the threshold. Taken together these findings show that the 94.0656 *m/z* fragment ion is a selective fragment ion for detection and discovery of pyrrolizidine alkaloids with high resolution mass spectrometry.

3.3.1. Possible origins and structure of the proposed target ion

Database searches were conducted to elucidate the most probable origins of the 94.0656 *m/z* fragment ion. We found that the fragment ion signal 94.0656 ± 0.001 *m/z* corresponding to $C_6H_8N^+$ (monoisotopic mass 94.0651 Da) can be obtained from molecules with such structural features as picoline, methylpyridine including *N*-methylpyridinium, aniline, 2,3,5,7a-tetrahydro-*1H*-pyrrolizine, pyrrolizidine, and tropane. The possible exact structures of the $C_6H_8N^+$ ion as a product ion from a tropane alkaloid have been proposed in the literature [36], where *N*-methylpyridinium structure was proposed. *In silico* models propose that the structure of the $C_6H_8N^+$ ion as a product ion from a pyrrolizidine alkaloid could be 1-methyl-3-methylidene-*3H*-pyrrol-1-ium (heuristic prediction by Mass Frontier 7.0 in mzCloud database). It could be argued that the $C_6H_8N^+$ fragment ion is a highly selective target fragment ion for the detection and discovery of pyrrolizidine alkaloids and, possibly, tropane alkaloids, provided that the experimental chromatography and mass spectrometry setup has high resolution and is optimal for broad MS^2 interrogation with narrow isolation, and provided that effective measures are taken to discern between the features originating from the sample and background contamination, as well as to fragment the precursor ions optimally.

3.3.2. Possibilities to further improve reliability of target ion screening

Most failures to detect the added alkaloids occurred among the later eluting compounds. Also, the absolute collision energies were used throughout the experiment instead of the Orbitrap normalised collision energy, thus pyrrolizidine alkaloids with larger molar mass were fragmented with relatively weaker collision energies, resulting in lower yield of the desired fragments. Furthermore, the Orbitrap exclusion list, being static apart from the active dynamic exclusion, was used throughout the entire chromatogram based on the first half of the chromatogram obtained from the reagent blank. Also, since the gradient was not linear, it can be expected that the number of compounds eluting simultaneously is much greater further down the chromatogram. These conditions could be considered non-ideal for the purpose of the experiment, therefore, the increase in failures to detect the added alkaloids

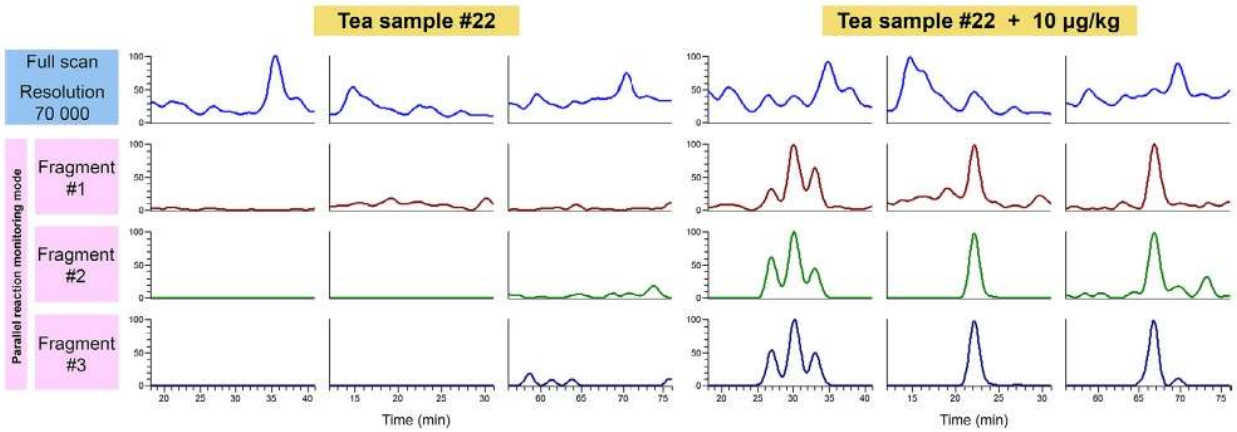

Fig. 4. Chromatographic features obtained by reanalysis of precursor ion hits above threshold in parallel reaction monitoring mode (PRM), compared to the precursor ion in full scan. The peaks in PRM mode are the following: echinatine *N*-oxide, 27 min; indicine *N*-oxide and intermedine *N*-oxide, 30 min; lycopsamine *N*-oxide, 33 min; europine, 22 min; seneciphylline *N*-oxide, 67 min.

Table 2
The total pyrrolizidine alkaloid concentrations measured in different foods of Latvian origin (the sum of 30 pyrrolizidine alkaloids is shown, including *N*-oxides).

Type of sample	*N*	Samples >LOQ,%	Minimum, µg/kg	Maximum, µg/kg	Mean, µg/kg
Herbal tea	15	47	5.8	215	71
Honey	40	33	0.14	74	9.4
Herbal tincture	15	0	< LOQ	–	–
Milk	10	0	< LOQ	–	–

with increasing molar mass and retention time is not surprising. Furthermore, the complexity of the matrix clearly has a significant effect on detection rate when the scanning capability is overwhelmed by the high number of coeluting compounds. To solve this issue, the inverse gradient technique could be applied, as well as a time-dependent variable exclusion list based on the reagent blank. Finally, normalised collision energies could be applied.

4. Concluding remarks

A nano-LC-MS method was developed for the determination of pyrrolizidine alkaloids in tea, honey, herbal tinctures, and milk samples. Different sample preparation procedures were evaluated. A QuEChERS procedure with dilution of samples achieved negligible matrix effects in comparison with the same procedure using a pre-concentration step or an SPE procedure. The nano-LC-MS method demonstrated superior sensitivity in comparison with a conventional flow LC-MS. Quantitative and screening analysis of pyrrolizidine alkaloids was performed. quantitation was performed with analytical standards. The screening analysis included MS^2 screening for fragment ions that are commonly produced by pyrrolizidine alkaloids during collision-induced dissociation. It is proposed that the $C_6H_8N^+$ fragment ion could be used as a highly selective target fragment ion for the detection and discovery of pyrrolizidine alkaloids using high resolution mass spectrometry.

The elaborated quantitative analysis method was applied for the occurrence study of pyrrolizidine alkaloids in various food products available on the Latvian market (Table 2), including samples of tea (n = 15), honey (n = 40), herbal tinctures (n = 15), and milk (n = 10). One herbal tea sample had a total pyrrolizidine alkaloid concentration of 215 µg kg^{-1}. In herbal tincture and milk samples, no pyrrolizidine alkaloids were detected above the LOQ values, while the presence of alkaloids was detected in 33% of honey samples and 47% of tea samples. Pyrrolizidine alkaloids in tea samples were mainly in the form of *N*-oxides. Lycopsamine type alkaloids were the most frequent in honey samples. Additionally, a risk assessment based on the product consumption data and benchmark dose was used to determine the maximum daily intake of pyrrolizidine alkaloids. Only one summer season honey from forest flowers with the total pyrrolizidine alkaloid concentration of 74 µg kg^{-1} exceeded the maximum recommended daily intake limit for children, while no other samples exceeded this limit for adults. The median LOQ over all analytes was 0.33 µg kg^{-1} in honey, 3.6 µg kg^{-1} in tea, 3.3 µg kg^{-1} in herbal tinctures, and 0.32 µg kg^{-1} in milk. The occurrence of pyrrolizidine alkaloids in various food products from the Latvian market was, in general, at low levels that are far below the maximum limit set by Commission Regulation (EU) 2020/2040.

Declaration of Competing Interest

The authors declare that they have no known competing financial interests or personal relationships that could have appeared to influence the work reported in this paper.

CRediT authorship contribution statement

Martins Jansons: Conceptualization, Validation, Software, Writing – original draft, Visualization, Investigation. **Deniss Fedorenko:** Methodology, Writing – review & editing. **Romans Pavlenko:** Writing – review & editing, Investigation. **Zane Berzina:** Writing – review & editing, Investigation. **Vadims Bartkevics:** Methodology, Resources, Writing – review & editing.

Supplementary materials

Supplementary material associated with this article can be found, in the online version, at doi:10.1016/j.chroma.2022.463269.

References

[1] O. Seremet, O. Olaru, C. Gutu, G. Nitulescu, M. Ilie, S. Negres, C. Zbarcea, C. Purdel, D. Spandidos, A. Tsatsakis, M. Coleman, D. Margina, Toxicity of plant extracts containing pyrrolizidine alkaloids using alternative invertebrate models, Mol. Med. Rep. 17 (2018) 7757–7763, doi:10.3892/mmr.2018.8795.

[2] E. Castells, P.P.J. Mulder, M. Pérez-Trujillo, Diversity of pyrrolizidine alkaloids in native and invasive Senecio pterophorus (Asteraceae): implications for toxicity, Phytochemistry 108 (2014) 137–146, doi:10.1016/j.phytochem.2014.09.006.
[3] I. Geburek, A. Preiss-Weigert, M. Lahrssen-Wiederholt, D. Schrenk, A. These, *In vitro* metabolism of pyrrolizidine alkaloids – metabolic degradation and GSH conjugate formation of different structure types, Food Chem. Toxicol. 135 (2020) 110868, doi:10.1016/j.fct.2019.110868.
[4] G. Osweiler, Veterinary Clinics of North America: Food Animal Practice. Ruminant Toxicology. Saunders an Imprint of, Elsevier, Philadelphia, USA, 2011.
[5] E. Kowalczyk, K. Kwiatek, Pyrrolizidine alkaloids in honey: determination with liquid chromatography-mass spectrometry method, J. Vet. Res. 62 (2018) 173–181, doi:10.2478/jvetres-2018-0027.
[6] C. Ma, Y. Liu, L. Zhu, H. Ji, X. Song, H. Guo, T. Yi, Determination and regulation of hepatotoxic pyrrolizidine alkaloids in food: a critical review of recent reseaarch, Food Chem. Toxicol. 119 (2018) 50–60, doi:10.1016/j.fct.2018.05.037.
[7] BfR (Bundesinstitut für Risikobewertung), Analytik und Toxizität von Pyrrolizidinalkaloiden sowie eine Einschätzung des gesundheitlichen Risikos durch deren Vorkommen in Honig, BfR-Stellungnahmen 38 (2011) 1–37 https://www.bfr.bund.de/cm/343/analytik-und-toxizitaet-von-pyrrolizidinalkaloiden.pdf. (Accessed 1 September 2020).
[8] M. Nold, Detect pyrrolizidine alkaloid contamination in food, Analytix Reporter (5) (2019) 14 https://www.sigmaaldrich.com/deepweb/assets/sigmaaldrich/marketing/global/documents/730/477/analytix-reporter-5-2019-mk.pdf. (Accessed 1 September 2020).
[9] C.T. Griffin, M. Danaher, C.T. Elliott, D.G. Kennedy, A. Furey, Detection of pyrrolizidine alkaloids in commercial honey using liquid chromatography–ion trap mass spectrometry, Food Chem. 136 (2013) 1577–1583, doi:10.1016/j.foodchem.2012.02.112.
[10] M. Martinello, C. Cristofoli, A. Gallina, F. Mutinelli, Easy and rapid method for the quantitative determination of pyrrolizidine alkaloids in honey by ultra performance liquid chromatography-mass spectrometry: an evaluation in commercial honey, Food Control 37 (2014) 146–152, doi:10.1016/j.foodcont.2013.09.037.
[11] D. Bodi, S. Ronczka, C. Gottschalk, N. Behr, A. Skibba, M. Wagner, M. Lahrssen-Wiederholt, A. Preiss-Weigert, A. These, Determination of pyrrolizidine alkaloids in tea, herbal drugs and honey, Food Addit. Contam. Part A 31 (2014) 1886–1895, doi:10.1080/19440049.2014.964337.
[12] J.F. Picron, M. Herman, E.V. Hoeck, S. Goscinny, Analytical strategies for the determination of pyrrolizidine alkaloids in plant based food and examination of the transfer rate during the infusion process, Food Chem. 266 (2018) 514–523, doi:10.1016/j.foodchem.2018.06.055.
[13] A. Dübecke, G. Beckh, C. Lüllmann, Pyrrolizidine alkaloids in honey and bee pollen, Food Addit. Contam. 28 (2011) 348–358 Part A, doi:10.1080/19440049.2010.541594.
[14] C. Mathon, P. Edder, S. Bieri, P. Christen, Survey of pyrrolizidine alkaloids in teas and herbal teas on the Swiss market using HPLC-MS/MS, Anal. Bioanal. Chem. 406 (2014) 7345–7354, doi:10.1007/s00216-014-8142-8.
[15] M.a Bolechová, J. Čáslavský, M. Pospíchalová, P. Kosubová, UPLC–MS/MS method for determination of selected pyrrolizidine alkaloids in feed, Food Chem 170 (2015) 265–270, doi:10.1016/j.foodchem.2014.08.072.
[16] K. Ewelina, K. Krzysztof, Use of a new LC-MS method for the determination of pyrrolizidine alkaloids in feeds, J. Vet. Res. 62 (2018) 183–191, doi:10.2478/jvetres-2018-0028.
[17] Alexandra Sixto, Silvina Niell, Horacio Heinzen, Straightforward determination of pyrrolizidine alkaloids in honey through simplified methanol extraction (QuPPE) and LC-MS/MS modes, ACS Omega 4 (2019) 22632–22637, doi:10.1021/acsomega.9b03538.
[18] M. Schulz, J. Meins, S. Diemert, P. Zagermann-Muncke, R. Goebel, D. Schrenk, M. Schubert-Zsilavecz, M. Abdel-Tawab, Detection of pyrrolizidine alkaloids in German licensed herbal medicinal teas, Phytomedicine 22 (2015) 648–656, doi:10.1016/j.phymed.2015.03.020.
[19] C. Ma, Y. Liu, L. Zhu, H. Ji, X. Song, H. Guo, T. Yi, Determination and regulation of hepatotoxic pyrrolizidine alkaloids in food: a critical review of recent research, Food Chem. Toxicol. 119 (2018) 50–60, doi:10.1016/j.fct.2018.05.037.
[20] C. Crews, B. Berthiller, R. Krska, Update on analytical methods for toxic pyrrolizidine alkaloids, Anal. Bioanal. Chem. 396 (2010) 327–338, doi:10.1007/s00216-009-3092-2.
[21] W. Zhang, W. Huai, Y. Zhang, J. Shen, X. Tang, X. Xie, K. Wang, H. Fan, Ultra-performance liquid chromatography hyphenated with quadrupole-orbitrap mass spectrometry for simultaneous determination of Necine-core-structure pyrrolizidine alkaloids in Crotalaria sessiliflora L. without all corresponding standards, Phytochem. Anal. 28 (2017) 365–373, doi:10.1002/pca.2683.
[22] B. Avula, S. Sagi, Y..H. Wang, J. Zweigenbaum, M. Wang, I.A. Khan, Characterization and screening of pyrrolizidine alkaloids and N-oxides from botanicals and dietary supplements using UHPLC-high resolution mass spectrometry, Food Chem. 178 (2015) 136–148, doi:10.1016/j.foodchem.2015.01.053.
[23] L. He, J. Diedrich, Y.Y. Chu, J.R. Yates, Extracting accurate precursor information for tandem mass spectra by Raw Converter, Anal. Chem. 87 (2015) 11361–11367, doi:10.1021/acs.analchem.5b02721.
[24] T. Kind, H. Tsugawa, T. Cajka, Y. Ma, Z. Lai, S. Mehta, G. Wohlgemuth, D. Barupal, M. Showalter, M. Arita, O. Fiehn, Identification of small molecules using accurate mass MS/MS search, Mass Spectrom. Rev. 37 (2018) 513–532, doi:10.1002/mas.21535.
[25] M. Willocx, I. Beeten, P. Asselman, L. Delgat, W. Baert, S. Janssens, F. Leliaert, J. Picron, C. Vanhee, Sorting out the plants responsible for a contamination with pyrrolizidine alkaloids in spice seeds by means of LC-MS/MS and DNA barcoding: proof of principle with cumin and anise spice seeds, Food Chem.: Mol. Sci. 4 (2022) 100070, doi:10.1016/j.fochms.2021.100070.
[26] E. Kowalczyk, K. Kwiatek, Use of a new LC-MS method for the determination of pyrrolizidine alkaloids in feeds, J. Vet. Res. 62 (2018) 183–191, doi:10.2478/jvetres-2018-0028.
[27] D. Bodi, S. Ronczka, C. Gottschalk, N. Behr, A. Skibba, M. Wagner, M. Wiederholt, A. Weigert, A. These, Determination of pyrrolizidine alkaloids in tea, herbal drugs and honey, Food Addit. Contam. Part A 31 (2014) 1886–1895, doi:10.1080/19440049.2014.964337.
[28] A. Kļaviņš, Gandrs Ltd., Enciklopēdija "Latvijas Daba", Encyclopedia 'Nature of Latvia'. https://www.latvijasdaba.lv/augi/senecio-jacobaea-l/, 2021 (accessed 1 September 2020).
[29] B. Huybrechts, A. Callebaut, Pyrrolizidine alkaloids in food and feed on the Belgian market, Food Addit. Contam. Part A 32 (2015) 1939–1951, doi:10.1080/19440049.2015.1086821.
[30] M. Martinello, A. Borina, R. Stella, D. Bovo, G. Biancotto, A. Gallina, F. Mutinellia, Development and validation of a QuEChERS method coupled to liquid chromatography and high resolution mass spectrometry to determine pyrrolizidine and tropane alkaloids in honey, Food Chem. 234 (2017) 295–302, doi:10.1016/j.foodchem.2017.04.186.
[31] European food safety authority, dietary exposure assessment to pyrrolizidine alkaloids in the European population, EFSA J. 14 (2016) 1–50, doi:10.2903/j.efsa.2016.4572.
[32] H. Knutsen, J. Alexander, L. Barregård, M. Bignami, B. Brüschweiler, S. Ceccatelli, B. Cottrill, M. Dinovi, L. Edler, B. Kraupp, C. Hogstrand, L. Hoogenboom, C. Nebbia, I. Oswald, A. Petersen, M. Rose, A. Roudot, T. Schwerdtle, C. Vleminckx, G. Vollmer, H. Wallace, J. Ruiz, M. Binaglia, EFSA Panel on Contaminants in the Food Chain (CONTAM), Risks for human health related to the presence of pyrrolizidine alkaloids in honey, tea, herbal infusions and food supplements, EFSA J. 15 (2017) 1–34, doi:10.2903/j.efsa.2017.4908.
[33] European Food Safety Authority, Use of the EFSA comprehensive European food consumption database in exposure assessment, EFSA J. 9 (2011) 1–34, doi:10.2903/j.efsa.2011.2097.
[34] A. These, D. Bodi, S. Ronczka, M. Lahrssen-Wiederholt, A. Preiss-Weigert, Structural screening by multiple reaction monitoring as a new approach for tandem mass spectrometry: presented for the determination of pyrrolizidine alkaloids in plants, Anal. Bioanal. Chem. 405 (2013) 9375–9383, doi:10.1007/s00216-013-7365-4.
[35] B. Avula, S. Sagi, Y.H. Wang, J. Zweigenbaum, M. Wang, I.A. Khan, Characterization and screening of pyrrolizidine alkaloids and N-oxides from botanicals and dietary supplements using UHPLC-high resolution mass spectrometry, Food Chem. 178 (2015) 136–148, doi:10.1016/j.foodchem.2015.01.053.
[36] R.M. Smith, J.F. Casale, The mass spectrum of cocaine: deuterium labeling and MS/MS studies, Microgram J. 7 (2010) 16–41 https://www.dea.gov/documents/2010/2010-01/2010-01-01/mass-spectrum-cocaine-deuterium-labeling-and-msms-studies.

Mycotoxins in cereals and pulses harvested in Latvia by nanoLC-Orbitrap MS

Reinholds, I; Jansons, M.; **Fedorenko, D.**; Pugajeva, I.; Zute, S.; Bartkiene, E.; Bartkevics, V.

Food Additives & Contaminants: Part B[4], **2021**, *14(2)*, 115-123.

[4] *Peer reviewed journal, imprint of Taylor & Francis (IF=3.964 (2022)), ISSN: 1939-3229*

Taylor & Francis

Food Additives & Contaminants: Part B

Surveillance

ISSN: (Print) (Online) Journal homepage: https://www.tandfonline.com/loi/tfab20

Mycotoxins in cereals and pulses harvested in Latvia by nanoLC-Orbitrap MS

Ingars Reinholds, Martins Jansons, Deniss Fedorenko, Iveta Pugajeva, Sanita Zute, Elena Bartkiene & Vadims Bartkevics

To cite this article: Ingars Reinholds, Martins Jansons, Deniss Fedorenko, Iveta Pugajeva, Sanita Zute, Elena Bartkiene & Vadims Bartkevics (2021): Mycotoxins in cereals and pulses harvested in Latvia by nanoLC-Orbitrap MS, Food Additives & Contaminants: Part B, DOI: 10.1080/19393210.2021.1892204

To link to this article: https://doi.org/10.1080/19393210.2021.1892204

FOOD ADDITIVES & CONTAMINANTS: PART B
https://doi.org/10.1080/19393210.2021.1892204

Taylor & Francis
Taylor & Francis Group

ARTICLE

Mycotoxins in cereals and pulses harvested in Latvia by nanoLC-Orbitrap MS

Ingars Reinholds[a,b], Martins Jansons[a,b], Deniss Fedorenko[a,b], Iveta Pugajeva[a], Sanita Zute[c], Elena Bartkiene[d], and Vadims Bartkevics[a,b]

[a]Institute of Food Safety, Animal Health and Environment "BIOR", Riga, Latvia; [b]Faculty of Chemistry, University of Latvia, Riga, Latvia; [c]Stende Research Centre, Institute of Agricultural Resources and Economics (AREI), Riga, Latvia; [d]Department of Food Safety and Quality, Lithuanian University of Health Sciences, Kaunas, Lithuania

ABSTRACT

Twenty-seven mycotoxins in unprocessed cereals (n = 110) and pulses (n = 23) harvested in Latvia were analysed by nanoflow liquid chromatography combined with Orbitrap high-resolution mass spectrometry. One or more mycotoxins were found in 99% of the cereals and 78% of the pulses. Deoxynivalenol, zearalenone and T-2 and HT-2 toxins were prevalent in 9 to 86% of the cereals, mostly below their maximum levels as set by the European regulations. Non-regulated type A and B trichothecenes were prevalent in 5 to 87% of the cereals, at concentrations of 0.27–83 µg kg^{-1} and 1.7–4,781 µg kg^{-1}, respectively. Quantification of emerging mycotoxins was also provided. Enniatins were detected in 94% of the cereals (3.5–2,073 µg kg^{-1}) and 13% of the pulses (4.4–17 µg kg^{-1}). *Alternaria* toxins were prevalent in 94% of the cereals at concentrations of 0.72–307 µg kg^{-1} and in 39% of the pulses at 0.69–10 µg kg^{-1}.

ARTICLE HISTORY
Received 16 September 2020
Accepted 14 February 2021

KEYWORDS
Multi-mycotoxin analysis; unprocessed cereals and pulses; nanoflow liquid chromatography; Orbitrap mass spectrometry

Introduction

Grain cereals are the most susceptible crops to mycotoxins. Filamentous fungi produce mycotoxins during pre-harvest and post-harvest periods under certain environmental and microclimatic conditions, such as high temperatures, high humidity, elevated moisture and CO_2 levels, causing economic losses to the agriculture across the world (Xia et al. 2020).

While more than 500 mycotoxins are known, the maximum levels of mycotoxins in European non-processed and processed cereals have been set only for nine compounds (European Commission 2006). The International Agency for Research on Cancer (IARC), classified these as group 1, human carcinogen, for aflatoxin B_1 (AFB_1) and the combination of four aflatoxins (AFs: AFB_1 + AFB_2 + AFG_1 + AFG_2), as possible human carcinogens (group 2B) for ochratoxin A (OTA) and not classifiable as to its carcinogenicity to humans for the fumonisins FB_1 and FB_2 and the *Fusarium* toxins deoxynivalenol (DON) and zearalenone (ZEN). According to Commission Recommendation 2013/165/EU (European Commission 2013), data of type A trichothecenes T-2 and HT-2 are limited and further extended screening of these toxins has been advised because of their relatively high prevalence and contamination levels in the cereals harvested in Europe (Pleadin et al. 2017; Chen et al. 2020).

Compared to cereals, legumes are a wider group of protein-rich crop varieties and include lentils, beans, cowpeas, peas, soybeans, lupin beans, etc. However, no limits have been set in Europe for the mycotoxin levels in processed grain legumes and unprocessed pulses. Driven by the vegetarian and vegan food preferences and the increase in adults and children following grain-free diets due to certain allergies or intolerances, the consumption of legume products has been growing steadily in recent years. These crops are commonly grown under mycotoxin-growth-inducing climatic conditions, thus being more susceptible to cross-contamination with filamentous fungi that form mycotoxins (Żelechowski et al. 2019).

Type A and type B trichothecenes T-2, HT-2, DON, nivalenol (NIV) and acetylated DON forms (3-AcDON, 15-AcDON) have been associated with certain acute human and animal health disorders such as gastroenteritis outbreaks, immune suppression and haemorrhaging effects. ZEN, a mycoestrogenic toxin, has been associated with adverse effects such as reproductive disorders in domestic animals and hyperestrogenic syndrome in humans (Haque et al. 2020; Holanda and Kim 2020). Emerging *Fusarium* enniatins (ENNs), beauvericin (BEA) and *Alternaria* toxins have also raised concerns of health-endangering effects because of their high prevalence in non-processed crops and cereal products

CONTACT Ingars Reinholds Ingars.Reinholds@bior.lv
Supplemental data for this article can be accessed on the publisher's website.

(Arcella et al. 2016; Orlando et al. 2019), including infant food products (Gotthardt et al. 2019).

High and ultra-performance liquid chromatography (HPLC and UHPLC, respectively) combined with triple quadrupole tandem mass spectrometry (MS/MS) is the most commonly used method for mycotoxin analysis. LC methods that use single quadrupole (MS), fluorescence, UV or photodiode array detectors, or commercially available enzyme-linked immunosorbent assays (ELISA) have been used mainly for the detection of individual mycotoxins (Pereira et al. 2014; Khaneghah et al. 2019).

Multi-mycotoxin HPLC-MS/MS methods have been extensively improved over the last two decades in terms of sample preparation, selectivity and sensitivity for the qualitative and quantitative mycotoxin analyses. Analyte losses during sample preparation through multi-step procedures based on solid-phase extraction or use of immunoaffinity columns and matrix effects limit multi-mycotoxin analysis. However, these limitations can be overcome by using the stable isotope dilution technique (Malachová et al. 2018; Yang et al. 2019; Rausch et al. 2020).

Over the last decade, high-resolution mass spectrometry techniques (HRMS) based on time-of-flight and the Orbitrap systems have been introduced for multi-mycotoxin analysis, including targeted and non-targeted applications. Compared to MS/MS methods based on low-resolution multi-monitoring (MRM), such applications provide advantages of high-resolution detection using different available mass spectrometric modes such as full-scan or parallel reaction monitoring (PRM) and facilitate accurate mass measurement (<5 ppm) and the elimination or reduction of the interference impact on analyte signal intensity during multi-compound analysis (Bryła et al. 2016; Khaneghah et al. 2019). While improvements in method specificity of HRMS can be attributed to the increase in MS resolution, ion suppression/enhancement phenomena due to matrix factors may occur in both MS/MS and HRMS approaches (Righetti et al. 2016).

Nano-flow-based LC separation methods in combination with sensitive HRMS techniques have gained attention because of the benefits of simplified sample preparation protocols and increased analyte separation (Schneider et al. 2005; Medina et al. 2020). Recently, researchers from the University of Jaén (Spain) analysed 64 pesticide residues in different food matrices and quantified 17 mycotoxins in different nuts through nano-LC-MS (Moreno-González et al. 2017; Alcántara-Durán et al. 2019). Outstanding reduction of matrix effects with simultaneous maintenance of high sensitivity due to the high sample dilution factors as well as the relevant reduction in solvent usage was noted as the main benefit of the nano-LC approach. The matrices tested in these mycotoxin analyses included fruit and vegetable products as well as olive oil, pesticide and nuts. Therefore, much emphasis was placed on the optimisation of sample preparation processes by considering the matrix effects of such food matrices rich in pigments, carbohydrates and lipids.

The objective of the present study was to expand the knowledge on the non-regulated and emerging mycotoxin occurrence in grain cereals and legumes harvested in Latvia. The current study aimed to employ a nano-LC -MS combined with an Orbitrap mass spectrometry detector for the analysis of protein- and starch-rich products of plant origin. The method was applied for the analysis of 27 mycotoxins, including the emerging *Fusarium* and *Alternaria* toxins, in a total of 133 samples of eight non-processed crop varieties (barley, rye, triticale, summer wheat, winter wheat, peas, field beans and lupin beans), which can be considered as matrices rich in proteins and carbohydrates and may provide an interesting challenge for nanoflow separation techniques.

Materials and methods

Chemicals and reagents

All the mycotoxin standards were with purities ranging from 97.4 to 99.5% and assay uncertainties of 2–5%: Aflatoxin B_1 (AFB_1), deoxynivalenol (DON), deoxynivalenol-3-glucoside (D3G), fusarenon X (FUS X), nivalenol (NIV), ochratoxin A (OTA), T-2 toxin (T-2), zearalenone (ZEN) were procured from Biopure-Romer Labs (Tulln, Austria). 15-acetyldeoxynivalenol (15-AcDON), 3-acetyldeoxynivalenol (3-AcDON), alternariol monomethyl ether (AME), enniatin B (ENN B), enniatin B_1,(ENN B_1), tentoxin (TEN) were purchased from Cayman Chemical (Ann Arbor, MI, USA) and 15-monoacetoxyscirpenol (15-MAS), aflatoxicol (AFL), altenuene (ALT), alternariol (AOH), altertoxin I (ATX I), fumonisin B_1 (FB_1), fumonisin B_2 (FB_2), fumonisin B_3 (FB_3), HT-2 toxin (HT-2), neosolaniol (NEO), ochratoxin B (OTB), T-2 toxin triol (T-2TRI) and T-2 tetraol (T-2TET) were purchased from Fermentek Ltd. (Jerusalem, Israel). Stock solutions of 1,000 mg L^{-1} concentrations were prepared in non-aqueous solvents and stored in a freezer at −20°C. Working standard solutions were prepared in 20% aqueous acetonitrile and stored frozen (−20°C) in amber glass bottles.

Formic acid (99%) was obtained from VWR Chemicals (Radnor, PA, USA). LC-MS grade ultra-

pure water and acetonitrile used for the preparation of mobile phases and sample extract diluents, as well as HPLC grade solvents used for sample extractions were obtained from Merck (Darmstadt, Germany).

The stability of multi-mycotoxin standard solutions prepared in 20% aqueous acetonitrile was evaluated by comparing the responses between peaks from fresh standard solution and a standard solution stored for 7, 30 and 50 days ($n = 5$). Evaluation based on unpaired t-tests was performed on groups of peak areas of a fresh standard and an aged one and $p < .05$ was interpreted as strong evidence against the null hypothesis. All mycotoxins were found stable for at least 50 days, except for AOH, AFB_1 and 15-MAS, which were stable for 30 days and NEO, OTB and D3G, which were stable for 7 days. Therefore, fresh multi-mycotoxin solutions of those standards were prepared weekly.

Samples

For this study, 133 agricultural crop samples (110 grain cereals and 23 pulses) harvested in 2019 were provided by the Institute of Agricultural Resources and Economics, from their two research centres located in Stende and Priekuli towns of Latvia. The cereals included rye ($n = 6$), triticale ($n = 7$), winter wheat ($n = 21$), summer wheat ($n = 12$), oat ($n = 32$) and barley ($n = 31$) varieties and pulses included broad beans ($n = 8$), peas ($n = 8$) and lupin beans ($n = 7$). The sample weight was around 200 g. The samples were crushed using disc type Laboratory mills 3303 (Perten Instruments AB., Huddinge, Sweden), homogenised and stored at −20°C until analysis.

Sample preparation

Five grams of each sample were weighed in 50 mL polypropylene tubes and were shaken after the addition of 10 mL of deionised water containing 2% formic acid to the tubes. Next, 10 mL of acetonitrile was added to the tubes, followed by shaking for 10 min in a programmable rotator. A mixture of QuEChERS salts, consisting of 4.0 g of anhydrous magnesium sulphate, 1.0 g of sodium chloride, 1.0 g of trisodium citrate and 0.5 g of disodium citrate were added to the tubes, followed by vigorous shaking for 3 min. The tubes were centrifuged (4,500 × g) at 15°C for 10 min and 7 mL of the acetonitrile layer was transferred to 15 mL polypropylene tubes, which were then capped and stored in a freezer at −80°C for 30 min. The tubes were then immediately centrifuged at 15°C (4,000 × g, 18 min). The samples were prepared by the addition of 47.5 µL of the supernatants and 2.5 µL of 20% acetonitrile or 500 µg L^{-1} of the standard mix (in the case of spiked extracts) by directly pipetting into 1,950 µL of LC-MS water containing 0.1% formic acid and 0.1% acetonitrile (dilution factor of 40). The final solvent composition of the extracts was 2.5% aqueous acetonitrile and 0.1% formic acid. The diluted extracts were filtered directly into 2 mL crimp cap vials (0.22 µm pore size, PVDF).

Method of analysis

Chromatographic separation was carried out on an EASY-Spray PepMap™ nano-LC capillary column (150 × 0.075 mm) with 3 µm C_{18} bonded silica particles (Thermo Scientific, Waltham, MA, USA). Electrospray ionisation was performed in the nano-electrospray ionisation mode using the EASY-Spray™ ionisation source. The analytical column was thermostated at 30°C; the autosampler was thermostated at 5°C; and injection volume was 1 µL. The following parameters were used for the ionisation source: ion transfer capillary temperature 250°C; spray voltage ±2.5 kV. The mobile phases were 0.1% formic acid in ultra-pure water (A) and 0.1% formic acid in acetonitrile (B). The gradient was 0–50 min 2.5% B to 99% B; 50–59 min 99% B; 59–67 min 99% B to 2.5% B, 67–80 min 2.5% B. The flow rate was set to 225 nL min^{-1}.

A Q-Exactive Focus Orbitrap-HRMS (Thermo Fisher Scientific, Waltham, MA, USA) detection system was used in the PRM mode. Precursor ions were isolated using an isolation window of 0.4 m/z at the corresponding elution windows and fragmented at the average optimum collision energy of all identified fragments of the corresponding precursor ion. Fragments were detected simultaneously at a resolution of 70,000. Ion injection time was set to 1,000 ms. The list of analytes, their retention times and precursor ions are given in Table 1. Table S1 of the Supplementary material lists all fragment ions which were used to construct the extracted ion chromatograms for the integration of mycotoxin concentrations.

Method validation

A one-point post-extraction standard addition calibration was performed at 50 µg kg^{-1}. In the case of higher concentrations present in the sample, the standard addition was increased accordingly up to 2,500 µg kg^{-1}, by decreasing the volume of sample extract with respect to the added standard solution. The decrease in volume of sample extract was compensated with an appropriate volume of LC-MS grade acetonitrile to maintain the composition of solution for injection at 2.5% acetonitrile.

For the quality analysis, in-house reference materials containing known concentrations of T-2 and HT-2 toxins

Table 1. Instrument parameters for the nano-LC-MS method.

Analyte	RT (min)	Precursor ion (*m/z*)	Polarity	CE (eV)
T-2TETR	15.4	343.1398	Negative	10
NIV	15.9	357.1190	Negative	10
D3G	17.5	503.1769	Negative	15
DON	18.0	341.1241	Negative	20
FUS X	20.6	355.1387	Positive	20
NEO	21.7	400.1965	Positive	20
15-AcDON	23.7	339.1438	Positive	10
3-AcDON	24.2	339.1438	Positive	10
15-MAS	24.7	342.1910	Positive	10
FB_1	25.6	722.3957	Positive	40
FB_3	27.1	706.4008	Positive	40
T-2TRI	27.6	400.2329	Positive	15
FB_2	28.1	706.4008	Positive	35
ALT	28.2	293.1019	Positive	15
AFB_1	29.5	313.0706	Positive	30
HT-2	30.9	442.2434	Positive	10
TEN	31.2	415.2339	Positive	25
AFL	31.5	315.0863	Positive	25
ATX I	31.6	351.0873	Negative	35
AOH	33.4	257.0454	Negative	30
OTB	35.0	370.1285	Positive	20
T-2	35.9	484.2540	Positive	15
OTA	38.5	402.0749	Negative	20
ZEN	38.6	317.1393	Negative	25
AME	40.1	271.0611	Negative	30
ENN B	50.6	657.4432	Positive	15
ENN B_1	52.3	671.4589	Positive	15

RT – retention time, CE – collision energy.

were analysed (barley and corn) and z-scores $|z| < 1.5$ were achieved, assuming a target standard deviation of 15%.

For the determination of method trueness (recovery, R (%)), precision and measurement uncertainty, a total of three replicates of six representative matrices (rye, oat, winter wheat, barley, beans and peas) were spiked with 50 µg kg^{-1} of standard solutions and were analysed over a three day period. The trueness (recovery) was determined from the extraction efficiency data according to Equation (1):

$$EEF = 100\% \cdot A_{spikedsample}/A_{spikedaliquot} \quad (1)$$

where $A_{spiked\ sample}/A_{spiked\ aliquot}$ is the ratio of analyte response from a blank matrix spiked prior to the extraction to the analyte response from a spiked extract aliquot from a sample that did not contain the analyte. The results for the analytes containing *EEF* (Equation 1) below 70% were corrected for extraction efficiency.

Analytes were confirmed on the basis of the presence of overlapping peaks from at least two different product ions where possible (the two characteristic ions for each analyte are expressed in Table 1). The sum of all of the observed fragments used for constructing the extracted ion chromatograms for the integration is summarised in the supplementary material (Table S1).

The inter-day repeatability expressed as relative standard deviation (RSD) values were calculated from the within-laboratory measurements. The expanded measurement uncertainties (U) were estimated according to Equation (2):

$$U = k \cdot \sqrt{RSD_{WR}^2 + RMS_{bias}^2 + u_{C_{ref}}{}^2} \quad (2)$$

where $k = 2$ (coverage factor at the 95% confidence interval), RSD_{WR} is the within-laboratory reproducibility, RMS_{bias} is the root-mean-squared bias and u_{Cref} is the relative uncertainty of the certified value for the pesticide standard.

The signal-to-noise (S/N) approach was used to estimate the limit of quantification (LOQ) using the chromatograms of spiked samples of six tested representative matrices. The LOQs were defined at levels resulting in S/N ≥ 10. The individual method performance indicators are summarised in Table 2.

In addition, the matrix effect was evaluated according to Equation (3):

$$ME_{underivatized} = 100\% \cdot (A_{matrix}/A_{solvent} - 1) \quad (3)$$

where $A_{matrix}/A_{solvent}$ is the ratio of analyte response from spiked blank matrix to the analyte response from standard in solvent.

Results and discussion

Nano-LC-MS fluidics and capillary column

The nano-flow LC approach was used in the development of the method, considering the suitability of the method for the analysis of emerging mycotoxins. The resolution for the separation of the mycotoxin analytes was evaluated for two different nano-LC-MS fused silica fluidic setups: (a) Acclaim PepMap™ capillary column combined with an EASY-Spray™ transfer line and an emitter and (b) EASY-Spray™ capillary column with an integrated emitter, both purchased from Thermo Scientific (San Jose, USA). Significant peak broadening was observed with the capillary column and the EASY-Spray™ transfer line containing the emitter due to increased system volume. The EASY-Spray™ capillary column with the integrated emitter afforded excellent separation that enabled successful high-resolution MS^2 acquisition of many analytes (Figure S1, Supplementary file).

Optimisation of the nano-LC-MS procedure

Due to the interferences in their mass spectra, some of the mycotoxins (for example, NEO and 15-MAS), could not be detected below the 50 µg kg^{-1} level in the full-scan mode. Therefore, PRM mode was used to ensure selectivity. No interferences were observed in the parallel reaction mode at a resolution of 70,000. An ion injection time of 1,000 ms was selected as a compromise between the co-elution and increased sensitivity due to the longer accumulation of ions in the ion trap. An ion injection time of <500 ms was found unfeasible due to droplet

Table 2. Performance parameters of the nano-LC-MS method.

Analyte	LOQ (µg kg^{-1})	Recovery (%) (mean, n = 18)	RSD (%) (mean, n = 18)	RMS_{bias} (%)	U (%)
15-MAS	0.64	104	18	4.3	37
15-AcDON	2.9	82	10	18	41
3-AcDON	0.70	77	6.6	23	48
AFL	4.5	93	13	6.5	29
AFB_1	0.24	91	11	8.8	28
ALT	0.21	91	6.2	8.8	22
AOH	1.3	86	14	14	39
AME	1.9	96	17	4.2	35
ATX I	0.98	90	6.0	1.0	24
DON	2.7	57	2.8	9.4	20
D3G	0.10	29	4.3	12	25
ENN B	2.3	107	27	6.9	57
ENN B_1	14	87	11	13	34
FB_1	0.15	48	18	19	52
FB_2	3.0	85	14	15	42
FB_3	0.26	96	21	4.4	45
FUS X	2.8	44	13	25	56
HT-2	0.79	96	11	4.2	23
NEO	0.26	99	10	1.0	20
NIV	68	60	11	28	61
OTA	0.53	84	5.6	16	34
OTB	0.13	82	10	18	41
T-2TETR	3.9	49	20	32	76
T-2	0.28	92	2.7	7.8	17
T-2TRI	0.78	94	6.3	5.6	17
TEN	0.62	84	24	16	57
ZEN	0.65	85	8.1	15	35

formation at the emitter tip during the highly aqueous segment of the gradient. Droplet formation at the emitter tip with highly aqueous mobile phase is a known problem while using nanoflow electrospray ionisation (Schneider et al. 2005). Because the droplets were transferred to the mass spectrometer at a low frequency, the gradient and flow rate was decreased accordingly to obtain a sufficient number of scans per peak. Three dilution factors of 100, 80, 40 and 20 were tested. The lowest allowed dilution factor for the sample extracts was optimised by injecting the standard solutions interlaced in the sequence with spiked sample extracts of decreasing dilution factors. The dilution factor of 40 was determined as the optimal as it did not significantly affect the signals in the standard solutions.

Method performance

The validation parameters for the developed nano-LC-MS method are summarised in Table 2. The estimated extraction efficiencies are given in Figure 1. The recovery rates calculated from the extraction data ranged between 77 and 104% and complied with the criterion established by the DG SANTE 2016/12089 guidelines (EC, 2016). The six mycotoxins, NIV, DON, D3G and other *Fusarium* metabolites that had a log $P < 0$ exhibited extraction efficiencies below 70%. Therefore, a correction for the extraction efficiency for these analytes was performed by applying standard addition (European Commission 2016).

The mean RSD values for most of the analytes were good, being 2.7–18%, except for ENN B, FB_3, T-2TETR and TE, which had RSD values at or above 20%. The individual values of the within-laboratory reproducibility and expanded uncertainty (U, %) are listed in Table 2. Within these studies, the in-house reference materials (barley and corn) that contained known concentrations of T-2 and HT-2 toxins were analysed. The average expanded measurement uncertainty was 38% and ranged between 17 and 61% for individual analytes. The high values of expanded uncertainty (>50%) determined in case of several mycotoxins can be associated with the matrix effects of grain and pulse varieties. Thus, to confirm this issue, the matrix effects were evaluated.

The determined matrix effects ranged between −36 and +26% for most of the analytes, except for AOH, AME, all ENNs and FBs, NIV, OTA, OTB. For these samples, the ME was far above 50% indicating an elevated ionisation enhancement effect (for example the ME of ZEN was 60%), whereas FUS X presented a strong ionisation suppression effect (ME was −60%). However, 14 analytes presented acceptable levels, e.g., AFB_1, AFL, T-2, TEN and ATX I and possessed moderate ionisation enhancement with an ME that ranged between 5 and 26%. In contrast, the other type A (15-MAS, HT-2, T-2TRI, T-2TETR and NEO) and type

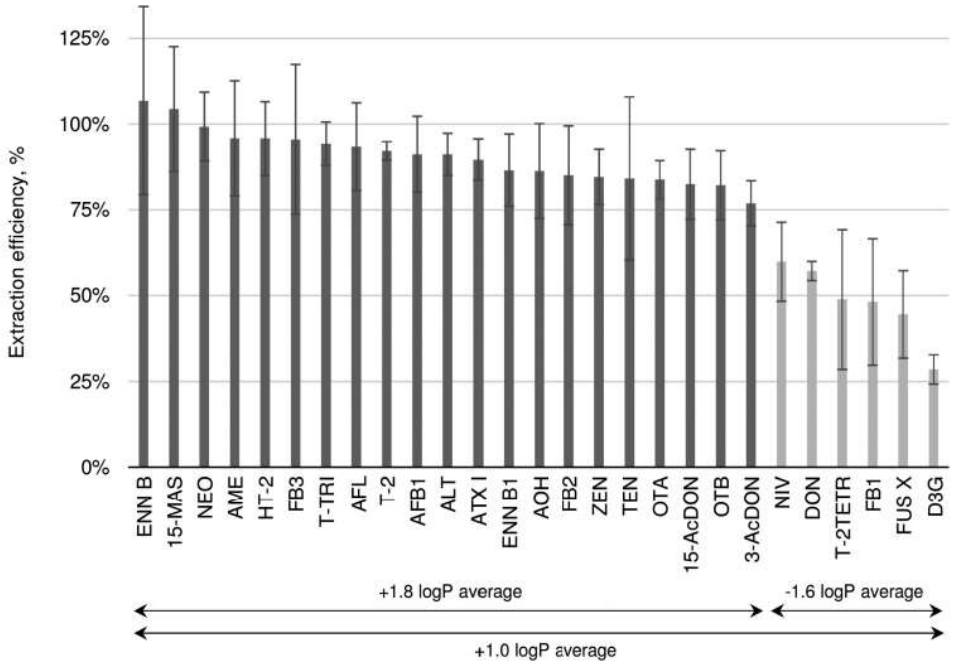

Figure 1. Extraction efficiencies.

B (DON, D3G, 3-AcDON and 15-AcDON) trichothecenes and ALT possessed a medium suppression effect with an ME that ranged between −36 and −13%.

The method sensitivity was evaluated from the calculated LOQ values, which ranged between 0.10 and 68 μg kg^{-1}. The sensitivity of the present method was sufficient for the quantification of the regulated and emerging mycotoxins and presented LOQs comparable or a slightly higher than those from the other recent studies for multi-mycotoxin analysis in cereals and pulse matrices (Rausch et al. Kunz et al. 2020). The LOQs for OTA, T-2, HT-2 and 3-AcDON of the present method also coincided with the LOQ values reported by Alcántara-Durán et al. (2019), who combined C18 and PSA sample treatment with nano-LC-MS analysis.

Mycotoxin levels in grain cereals and pulses

The developed nano-LC-MS method was applied for the analysis of the agricultural crop samples collected from the Stende and Priekuli Research centres in Latvia. Among them, 95% (n = 127) of the analysed samples were positive for contamination with 23 different mycotoxins. Only one among the oat cereals, four among peas and one lupin bean sample were mycotoxin free according to the method's quantification levels. AFB_1, AFL, OTA and FB_2 were absent in the cereal and pulses samples. OTB, the dechlorinated OTA metabolite and FB_3 both co-occurred in only one oat sample at concentrations of 0.34 and 0.27 μg kg^{-1}, respectively. The ranges of the concentration levels of the other 21 mycotoxins in cereals and legumes are presented in Figure 2.

A comparison of the regulated mycotoxins indicated that the T-2 and HT-2 toxins co-occurred in 72% (n = 85) of the total 110 analysed cereal samples and their individual concentrations were 0.30–7.6 μg kg^{-1} and 0.79–118 μg kg^{-1}, respectively. Winter wheat (18/21), barley (25/31), triticale (6/7) and rye (5/6) were the most contaminated with the T-2 and HT-2 toxins compared to oat (23/33) and summer wheat (6/12) varieties. The total concentration of T-2 and HT-2 levels in the cereals ranged between 1.1 and 205 μg kg^{-1}, with a mean value of 14 μg kg^{-1} and slightly exceeded the maximum limit 0 f 200 μg kg^{-1}, as set for nonprocessed grains only in the case of one barley sample (EC, 2013). T-2 and HT-2 toxins were also frequently detected in seven broad beans and three lupin beans at the levels of 0.52–27 μg kg^{-1} and 1.7 and 15 μg kg^{-1}, respectively. Other type A trichothecenes (15-MAS, T-TRI, T-2TETR and NEO) were determined only in the cereals at low concentrations (0.27–26 μg kg^{-1}), except for one barley sample with a T-2TETR concentration of 83 μg kg^{-1}.

The type B trichothecenes were determined only in cereals. DON was detected in 54% of the analysed samples at concentrations ranging between 2.8 and 429 μg kg^{-1} and a mean value of 67 μg kg^{-1}, which were considerably lower than the maximum limits (1250–1750 μg kg^{-1}) set for DON in unprocessed

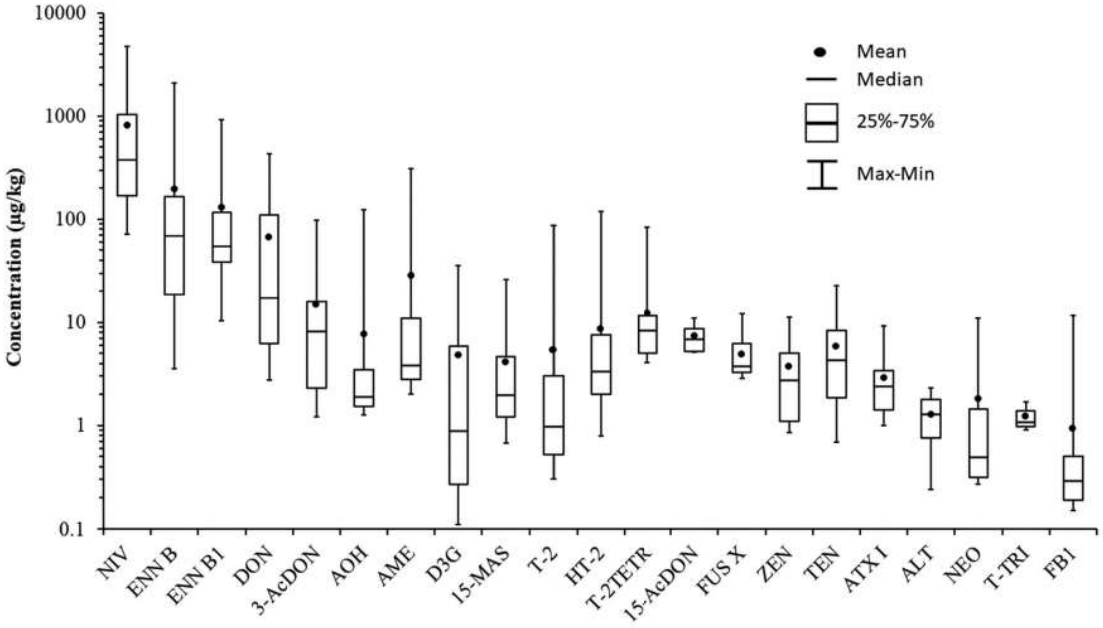

Figure 2. Mycotoxins in legume and cereal samples.

cereals (EC, 2006). Barley (20/31), oat (19/33) and winter wheat (12/21) cereals were mostly contaminated with DON compared to triticale (3/7), summer wheat (5/12) and rye (1/6) varieties The non-regulated modified DON derivatives (D3G, 3-AcDON, 15-AcDON and NIV) were mainly detected in all cereal varieties: barley (30/31), oat (32/33), winter wheat (18/21), summer wheat (9/12) and triticale (5/7), except for rye samples (1/6). While NIV was detected in 83% of the analysed cereal samples, the uncertainty was rather high, the concentrations ranging between 71 and 4,780 µg kg^{-1}. Other class B trichothecenes detected were 15-AcDON, FUS X, 3-AcDON, D3G, in 4, 14, 24 and 58% of the analysed cereals at concentrations below 50 µg kg^{-1}, taking expanded measurement uncertainty into account for one oat sample that contained 96 µg kg^{-1} 3-AcDON. ZEN was detected in very low concentrations between 0.86 and 11 µg kg^{-1} in one triticale, three oat and seven barley samples. FB_1 was determined at trace levels (0.15–1.6 µg kg^{-1}) in three barley, seven oat and 10 winter wheat samples.

The emerging mycotoxins ENN B and ENN B_1 were frequently detected in all analysed cereal varieties, at individual concentrations of 3.5–2,073 µg kg^{-1} and 10–922 µg kg^{-1}, respectively. Only one summer wheat, two rye and two barley samples were tested positive for ENN concentrations above 1,000 µg kg^{-1}. Among the pulse samples, only ENN B was determined at concentrations of 4.4–17 µg kg^{-1} in one bean and two lupin samples.

TEN was the most prevalent among *Alternaria* toxins determined in 80–100% of all analysed cereal varieties at low concentrations of 0.72–23 µg kg^{-1}. TEN was the only mycotoxin determined at 0.69–3.8 µg kg^{-1} in peas (n = 8) and lupin beans (n = 5). AOH ranged between 1.3 and 125 µg kg^{-1} in oat (21/33), rye (5/6), winter wheat (2/21) and barley (7/31) varieties and was also determined in lupin beans (n = 4) in the range of 1.5–2.9 µg kg^{-1}. AME was mostly determined in oats (8/33) at concentrations of 2.52–28 µg kg^{-1}, except for the one oat sample that simultaneously contained 307 µg kg^{-1} of AME and 125 µg kg^{-1} of AOH. ATX I was detected in trace levels (1.0 and 9.2 µg kg^{-1}) in 50% (n = 55) of the analysed cereals and also co-occurred with in one lupin bean sample (3.3 µg kg^{-1}).

These results, particularly of the emerging toxins, were compared with previously reported results of European cereals. Bryła et al. (2016) reported high DON and ZEN contamination in grains from Poland, triticale being 100% contaminated with ZEN and DON and the sum of 3- and 15-AcDON and ENNs ranging between 8 and 3,328 µg kg^{-1}. Furthermore, the ENN levels in Latvian cereals were lower than those determined in the Polish survey. The absence of OTA and aflatoxins in the cereal varieties was in good agreement with the results of the present study.

A comparison of literature data for *Alternaria* toxins indicated good agreement with the overall prevalence of

TEN, OTA and AME, which were determined as the predominant contaminants in wheat samples (Fraeyman et al. 2017).

Comparing pulse varieties, Carballo et al. (2018) included beauvericin (BEA) and four ENNs among the 27 mycotoxins analysed in legumes and other food matrices. This study also reported HT-2 as the most prevailing mycotoxin in legumes (56%) at concentrations between 4.0 and 7.8 μg kg^{-1} in grain and legume samples.

Oviedo et al. (2012) reported a high prevalence (60%) of AOH (25–211 μg kg^{-1}) and AME (62–1,153 μg kg^{-1}) in soybean samples from Argentina. However, studies on *Alternaria* toxins in other legume varieties are scarce, with the exception of a recent report from the European Food Safety Authority (EFSA), which indicated the high prevalence (>80%) of AOH, AME and TEN in legumes, while only carob fruit and soy bean samples were included in the study (Arcella et al. 2016). Compared to these previous reports, the present study confirms the high prevalence of *Alternaria* mycotoxins in different grain legumes, especially of the lupin variety.

Conclusions

The developed nano-LC separation technique for the analysis of 27 multi-class mycotoxins in grain cereals and legumes possessed sufficient accuracy and precision for analysing most of the analytes. The mobile phase consumption, including acetonitrile, was significantly reduced compared to that for conventional methods. The method was successfully applied for the analysis of a total of 133 samples of nine crop varieties and indicated 99% of the analysed cereals (n = 109) and 78% of the pulses (n = 18) as positive for 1 to 16 of the 27 analysed mycotoxins, including four *Alternaria* toxins and and The regulated mycotoxins (DON, ZEN, sum of T_2 and HT-2 toxins and F_1) were found prevalent in the analysed grain samples at concentrations far below their maximum tolerable levels High distributions of enniatins and *Alternaria* toxins were observed that raise concerns of future work on any regulatory limits for those toxins in cereals.

Acknowledgments

Funding of the sample and reagent purchase by the European Regional Development Fund, within the Project activity 1.1.1.2 "Post-doctoral Research Aid" (Project No. 1.1.1.2/VIAA/1/16/219) is greatly acknowledged. Tandem Taylor & Francis Editing Services are acknowledged for language editing.

Authorship contribution statement

The contribution was as follows: Ingars Reinholds: Conceptualisation, resource gathering, data curation, original draft preparation & editing, visualisation and investigation. Martins Jansons: Data curation, original draft preparation, conceptualisation, methodology and validation. Deniss Fedorenko: Methodology and validation. Iveta Pugajeva: Methodology, investigation and resource gathering. Sanita Zute: Resource gathering and investigation. Jelena Bartkiene: Conceptualisation and investigation. Vadims Bartkevics: Conceptualisation, supervision and investigation.

Disclosure statement

The authors declare no conflicts of interest.

Funding

This work was supported by the European Regional Development Fund under project No. 1.1.1.2/VIAA/I/16/001, Post-doctoral research project No. 1.1.1.2/VIAA/1/16/219.

ORCID

Ingars Reinholds http://orcid.org/0000-0002-6910-3054
Martins Jansons http://orcid.org/0000-0002-9017-6135
Vadims Bartkevics http://orcid.org/0000-0002-6193-7409

References

Alcántara-Durán J, Moreno-González D, García-Reyes JF, Molina-Díaz A. 2019. Use of a modified QuEChERS method for the determination of mycotoxin residues in edible nuts by nano flow liquid chromatography high resolution mass spectrometry. Food Chem. 279:144–149. doi:10.1016/j.foodchem.2018.11.149.

Arcella D, Eskola M, Gómez Ruiz JA. 2016. Dietary exposure assessment to Alternaria toxins in the European population. Efsa J. 14(12):e04654. doi:10.2903/j.efsa.2016.4654.

Bryła M, Waśkiewicz A, Podolska G, Szymczyk K, Jędrzejczak R, Damaziak K, Sułek A. 2016. Occurrence of 26 mycotoxins in the grain of cereals cultivated in Poland. Toxins. 8(6):160. doi:10.3390/toxins8060160.

Carballo D, Moltó JC, Berrada H, Ferrer E. 2018. Presence of mycotoxins in ready-to-eat food and subsequent risk assessment. Food Chem Toxicol. 121:558–565. doi:10.1016/j.fct.2018.09.054.

Chen P, Xiang B, Shi H, Yu P, Song Y, Li S. 2020. Recent advances on type A trichothecenes in food and feed: analysis, prevalence, toxicity, and decontamination techniques. Food Control. 118:107371. doi:10.1016/j.foodcont.2020.107371.

European Commission. 2006. Commission Regulation (EC) No 1881/2006 of 19 December 2006 setting maximum levels for certain contaminants in foodstuffs. Off J Eur Union. 364:324–365.

European Commission. 2013. Commission recommendation of 27 March 2013 on the presence of T-2 and HT-2 toxin in cereals and cereal products. Off J Eur Union. 91:12–15.

European Commission. 2016. Guidance document on identification of mycotoxins in food and feed, SANTE/12089/2016.

Fraeyman S, Croubels S, Devreese M, Antonissen G. 2017. Emerging *Fusarium* and *Alternaria* mycotoxins: occurrence, toxicity and toxicokinetics. Toxins. 9(7):228. doi:10.3390/toxins9070228.

Gotthardt M, Asam S, Gunkel K, Moghaddam AF, Baumann E, Kietz R, Rychlik M. 2019. Quantitation of six *Alternaria* toxins in infant foods applying stable isotope labeled standards. Front Microbiol. 10:109. doi:10.3389/fmicb.2019.00109.

Haque MA, Wang Y, Shen Z, Li X, Saleemi MK, He C. 2020. Mycotoxin contamination and control strategy in human, domestic animal and poultry: a review. Microb Pathogen. 142:104095. doi:10.1016/j.micpath.2020.104095.

Holanda DM, Kim SW. 2020. Efficacy of mycotoxin detoxifiers on health and growth of newly-weaned pigs under chronic dietary challenge of deoxynivalenol. Toxins. 12(5):311. doi:10.3390/toxins12050311.

Khaneghah AM, Fakhri Y, Gahruie HH, Niakousari M, Sant'Ana AS. 2019. Mycotoxins in cereal-based products during 24 years (1983–2017): a global systematic review. Trends Food Sci Tehnol. 91:95–105. doi:10.1016/j.tifs.2019.06.007.

Kunz BM, Wanko F, Kemmlein S, Bahlmann A, Rohn S, Maul R. 2020. Development of a rapid multi-mycotoxin LC-MS/MS stable isotope dilution analysis for grain legumes and its application on 66 market samples. Food Control. 109:106949. doi:10.1016/j.foodcont.2019.106949.

Malachová A, Stránská M, Václavíková M, Elliott CT, Black C, Meneely J, Hajšlová J, Ezekiel CN, Schuhmaker R, Krska R. 2018. Advanced LC–MS-based methods to study the co-occurrence and metabolization of multiple mycotoxins in cereals and cereal-based food. Anal Bioanal Chem. 410(3):801–825. doi:10.1007/s00216-017-0750-7.

Medina DAV, Maciel EVS, de Toffoli AL, Lanças FM. 2020. Miniaturization of liquid chromatography coupled to mass spectrometry. 2. Achievements on modern instrumentation for miniaturized liquid chromatography coupled to mass spectrometry. TrAC Trends Anal Chem. 128:115910. doi:10.1016/j.trac.2020.115910.

Moreno-González D, Pérez-Ortega P, Gilbert-López B, Molina-Díaz A, García-Reyes JF, Fernández-Alba AR. 2017. Evaluation of nanoflow liquid chromatography high resolution mass spectrometry for pesticide residue analysis in food. J Chromatogr A. 1512:78–87. doi:10.1016/j.chroma.2017.07.019.

Orlando B, Grignon G, Vitry C, Kashefifard K, Valade R. 2019. *Fusarium* species and enniatin mycotoxins in wheat, durum wheat, triticale and barley harvested in France. Mycotoxin Res. 35(4):369–380. doi:10.1007/s12550-019-00363-x.

Oviedo MS, Barros GG, Chulze SN, Ramirez ML. 2012. Natural occurrence of alternariol and alternariol monomethyl ether in soya beans. Mycotoxin Res. 28(3):169–174. doi:10.1007/s12550-012-0132-0.

Pereira VL, Fernandes JO, Cunha SC. 2014. Mycotoxins in cereals and related foodstuffs: a review on occurrence and recent methods of analysis. Trends Food DSci Technol. 36(2):96–136. doi:10.1016/j.trac.2009.04.01.

Pleadin J, Vasilj V, Kudumija N, Petrović D, Vilušić M, Škrivanko M. 2017. Survey of T-2/HT-2 toxins in unprocessed cereals, food and feed coming from Croatia and Bosnia & Herzegovina. Food Chem. 224:153–159. doi:10.1016/j.foodchem.2016.12.063.

Rausch AK, Brockmeyer R, Schwerdtle T. 2020. Development and validation of a QuEChERS-based liquid chromatography tandem mass spectrometry multi-method for the determination of 38 native and modified mycotoxins in cereals. J Agric Food Chem. 68(16):4657–69. doi:10.1021/acs.jafc.9b07491.

Righetti L, Paglia G, Galaverna G, Dall'Asta C. 2016. Recent advances and future challenges in modified mycotoxin analysis: why HRMS has become a key instrument in food contaminant research. Toxins. 8(12):361. doi:10.3390/toxins8120361.

Schneider BB, Guo X, Fell LM, Covey TR. 2005. Stable gradient nanoflow LC-MS. J Am Soc Mass Spectrom. 16(9):1545–1551. doi:10.1016/j.jasms.2005.05.004.

Xia R, Schaafsma AW, Wu F, Hooker DC. 2020. Impact of the improvements in *Fusarium* head blight and agronomic management on economics of winter wheat. World Mycotoxin J. 1–18. doi:10.3920/WMJ2019.2518.

Yang X, Gao J, Liu Q, Yang D. 2019. Co-occurrence of mycotoxins in maize and maize-derived food in China and estimation of dietary intake. Food Addit Contam Part B. 12(2):124–134. doi:10.1080/19393210.2019.1570976.

Żelechowski M, Olszewski J, Kulik T. 2019. A preliminary survey of cultured fusaria from symptomatic legume grains in North-Eastern Poland. Toxins. 11(10):569. doi:10.3390/toxins11100569.

Recent Applications of Nano-Liquid Chromatography in Food Safety and Environmental Monitoring: A Review

Fedorenko, D.; Bartkevics, V. *Critical Reviews in Analytical Chemistry*[5] **2021**, 1–25.

[5] *Peer reviewed journal, imprint of Taylor & Francis (IF=5.686 (2022)), ISSN: 1547-6510*

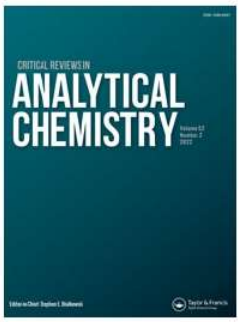

Critical Reviews in Analytical Chemistry

ISSN: (Print) (Online) Journal homepage: https://www.tandfonline.com/loi/batc20

Recent Applications of Nano-Liquid Chromatography in Food Safety and Environmental Monitoring: A Review

Deniss Fedorenko & Vadims Bartkevics

To cite this article: Deniss Fedorenko & Vadims Bartkevics (2021): Recent Applications of Nano-Liquid Chromatography in Food Safety and Environmental Monitoring: A Review , Critical Reviews in Analytical Chemistry, DOI: 10.1080/10408347.2021.1938968

To link to this article: https://doi.org/10.1080/10408347.2021.1938968

Published online: 15 Aug 2021.

CRITICAL REVIEWS IN ANALYTICAL CHEMISTRY
https://doi.org/10.1080/10408347.2021.1938968

Taylor & Francis
Taylor & Francis Group

REVIEW ARTICLE

Recent Applications of Nano-Liquid Chromatography in Food Safety and Environmental Monitoring: A Review

Deniss Fedorenko[a,b] and Vadims Bartkevics[a,b]

[a]Institute of Food Safety, Animal Health and Environment "BIOR", Riga, Latvia; [b]University of Latvia, Faculty of Chemistry, Riga, Latvia

ABSTRACT

In recent years, a trend toward instrument miniaturization has led to the development of new and sophisticated analytical systems, such as nano-liquid chromatography (nano-LC), which has enabled improvements of sensitivity, as well as chromatographic resolution. The growing interest in nano-LC methodology has resulted in a variety of innovative and promising applications. In this article, we review the applications of nano-LC separation methods coupled with mass spectrometry in the analysis of food and environmental samples. An assessment of sample preparation methods and analytical performance are provided, along with comparison to other, more established analytical techniques. Three main groups of compounds that are crucial for food safety assessment are considered in this review: pharmaceuticals (including antibiotics), pesticides, and mycotoxins. Recent practical applications of the nano-LC method in the determination of these compounds are discussed. Furthermore, we also focus on methods for the determination of various environmental contaminants using nano-LC methods. Future perspectives for the development of nano-LC methods are discussed.

KEYWORDS

Mass spectrometry; mycotoxins; nano-liquid chromatography; pesticides; veterinary drugs

Introduction

The rapid development of separation science has resulted in the availability of advanced chromatography equipment, such as nano-liquid chromatography (nano-LC) instrumentation. The advent of nano-LC represents the next step in the miniaturization and automation of liquid chromatography systems. The theoretical background of capillary and nano-LC methods was developed by research groups including those of Novotny and Karlsson,[1,2] as well as Knox and Gilbert[3,4] who studied separation processes on microcolumns. Since, then, the technological development trends have been aimed toward the miniaturization of column size, decreasing the sorbent particle size, and improving the separation efficiency.

The development of liquid chromatography has come a long way: from the introduction of high performance liquid chromatography (HPLC), to subsequent development of ultra-high performance liquid chromatography (UHPLC), the elaboration of capillary LC, and to the recent development of nano-LC. No clear definition of nano-liquid chromatography was initially established.[5,6] Later on, it was agreed by various researchers, that the term "nano-liquid chromatography" should refer to nanoflow liquid chromatography, meaning that the flow rate is generally measured in nanoliters per minute and the injection volume is also in nanoliters.[6,7] For example, Chervet et al.[5] and some other research groups have categorized nano-liquid chromatography according to such parameters as $10-1{,}000$ $\mathrm{nL\cdot min^{-nL}}$flow rate and $10-150\,\mu$m column inner diameter. Nevertheless, nowadays, it is agreed that the flow rates relevant to nano-liquid chromatography are on the scale of nanoliters per minute. The criterion for injection volume is analogous, however, usually no classification is given based the injection volume only. The injection volume depends on the analytical procedure, especially when a preconcentration step is implemented.

Nano-LC methods have found a considerable range of applications, for example, in biochemistry and proteomics, analysis of pharmaceutical compounds, including chiral compounds.[7,8] Additionally, it is used for the analysis of environmental samples, in forensics, and in food safety applications. The most common application of nano-LC methods is proteomics. The number of publications related to nano-LC methods in food analysis is significantly lower, despite the key benefit that all sample types currently analyzed by conventional HPLC and UHPLC can be also analyzed by nano-LC methods,[8] as shown by the variety of sample types and analytes that have been described in the literature. Nano-LC can be used with a variety of detectors, for example, ultraviolet diode array detectors (UV-DAD)[9,10] and MS detectors, for example, MS-MS, TOF, Q-Trap, and Orbitrap.[11]

The advantages of nano-LC methods are numerous. Due to the reduced flow rates, consumption of solvents is decreased,[6,12,13] in line with the green chemistry principles, reducing both the environmental impact and the cost of analysis. An additional advantage is the opportunity to use

CONTACT Deniss Fedorenko deniss.fedorenko@bior.lv Institute of Food Safety, Animal Health and Environment "BIOR", Riga, Latvia.

stationary phases that are commonly available for HPLC, such as reversed phase C_{18} sorbents with $3-5\,\mu m$ or smaller particle size, which are known to enable high separation efficiency.[7,12,14] Other types of columns, such as monolithic and open tubular columns, also can be used with nano-LC methods.[8,12,15]

When comparing nano-LC with other variants of liquid chromatography, it is important to acknowledge several facts. It is known that the mass sensitivity is higher in nano-LC because of lower flow rates, resulting in reduced chromatographic dilution.[12,16,17] The amount of sample required for nano-LC analysis is smaller, and the injection volume also is lower. Although this may not be a concern in the analysis of pharmaceutical substances, it can be very important in proteomics and forensics.[18]

Different chemical contaminants can be found in foods and in the environment. For example, the topic of antibiotics residues is one of the most challenging in this regard, and the presence of antibiotics in foods is a very important concern, especially in the light of emerging antibiotics resistance in pathogens.[19] There are several pathways for the entry of pharmaceuticals into the environment, for example, from incomplete waste water treatment, the use of wastewater sludge in agricultural soil, improper disposal of unused drugs.[20–22] This type of environmental contamination not only may exert a significant impact on living organisms but also represents a potential threat to human health.

Various regulations have been implemented to control the levels of harmful chemicals in food and environment, to ensure consumer safety and to preserve pristine natural resources. The regulations, such as European Union Commission Regulation No 37/2010, have established the maximum residue levels (MRLs) for a range pharmaceutical compounds in food. Similarly, regulation No 396/2005 of the European Parliament has established the maximum residue levels of pesticides in food and feed[23] and the Commission Regulation (EC) No 1881/2006 covers mycotoxins.[24] Over the years, those limits have been repeatedly revised according to the most recent toxicity and occurrence data for those pharmaceuticals gradually becoming lower over time. Additionally, some antibiotics and antimicrobials, such as chloramphenicol, nitrofurans, and some others have been banned for application in any food-producing animal species, as stated in Commission Regulation No 37/2010,[25] therefore, the quantitation limits of analytical methods for those compounds must meet the minimum required performance limits according to the Commission Decision 2002/657/EC.[26,27] This brings the consideration of analytical technology into account, as the chromatographic methods for the determination of those compounds often must be adapted for more sensitive detectors or more selective chromatography techniques. This highlights a challenge for the laboratories to ensure the appropriate level of the technical equipment and to apply the analytical methods able to meet the requirements of those regulations. From this point of view, to have an ability to properly assess an impact of this kind of contaminants, it is crucial to have the capability for the analysis of those compounds at low levels. Therefore, the nano-LC methodology has a potential to provide better analytical performance in comparison with other chromatography methods.

The aim of this review is to provide an outlook on recent applications of the nano-LC method in the analysis of various food and environment samples. Three main groups of analytes are considered: pharmaceuticals, including antibiotics and nonsteroid anti-inflammatory drugs (NSAIDs), pesticides, and mycotoxins. Several advantages and drawbacks, as well as potential directions of improvement are discussed.

Some theoretical aspects and technology outline

The theoretical background of the nano-LC method has been influenced by several studies presented elsewhere.[1–4] The main point of interest relates to the chromatographic dilution, which depends on the internal diameter of a column (i.d.). Chromatographic dilution D decreases proportionally to the square of column i.d. (denoted as d) if other parameters stay the same.[8,14] Formula 2.1. shows the relationship between those parameters, where H and L are the plate height and column length respectively, ε is the column porosity and V_{inj} is the injection volume.[28,29]

$$D = \frac{\pi d_c^2 \varepsilon (1+k)\sqrt{2HL\pi}}{4V_{inj}} \tag{2.1}$$

Additionally, another point of interest in the nano-LC method is the decreased flow rate. Schmidt et al.[30] studied low flow rates that are typical in nano-LC. In their thorough investigation of the signal intensity dependence on flow rate, it was found that the signal intensity in MS detector improved with a slower flow rate. Several explanations of this phenomenon were proposed. It was concluded that lower flow rate resulted in a more stable spray, improved ionization, and better coupling with MS, because the droplet size was smaller at lower flow rate.[8,14,31,32]

Historically, the first commercially available nano-LC system was UltiMate NanoLC, developed in 1998 by LC-Packing.[14] Before commercial columns were available, the nano-LC columns were packed in-house, meaning that each column had to be prepared using one of column packing methods. Initially, the choice of efficient pumps was limited. It has been reported that, to achieve a low flow rate measured in nanoliters per minute, passive split pumps were proposed.[14] A passive split system consisted of typical HPLC pump feeding two tubes with different diameters. The flow from the pump was, thus, mechanically split into two, and the smaller diameter tube led to the column, while the larger diameter tube led to waste, meaning that most of the solvent was discarded.[8,14,33] The pump must provide an accurate, stable, and reproducible flow, especially under gradient conditions, and mechanical split systems were not able to meet these requirements. Therefore, further developments of the nano-LC technology were not imaginable without advances in pump systems. Consequently, new splitless types of pumps were developed, such as continuous flow and solvent refill pumps.[8,13,14]

Ionization process, implemented in the nano-LC MS detectors, has the same physical basis as in regular HPLC-MS instrumentation. Currently, multiple studies are using electrospray ionization (ESI), which can be miniaturized to match the scale of nano-LC applications. Because of the small capillary diameter and low flow rates, the effects of mixing are more pronounced and can degrade the results as mentioned by Noga et al.[34] Therefore, it is important to reduce the possible band broadening due to dead volume and imperfections in fittings between capillaries. Another type of ionization used in nano-LC MS detectors is direct electron ionization (direct-EI), which features direct connection between nano-LC system and MS by introducing the solution from LC directly into the EI source, where transition into gas phase followed by ionization occur.[35,36] Commercially available nano-ESI sources include, for example, EASY-Spray by ThermoFisher, featuring nanoViper fittings with zero dead volume, and integrated nano-LC column with temperature control, which have been used by Moreno-González et al.,[37] Nakashima et al.,[38] and by others.

Nano-spray emitters are used for the creation of electrospray and represent miniaturized capillaries. Several other specific tools for nano-LC have been introduced in the recent years. For example, Newomics emitters[39] are reported to improve the ionization process and increase sensitivity by splitting a flow from a column into several channels, further decreasing a size of initial droplets. However, no studies to date feature this type of emitters in area of food analysis. Other types of emitters are coated fused silica emitters, for example, from New Objective.[40,41] Various types of nano-spray emitters are available, including materials such as fused silica or metal with different geometry and spatial dimensions that are designed for various flow rates and applications. Voltage can be applied to the emitter on different points of the emitter surface by conductive coating: to the tip of the emitter, to distal end of the emitter, or to fitting holding the emitter. This allows the use of either polymer fittings or metal fittings.[42] Stability of emitter in nano-LC can be an additional point of concern. Miniaturized emitters can be more easily damaged in contact with other objects. Not only that but also increased voltage could result in electric discharge at the tip, resulting in rapid performance decay. In a study by Wilson et al.[41] this phenomenon was observed, and it was concluded, that appropriate voltage must be used to reduce degradation. In this study, it was also demonstrated, that stability over the time of five days, expressed as a signal intensity, was almost unaffected.

Clearly, the analytical column is a crucial component of any nano-LC system. Currently, still only a limited variety of columns are commercially available. The most common commercially available columns are packed C_{18} reversed phase columns.[43] It should be noted that while commercial columns are available, some researchers prefer in-house packed columns that allow modification of stationary phase chemistry.[43–45] Core-shell phenyl-hexyl stationary phase[46] and polysaccharide derivatives[45,47,48] have been successfully used for separations with nano-LC equipment. Comparison between different stationary phases such as C_{18}, phenyl, and CN was performed by Buonasera et al.,[49] who found that phenyl stationary phase was more suitable for separation of organophosphorus pesticides. Besides packed C_{18} columns, other column types have been reported: open tubular column (OT), hydrophilic interaction column (HILIC), pillar array columns, and a chip format column.[43,50] For example, nano-LC methods can be successfully employed for the separation of enantiomers and racemic mixtures.[44,48,51,52] Polysaccharide-based chiral stationary phases can be used for this purpose.[45] Various modifications in HILIC stationary phases for capillary and nano-LC can be carried out by selecting the monomers for *in situ* polymerization, which results in different monoliths that have different properties and are suitable for different applications, for example, for the separation of phenolic compounds and inorganic ions (including nitrates and nitrites).[53–55] Additionally, colistin sulfate stationary phase has been employed in nano-LC settings for chiral separation of various classes of pharmaceutical compounds.[44] There are also possibilities of using two stationary phases in one column, where the first phase provides on-line preconcentration and the second phase achieves the separation.[16] For example, D'Orazio and Fanali[16] prepared a column in-house by combining two stationary phases: silica modified-teicoplanin particles and a C_{18} sorbent, the first being used for preconcentration.

Preconcentration or on-column focusing is a widely employed method that allows to increase sensitivity.[12] Similar to other liquid chromatography techniques, preconcentration is also a common method in nano-liquid chromatography. In a typical method involved the preconcentration technique, two columns are usually used: analytical column for separation of compounds, and trap column or pre-column for focusing of analytes. On-column focusing allows to analyze diluted samples, and this is a way of overcoming a low sensitivity issue that is likely to occur in the method with injection volume of several nanoliters.[12,16]

Despite its advantages aforementioned, several drawbacks are present with this type of miniaturized liquid chromatography that affect the applicability of this method. In general, some parameters of nano-LC methods require more attention than regular HPLC. Typically, lower flow rates result in longer equilibration time and time of analysis, resulting in decreased sample throughput. Another concern is that it is especially important to pay attention to the void volume and dead volume[8,12,14] by making sure that all fittings are correct and the length of tubes is appropriate. In regular HPLC, leakages usually can be spotted easily. However, the flow rates in nano-LC are significantly slower and leakages are harder to spot.[34] Therefore, precisely matching fittings must be used and more attention should be given to this problem. Smaller capillaries also result in higher chances of clogging; therefore, filtering of the samples is often crucial. Lower injection volume also means, that without any additional measures the sensitivity of the method most likely will be decreased.[56] To overcome this issue, it has been

proposed to use off-column preconcentration, on-column focusing, or MS detectors with high sensitivity.[12,16] A column has smaller dimensions and has less amount of sorbent, meaning that high concentration of matrix components could easily oversaturate a column, reducing efficiency, and decreasing its lifespan. Therefore, sample dilution is often used.[37,57,58] Narrower bands in nano-LC in comparison with HPLC and UHPLC indicate, that a detector must be fast enough to have sufficient scanning time to obtain the adequate number of scans per band. Another issue with nano-ESI is the selection of proper voltage for the analysis. Under isocratic conditions, an acceptable voltage for ionization can be found experimentally and is equally applicable throughout the chromatographic run. However, the changing mobile phase composition under gradient conditions leads to changes in viscosity and surface tension, which affect electrospray efficiency. This phenomenon was studied by Marginean et al.,[59] who proposed the application of voltage-control algorithms. The robustness of the technique is considered in practical applications,[60] and therefore, disadvantages must be assessed to evaluate whether a method is fit for purpose.

An alternative way of miniaturizing chromatographic separation is illustrated by the lab-on-chip approach. In this method, chromatographic column is etched out of a flat substrate (chip), and several auxiliary elements, such as sample preparation section and connection to MS, are usually present.[39,50,61,62] This application of the nano-LC concept has several advantages, for example, easier connectivity with separation and reaction processes either before or after the column, as well as reduced connector volumes, which can eliminate dead volumes.[50,61] There is an ongoing research and development effort aimed at providing more practical applications of this type of liquid chromatography for food safety analysis, and several methods have been reported for the determination of mycotoxins,[62] pesticides,[63] and pharmaceutical compounds.[64]

Applications of the nano-LC method

Table 1 lists recent literature sources reporting the applications of nano-LC methods for the analysis of various contaminants and drug residues relevant to food safety, as well as some applications for environment sample analysis. Table 1 also provides an overview of the liquid chromatography (LC) conditions and detector types employed in nano-LC analysis by various researchers. MS detectors are used the most frequently, but UV detectors also have been applied. Orbitrap MS is the most commonly implemented detection method in nano-LC. The composition of mobile phases is generally MeCN and H_2O with or without some amount of formic acid. Other mobile phases have also been used. Both gradient and isocratic conditions are implemented in the nano-LC analytical methods, with the typical injection volumes and flow rates also shown in Table 1. Additionally, it should be mentioned that numerous studies involve a preconcentration step due to its advantages. It should be noted that the time of nano-LC analysis, or the time required for separation, varies significantly, similarly to other, more established liquid chromatography methods. Based on the literature precedents listed in Table 1, possibilities for nano-LC method optimization are apparent and such methods do not always have to be time-consuming, despite the slower flow rate.

Comparison of sample preparation procedures

A range of significantly different sample preparation procedures have been used with nano-LC methods of analysis (Table 2). For example, even though pesticides can be determined by a nano-LC method with instrumental parameters that are similar to each other, sample preparation may differ in each study. Therefore, when comparing nano-LC methods with HPLC and UHPLC methods, the sample preparation procedures must be considered as well.

There are many similarities in the sample preparation procedures between nano-LC and other methods. Sample preparation for nano-LC usually has fewer steps, as it can be seen from Table 2. A typical sample preparation procedure results in obtaining the extract and dilution of it. Dilution is useful for decreasing matrix effects, for instance, a dilution factor of up to 100 resulted in significant reduction of matrix effects.[57] Dilution factors of 10, 20, and 50 are also reported to substantially decrease matrix effects.[37,58]

Table 2 provides a comparison of sample preparation methods for various types of sample matrices and liquid chromatography techniques. In this review, comparison is made with the most typical methods that are representative of the respective classes of analytes.

Sample homogenization is a critical step that is used in the majority of described methods. Therefore, it was not included in this comparison. We consider the extraction of analytes using different solvents and mixing of samples for achieving optimal extraction efficiency. After that, SPE is performed either by dSPE, or by using a regular SPE cartridge. The sample preparation can be concluded with evaporation and reconstitution, or extracts can be analyzed directly. To avoid contamination of instruments with solid particles and for additional cleanup, filtration is generally used.

One of the most crucial differences between sample preparation for nano-LC analysis and for other types of liquid chromatography is that the majority of reported methods rely on a reduced number of sample preparation steps. This brings several benefits, such as shortened sample preparation time, lighter workload of laboratory equipment, and lower consumption of reagents. These factors are important, especially in routine laboratories providing services in the area of food safety and environmental monitoring, as they allow to reduce the costs of analysis, while maintaining or in some cases even improving the analytical performance.

Comparison of analytical performance

When comparing the analytical parameters of the nano-LC methods and other liquid chromatography methods it is important to keep in mind the fact that mass spectrometers

Table 1. Several applications of nano-LC methods and their overall characteristics.

Analytes	Samples	Detector	LC mobile phase	Column	Conditions and flow rate	Injection volume	Time of analysis	Reference
Antibiotics (penicillin group)	Pharmaceuticals, bovine milk, porcine tissues (liver and kidney)	UV detector; quadrupole ion trap MS	0.1% FA in H_2O and MeCN	In-house packed C_{18} column, 3 μm, 100 μm i.d. × 100 mm	Gradient, 200 nL·min^{-1}	50 – 1,000 nL	45 min	[10]
Antibiotics and pesticides (two methods)	Milk and honey	UV-vis detector; Orbitrap MS	MeCN:MeOH:H_2O, 75:15:10 with 3 – 5% (v/v) FA	In-house packed monolith column with multiwalled carbon nanotubes (MWCNTs), 75 μm i.d. × 100 mm	Isocratic, 800 nL·min^{-1}	1,000 nL	20 – 25 min	[65]
Phenolic acids, flavonoids	Cranberry syrup	TOF MS	1% FA in H_2O and MeCN	NanoSeparations C_{18} column, 3 μm, i.d. 75 μm, with preconcentration	Gradient, 300 nL·min^{-1}	1,000 nL	40 min	[66]
Antibiotics (sulfonamides)	Pasteurized bovine milk	Ion trap MS	0.1% FA in H_2O and 0.1% FA in MeCN	In-house packed C_{18} column, core-shell, 2.6 μm, 100 μm i.d. × 250 mm, with preconcentration	190 nL·min^{-1}	200 – 1,200 nL	40 min	[67]
64 multiclass pesticides	Tomato, orange, fruit-based jam, baby food and olive oil	Orbitrap MS	0.1% FA in H_2O and 0.1% FA in MeCN	Thermo EASY-Spray C_{18} PepMap column, 3 μm, i.d. 75 μm, with preconcentration	Gradient, 300 nL·min^{-1}	1,000 nL	48 min	[37]
162 multiclass pesticides	Olive oil	Orbitrap MS	0.1% FA in H_2O and 0.1% FA in MeCN	Thermo EASY-Spray PepMap C_{18} column, 3 μm, i.d. 75 μm	Gradient, 200 nL·min^{-1}	1,000 nL	37 min	[68]
Pesticides	Apples and baby food	Orbitrap MS with ambient dielectric barrier discharge ionization source	H_2O:MeCN, 95:5 with 0.05% FA and MeCN with 0.05% FA	AB Sciex C_{18} column, 3 μm, 75 μm i.d. × 150 mm	Gradient, 800 nL·min^{-1}	5,000 nL	33 min	[69]
Pharmaceuticals	Benthic invertebrates (*Potamopyrgus antipodarum* and *Valvata piscinalis*)	Qtrap MS	H_2O:MeCN, 98:2 with 0.1% FA and MeCN:H_2O, 80:20 with 0.1% FA	Themo PepMap C_{18} column, 3 μm, i.d. 75 μm, with preconcentration	Gradient, 300 nL·min^{-1}	1,000 nL	35 min	[70]
Pharmaceuticals	Wastewater and sludge	Ion trap MS	0.3% FA and 0.1% ammonium formate in H_2O, MeCN with 0.1% FA	In-house packed column, 3 μm, i.d. 75 μm × 110 mm	Gradient, 300 nL·min^{-1}	1,000 nL	33 min	[71]
35 emerging pollutants (various classes of pharmaceuticals, steroids, pesticides and others)	Benthic invertebrates (*Potamopyrgus antipodarum*, *Gammarus fossarum*, and *Chironomus riparius*)	Qtrap MS	For positive ion mode: 0.1% FA in H_2O and MeOH:MeCN:H_2O, 45:45:10 with 0.1% FA. For negative ion mode: 0.1 mM NH_4OAc in H_2O and 0.1 mM NH_4OAc in MeCN:MeOH:H_2O, 45:45:10	Thermo PepMap C_{18} column, 3 μm, i.d. 75 μm × 150 mm, with preconcentration	Gradient, 300 nL·min^{-1}	1,000 nL	64 and 57 min	[72]
Perfluorooctanoic acid, perfluorooctane sulfonate	River water	TOF MS	10 mM NH_4OAc in MeCN:H_2O, 10:90; 10 mM NH_4OAc in MeCN:H_2O, 90:10	G&T Septech C_{18} column, 3.5 μm, i.d. 100 μm × 150 mm, with preconcentration	Gradient, 700 nL·min^{-1}	0.02 – 1,000 μL	14 min	[41]
Mycotoxins	Edible nuts (peanuts, pistachios, almonds)	Orbitrap MS	0.1% FA in H_2O and 0.1% FA in MeCN	Thermo PepMap C_{18} column, 3 μm, i.d. 75 μm× 150 mm, with preconcentration	Gradient, 200 nL·min^{-1}	100 nL	28 min	[73]

(*continued*)

Table 1. Continued.

Analytes	Samples	Detector	LC mobile phase	Column	Conditions and flow rate	Injection volume	Time of analysis	Reference
Pesticides (aldicarb, atrazine, methomyl, propazine)	River water	Single quadrupole MS	H_2O and MeCN	Agilent C_{18} Zorbax-SB, 3.5 μm, 75 μm i.d. × 150 mm	Gradient, 300 nL·min^{-1}	60 nL	40 min	[36]
Veterinary drugs and antibiotics	Honey, veal muscle, eggs and milk	Orbitrap MS	0.1% FA in H_2O and 0.1% FA in MeCN	Thermo EASY-Spray PepMap C_{18} column, 3 μm, 75 μm i.d. × 150 mm	Gradient, 200 nL·min^{-1}	1,000 nL	35 min	[57]
Pesticides	Milli-Q water (spiked)	UV detector	0.1% FA in H_2O and 0.1% FA in MeCN	In-house packed phenyl column, 3 μm, 100 μm i.d., 250 mm, with preconcentration	Gradient, 500 nL·min^{-1}	20 μL	25 min	[74]
Pesticides	Honeybees	Orbitrap MS	0.1% FA in H_2O and 0.1% FA in MeCN	Thermo EASY-Spray PepMap C_{18} column, 3 μm, 75 μm i.d. × 150 mm	Gradient, 200 nL·min^{-1}	1,000 nL	37 min	[75]
Insecticides and pesticides	Honey and pollen	Orbitrap MS	0.1% FA in H_2O and 0.1% FA in MeCN	Thermo EASY-Spray PepMap C_{18} column, 3 μm, 75 μm i.d. × 150 mm	Gradient, 300 nL·min^{-1}	1,000 nL	37 min	[76]
Pesticides	Baby food	UV detector	H_2O and MeCN (20:80, v/v)	In-house packed phenyl column, 3 μm, 100 μm i.d. × 255 mm, with preconcentration	Isocratic, 300 nL·min^{-1}	1,000 nL	32 min	[49]
Pesticides, drugs of abuse, performance enhancing drugs, environmental contaminants	Food (leek, lemon, olive oil), human urine, wastewater	Orbitrap MS	0.1% FA in H_2O and 0.1% FA in MeCN	Thermo EASY-Spray PepMap C_{18} column, 2 μm, 75 μm i.d. × 500 mm and 3 μm, 75 μm i.d. × 150 mm	Gradient, 300 nL·min^{-1}	1,000 nL	45 min and 37 min	[58]
Aflatoxins	Peanut products (peanuts, peanut butter, peanut powder)	QqQ MS	0.1 mM NH_4OAc in H_2O and MeCN:MeOH (25:75, v/v) with 1 mM NH_4OAc	Agilent nanoLC-chips with Zorbax SB-C_8 stationary phase, 5 μm, 75 μm i.d. × 150 mm, with preconcentration	Gradient, 300 nL·min^{-1}	8,000 nL	25 min	[62]

Abbreviations: FA: formic acid; MeCN: acetonitrile; MeOH: methanol; UV: ultraviolet; TOF MS: time of flight MS; i.d.: internal diameter; NH_4OAc: ammonium acetate; IAC: immunoaffinity cartridges; QqQ MS: triple quadrupole MS.

Table 2. Comparison of different sample preparation methods for chromatographic separation of antibiotics, pesticides, and pharmaceuticals, including the application of nano-LC methods.

Analytes	Equipment	Samples	Main steps of sample preparation procedure	SPE	Evaporation	Prior analysis	Reference
Antibiotics							
Antibiotics (penicillin group)	Nano-LC, Ion-trap MS	Bovine milk	Centrifuged, mixed with 0.1 M phosphate buffer (pH 8), LLE with *n*-hexane, SPE	Supelco LC −18 C_{18} SPE cartridge	40 − 45 °C, nitrogen	Reconstituted in H_2O, filtered	[10]
Antibiotics (penicillin group)	Nano-LC, Ion-trap MS	Porcine tissues (liver and kidney)	Vortex mixed with MeOH, centrifuged	–	40 − 45 °C, nitrogen	Reconstituted in H_2O, filtered	[10]
Antibiotics (sulfonamides)	Nano-LC, Ion-trap MS	Pasteurized bovine milk	Mixed with TFA solution, added McIlvaine buffer, pH adjusted to 4.5, centrifuged, SPE, eluted with MeOH and 95% MeOH with 2% ammonium hydroxide	Oasis HLB	32 °C, rotary evaporator	Reconstituted in 5% MeOH, ultra-sonicated, centrifuged	[67]
Antibiotics and pesticides	Nano-LC, Orbitrap MS	Milk	Filtered, SPE	Captiva ND cartridge	–	–	[65]
Veterinary drugs and antibiotics	Nano-LC, Orbitrap MS	Veal muscle, egg and milk	Added extraction buffer (EDTA, oxalic acid, pH 3 with ammonium sulfate) and MeCN, shook, centrifuged, transferred into another tube with ammonium sulfate, SPE	HLB cartridge	–	Diluted (d = 40 and 100)	[57]
Veterinary drugs and antibiotics	Nano-LC, Orbitrap MS	Honey	Mixed with water, added EDTA, homogenized, added ethyl acetate, stirred, added sodium sulfate, C_{18} sorbent, and PSA, shook, centrifuged	–	–	Diluted (d = 40 and 100)	[57]
Antibiotics	UHPLC –MS/MS	Animal tissues (liver, kidney, and muscle)	Added McIlvaine buffer, mixed, centrifuged, added phosphate buffer, SPE	Waters Oasis HLB	45 °C, nitrogen	Reconstituted and filtered	[77]
Veterinary drugs (including antibiotics)	UHPLC, TOF MS	Animal tissues (liver, kidney, and muscle)	Added MeCN, ammonium sulfate and extraction solution, centrifuged, transferred into a Syncore vessel, added ammonium sulfate, evaporated. Then, pH of the aqueous phase was adjusted to 6.5, centrifuged, SPE, added DMSO, evaporated until 0.5 mL remained	Waters Oasis HLB	In Syncore vessel at 50 °C, and after SPE	Diluted	[78]
Veterinary drugs and antibiotics	UHPLC, QqQ MS	Bovine muscle	Added MeCN, shook, centrifuged, evaporated until 1 mL was left. Repeated extraction with extraction solution (NH_4OAc, EDTA, NaCl, TCA in H_2O), vortexed, shook, centrifuged. Decanted extracts, adjusted pH to 6.5, SPE	Waters Oasis HLB	30 °C, nitrogen	Combined extracts, filtered	[79]
Veterinary drugs	UHPLC, QqQ MS	Milk	Added 1% of acetic acid in MeCN and Na_2EDTA solution, vortexed, added $MgSO_4$, NaOAc, shook, centrifuged	–	–	Filtered, diluted	[80]
Antibiotics	HPLC, QqQ MS	Milk	Quinolones and fluoroquinolones: added 0.1% FA in MeCN, vortexed, froze (–20 °C), centrifuged, evaporated, reconstituted. Sulfonamides, trimethoprim and bromhexine: added ethanol and acetic acid, mixed, froze (–20 °C), centrifuged, diluted.	–	45 °C, nitrogen	Reconstituted and centrifuged or diluted	[81]

(*continued*)

Table 2. Continued.

Analytes	Equipment	Samples	Main steps of sample preparation procedure	SPE	Evaporation	Prior analysis	Reference
Veterinary drugs and antibiotics	HPLC, Orbitrap MS	Milk	Added 1% of acetic acid in MeCN and Na_2EDTA solution, vortexed, added $MgSO_4$, NaOAc, shook, centrifuged, diluted with methanol and aqueous formic acid solution	–	–	Filtered and diluted	[82]
Antibiotics	HPLC, QqQ MS	Honey	Added Na_2EDTA solution, citric acid and H_2O, shook, added 1% acetic acid in MeCN, Na_2SO_4 and NaCl, dSPE	Dispersive SPE with PSA, C_{18}, and Na_2SO4	–	Filtered and diluted	[83]
Pesticides							
64 multiclass pesticides	Nano-LC, Orbitrap MS	Tomatoes, oranges, fruit-based jam, baby food	Mixed with MeCN, added $MgSO_4$ and NaCl, shook, centrifuged, dSPE with PSA and $MgSO_4$	Dispersive SPE with PSA and $MgSO_4$	–	Filtered and diluted (d = 50)	[37]
64 multiclass pesticides	Nano-LC, Orbitrap MS	Olive oil	Mixed with 1% FA in MeCN, added $MgSO_4$ and NaCl, centrifuged and treated with PSA, $MgSO_4$, and C_{18} sorbent	Dispersive SPE with PSA, $MgSO_4$, and C_{18} sorbent	–	Filtered and diluted (d = 20 and 50)	[37]
162 multiclass pesticides	Nano-LC, Orbitrap MS	Olive oil	Mixed with H_2O, MeCN with 1% acetic acid, added $MgSO_4$ and NaCl, added EMR sorbent and dSPE with $MgSO_4$ and NaCl	Dispersive SPE, EMR sorbent and with $MgSO_4$ and NaCl	–	Filtered and diluted	[68]
Multiclass pesticides	Nano-LC, Orbitrap MS	Apples, baby food	Extraction by QuEChERS method CEN 15662, without dispersive SPE	–	–	Filtered	[69]
Pesticides	Nano-LC, passive split, UV detector	Baby food	Added ethyl acetate, sonicated, centrifuged, transferred the top layer, repeated the extraction, added Na_2SO_4 to combined extract, filtered, evaporated, SPE	Waters Sep-Pak Vac C_{18} SPE	After filtration and after SPE	Reconstituted	[49]
Pesticides	Nano-LC, Orbitrap MS	Leek and lemon	Mixed with MeCN, added NaCl and $MgSO_4$, shook, centrifuged, dSPE, centrifuged	Dispersive SPE with $MgSO_4$ and PSA	–	Filtered and diluted (d = 20 or 50)	[58]
Pesticides	Nano-LC, Orbitrap MS	Olive oil	Mixed with water and 1% acetic acid in MeCN, added NaCl and $MgSO_4$, shook, centrifuged, dSPE, centrifuged	Dispersive SPE with $MgSO_4$, C_{18}, and PSA	–	Filtered and diluted (d = 20 or 50)	[58]
Insecticides and pesticides	Nano-LC, Orbitrap MS	Nectar	Diluted in methanol-water solution, filtered	–	–	Filtered and diluted (d = 40)	[76]
Insecticides and pesticides	Nano-LC, Orbitrap MS	Pollen	Added water, shook, added MeCN, shook, added salts (NaCl and $MgSO_4$), shook, centrifuged, dSPE	Dispersive SPE with $MgSO_4$, C_{18} and PSA	–	Filtered and diluted (d = 5)	[76]
Pesticides	UHPLC, QqQ MS	Fruits (pakchoi, cowpea, pepper) and vegetables (peach, grape and watermelon)	Added MeCN, mixed, added NaCl, mixed, centrifuged, left for 60 min, transferred into a tube with C_{18} sorbent, PSA, $MgSO_4$, and GCB, mixed, centrifuged	Dispersive SPE (C_{18} sorbent, PSA, $MgSO_4$, and GCB)	–	Filtered	[84]
Pesticides	UHPLC, TOF MS	Fruits (starfruits and Indian jujubes)	Mixed with MeCN, filtered through a paper filter, added NaCl, mixed, centrifuged, transferred into a tube with PSA and $MgSO_4$, evaporated	Dispersive SPE (PSA and $MgSO_4$)	Vacuum rotary evaporator, 36 °C	Reconstituted, filtered	[85]

(*continued*)

Table 2. Continued.

Analytes	Equipment	Samples	Main steps of sample preparation procedure	SPE	Evaporation	Prior analysis	Reference
Pesticides	UHPLC, QqQ MS	Edible oils (olive, soy, sunflower)	Mixed with MeCN, added $MgSO_4$, NaCl, sodium citrate and disodium hydrogencitrate, mixed, centrifuged, froze in dry ice, the MeCN extract was transferred into a tube with EMR-Lipid dSPE and H_2O, vortexed, centrifuged, dSPE with NaCl and $MgSO_4$, homogenized, centrifuged, FA was added	Dispersive SPE with EMR-Lipid dSPE, another with NaCl and $MgSO_4$	–	Acidified and diluted (d = 5)	[86]
Pesticides	HPLC, QqQ MS	Olive oil and olives	Mixed with MeCN, stored in a freezer (–18 °C) for 12 h, transferred into a tube with PSA, GCB, $MgSO_4$, shook, centrifuged, the extract was filtered	Dispersive SPE (PSA, GCB, $MgSO_4$)	–	Filtered	[87]
Pesticides	HPLC, QqQ MS	Honeybees, honey and bee pollen	Extraction with MeCN, 2% TEA in MeCN, hexane, H_2O, mixed, added $MgSO_4$, NaOAc, PSA, vortexed, centrifuged, another dSPE, SPE, evaporation	Dispersive SPE with $MgSO_4$, NaOAc, PSA, another with PSA and $MgSO_4$; SPE with Scharlau Extra Bond C_{18} cartridge	Evaporation after SPE	Reconstituted and filtered	[88]
Pesticides	HPLC, ToF MS	Vegetables and fruits (eggplant, cabbage, cauliflower, guava, okra, onions, potatoes, apples, bananas, grapes, mangoes, oranges, and pomegranates)	Added MeCN-MeOH mixture, vortexed, added NaCl, vortexed, centrifuged, evaporated, reconstituted with MeCN-MeOH mixture, SPE, evaporated, reconstituted	SPE with Supelco GCB/PSA cartridge	Evaporation before and after SPE	Reconstituted and filtered	[89]
Pesticides	UHPLC, QqQ MS	Vegetables (tomatoes, bell peppers, eggplants, cucumbers, zucchinis, cabbage, carrots, potatoes) and fruits (strawberries, watermelons, apples, and grapes)	Mixed with MeCN, added $MgSO_4$ and NaCl, centrifuged, dSPE with PSA, GCB and $MgSO_4$, diluted	dSPE with PSA, GCB and $MgSO_4$	–	Diluted	[90]
Pesticides	UHPLC, QqQ MS	Baby food (fruit and vegetable-based juices and purees)	Shook with MeCN, added $MgSO_4$, NaCl, followed by sodium citrate and disodium hydrogencitrate, shook, centrifuged, dSPE	dSPE with PSA and $MgSO_4$	Evaporation after dSPE	Reconstituted	[91]
Pesticides	UHPLC, Orbitrap MS	Baby food (meat, fish, and vegetable-based)	Added water, MeCN with 1% FA, shook, centrifuged, SPE	Florisil Cartridge SPE	–	–	[92]
Mycotoxins							
Mycotoxins	Nano-LC, Orbitrap MS	Edible nuts (peanuts, pistachios, almonds)	Homogenized, added water, then MeCN with formic acid, mixed, added salt mix, mixed and centrifuged, dSPE	Dispersive SPE (EMR sorbent)	–	Diluted and filtered (d = 50)	[73]

(*continued*)

Table 2. Continued.

Analytes	Equipment	Samples	Main steps of sample preparation procedure	SPE	Evaporation	Prior analysis	Reference
Aflatoxins	Nano-LC, QqQ MS	Peanut products (peanuts, peanut butter, peanut powder)	Mixed with NaCl and 60% MeOH, homogenized, centrifuged, diluted, filtered (paper filter), SPE	Vicam AflaTest SPE with IAC	Evaporation after SPE	Reconstituted	[62]
Mycotoxins	UHPLC, QqQ MS	Nuts (almonds, hazelnuts, peanuts, pistachios, walnuts)	Mixed with MeCN and H_2O solution, added Na_2SO_4 and NaCl, shook, centrifuged, dSPE	Dispersive SPE with C_{18}	–	Filtered	[93]
Mycotoxins	UHPLC, QqQ MS	Nuts and seeds (almonds, peanuts, sunflower seeds, pumpkin seeds, walnuts, macadamia nuts, pistachios, hazelnuts, pine nuts)	Added H_2O, mixed, added 5% FA in MeCN, shook, added QuEChERS mixture, shook, centrifuged, evaporated, reconstituted; additionally, for aflatoxins: MeCN layer after QuEChERS was evaporated, reconstituted, H_2O and NaCl were added, extracted with chloroform, mixed, centrifuged, evaporated, reconstituted	–	Evaporation after QuEChERS	Reconstituted and filtered	[94]
Mycotoxins	UHPLC, QqQ MS	Rice, maize, peanut paste	Added 2% FA in water, MeCN, vortexed, added $MgSO_4$, NaCl, shook, centrifuged, dSPE, shook, centrifuged, added DMSO to clear extract, evaporated, diluted DMSO residue	dSPE with C_{18} and $MgSO_4$	Evaporation after dSPE	Diluted with DMSO residue, filtered	[95]
Mycotoxins	UHPLC, QqQ MS	Nuts (almonds, peanuts, walnuts, hazelnuts, pecan nuts, cashews, Brazil nut, pine nuts)	Added H_2O, shook, added 5% FA in MeCN, $MgSO_4$, NaCl, shook, centrifuged, dSPE, evaporated, reconstituted	dSPE with C_{18} and Z-Sep+ sorbent	Evaporation after dSPE	Reconstituted	[96]

Abbreviations: PSA: primary-secondary amine sorbent; NH_4OAc: ammonium acetate; AcOH: acetic acid; EMR: Enhanced Matrix Removal-Lipid sorbent; TFA: trifluoroacetic acid; LLE: liquid–liquid extraction; DMSO: dimethyl sulfoxide; GCB: graphitized carbon black, TEA: triethylamine; EMR: enhanced matrix removal-lipid sorbent; d: dilution factor; FA: formic acid.

are the same as in other techniques. Therefore, improvements of sensitivity can be achieved due to reduced flow rates and the size of droplets, as well by suppressing matrix effects. However, there are fundamental limitations regarding how far those analytical parameters can be optimized and it is principally important to not overestimate the potential capabilities of nano-LC methods. Comparison of analytical performance is provided in Table 3.

The comparison was focused on the most crucial analytical parameters: range, limit of detection (LOD), limit of quantitation (LOQ), recovery, and the matrix effects. Range is expressed either as linear dynamic range, or as calibration range in validations. LOD is defined as the lowest concentration of an analyte that can be determined with analytical signal reliably distinguished from zero.[97] And typically, LOD is determined as signal to noise ratio $S/N > 3$. LOQ shows the concentration of analyte that can be confidently quantitated with known accuracy and precision.[98] It should be determined according to the minimum concentration that provides suitable recovery and RSD values corresponding to the respective regulation (e.g., veterinary drugs or pesticides). The estimation of LOQ values can be done using several methods. Typically, LOQ values are established on the basis of signal to noise ratio ($S/N > 10$). However, noise levels are often negligible with high resolution mass spectrometry (HRMS) such as Orbitrap MS or ToF MS. To not overestimate the method sensitivity in the case of HRMS detectors, LOQ can be assumed as the lowest concentration level that has been tested.[68]

Matrix effects are certainly one of the key parameters of analytical performance. When analyzing samples of different origin, for example, animal products, fruit and vegetable products, or other environmental samples, it is worth mentioning that sample preparation does not eliminate all matrix components. As a result, the presence of residual matrix components may affect the analytical signal, leading to signal suppression or enhancement.[36] One of the benefits of the nano-LC methods is attributed to the potential for a significant decrease of matrix effects. This is achieved by injecting diluted samples. In numerous examples,[37,57,58] it has been proven that the dilution of samples decreased matrix effects while maintaining reasonable sensitivity.

Table 3. Comparison of analytical performance of the determination procedures of antibiotics, pesticides, mycotoxins, and pharmaceuticals, including the applications of nano-LC methods.

Analytes	Samples	Equipment	Column	Range	LOD	LOQ	Recovery	Matrix effects	Reference
Antibiotics									
Antibiotics (penicillin group)	Pharmaceuticals, bovine milk, porcine tissues (liver and kidney)	Thermo UltiMate 3000 nano-LC with ion trap MS	In-house packed C_{18} column, 3 μm, 100 μm i.d. × 100 mm	0.05 – 5 $\mu g \cdot mL^{-1}$ (UV), from 0.1 – 10 to 1 – 100 $\mu g \cdot L^{-1}$ (MS)	2.27 – 4.06 $\mu g \cdot L^{-1}$ (UV); 0.01 – 0.51 $\mu g \cdot L^{-1}$ (MS)	7.57 – 13.5 $\mu g \cdot L^{-1}$ (UV); 0.04 – 1.71 $\mu g \cdot L^{-1}$ (MS);	104 – 116% (UV); 100 – 117% (MS)	ND	[10]
Antibiotics (sulfonamides)	Pasteurized bovine milk	LC Packing Dionex Ultimate Capillary HPLC with UV detector; Thermo LCQ Ion-trap MS	In-house packed C_{18} column, core-shell, 2.6 μm, 100 μm i.d. × 250 mm, with preconcentration	From 50 – 500 to 120 – 1,200 $ng \cdot mL^{-1}$	8 – 96 $\mu g \cdot kg^{-1}$	2 – 40 $\mu g \cdot kg^{-1}$	85 – 105%	Significant (signal reduced up to four times in matrix)	[67]
Antibiotics	Milk	UltiMate 3000 nano-LC; Exactive Plus Orbitrap MS	In-house packed monolith column with multiwalled carbon nanotubes (MWCNTs), 75 μm i.d. × 100 mm	0.1 – 25 $\mu g \cdot kg^{-1}$	0.10 – 0.14 $\mu g \cdot kg^{-1}$	0.21 $\mu g \cdot kg^{-1}$	77 – 89%	From 0 to 0.1%	[65]
Veterinary drugs and antibiotics	Honey, veal muscle, egg, and milk	Thermo EASY-nLC 1000 nano-LC system, Thermo Q-Exactive Orbitrap MS	Thermo EASY-Spray PepMap C_{18} column, 3 μm, 75 μm i.d. × 150 mm	0.1 – 1,000 $\mu g \cdot kg^{-1}$	ND	0.1 – 1 $\mu g \cdot kg^{-1}$	73.8 – 121% for milk, veal and honey, 86.9 – 120% for eggs (except tetracyclines)	0 – 1.9% for milk, 0 – 9.2 for veal, 0 – 1.6 for eggs, 0 – 9.6% for honey	[57]
Antibiotics	Animal tissues (liver, kidney, and muscle)	Waters Acquity UHPLC; Waters Micromass Xevo TQ-S MS/MS	Waters Acquity BEH C_{18}, 1.7 μm, 2.1 mm i.d. × 50 mm	From 0.2 – 500 to 4 – 500 $\mu g \cdot kg^{-1}$	0.2 – 4 $\mu g \cdot kg^{-1}$	0.5 – 10 $\mu g \cdot kg^{-1}$	54 – 102%	From – 86% to 117%	[77]
Veterinary drugs (including antibiotics)	Animal tissues (liver, kidney, and muscle)	Acquity system UHPLC, Waters LCT Premier TOF MS	Waters HSS T3, 1.8 μm, 2.1 mm i.d. × 100 mm	1 – 100 $\mu g \cdot kg^{-1}$ and 10 – 1,000 $\mu g \cdot kg^{-1}$	ND	0.2 – 10.9 $\mu g \cdot kg^{-1}$	14 – 144%	31 – 243%	[78]
Veterinary drugs and antibiotics	Bovine muscle	Thermo Accela UHPLC, Thermo TSQ Quantum Access QqQ MS	Waters Acquity UPLC BEH HILIC column, 1.7 μm, 2.1 mm i.d. × 100 mm	0.25 – 4 × validation levels (based on MRLs)	ND	0.03 – 178 $\mu g \cdot kg^{-1}$	37 – 106%	From – 99% to 117%	[79]
Veterinary drugs	Milk	Waters Acquity UPLC system; Waters Acquity TQD QqQ Ms	Waters Acquity UPLC BEH HILIC column, 1.7 μm, 2.1 mm i.d. × 100 mm	5 – 200 $\mu g \cdot kg^{-1}$	1 – 4 $\mu g \cdot kg^{-1}$	3 – 10 $\mu g \cdot kg^{-1}$	70 – 110%	1.5 – 1001%	[80]
Antibiotics	Milk	Waters Alliance Separations Module 2695 HPLC; Waters Quattro Micro QqQ MS	Waters Symmetry C_{18}, 3.5 μm, 4.6 mm i.d. × 75 mm	0.25 – 2.0 × MRL	0.2 – 10 $ng \cdot mL^{-1}$	2.5 – 25 $ng \cdot mL^{-1}$	62 – 108%	37 – 308%	[81]
Veterinary drugs and antibiotics	Milk	Thermo Transcend 600 LC, Thermo Exactive Orbitrap MS	Thermo Hypersil GOLD aQ C_{18} column, 1.7 μm, 2.1 mm i.d. × 100 mm	5 – 100 $\mu g \cdot kg^{-1}$	ND	0.2 – 25 $\mu g \cdot kg^{-1}$	ND	ND	[82]
Antibiotics	Honey	Agilent 1200 series HPLC system; Agilent 6460 QqQ MS	Agilent Poroshell 120, EC- C_{18}, 2.7 μm, 2.1 mm i.d. × 100 mm	ND	0.14 – 2.91 $\mu g \cdot kg^{-1}$	0.5 – 9.7 $\mu g \cdot kg^{-1}$	81 – 110%	From – 59 to 19%	[83]

(*continued*)

Table 3. Continued.

Analytes	Samples	Equipment	Column	Range	LOD	LOQ	Recovery	Matrix effects	Reference
Pesticides									
64 multiclass pesticides	Tomatoes, oranges, fruit-based jam, baby food, and olive oil	Thermo EASY-nLC 1000 nano-LC, Thermo Q-Exactive Orbitrap MS	Thermo EASY-Spray C_{18} PepMap column, 3 μm, i.d. 75 μm, with preconcentration	0.002 – 200 $\mu g \cdot kg^{-1}$	ND	0.001 – 0.114 $\mu g \cdot kg^{-1}$	ND	From – 11% to 10%, with d = 50	[37]
162 multiclass pesticides	Olive oil	Thermo EASY-nLC 1000 nano-LC, Thermo Q-Exactive Orbitrap MS	Thermo EASY-Spray PepMap C_{18} column, 3 μm, i.d. 75 μm	0.05 – 500 $\mu g \cdot kg^{-1}$	ND	0.05 $\mu g \cdot kg$-1	75 – 119%	From – 20% to 9%	[68]
Pesticides	Apples and baby food	AB Sciex Eksigent Ekspert nano-LC 400, Thermo LTQ-Orbitrap MS with ambient dielectric barrier discharge ionization source	AB Sciex C_{18} columm, 3 μm, 75 μm i.d. × 150 mm	1.8 $ng \cdot mL^{-1}$ – 1 $\mu g \cdot mL^{-1}$	11 – 598 $pg \cdot mL^{-1}$	33 – 1,812 $pg \cdot mL^{-1}$	ND	From – 14.9% to 29.4%	[69]
Pesticides	Baby food	LC Packings Dionex Ultimate Capillary HPLC unit with mechanical spilt and UV detector	In-house packed phenyl column, 3 μm, 100 μm i.d. × 255 mm, with preconcentration	10 – 1,250 $ng \cdot mL^{-1}$	4.4 – 37.5 $ng \cdot mL^{-1}$	14.5 – 125.0 $ng \cdot mL^{-1}$	37 – 119%	ND	[49]
Pesticides	Food (leeks, lemons, olive oil)	Thermo EASY-nLC 1000 nano-LC system, Thermo Q-Exactive Orbitrap MS	Thermo EASY-Spray PepMap C_{18} column, 3 μm, 75 μm i.d. × 150 mm	0.001 – 10 $\mu g \cdot L^{-1}$	ND	0.003 – 0.083 $\mu g \cdot kg^{-1}$	ND	From – 6 to 0% (lemon), from – 7 to 0% (olive oil), from – 7 to 0% (leek)	[58]
Insecticides and pesticides	Honey and pollen	Thermo EASY-nLC 1000 nano-LC system, Thermo Q-Exactive Orbitrap MS	Thermo EASY-Spray PepMap C_{18} column, 3 μm, 75 μm i.d. × 150 mm	0.05 – 500 $\mu g \cdot kg^{-1}$ (pollen), 0.04 – 400 $\mu g \cdot kg^{-1}$ (nectar)	ND	0.5 $\mu g \cdot kg^{-1}$ (pollen), 0.4 $\mu g \cdot kg^{-1}$ (nectar)	85 – 97%	From – 4% to – 9% (pollen) and from – 5 to – 8% (nectar)	[76]
Pesticides	Fruits (pakchoi, cowpea, pepper) and vegetables (peach, grape and watermelon)	Agilent 1290 UPLC; Agilent 6460 QqQ MS	Agilent Zorbax Eclipse Plus- C_{18} column, 3.5 μm, 3.0 mm i.d. × 150 mm	15 – 500 $\mu g \cdot kg^{-1}$	0.003 – 2 $\mu g \cdot kg^{-1}$	0.1 – 6.67 $\mu g \cdot kg^{-1}$	73 – 134%	ND	[84]
Pesticides	Fruits (starfruits and Indian jujubes)	Agilent 1290 Infinity UPLC; AB Sciex TripleTOF 5600^{+}	Agilent Eclipse Plus C_{18} RRHD column, 1.8 μm, 2.1 mm i.d. × 50 mm	10 – 200 $ng \cdot mL^{-1}$	0.03 – 4 $\mu g \cdot kg^{-1}$	0.1 – 12 $\mu g \cdot kg^{-1}$	63 – 119%	48 – 120%	[85]
Pesticides	Edible oils (olive, soya, sunflower)	Agilent UHPLC 1290 Series; Agilent Technologies 6490 QqQ MS	Agilent Zorbax Eclipse Plus C_8 column, 1.8 μm, 2.1 mm i.d. × 100 mm	10 – 500 $\mu g \cdot kg^{-1}$	ND	10 – 50 $\mu g \cdot kg^{-1}$	60 – 120% (for the majority of compounds)	From – 50 to 50% (for the majority of compounds)	[86]
Pesticides	Olive oil and olives	Agilent Series 1200 HPLC, Agilent 6410 QqQ MS	Varian Zorbax Eclipse XDB C_{18}, 3.5 μm, 2.1 mm i.d. × 150 mm	10 – 300 $\mu g \cdot L^{-1}$	3 $\mu g \cdot kg^{-1}$	10 $\mu g \cdot kg^{-1}$	70 – 126% (for the majority of compounds)	Variable (assessment by t test)	[87]
Pesticides	Honeybees, honey and bee pollen	Agilent Technologies 6410 Triple Quad LC-MS system	Agilent Zorbax Eclipse XDB- C_{18}, 3.5 μm, 2.1 mm i.d. × 150 mm	0.5 – 700 $\mu g \cdot kg^{-1}$	0.03 – 23.3 $\mu g \cdot kg^{-1}$	0.1 – 78 $\mu g \cdot kg^{-1}$	58 – 117%	Variation (assessment by t test)	[88]

Pesticides	Vegetables and fruits (eggplant, cabbage, cauliflower, guava, okra, onions, potatoes, apples, bananas, grapes, mangoes, oranges, and pomegranates)	Waters Acquity UHPLC; Waters Synapt TOF MS	Waters UPLC BEH C_{18} column, 1.7 μm, 2.1 mm i.d. × 50 mm	10 – 750 $\mu g \cdot L^{-1}$	0.3 – 3.8 $\mu g \cdot kg^{-1}$	0.8 – 11.8 $\mu g \cdot kg^{-1}$	74 – 111%	Strong matrix effects	[89]
Pesticides	Vegetables (tomatoes, bell peppers, eggplants, cucumbers, zucchinis, cabbage, carrots, potatoes) and fruits (strawberries, watermelons, apples and grapes)	Agilent 1200 UHPLC; Agilent 6460 QqQ MS	Agilent Zorbax C_{18} column, 1.8 μm, 2.1 mm i.d. × 50 mm	ND	0.7 – 214 $\mu g \cdot kg^{-1}$	2.9 – 452 $\mu g \cdot kg^{-1}$	85– 106%	ND	[90]
Pesticides	Baby food (fruit and vegetable-based juices and purees)	Agilent 1200 LC; Agilent 6410 QqQ MS	Agilent Zorbax Eclipse XDB-C_{18} column, 1.8 μm, 4.6 mm i.d. × 50 mm	5 – 250 $\mu g \cdot kg^{-1}$	ND	5 – 10 $\mu g \cdot kg^{-1}$	86 – 114%	From – 20% to 34%	[91]
Pesticides	Baby food (meat, fish, and vegetable-based)	Thermo Transcend 600 LC, Thermo Exactive Orbitrap MS	Thermo Hypersil GOLD aQ C_{18} column, 1.7 μm, 2.1 mm i.d. × 100 mm	2.5 – 100 $\mu g \cdot L^{-1}$	0.5 – 50 $\mu g \cdot kg^{-1}$	10 – 100 $\mu g \cdot kg^{-1}$	70 – 120% (for the majority of compounds)	From – 20% to 20% (for the majority of compounds)	[92]
Mycotoxins									
Mycotoxins	Edible nuts (peanuts, pistachios, almonds)	Thermo EASY-nLC 1000 nano-LC system and Thermo Q-Exactive Orbitrap MS	Thermo PepMap C_{18} column, 3 μm, i.d. 75 μm× 150 mm, with preconcentration	0.05 – 50 $\mu g \cdot kg^{-1}$	ND	0.05 – 5 $\mu g \cdot kg^{-1}$	75 – 98%	0 – 6%	[73]
Aflatoxins	Peanut products (peanuts, peanut butter, peanut powder)	Agilent 1200 nano-HPLC; Agilent 6410 series TripleQuad MS	Agilent nanoLC-chips with Zorbax SB-C_8 stationary phase, 5 μm, 75 μm i.d. × 150 mm, with preconcentration	0.048 – 16 $\mu g \cdot kg^{-1}$	0.004 – 0.008 $\mu g \cdot kg^{-1}$	0.048 $\mu g \cdot kg^{-1}$	91 – 100%	ND	[62]
Mycotoxins	Nuts (almonds, hazelnuts, peanuts, pistachios, walnuts)	Agilent series 1290 LC; Agilent 6460 A QqQ MS	Agilent Zorbax plus C_{18} column, 1.8 μm, 2.1 mm i.d. × 100 mm	0.5 – 250 $\mu g \cdot L^{-1}$	ND	0.5 – 1.0 $\mu g \cdot kg^{-1}$	70 – 118%	From – 40 to 82%	[93]
Mycotoxins	Nuts and seeds (almonds, peanuts,	Agilent 1290 Infinity LC; AB Sciex API 3200 QqQ MS	Agilent Zorbax Eclipse Plus RR HD column,	From 0.57 – 50 $\mu g \cdot kg^{-1}$ to 150 – 5,000 $\mu g \cdot kg^{-1}$	0.17 – 45.1 $\mu g \cdot kg^{-1}$	0.57 – 150 $\mu g \cdot kg^{-1}$	61 – 104%	From – 61 to – 12%	[94]

(*continued*)

Table 3. Continued.

Analytes	Samples	Equipment	Column	Range	LOD	LOQ	Recovery	Matrix effects	Reference
	sunflower seeds, pumpkin seeds, walnuts, macadamia nuts, pistachios, hazelnuts, pine nuts)		1.8 μm, 2.1 mm i.d. × 50 mm						
Mycotoxins	Rice, maize, peanut paste	Waters Acquity UPLC, Waters Xevo TQ-S QqQ MS	Waters Cortecs UPLC C_{18} column, 1.6 μm, 2.1 mm i.d. × 100 mm	ND	0.005 – 125 $\mu g \cdot kg^{-1}$ (in solvent)	0.01 – 250 $\mu g \cdot kg^{-1}$ (in solvent)	ND	ND	[95]
Mycotoxins	Nuts (almonds, peanuts, walnuts, hazelnuts, pecan nuts, cashews, Brazil nut, pine nuts)	Waters Alliance 2695 LC, Waters Quattro Micro QqQ MS	Phenomenex Kinetex C_{18} column, 2.6 μm, 4.6 mm i.d. × 150 mm	From 1.25 – 500 to 5 – 500 $\mu g \cdot kg^{-1}$	0.3 – 3.5 $\mu g \cdot kg^{-1}$	1.25 – 5 $\mu g \cdot kg^{-1}$	78 – 102%	64 – 94%	[96]

Abbreviations: ND: no data; d: dilution factor.

Recovery is an important criterion for deciding whether the particular analytical method is suitable for the analysis of a specific compound. Different regulations have set forth the requirements for the acceptable level of recovery of certain contaminants. For example, the SANTE guidelines requires 70% to 120% recovery of pesticide residues.[99] For veterinary drugs recovery levels from 50 – 120% to 80 – 110% depending on concentration levels are required by the European Commission guideline 2002/657/EC.[27] Achieving an acceptable recovery might be a challenge due to both instrumental factors and the characteristics of the individual compound. Table 3 shows generally acceptable recoveries, although for several compounds the recoveries might not be ideal. While the optimization of sample preparation and instrumental parameters is relatively straightforward in methods intended for few analytes, the same task may become rather difficult in multi methods that are widely used in routine laboratories for a larger number of analytes with significantly different chemical properties, logP and pKa values.

The recovery parameters and matrix effects are reported in Table 3 as ranges from the minimum to the maximum value, meaning that the distribution of those values can vary significantly. This is especially important for matrix effects, where several compounds can show significant signal suppression or enhancement while others have acceptable matrix effects, and the resulting data will have a higher variance.

As can be observed from the Table 3, two types of detectors have been employed: MS and UV. When comparing those methods, it should be noted that the sensitivity expressed as LOQ values is typically lower with UV detectors than with MS detectors. This is logical, because UV detectors have limited selectivity and sensitivity in comparison with MS detectors.

Another issue with UV detectors is that they are suitable for screening, but not for confirmatory analysis of veterinary drug residues. Regulation 2002/657/EC implements requirements for analytical methods that must meet certain criteria to confirm that sample contains a compound. Four identification points are required for banned substances, and they can be obtained based on the type of ion (precursor or product ion) and the resolution of mass spectra. Thus, according to this criterion, the applications of UV detectors are limited to screening analysis only.

The analytical parameters of nano-LC methods are comparable to those of other liquid chromatography variants, such as UHPLC and HPLC. Figure 1 (based on Table 3) and Figure 2 (based on Table 5) compares the LOQ values between various methods that have been used for the determination of various groups of analytes.

In this review, it has been found that analytical parameters of various nano-LC methods are comparable. The differences can be explained on the basis of different instrumental setups, used by each group of researchers. From Figure 1, it is clear that nano-LC methods tend to have comparable or better sensitivity than UHPLC and HPLC methods. Noticeable was advantages found when the

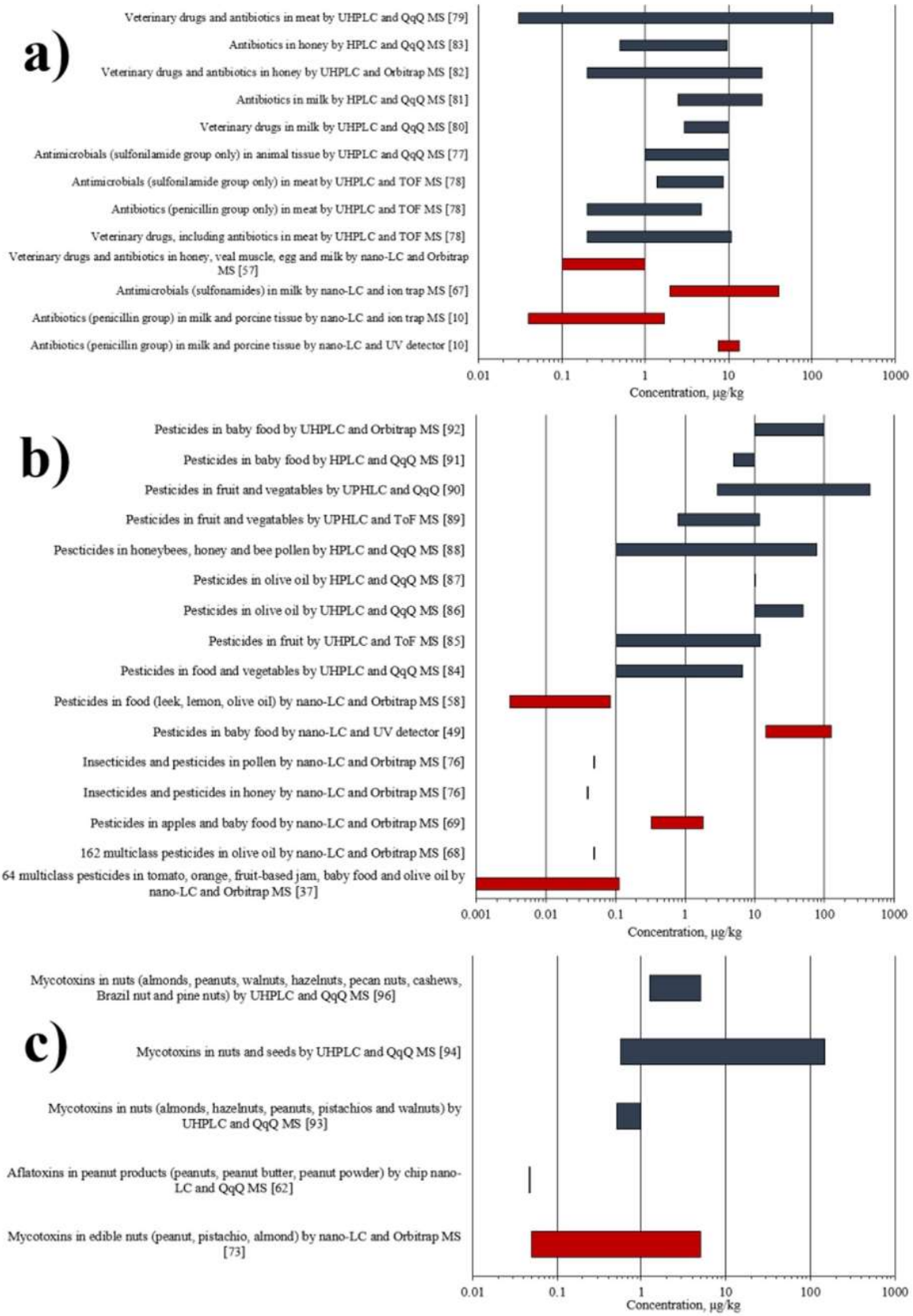

Figure 1. Comparison between LOQ values of nano-LC, HPLC, and UHPLC methods for the determination of (a) veterinary drugs and antibiotics, (b) pesticides, and (c) mycotoxins.

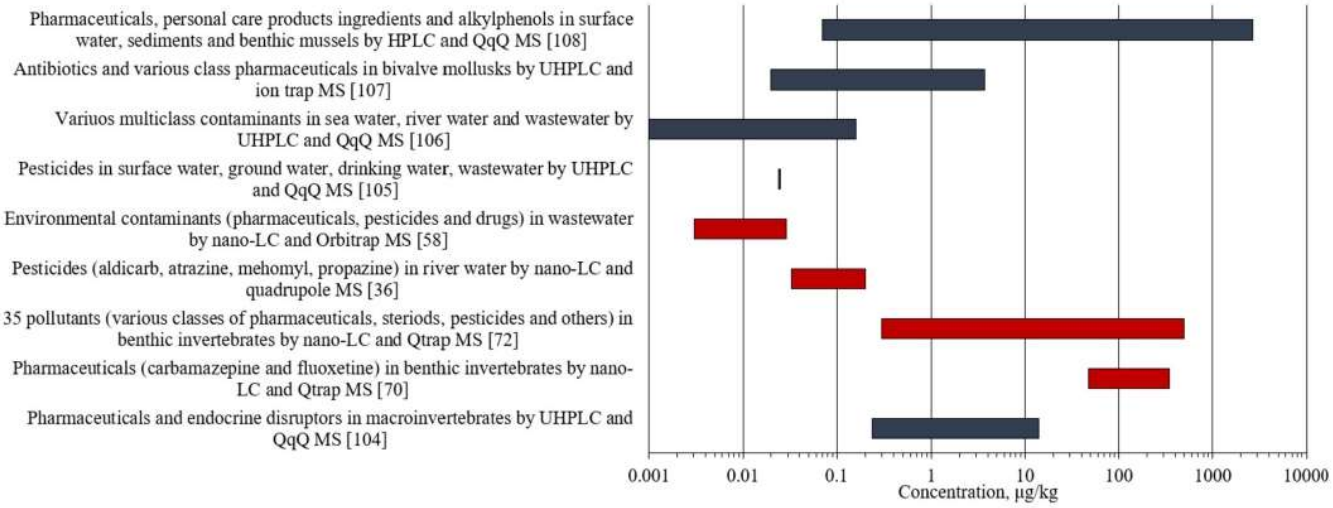

Figure 2. A comparison of LOQ values obtained by nano-LC and UHPLC methods with regard to various environmental contaminants.

nano-LC method was applied to pesticide analysis in comparison to other types of liquid chromatography. Not only the sample preparation in general consisted of fewer steps but also much more significant enhancement of sensitivity was achieved, compared to antibiotics and veterinary drugs. For mycotoxins, however, the sample preparation procedures were very similar and only minimal reduction in sample preparation efforts have been achieved to date. At the time, it is obvious that great improvements of method sensitivity have been achieved (Figure 1). It can be anticipated that nano-LC methods for mycotoxins could also in the future benefit from considerable reduction in sample preparation steps, analogously to the advancements in pesticides analysis.

Numerous nano-LC methods have been developed for the determination of low molecular mass compounds that are important for food safety control. In addition, several publications that do not describe real sample analysis also provide valuable information and demonstrate the capabilities of nano-LC methods. Aqai et al.[100] proposed a method for the determination of ochratoxins in wheat and cereal using a Waters nanoACQUITY UPLC, a commercial C_{18} column, and qTOF mass spectrometer, achieving LOD of 0.15 $\mu g \cdot kg^{-1}$. D'Orazio and Fanali[16] developed a method for basic drugs (acebutolol, alprenolol, nadolol, oxprenolol, and terbutaline), using custom built instrumentation with passive mechanical split under isocratic conditions, with in-house packed column coupled to a UV detector. The LOD values in standard solutions were found to be from 5 to 20 $\mu g \cdot kg^{-1}$. Another article by D'Orazio et al.[33] included the development of two methods for the analysis of NSAIDs and steroids in standard solutions using custom built instrumentation with a passive mechanical split under isocratic regime and an in-house packed column coupled with UV detector. The LOD values were from 10 to 40 $\mu g \cdot kg^{-1}$. In a study by Cappiello et al.,[101] three methods were developed for the determination of nitrated polycyclic aromatic hydrocarbons, pesticides, and human hormones, and standard solutions were analyzed. A Kontron LC system was used with a passive mechanical split, a commercial column (3 μm particle size, 75 μm × 15 cm), and a quadrupole mass spectrometer. Another article by D'Orazio and Fanali[102] featured the development and application of a new nano-junction interface for the analysis of organophosphorus pesticides and acidic drugs, including acidic NSAIDs. The authors used Agilent 1100 series LC with passive mechanical split and ion-trap MS, as well as an in-house packed C_{18} column (5 μm particle size, 100 μm × 345 mm). The LOD values were reported from 0.3 to 8.2 μg/mL. Fanali et al.[56] developed a method for the determination of β-blockers (nadolol, oxprenolol, alprenolol, and propranolol) with in-house assembled instrumentation, using a mechanical split, in-house packed column with two stationary phases, and an ion trap MS, achieving LODs from 0.5 to 100 $ng \cdot mL^{-1}$.

It is worth noting that other types of analytes relevant to food quality have been also investigated using nano-LC methods. Contreras et al.[66] developed a method for the determination of phenolic acids and flavonoids in cranberry syrups using a Bruker EASY-nLC liquid chromatograph, a Bruker micrOTOF mass spectrometer, and a NanoSeparations C_{18} column (3 μm particle size, 75 μm i.d. × 101 mm) with a pre-column under gradient conditions. The LOQ values achieved were $2.0 - 62.5\ ng \cdot mL^{-1}$.

There are several other studies dedicated to the comparison between nano-LC methods and other liquid chromatography methods. The researchers have demonstrated the advantages of nano-LC methods by providing indisputable evidence of improvements in sensitivity and considerable decrease of the matrix effects. In a study by Moreno-González et al.[37] the proposed method of determination of 64 pesticides was compared with other UHPLC methods and LOQ values for the nano-LC method was $<0.01\ \mu g \cdot kg^{-1}$ for 80% of analytes, while for UHPLC methods it was in a range of $1 - 25$ to $1 - 100\ \mu g \cdot kg^{-1}$. Similarly, matrix effects of the nano-LC method were negligible for 90% of analytes, while for others they were either not reported, or moderate for 80% of analytes. Alcántara-Durán et al.[73] presented a nano-LC method for mycotoxins in edible nuts and also compared their results. In the comparison with other LC methods, sensitivity was $0.05 - 5\ \mu g \cdot kg^{-1}$ with negligible

matrix effects for 100% of analytes, but other LC methods had substantially strong matrix effects. Moreover, sensitivity of other UHPLC methods was $0.61-150\,\mu g{\cdot}kg^{-1}$ and $1.25-5\,\mu g{\cdot}kg^{-1}$. In a study by Moreno-González et al.,[68] who developed a nano-LC method for analysis of pesticides in olive oil, the obtained sensitivity was $0.05-50\,\mu g{\cdot}kg^{-1}$ while comparable UHPLC methods not only had fewer analytes, but also had sensitivity of $0.1-91$ and $10-50\,\mu g{\cdot}kg^{-1}$. Matrix effects were also significantly decreased in comparison with other methods. Chip-based approach of nano-LC resulted in a significant improvement of sensitivity as was reported by Liu et al.[62] who developed a method for the determination of mycotoxins in peanuts. Other UHPLC and HPLC methods provided LODs of about $0.09-1.4\,\mu g{\cdot}kg^{-1}$, however, the nano-LC method was able to achieve LODs of $0.004-0.008\,\mu g{\cdot}kg^{-1}$.

Analysis of contaminants in environment samples by nano-LC methods

The determination of various chemical contaminants in the environment is a key task for advanced analytical techniques, including nano-LC. Sometimes the determination of a specific chemicals directly in water is not efficient or does not provide meaningful information about their distribution in the ecosystem. For this reason, it is common to use certain species of benthic invertebrates as bioindicators of environmental pollution.[103]

Some examples of such analytes are pesticides, pharmaceuticals including antibiotics, perfluorinated compounds, polycyclic aromatic compounds, and monomers of commercially significant polymers. In this review, we mainly focus on determination of pharmaceutical compounds and pesticides. Table 4 lists various sample preparation techniques for nano-LC and for other methods.

A variety of methods have been reported for the analytical determination of pharmaceutical compounds and pesticides in environmental samples, including liquid chromatography and mass spectrometry methods.

Typical sample preparation procedures in this area consist of sample homogenization, extraction, sometimes SPE and evaporation, following by reconstitution and instrumental analysis, as also listed in Table 2. Generally, water samples require less sample preparation, but larger amounts of samples are necessary for the analysis. Several examples of sample preparation methods for nano-LC methods are also listed in Table 4. Environmental sample preparation for nano-LC, compared to the methods for antibiotics, pesticides, and other analytes mentioned in Table 2, was not significantly shortened. This can be explained by the fact that, regardless of the chromatographic method, the preparation of environmental samples consumes less time and resources, especially for water samples.

The analytical performance of nano-LC methods is compared to UHPLC methods in Table 5.

The nano-LC method has its advantages in sample preparation and reducing LODs, as described previously in subsections Comparison of sample preparation procedures and Comparison of analytical performance. Similar observations were also made with environmental samples. However, the number nano-LC applications in the analysis of environmental samples was rather limited, compared to analyses related to food safety.

Additionally, there are several more meaningful examples illustrating this topic. González-Fuenzalida et al.[109] developed a method for the determination of diclofenac in river water utilizing nanomaterials for capillary column packing and achieved LOQ of $3.3\,ng{\cdot}mL^{-1}$. In a study by D'Orazio et al.,[110] a method for the determination of estrogenic compounds was developed, achieving LODs of $1.4-55.4\,ng{\cdot}L^{-1}$ with spiked Milli-Q water. They used an Agilent 1100 series LC with passive split and compared several types of stationary phases (C_{18}, phenyl, C_{18} bidentate silica hydrate), with C_{18} stationary phase found to be more suitable for this method.

Some other types of contaminants have also been successfully determined by nano-LC methods. Serra-Mora et al.[111] developed a method for the determination of triazines and their degradation products in water samples by using a UV-DAD detector. In their study, a Zorbax 300SB C_{18} column ($3.5\,\mu m$, $75\,\mu m$ i.d., 50 mm, 300 Å) was connected to Agilent 1260 Infinity LC system and isocratic conditions were selected, with a flow rate of 700 nL/min. Additionally, the authors performed a comparison between capillary and nano-LC methods for the determination of same compounds (triazines) and demonstrated that the nano-LC method provided a significant advantage in terms of method sensitivity.

An interesting approach for environment contamination assessment was designed by Berlioz-Barbier et al.[112] They performed a nontargeted analysis of benthic invertebrates (*Chironomus riparius*) that were exposed to the effluents of a wastewater treatment plant, using Thermo Ultimate 3000 nano-LC system with a Bruker microToF QII MS and Thermo Scientific Acclaim PepMap 100 C_{18} column ($3\,\mu m$, $75\,\mu m$ i.d. × 150 mm, 100 Å) for separation. Endogenous biomarkers such as fatty acids were identified, along with xenobiotics including ibuprofen and propranolol. Another method for the determination of fatty acids via nano-LC analysis was developed by Albergamo et al.[113] They studied anthropogenic impact on the environment and assessed marine pollution based on the fatty acid profile in mussels. A method for similar analytes in a similar matrix was developed by Rigano et al.[114] In a study by Serra-Mora et al.,[115] a method for the determination of herbicide Tribenuron-methyl in environmental waters was developed by using an Agilent 1260 Infinity nanoLC with a UV diode array detector.

Discussion

It is important to emphasize that still only a limited number of scientific articles describe the development and applications of nano-LC methods for food safety analysis. However, this situation provides an opportunity to develop new, more advanced methods with better analytical performance. A typical goal in food safety analysis is to increase the number of

Table 4. Comparison of sample preparation between nano-LC and UHPLC methods for analysis of the environmental samples.

Analytes	Equipment	Samples	Main sample treatment steps	SPE	Evaporation	Prior analysis	Reference
Pharmaceuticals (carbamazepine and fluoxetine)	Nano-LC, Qtrap MS	Benthic invertebrates (*Potamopyrgus antipodarum* and *Valvata piscinalis*)	Homogenized, added MeCN, H_2O, hexane and citrate QuEChERS, shaken, centrifuged	Dispersive SPE	–	Diluted	[70]
35 emerging pollutants (various classes of pharmaceuticals, steroids, pesticides and others)	Nano-LC, QqQ MS	Benthic invertebrates (*Potamopyrgus antipodarum*, *Gammarus fossarum*, and *Chironomus riparius*)	Homogenized, added MeCN, H_2O, hexane and citrate QuEChERS, shaken, centrifuged, evaporation	Dispersive SPE	Room temperature, nitrogen	Reconstituted	[72]
Environmental contaminants (pharmaceuticals, pesticides and drugs)	Nano-LC, Orbitrap MS	Wastewater	Passed through Oasis HLB SPE cartridge, evaporated	Waters Oasis HLB SPE cartridge	37 °C, nitrogen	Reconstituted, diluted (d = 20 or 50)	[58]
Pesticides	Nano-LC, Orbitrap MS	Honeybees	Added MeCN, sonicated, centrifuged	–	–	Diluted and filtered (d = 5)	[75]
Pesticides (aldicarb, atrazine, methomyl, propazine)	Nano-LC, single quadrupole MS	River water	Performed SPE, evaporation, reconstitution	Waters Oasis HLB SPE cartridge	Evaporated after SPE	Reconstituted	[36]
Perfluorooctanoic acid, perfluorooctane sulfonate	Nano-LC, ToF MS	River water	Filtered, added PFHA solution	–	–	Filtered	[41]
41 pharmaceuticals and 21 endocrine disruptors	UHPLC, QqQ MS	Macroinvertebrates (*Ancylus fluviatilis*, *Hydropsyche spp.*, *Phagocata spp.*)	Ultrasonicated with solvent (MeOH or H_2O/MeCN with FA), centrifuged, SPE, evaporated, reconstituted with H_2O/MeCN with FA, SPE, evaporated	Waters Ostro SPE	Evaporated after SPE	Reconstituted	[104]
Pesticides	UHPLC, QqQ MS	Surface water, ground water, drinking water, wastewater	Centrifuged, added FA, SPE, evaporated, reconstituted	Waters Oasis HLB SPE cartridge	Evaporated after SPE (40 °C, nitrogen)	Reconstituted	[105]
46 various multiclass contaminants	UHPLC, QqQ MS	Water (sea, river), wastewater	SPE, evaporated and reconstituted	Waters Oasis HLB SPE	Evaporated after SPE (40 °C, nitrogen)	Reconstituted, centrifuged	[106]
Antibiotics and various classes of pharmaceuticals	UHPLC, QqQ MS	Bivalve mollusks (*Crassostrea gigas*, *Mytilus galloprovincialis*, *Chamelea gallina*)	Extracted by PLE, the eluate was concentrated (to 30%), added water and Na_2EDTA, SPE, evaporated, reconstituted	Waters Oasis HLB SPE	Evaporated after SPE	Reconstituted	[107]
Pharmaceutical ingredients of personal care products, alkylphenols	HPLC, QqQ MS	Surface water, sediments and benthic mussels (*Geukensia demissa*)	For PPCPs in sediment and water: extracted with aqueous phosphate buffer or ammonia solution, extracted with MeCN, evaporated, filtered, adjusted pH to 2 or 10, added Na_4EDTA (for acidic extracts), SPE. Tissues: extracted with MeCN, followed by buffers, the rest as with sediment and water samples. For APs in water and sediment: extracted with MeOH containing KOH, then with hexane, acetylated, adjusted pH, cleaned up by silica gel column chromatography. Tissue: extracted with isooctane and SPE	Waters Oasis HLB SPE (for PPCPs) or aminopropyl cartrigde SPE (APs)	Only for PPCPs in water and sediment samples	Filtered	[108]

Abbreviations: PLE: pressurized liquid extraction; PFHA: perfluoroheptanoic acid; PPCP: personal care products ingredients; AP: alkylphenols.

Table 5. Comparison of the analytical performance of nano-LC methods to UHPLC in the analysis of environmental samples.

Analytes	Samples	Instruments	Column	Range	LOD	LOQ	Recovery	Matrix effects	Source
Pharmaceuticals (carbamazepine and fluoxetine)	Benthic invertebrates (*Potamopyrgus antipodarum* and *Valvata piscinalis*)	Thermo Ultimate3000 nano-LC, Sciex Qtrap 3200 MS	Themo PepMap C_{18} column, 3 μm, i.d. 75 μm, with preconcentration	5 × LOQ – 50 × LOQ	18 and 128 $\mu g \cdot kg^{-1}$	48 and 343 $\mu g \cdot kg^{-1}$	85 and 98%	−22% and – 14%	[70]
35 pollutants (various classes of pharmaceuticals, steroids, pesticides and others)	Benthic invertebrates (*Potamopyrgus antipodarum*, *Gammarus fossarum*, and *Chironomus riparius*)	Thermo Ultimate 3000 nano-LC, AB Sciex Qtrap 5500	Thermo PepMap C_{18} column, 3 μm, i.d. 75 μm × 150 mm, with preconcentration	From LOQ up to 40 – 50 × LOQ	ND	0.3 – 490 $\mu g \cdot kg^{-1}$	40 – 121%	Vary significantly	[72]
Perfluorooctanoic acid, perfluorooctane sulfonate	River water	Agilent Series 1100 capillary gradient pump, Micromass LCT TOF MS	Thermo PepMap C_{18} column, 3 μm, i.d. 75 μm × 150 mm, with preconcentration	20 – 500 $ng \cdot L^{-1}$	500 and 1,000 $pg \cdot L^{-1}$	ND	95%	ND	[41]
Pesticides	Honeybees	Thermo EASY-nLC 1000 nano-LC system, Thermo Q-Exactive Orbitrap MS	Thermo EASY-Spray PepMap C_{18} column, 3 μm, 75 μm i.d. × 150 mm	From $6 \cdot 10^1$ to $6 \cdot 10^6$ $pg \cdot bee^{-1}$	ND	$6 \cdot 10^1$ to $6 \cdot 10^3$ $pg \cdot bee^{-1}$	70 – 105%	From – 12 to 8%	[75]
Pesticides (aldicarb, atrazine, methomyl, propazine)	River water	Agilent 1100 series nano- LC system; direct-EI-MS; Agilent 5975B Inert MSD MS (with ESI)	Agilent C_{18} Zorbax-SB, 3.5 μm, 75 μm i.d. × 150 mm	From 10 pg – 10 ng to 60 pg – 600 ng	10 – 60 pg	33 – 200 pg	ND	From – 3 to 15%	[36]
Environmental contaminants (pharmaceuticals, pesticides and drugs)	Wastewater	Thermo EASY-nLC 1000 nano-LC system, Thermo Q-Exactive Orbitrap MS	Thermo EASY-Spray PepMap C_{18} column, 3 μm, 75 μm i.d. × 150 mm	0.001 – 10 $\mu g \cdot L^{-1}$	ND	0.3 to 29.4 $ng \cdot L^{-1}$	ND	From – 7 to 0%	[58]
41 pharmaceuticals and 21 endocrine disruptors	Macroinvertebrates (*Ancylus fluviatilis*, *Hydropsyche spp.*, *Phagocata spp.*)	Waters UPLC; Applied Biosystems Qtrap 5500	Waters Acquity HSS T3 column or Acquity BEH C_{18} column	0.1 – 100 $\mu g \cdot kg^{-1}$	0.080 – 2.4 $\mu g \cdot kg^{-1}$ (endocrine disruptors), 0.06 – 4.3 $\mu g \cdot kg^{-1}$ (pharmaceuticals)	0.27 – 8.0 $\mu g \cdot kg^{-1}$ (endocrine disruptors), 0.24 – 14 $\mu g \cdot kg^{-1}$ (pharmaceuticals)	34 – 125% (pharmaceuticals), 48 – 117% (endocrine disruptors)	Up to – 20%	[104]
Pesticides	Surface water, ground water, drinking water, wastewater	Waters Acquity UPLC; Waters TDQ QqQ MS	Waters Acquity UPLC HSS T3 column, 1.8 µm, 2.1 mm i.d. × 50 mm	0.5 – 100 $\mu g \cdot L^{-1}$	ND (instrument LOD 0.05 – 1 $\mu g \cdot L^{-1}$)	0.025 $\mu g \cdot L^{-1}$	40 – 130% (majority of compounds)	From 40 to 120% (majority of compounds)	[105]
46 various multiclass contaminants	Water (sea, river), wastewater	Varian LC system (ProStar 410 autosampler, ProStar 210 pumps); Varian 1200 L QqQ MS	Varian Polaris C_{18}-Ether column, 3 μm, 2 mm i.d. × 150 mm	From 2.5 – 750 to 12.5 – 1,0000 $ng \cdot L^{-1}$	ND	1.2 to 28 $ng \cdot L^{-1}$ (seawater), 5.0 to 160 $ng \cdot L^{-1}$ wastewater	10 – 110%	Signal suppression	[106]

(*continued*)

Table 5. Continued.

Analytes	Samples	Instruments	Column	Range	LOD	LOQ	Recovery	Matrix effects	Source
Antibiotics and various classes of pharmaceuticals	Bivalve mollusks (*Crassostrea gigas*, *Mytilus galloprovincialis*, *Chamelea gallina*)	Waters Acquity Ultra-Performance LC, Applied Biosystems Qtrap 5500	Waters Acquity HSS T3 column, 1.8 µm, 2.1 mm i.d. × 50 mm and Waters Acquity BEH C_{18} column, 1.7 µm 2.1 mm i.d. × 50 mm	0.1 – 100 $\mu g \cdot kg^{-1}$	0.01 – 1.11 $\mu g \cdot kg^{-1}$	0.02 – 3.7 $\mu g \cdot kg^{-1}$	30 – 116%	From 0 to – 80% (the majority of compounds)	[107]
Pharmaceuticals, personal care products ingredients and alkylphenols	Surface water, sediments and benthic mussels (*Geukensia demissa*)	Waters 2795 HPLC, Micromass Quattro Ultima QqQ MS	Waters Xterra C_{18} column, 3.5 µm, 2.1 mm i.d. × 100 mm or Waters Atlantis HILIC column, 3.0 µm, 2.1 mm i.d. × 100 mm	ND	ND	Water 0.1 – 2,300 $ng \cdot L^{-1}$; sediments 0.1 – 2,660 $\mu g \cdot kg^{-1}$ and mussels 0.07 – 1,400 $\mu g \cdot kg^{-1}$	Water: 33 – 130%; sediments: 54 – 140%; mussels: 56 – 150% (for the majority of compounds)	ND	[108]

Abbreviations: ND: no data.

compounds in a scope of the analytical procedure. However, the number of compounds determined by nano-LC methods is generally lower, and only a few authors have proposed truly multi-analyte methods. To our knowledge, only one multi-analyte method for veterinary drugs, as well as one multi-analyte method for mycotoxins have been proposed by Alcántara-Durán et al.[57,73] A method for determining 64 and 162 multiclass pesticides was proposed by Moreno-González et al.[37,68] In recent years, there has been a growing interest in this topic, and more multi-analyte nano-LC methods have been proposed, leading to an increasing appeal of the nano-LC techniques for routine analysis.

One of the critical points of interest is the sensitivity of the analytical method. As it was demonstrated in this review, improved sensitivity has been often declared as an advantage of nano-LC methods. This trend is in line with the theoretical predictions and is illustrated by the low LOD values of methods developed by various researchers. At the same time, the methodologies for estimating LOD values are not always consistent and there may be significant variations even in the same group of analytes. Overall, nano-LC methods have brought significant improvements in sensitivity to applications in proteomics while for the determination of low molecular mass compounds, such as pharmaceuticals and pesticides, the sensitivity advantages of nano-LC methods are less pronounced, but still meaningful. It should be noted that the applications of nano-LC methods for the quantification of pharmaceuticals, mycotoxins, and pesticides still provide other benefits, for instance, lower solvent consumption, better chromatographic separation, and better ionization in mass spectrometers.

One of the concerns regarding the development of nano-LC methods is the lack of variety of chromatographic columns for nano-LC. As aforementioned, there are packed and monolithic columns. However, typically they are reversed phase C_{18} columns with different particle sizes. Some research groups are still advancing in the field using in-house packed columns, as well as in-house assembled chromatography systems. While such approach clearly has the benefits of versatility, there are also the drawbacks of method transfer or replication when nonstandardized custom-built instrumentation is involved.

It is worth mentioning that there is still a limited number of nano-LC method applications in routine sample analysis, such as the methods by Moreno-González et al.[37,68] for determining multiclass pesticides and by Contreras et al.[66] for determining phenolic compounds and flavonoids. This can be explained by concerns about the time of analysis, as lower flow rates result in longer equilibration time and gradient delay, although there are possibilities for optimization. Applications of the nano-LC method for environment sample analysis are promising; however, to date there is only limited number of studies.

Future directions of research

Nano-LC methods have been known for many years and there has been a considerable progress in method development. Numerous studies have demonstrated encouraging results for the application of nano-LC methods in food

safety and environmental sample analysis. Despite that, several groups of compounds are yet to be analyzed with this technology. Similarly, to date, the lab-on-chip approach of nano-LC has been adapted for the analysis of mycotoxins,[62] but no chip-based methods have been reported for the determination of other compounds. Likewise, it introduces great opportunities for reducing some of the drawbacks that are common to regular implementation of this method. That is why the future studies incorporating the development, validation, and application of multi-analyte methods for antibiotics, other pharmaceuticals, and mycotoxins could substantiate the suitability of nano-LC method for a wider range of tasks.

The trends toward miniaturization also affect the design of analytical columns. The development of microcapillaries has allowed to further decrease the ID of columns,[18] and open capillary columns with ID $<20\,\mu$m and even $<10\,\mu$m are being investigated and applied for proteomics.[18,43,61] Clearly, the efforts toward the design of such columns will benefit from more rigorous, systematic approach and theoretical analysis, which should lead to the implementation of appropriate technical solutions, followed by commercialization.

It has been proposed that it should be possible to substantially decrease matrix effects by using the nanoLC-Direct-EI MS approach,[31] and several examples of applications have been presented.[35,36,101] However, this particular type of interface is not commonly used by other researchers and no applications for food analysis have been reported. Moreno-González et al.[68] reported that, in comparison to other liquid chromatography methods, a nano-LC method combined with QuEChERS (Quick Easy Cheap Effective Rugged Safe) sample preparation provides for substantially lower matrix effects. Additionally, to mitigate such negative effects as bubble formation during nano-LC analysis, nano-liquid–junction interface has been proposed.[102]

In proteomics, several applications of 2D nano-LC methods have been previously described.[14,116–119] However, to date, there have been no reports about the application of 2D nano-LC methods in the field of food safety and environmental sample analysis. Considering the significant decrease of matrix effects and the extended range of analyzed compounds that 2D chromatography can provide, this direction of research and method development can be expected to have a great potential.

Conclusions

Without a doubt, nano-LC methods represent a major category of separation methods that has applications in a variety of fields. Since the beginning of liquid chromatography as a method of separation, it has developed rapidly and became one of the key methods in analytical chemistry.

This review provided an outlook on the wide variety of applications of nano-LC methods for the determination of antibiotics, veterinary drugs, pesticides, mycotoxins, and environmental contaminants. Comparisons of sample preparation procedures and analytical performance were provided. The reviewed sources have clearly demonstrated that despite some drawbacks discussed in this article nano-LC methods offer important improvements in analytical performance, such as sensitivity. In addition, numerous examples of simplified sample preparation steps were presented.

Considering the increasing regulatory requirements for the detection of contaminants, there is a strong demand for more capable analytical methods. Both the technological aspects of liquid chromatography and approaches to method development have undergone significant improvements throughout the years. Still, there are vast opportunities for nano-LC method development for the analysis of contaminants in food and environmental samples. Since the number of published nano-LC applications to food safety control is rather limited, it should be considered as an opportunity for further research and method development.

Rather than being a single step in the development of liquid chromatography, the nano-LC techniques can be expected to undergo iterative optimization and the implementation of innovative ideas. The next steps of future development in liquid chromatography miniaturization may include further decrease of column internal diameter, as well as the application of lab-on-chip designs to 2D nano-LC instrumentation in food and environmental sample analysis.

Conflicts of interests

Authors declare no conflicts of interest.

Funding

This work was supported by the Latvian Council of Science under the project No. lzp-2020/2-0128.

ORCID

Deniss Fedorenko http://orcid.org/0000-0001-7577-6864
Vadims Bartkevics http://orcid.org/0000-0002-6193-7409

References

[1] Novotny, M. Microcolumns in Liquid Chromatography. *Anal. Chem.* **1981**, *53*, 1294A–1308A. DOI: 10.1021/ac00235a001.
[2] Karlsson, K. E.; Novotny, M. Separation Efficiency of Slurry-Packed Liquid Chromatography Microcolumns with Very Small Inner Diameters. *Anal. Chem.* **1988**, *60*, 1662–1665. DOI: 10.1021/ac00168a006.
[3] Knox, J. H. Theoretical Aspects of LC with Packed and Open Small-Bore Columns. *J. Chromatogr. Sci.* **1980**, *18*, 453–461. DOI: 10.1093/chromsci/18.9.453.
[4] Knox, J. H.; Gilbert, M. T. Kinetic Optimization of Straight Open-Tubular Liquid Chromatography. *J. Chromatogr. A* **1979**, *186*, 405–418. DOI: 10.1016/S0021-9673(00)95263-4..
[5] Chervet, J. P.; Ursem, M.; Salzmann, J. P. Instrumental Requirements for Nanoscale Liquid Chromatography. *Anal. Chem.* **1996**, *68*, 1507–1512. DOI: 10.1021/ac9508964.
[6] Yandamuri, N.; Nagabattula, K. R. S.; Kurra, S. S.; Batthula, S.; Allada, L. P. S. N.; Bandam, P. Comparative Study of New Trends in HPLC: A Review. *Int. J. Pharm. Sci. Rev. Res.* **2013**, 23, 167–172.
[7] Fanali, S. An Overview to Nano-Scale Analytical Techniques: Nano-Liquid Chromatography and Capillary

Electrochromatography. *Electrophoresis* **2017**, *38*, 1822–1829. DOI: 10.1002/elps.201600573.

[8] Gama, M. R.; Collins, C. H.; Bottoli, C. B. G. Nano-Liquid Chromatography in Pharmaceutical and Biomedical Research. *J. Chromatogr. Sci.* **2013**, *51*, 694–703. DOI: 10.1093/chromsci/bmt023.

[9] Xie, X.; Tolley, L. T.; Truong, T. X.; Tolley, H. D.; Farnsworth, P. B.; Lee, M. L. Dual-Wavelength Light-Emitting Diode-Based Ultraviolet Absorption Detector for Nano-Flow Capillary Liquid Chromatography. *J. Chromatogr. A* **2017**, *1523*, 242–247. DOI: 10.1016/j.chroma.2017.07.097.

[10] Hsieh, S.-H.; Huang, H.-Y.; Lee, S. Determination of Eight Penicillin Antibiotics in Pharmaceuticals, Milk and Porcine Tissues by Nano-Liquid Chromatography. *J. Chromatogr. A* **2009**, *1216*, 7186–7194. DOI: 10.1016/j.chroma.2009.05.080.

[11] Fanali, C.; Asensio-Ramos, M.; D'Orazio, G.; Hernández-Borges, J.; Rocco, A.; Fanali, S. Nano-Liquid Chromatographic Separations. In *Handbook of Advanced Chromatography/Mass Spectrometry Techniques;* Holčapek, M., Byrdwell, Wm. C., Eds.; AOCS Press: Urbana, Illinois, **2017**; Chapter 9, pp 309–363. DOI: 10.1016/B978-0-12-811732-3.00009-1.

[12] Fanali, C.; Dugo, L.; Dugo, P.; Mondello, L. Capillary-Liquid Chromatography (CLC) and Nano-LC in Food Analysis. *TrAC Trends Anal. Chem.* **2013**, *52*, 226–238. DOI: 10.1016/j.trac.2013.05.021.

[13] Yandamuri, N.; Dinakaran, S. K. Advanced Study of Nano Liquid Chromatography and Its Application-A Review. *World J. Pharm. Res.* **2015**, *4*, 1355–1367.

[14] Šesták, J.; Moravcová, D.; Kahle, V. Instrument Platforms for Nano Liquid Chromatography. *J. Chromatogr. A* **2015**, *1421*, 2–17. DOI: 10.1016/j.chroma.2015.07.090.

[15] Vehus, T.; Roberg-Larsen, H.; Waaler, J.; Aslaksen, S.; Krauss, S.; Wilson, S. R.; Lundanes, E. Versatile, sensitive liquid chromatography mass spectrometry – Implementation of 10 μm OT columns suitable for small molecules, peptides and proteins. *Sci Rep* **2016**, *6*, 37507. DOI: 10.1038/srep37507

[16] D'Orazio, G.; Fanali, S. Combination of Two Different Stationary Phases for on-Line Pre-Concentration and Separation of Basic Drugs by Using Nano-Liquid Chromatography. *J. Chromatogr. A* **2013**, *1285*, 118–123. DOI: 10.1016/j.chroma.2013.02.035.

[17] Wilson, S. R.; Vehus, T.; Berg, H. S.; Lundanes, E. Nano-LC in Proteomics: Recent Advances and Approaches. *Bioanalysis* **2015**, *7*, 1799–1815. DOI: 10.4155/bio.15.92.

[18] Shimizu, H.; Smirnova, A.; Mawatari, K.; Kitamori, T. Extended-Nano Chromatography. *J. Chromatogr. A* **2017**, *1490*, 11–20. DOI: 10.1016/j.chroma.2016.09.012.

[19] Kovalakova, P.; Cizmas, L.; McDonald, T. J.; Marsalek, B.; Feng, M.; Sharma, K. V. Occurrence and Toxicity of Antibiotics in the Aquatic Environment: A Review. *Chemosphere* **2020**, *251*, 126351. DOI: 10.1016/j.chemosphere.2020.126351.

[20] Gunther, F. A.; Whitacre, D. M.; Albert, L. A.; Hutzinger, O.; Knaak, J. B.; Mayer, F. L.; Morgan, D. P.; Park, D. L.; Tjeerdema, R. S.; de Voogt, P. Occurrence and Fate of Human Pharmaceuticals in the Environment. In *Reviews of Environmental Contamination and Toxicology*; Springer New York: New York, NY, **2010**; Vol. 202, pp 53–154. DOI: 10.1007/978-1-4419-1157-5_2.

[21] Sui, Q.; Cao, X.; Lu, S.; Zhao, W.; Qiu, Z.; Yu, G. Occurrence, Sources and Fate of Pharmaceuticals and Personal Care Products in the Groundwater: A Review. *Emerg. Contam.* **2015**, *1*, 14–24. DOI: 10.1016/j.emcon.2015.07.001.

[22] Gross, B.; Montgomery-Brown, J.; Naumann, A.; Reinhard, M. Occurrence and Fate of Pharmaceuticals and Alkylphenol Ethoxylate Metabolites in an Effluent-Dominated River and Wetland. *Environ. Toxicol. Chem.* **2004**, *23*, 2074–2083. DOI: 10.1897/03-606.

[23] Regulation (EC) No 396/2005 of the European Parliament and of the Council of 23 February **2005** on maximum residue levels of pesticides in or on food and feed of plant and animal origin and amending Council Directive 91/414/EECText with EEA relevance.

[24] Commission Regulation (EC) No 1881/2006 of 19 December 2006 setting maximum levels for certain contaminants in foodstuffs.

[25] Commission Regulation (EU) No 37/2010 of 22 December 2009 on pharmacologically active substances and their classification regarding maximum residue limits in foodstuffs of animal origin.

[26] Commission Decision of 14 August 2002 implementing Council Directive 96/23/EC concerning the performance of analytical methods and the interpretation of results.

[27] 2002/657/EC: Commission Decision of 12 August 2002 implementing Council Directive 96/23/EC concerning the performance of analytical methods and the interpretation of results.

[28] Szumski, M.; Buszewski, B. State of the Art in Miniaturized Separation Techniques. *Crit. Rev. Anal. Chem.* **2002**, *32*, 1–46. DOI: 10.1080/10408340290765434.

[29] Vissers, J. P. C.; Claessens, H. A.; Cramers, C. A. Microcolumn Liquid Chromatography: Instrumentation, Detection and Applications. *J. Chromatogr. A* **1997**, *779*, 1–28. DOI: 10.1016/S0021-9673(97)00422-6.

[30] Schmidt, A.; Karas, M.; Dülcks, T. Effect of Different Solution Flow Rates on Analyte Ion Signals in Nano-ESI MS, or: When Does ESI Turn into Nano-ESI? *J. Am. Soc. Mass Spectrom.* **2003**, *14*, 492–500. DOI: 10.1016/S1044-0305(03)00128-4.

[31] Rigano, F.; Tranchida, P. Q.; Dugo, P.; Mondello, L. High-Performance Liquid Chromatography Combined with Electron Ionization Mass Spectrometry: A Review. *TrAC Trends Anal. Chem.* **2019**, *118*, 112–122. DOI: 10.1016/j.trac.2019.05.032.

[32] El-Faramawy, A.; Siu, K. W. M.; Thomson, B. A. Efficiency of Nano-Electrospray Ionization. *J. Am. Soc. Mass Spectrom.* **2005**, *16*, 1702–1707. DOI: 10.1016/j.jasms.2005.06.011.

[33] D'Orazio, G.; Rocco, A.; Fanali, S. Fast-Liquid Chromatography Using Columns of Different Internal Diameters Packed with Sub-2 Mm Silica Particles. *J. Chromatogr. A* **2012**, *1228*, 213–220. DOI: 10.1016/j.chroma.2011.05.053.

[34] Noga, M.; Sucharski, F.; Suder, P.; Silberring, J. A Practical Guide to Nano-LC Troubleshooting. *J. Sep. Sci.* **2007**, *30*, 2179–2189. DOI: 10.1002/jssc.200700225.

[35] Cappiello, A.; Famiglini, G.; Pierini, E.; Palma, P.; Trufelli, H. Advanced Liquid Chromatography – Mass Spectrometry Interface Based on Electron Ionization. *Anal. Chem.* **2007**, *79*, 5364–5372. DOI: 10.1021/ac070468l.

[36] Cappiello, A.; Famiglini, G.; Palma, P.; Pierini, E.; Termopoli, V.; Trufelli, H. Overcoming Matrix Effects in Liquid Chromatography – Mass Spectrometry. *Anal. Chem.* **2008**, *80*, 9343–9348. DOI: 10.1021/ac8018312.

[37] Moreno-González, D.; Pérez-Ortega, P.; Gilbert-López, B.; Molina-Díaz, A.; García-Reyes, J. F.; Fernández-Alba, A. R. Evaluation of Nanoflow Liquid Chromatography High Resolution Mass Spectrometry for Pesticide Residue Analysis in Food. *J. Chromatogr. A* **2017**, *1512*, 78–87. DOI: 10.1016/j.chroma.2017.07.019.

[38] Nakashima, A.; Yamaguchi, H.; Kodani, Y.; Kaneko, Y. S.; Kawata, M.; Nagasaki, H.; Nagatsu, T.; Ota, A. Identification by Nano-LC-MS/MS of NT5DC2 as a Protein Binding to Tyrosine Hydroxylase: Down-Regulation of NT5DC2 by SiRNA Increases Catecholamine Synthesis in PC12D Cells. *Biochem. Biophys. Res. Commun.* **2019**, *516*, 1060–1065. DOI: 10.1016/j.bbrc.2019.06.156.

[39] Oedit, A.; Vulto, P.; Ramautar, R.; Lindenburg, P. W.; Hankemeier, T. Lab-on-a-Chip Hyphenation with Mass Spectrometry: Strategies for Bioanalytical Applications. *Curr. Opin. Biotechnol.* **2015**, *31*, 79–85. DOI: 10.1016/j.copbio.2014.08.009.

[40] Kim, W.; Guo, M.; Yang, P.; Wang, D. Microfabricated Monolithic Multinozzle Emitters for Nanoelectrospray Mass

Spectrometry. *Anal. Chem.* **2007**, *79*, 3703–3707. DOI: 10.1021/ac070010j.

[41] Wilson, S. R.; Malerod, H.; Holm, A.; Molander, P.; Lundanes, E.; Greibrokk, T. On-Line SPE–Nano-LC–Nanospray-MS for Rapid and Sensitive Determination of Perfluorooctanoic Acid and Perfluorooctane Sulfonate in River Water. *J. Chromatogr. Sci.* **2007**, *45*, 146–152. DOI: 10.1093/chromsci/45.3.146.

[42] New Objective : Innovation in High-Performance LC-MS http://www.newobjective.com/products/emitters/coatings.shtml (accessed Oct 29, 2020).

[43] Wilson, S. R.; Olsen, C.; Lundanes, E. Nano Liquid Chromatography Columns. *Analyst* **2019**, *144*, 7090–7104. DOI: 10.1039/c9an01473j.

[44] Fouad, A.; Shaykoon, M. S. A.; Ibrahim, S. M.; El-Adl, S. M.; Ghanem, A. Colistin Sulfate Chiral Stationary Phase for the Enantioselective Separation of Pharmaceuticals Using Organic Polymer Monolithic Capillary Chromatography. *Molecules* **2019**, *24*, 833. DOI: 10.3390/molecules24050833.

[45] Chankvetadze, B. Recent Developments on Polysaccharide-Based Chiral Stationary Phases for Liquid-Phase Separation of Enantiomers. *J Chromatogr A* **2012**, *1269*, 26–51. DOI: 10.1016/j.chroma.2012.10.033.

[46] Fanali, S.; Rocchi, S.; Chankvetadze, B. Use of Novel Phenyl-Hexyl Core-Shell Particles in Nano-LC. *Electrophoresis* **2013**, *34*, 1737–1742. DOI: 10.1002/elps.201200639.

[47] D'Orazio, G.; Fanali, C.; Fanali, S.; Gentili, A.; Karchkhadze, M.; Chankvetadze, B. Further Study on Enantiomer Resolving Ability of Amylose Tris(3-Chloro-5-Methylphenylcarbamate) Covalently Immobilized onto Silica in Nano-Liquid Chromatography and Capillary Electrochromatography. *J. Chromatogr. A* **2020**, *1623*, 461213. DOI: 10.1016/j.chroma.2020.461213.

[48] D'Orazio, G.; Fanali, C.; Fanali, S.; Gentili, A.; Chankvetadze, B. Comparative Study on Enantiomer Resolving Ability of Amylose Tris(3-Chloro-5-Methylphenylcarbamate) Covalently Immobilized onto Silica in Nano-Liquid Chromatography and Capillary Electrochromatography. *J. Chromatogr. A* **2019**, *1606*, 460425. DOI: 10.1016/j.chroma.2019.460425.

[49] Buonasera, K.; D'Orazio, G.; Fanali, S.; Dugo, P.; Mondello, L. Separation of Organophosphorus Pesticides by Using Nano-Liquid Chromatography. *J. Chromatogr. A* **2009**, *1216*, 3970–3976. DOI: 10.1016/j.chroma.2009.03.005.

[50] Vasconcelos Soares Maciel, E.; de Toffoli, A. L.; Sobieski, E.; Domingues Nazário, C. E.; Lanças, F. M. Miniaturized Liquid Chromatography Focusing on Analytical Columns and Mass Spectrometry: A Review. *Anal. Chim. Acta* **2020**, *1103*, 11–31. DOI: 10.1016/j.aca.2019.12.064.

[51] Fanali, S. Nano-Liquid Chromatography Applied to Enantiomers Separation. *J. Chromatogr. A* **2017**, *1486*, 20–34. DOI: 10.1016/j.chroma.2016.10.028.

[52] Pérez-Fernández, V.; Dominguez-Vega, E.; Chankvetadze, B.; Crego, A. L.; García, M. Á.; Marina, M. L. Evaluation of New Cellulose-Based Chiral Stationary Phases Sepapak-2 and Sepapak-4 for the Enantiomeric Separation of Pesticides by Nano Liquid Chromatography and Capillary Electrochromatography. *J. Chromatogr. A* **2012**, *1234*, 22–31. DOI: 10.1016/j.chroma.2012.01.035.

[53] Aydoğan, C. A New Anion-Exchange/Hydrophobic Monolith as Stationary Phase for Nano Liquid Chromatography of Small Organic Molecules and Inorganic Anions. *J. Chromatogr. A* **2015**, *1392*, 63–68. DOI: 10.1016/j.chroma.2015.03.014.

[54] Aydoğan, C.; Yı lmaz, F.; Denizli, A. Cation Exchange/Hydrophobic Interaction Monolithic Chromatography of Small Molecules and Proteins by Nano Liquid Chromatography. *J. Sep. Sci.* **2013**, *36*, 1685–1692. DOI: 10.1002/jssc.201300089.

[55] Aydoğan, C.; Gökaltun, A.; Denizli, A.; El-Rassi, Z. Organic Polymer-Based Monolithic Capillary Columns and Their Applications in Food Analysis. *J. Sep. Sci.* **2019**, *42*, 962–979. DOI: 10.1002/jssc.201801051.

[56] Fanali, S.; Aturki, Z.; D'Orazio, G.; Rocco, A. Separation of Basic Compounds of Pharmaceutical Interest by Using Nano-Liquid Chromatography Coupled with Mass Spectrometry. *J. Chromatogr. A* **2007**, *1150*, 252–258. DOI: 10.1016/j.chroma.2006.10.021.

[57] Alcántara-Durán, J.; Moreno-González, D.; Gilbert-López, B.; Molina-Díaz, A.; García-Reyes, J. F. Matrix-Effect Free Multi-Residue Analysis of Veterinary Drugs in Food Samples of Animal Origin by Nanoflow Liquid Chromatography High Resolution Mass Spectrometry. *Food Chem.* **2018**, *245*, 29–38. DOI: 10.1016/j.foodchem.2017.10.083.

[58] Moreno-González, D.; Alcántara-Durán, J.; Gilbert-López, B.; García-Reyes, J. F.; Molina-Díaz, A. Matrix-Effect Free Quantitative Liquid Chromatography Mass Spectrometry Analysis in Complex Matrices Using Nanoflow Liquid Chromatography with Integrated Emitter Tip and High Dilution Factors. *J. Chromatogr. A* **2017**, *1519*, 110–120. DOI: 10.1016/j.chroma.2017.09.006.

[59] Marginean, I.; Kelly, R. T.; Moore, R. J.; Prior, D. C.; LaMarche, B. L.; Tang, K.; Smith, R. D. Selection of the Optimum Electrospray Voltage for Gradient Elution LC-MS Measurements. *J. Am. Soc. Mass Spectrom.* **2009**, *20*, 682–688. DOI: 10.1016/j.jasms.2008.12.004.

[60] Lehotay, S. J.; Chen, Y. Hits and Misses in Research Trends to Monitor Contaminants in Foods. *Anal. Bioanal. Chem.* **2018**, *410*, 5331–5351. DOI: 10.1007/s00216-018-1195-3.

[61] Desmet, G.; Eeltink, S. Fundamentals for LC Miniaturization. *Anal. Chem.* **2013**, *85*, 543–556. DOI: 10.1021/ac303317c.

[62] Liu, H.-Y.; Lin, S.-L.; Chan, S.-A.; Lin, T.-Y.; Fuh, M.-R. Microfluidic Chip-Based Nano-Liquid Chromatography Tandem Mass Spectrometry for Quantification of Aflatoxins in Peanut Products. *Talanta* **2013**, *113*, 76–81. DOI: 10.1016/j.talanta.2013.03.053.

[63] Eikel, D.; Henion, J. Liquid Extraction Surface Analysis (LESA) of Food Surfaces Employing Chip-Based Nano-Electrospray Mass Spectrometry. *Rapid Commun. Mass Spectrom.* **2011**, *25*, 2345–2354. DOI: 10.1002/rcm.5107.

[64] Sainiemi, L.; Nissilä, T.; Kostiainen, R.; Franssila, S.; Ketola, R. A. A Microfabricated Micropillar Liquid Chromatographic Chip Monolithically Integrated with an Electrospray Ionization Tip. *Lab Chip* **2012**, *12*, 325–332. DOI: 10.1039/c1lc20874h.

[65] Aydoğan, C.; Rassi, Z. E. MWCNT Based Monolith for the Analysis of Antibiotics and Pesticides in Milk and Honey by Integrated Nano-Liquid Chromatography-High Resolution Orbitrap Mass Spectrometry. *Anal. Methods* **2019**, *11*, 21–28. DOI: 10.1039/C8AY02173B.

[66] Contreras, M. d M.; Arráez-Román, D.; Fernández-Gutiérrez, A.; Segura-Carretero, A. Nano-Liquid Chromatography Coupled to Time-of-Flight Mass Spectrometry for Phenolic Profiling: A Case Study in Cranberry Syrups. *Talanta* **2015**, *132*, 929–938. DOI: 10.1016/j.talanta.2014.10.049.

[67] D'Orazio, G.; Rocchi, S.; Fanali, S. Nano-Liquid Chromatography Coupled with Mass Spectrometry: Separation of Sulfonamides Employing Non-Porous Core–Shell Particles. *J. Chromatogr. A* **2012**, *1255*, 277–285. DOI: 10.1016/j.chroma.2012.03.032.

[68] Moreno-González, D.; Alcántara-Durán, J.; Addona, S. M.; Beneito-Cambra, M. Multi-Residue Pesticide Analysis in Virgin Olive Oil by Nanoflow Liquid Chromatography High Resolution Mass Spectrometry. *J. Chromatogr. A* **2018**, *1562*, 27–35. DOI: 10.1016/j.chroma.2018.05.053.

[69] Mirabelli, M. F.; Wolf, J.-C.; Zenobi, R. Pesticide Analysis at Ppt Concentration Levels: Coupling Nano-Liquid Chromatography with Dielectric Barrier Discharge Ionization-Mass Spectrometry. *Anal. Bioanal. Chem.* **2016**, *408*, 3425–3434. DOI: 10.1007/s00216-016-9419-x.

[70] Berlioz-Barbier, A.; Baudot, R.; Wiest, L.; Gust, M.; Garric, J.; Cren-Olivé, C.; Buleté, A. MicroQuEChERS–Nanoliquid Chromatography–Nanospray–Tandem Mass Spectrometry for the Detection and Quantification of Trace Pharmaceuticals in

Benthic Invertebrates. *Talanta* **2015**, *132*, 796–802. DOI: 10.1016/j.talanta.2014.10.030.

[71] Quality of wastewater in the El Paso, Texas region — Analysis of pharmaceuticals and personal care products using high performance liquid chromatography tandem mass spectrometry - ProQuest https://search.proquest.com/docview/916754906/?pq-origsite=primo (accessed Nov 4, **2019**.

[72] Berlioz-Barbier, A.; Buleté, A.; Faburé, J.; Garric, J.; Cren-Olivé, C.; Vulliet, E. Multi-Residue Analysis of Emerging Pollutants in Benthic Invertebrates by Modified Micro-Quick-Easy-Cheap-Efficient-Rugged-Safe Extraction and Nanoliquid Chromatography–Nanospray–Tandem Mass Spectrometry Analysis. *J. Chromatogr. A* **2014**, *1367*, 16–32. DOI: 10.1016/j.chroma.2014.09.044.

[73] Alcántara-Durán, J.; Moreno-González, D.; García-Reyes, J. F.; Molina-Díaz, A. Use of a Modified QuEChERS Method for the Determination of Mycotoxin Residues in Edible Nuts by Nano Flow Liquid Chromatography High Resolution Mass Spectrometry. *Food Chem.* **2019**, *279*, 144–149. DOI: 10.1016/j.foodchem.2018.11.149.

[74] Asensio-Ramos, M.; D'Orazio, G.; Hernandez-Borges, J.; Rocco, A.; Fanali, S. Multi-Walled Carbon Nanotubes–Dispersive Solid-Phase Extraction Combined with Nano-Liquid Chromatography for the Analysis of Pesticides in Water Samples. *Anal. Bioanal. Chem.* **2011**, *400*, 1113–1123. DOI: 10.1007/s00216-011-4885-7.

[75] Moreno-González, D.; Cutillas, V.; Hernando, M. D.; Alcántara-Durán, J.; García-Reyes, J. F.; Molina-Díaz, A. Quantitative Determination of Pesticide Residues in Specific Parts of Bee Specimens by Nanoflow Liquid Chromatography High Resolution Mass Spectrometry. *Sci. Total Environ.* **2020**, *715*, 137005. DOI: 10.1016/j.scitotenv.2020.137005.

[76] Moreno-González, D.; Alcántara-Durán, J.; Gilbert-López, B.; Beneito-Cambra, M.; Cutillas, V. M.; Rajski, Ł.; Molina-Díaz, A.; García-Reyes, J. F. Sensitive Detection of Neonicotinoid Insecticides and Other Selected Pesticides in Pollen and Nectar Using Nanoflow Liquid Chromatography Orbitrap Tandem Mass Spectrometry. *J. AOAC Int.* **2018**, *101*, 367–373. DOI: 10.5740/jaoacint.17-0412.

[77] Zhang, Z.; Li, X.; Ding, S.; Jiang, H.; Shen, J.; Xia, X. Multiresidue Analysis of Sulfonamides, Quinolones, and Tetracyclines in Animal Tissues by Ultra-High Performance Liquid Chromatography–Tandem Mass Spectrometry. *Food Chem.* **2016**, *204*, 252–262. DOI: 10.1016/j.foodchem.2016.02.142.

[78] Kaufmann, A.; Butcher, P.; Maden, K.; Widmer, M. Quantitative Multiresidue Method for about 100 Veterinary Drugs in Different Meat Matrices by Sub 2-Mm Particulate High-Performance Liquid Chromatography Coupled to Time of Flight Mass Spectrometry. *J. Chromatogr. A* **2008**, *1194*, 66–79. DOI: 10.1016/j.chroma.2008.03.089.

[79] Dasenaki, M. E.; Michali, C. S.; Thomaidis, N. S. Analysis of 76 Veterinary Pharmaceuticals from 13 Classes Including Aminoglycosides in Bovine Muscle by Hydrophilic Interaction Liquid Chromatography–Tandem Mass Spectrometry. *J. Chromatogr. A* **2016**, *1452*, 67–80. DOI: 10.1016/j.chroma.2008.03.089.

[80] Aguilera-Luiz, M. M.; Martínez Vidal, J. L.; Romero-González, R.; Frenich, A. G. Multi-Residue Determination of Veterinary Drugs in Milk by Ultra-High-Pressure Liquid Chromatography–Tandem Mass Spectrometry. *J. Chromatogr. A* **2008**, *1205*, 10–16. DOI: 10.1016/j.chroma.2008.07.066.

[81] Martins, M. T.; Barreto, F.; Hoff, R. B.; Jank, L.; Arsand, J. B.; Motta, T. M. C.; Schapoval, E. E. C. Multiclass and Multi-Residue Determination of Antibiotics in Bovine Milk by Liquid Chromatography–Tandem Mass Spectrometry: Combining Efficiency of Milk Control and Simplicity of Routine Analysis. *Int. Dairy J.* **2016**, *59*, 44–51. DOI: 10.1016/j.idairyj.2016.02.048.

[82] Romero-González, R.; Aguilera-Luiz, M. M.; Plaza-Bolaños, P.; Garrido Frenich, A.; Martínez Vidal, J. L. Food Contaminant Analysis at High Resolution Mass Spectrometry: Application for the Determination of Veterinary Drugs in Milk. *J. Chromatogr. A* **2011**, *1218*, 9353–9365. DOI: 10.1016/j.chroma.2011.10.074.

[83] Jin, Y.; Zhang, J.; Zhao, W.; Zhang, W.; Wang, L.; Zhou, J.; Li, Y. Development and Validation of a Multiclass Method for the Quantification of Veterinary Drug Residues in Honey and Royal Jelly by Liquid Chromatography–Tandem Mass Spectrometry. *Food Chem.* **2017**, *221*, 1298–1307. DOI: 10.1016/j.foodchem.2016.11.026.

[84] Xiu-Ping, Z.; Lin, M.; Lan-Qi, H.; Jian-Bo, C.; Li, Z. The Optimization and Establishment of QuEChERS-UPLC–MS/MS Method for Simultaneously Detecting Various Kinds of Pesticides Residues in Fruits and Vegetables. *J. Chromatogr. B* **2017**, *1060*, 281–290. DOI: 10.1016/j.jchromb.2017.06.008.

[85] Yang, X.; Luo, J.; Duan, Y.; Li, S.; Liu, C. Simultaneous Analysis of Multiple Pesticide Residues in Minor Fruits by Ultrahigh-Performance Liquid Chromatography/Hybrid Quadrupole Time-of-Fight Mass Spectrometry. *Food Chem.* **2018**, *241*, 188–198. DOI: 10.1016/j.foodchem.2017.08.102.

[86] Dias, J. V.; Cutillas, V.; Lozano, A.; Pizzutti, I. R.; Fernández-Alba, A. R. Determination of Pesticides in Edible Oils by Liquid Chromatography-Tandem Mass Spectrometry Employing New Generation Materials for Dispersive Solid Phase Extraction Clean-Up. *J. Chromatogr. A* **2016**, *1462*, 8–18. DOI: 10.1016/j.chroma.2016.07.072.

[87] Anagnostopoulos, C.; Miliadis, G. E. Development and Validation of an Easy Multiresidue Method for the Determination of Multiclass Pesticide Residues Using GC–MS/MS and LC–MS/MS in Olive Oil and Olives. *Talanta* **2013**, *112*, 1–10. DOI: 10.1016/j.talanta.2013.03.051.

[88] Kasiotis, K. M.; Anagnostopoulos, C.; Anastasiadou, P.; Machera, K. Pesticide Residues in Honeybees, Honey and Bee Pollen by LC–MS/MS Screening: Reported Death Incidents in Honeybees. *Sci. Total Environ.* **2014**, *485–486*, 633–642. DOI: 10.1016/j.scitotenv.2014.03.042.

[89] Sivaperumal, P.; Anand, P.; Riddhi, L. Rapid Determination of Pesticide Residues in Fruits and Vegetables, Using Ultra-High-Performance Liquid Chromatography/Time-of-Flight Mass Spectrometry. *Food Chem.* **2015**, *168*, 356–365. DOI: 10.1016/j.foodchem.2014.07.072.

[90] Jallow, M. F. A.; Awadh, D. G.; Albaho, M. S.; Devi, V. Y. Monitoring of Pesticide Residues in Commonly Used Fruits and Vegetables in Kuwait. *Int. J. Environ. Res. Public. Health* **2017**, *14*, 833, DOI: 10.3390/ijerph14080833.

[91] Vuković, G.; Shtereva, D.; Bursić, V.; Mladenova, R.; Lazić, S. Application of GC–MSD and LC–MS/MS for the Determination of Priority Pesticides in Baby Foods in Serbian Market. *LWT - Food Sci. Technol.* **2012**, *49*, 312–319. DOI: 10.1016/j.lwt.2012.07.021.

[92] Gómez-Pérez, M. L.; Romero-González, R.; Vidal, J. L. M.; Frenich, A. G. Analysis of Pesticide and Veterinary Drug Residues in Baby Food by Liquid Chromatography Coupled to Orbitrap High Resolution Mass Spectrometry. *Talanta* **2015**, *131*, 1–7. DOI: 10.1016/j.talanta.2014.07.066.

[93] Hidalgo-Ruiz, J. L.; Romero-González, R.; Vidal, J. L. M.; Frenich, A. G. Determination of Mycotoxins in Nuts by Ultra High-Performance Liquid Chromatography-Tandem Mass Spectrometry: Looking for a Representative Matrix. *J. Food Compos. Anal.* **2019**, *82*, 103228. DOI: 10.1016/j.jfca.2019.05.011.

[94] Arroyo-Manzanares, N.; Huertas-Pérez, J. F.; Gámiz-Gracia, L.; García-Campaña, A. M. A New Approach in Sample Treatment Combined with UHPLC-MS/MS for the Determination of Multiclass Mycotoxins in Edible Nuts and Seeds. *Talanta* **2013**, *115*, 61–67. DOI: 10.1016/j.talanta.2013.04.024.

[95] Manizan, A. L.; Oplatowska-Stachowiak, M.; Piro-Metayer, I.; Campbell, K.; Koffi-Nevry, R.; Elliott, C.; Akaki, D.; Montet, D.; Brabet, C. Multi-Mycotoxin Determination in Rice, Maize and Peanut Products Most Consumed in Côte D'Ivoire by UHPLC-MS/MS. *Food Control* **2018**, *87*, 22–30. DOI: 10.1016/j.foodcont.2017.11.032.

[96] Cunha, S. C.; Sá, S. V. M.; Fernandes, J. O. Multiple Mycotoxin Analysis in Nut Products: Occurrence and Risk Characterization. *Food Chem. Toxicol.* **2018**, *114*, 260–269. DOI: 10.1016/j.fct.2018.02.039.

[97] Thompson, M.; Ellison, S. L. R.; Wood, R. Harmonized Guidelines for Single-Laboratory Validation of Methods of Analysis (IUPAC Technical Report). *Pure Appl. Chem.* **2002**, *74*, 835–855. DOI: 10.1351/pac200274050835.

[98] ICH Q2(R1) Validation of Analytical Procedures: Text and Methodology - ECA Academy. https://www.gmp-compliance.org/guidelines/gmp-guideline/ich-q2r1-validation-of-analytical-procedures-text-and-methodology (accessed Aug 1, 2020).

[99] Method Validation and Quality Control Procedures for Pesticide Residues Analysis in Food and Feed (SANTE/12682/2019) https://www.eurl-pesticides.eu/docs/public/tmplt_article.asp?CntID=727&LabID=100&Lang=EN (accessed Aug 1, 2020).

[100] Aqai, P.; Peters, J.; Gerssen, A.; Haasnoot, W.; Nielen, M. W. F. Immunomagnetic Microbeads for Screening with Flow Cytometry and Identification with Nano-Liquid Chromatography Mass Spectrometry of Ochratoxins in Wheat and Cereal. *Anal. Bioanal. Chem.* **2011**, *400*, 3085–3096. DOI: 10.1007/s00216-011-4974-7.

[101] Cappiello, A.; Famiglini, G.; Mangani, F.; Palma, P.; Siviero, A. Nano-High-Performance Liquid Chromatography–Electron Ionization Mass Spectrometry Approach for Environmental Analysis. *Anal. Chim. Acta* **2003**, *493*, 125–136. DOI: 10.1016/S0003-2670(03)00868-7.

[102] D'Orazio, G.; Fanali, S. Pressurized Nano-Liquid–Junction Interface for Coupling Capillary Electrochromatography and Nano-Liquid Chromatography with Mass Spectrometry. *J. Chromatogr. A* **2013**, *1317*, 67–76. DOI: 10.1016/j.chroma.2013.08.052.

[103] Li, L.; Zheng, B.; Liu, L. Biomonitoring and Bioindicators Used for River Ecosystems: Definitions, Approaches and Trends. *Proc. Environ. Sci.* **2010**, *2*, 1510–1524. DOI: 10.1016/j.proenv.2010.10.164.

[104] Huerta, B.; Jakimska, A.; Llorca, M.; Ruhí, A.; Margoutidis, G.; Acuña, V.; Sabater, S.; Rodriguez-Mozaz, S.; Barcelò, D. Development of an Extraction and Purification Method for the Determination of Multi-Class Pharmaceuticals and Endocrine Disruptors in Freshwater Invertebrates. *Talanta* **2015**, *132*, 373–381. DOI: 10.1016/j.talanta.2014.09.017.

[105] Marín, J. M.; Gracia-Lor, E.; Sancho, J. V.; López, F. J.; Hernández, F. Application of Ultra-High-Pressure Liquid Chromatography–Tandem Mass Spectrometry to the Determination of Multi-Class Pesticides in Environmental and Wastewater Samples: Study of Matrix Effects. *J. Chromatogr. A* **2009**, *1216*, 1410–1420. DOI: 10.1016/j.chroma.2008.12.094.

[106] Nödler, K.; Licha, T.; Bester, K.; Sauter, M. Development of a Multi-Residue Analytical Method, Based on Liquid Chromatography–Tandem Mass Spectrometry, for the Simultaneous Determination of 46 Micro-Contaminants in Aqueous Samples. *J. Chromatogr. A* **2010**, *1217*, 6511–6521. DOI: 10.1016/j.chroma.2010.08.048.

[107] Alvarez-Muñoz, D.; Huerta, B.; Fernandez-Tejedor, M.; Rodríguez-Mozaz, S.; Barceló, D. Multi-Residue Method for the Analysis of Pharmaceuticals and Some of Their Metabolites in Bivalves. *Talanta* **2015**, *136*, 174–182. DOI: 10.1016/j.talanta.2014.12.035.

[108] Klosterhaus, S. L.; Grace, R.; Hamilton, M. C.; Yee, D. Method Validation and Reconnaissance of Pharmaceuticals, Personal Care Products, and Alkylphenols in Surface Waters, Sediments, and Mussels in an Urban Estuary. *Environ. Int.* **2013**, *54*, 92–99. DOI: 10.1016/j.envint.2013.01.009.

[109] González-Fuenzalida, R. A.; López-García, E.; Moliner-Martínez, Y. Campíns-Falcó, P. Adsorbent Phases with Nanomaterials for in-Tube Solid-Phase Microextraction Coupled on-Line to Liquid Nanochromatography. *J. Chromatogr. A* **2016**, *1432*, 17–25. DOI: 10.1016/j.chroma.2016.01.009.

[110] D'Orazio, G.; Hernández-Borges, J.; Asensio-Ramos, M.; Rodríguez-Delgado, M. Á.; Fanali, S. Capillary Electrochromatography and Nano-Liquid Chromatography Coupled to Nano-Electrospray Ionization Interface for the Separation and Identification of Estrogenic Compounds. *Electrophoresis* **2016**, *37*, 356–362. DOI: 10.1002/elps.201500327.

[111] Serra-Mora, P.; Jornet-Martinez, N.; Moliner-Martinez, Y. Campíns-Falcó, P. In Tube-Solid Phase Microextraction-Nano Liquid Chromatography: Application to the Determination of Intact and Degraded Polar Triazines in Waters and Recovered Struvite. *J. Chromatogr. A* **2017**, *1513*, 51–58. DOI: 10.1016/j.chroma.2017.07.053.

[112] Berlioz-Barbier, A.; Buleté, A.; Fildier, A.; Garric, J.; Vulliet, E. Non-Targeted Investigation of Benthic Invertebrates (Chironomus Riparius) Exposed to Wastewater Treatment Plant Effluents Using Nanoliquid Chromatography Coupled to High-Resolution Mass Spectrometry. *Chemosphere* **2018**, *196*, 347–353. DOI: 10.1016/j.chemosphere.2018.01.001.

[113] Albergamo, A.; Rigano, F.; Purcaro, G.; Mauceri, A.; Fasulo, S.; Mondello, L. Free Fatty Acid Profiling of Marine Sentinels by NanoLC-EI-MS for the Assessment of Environmental Pollution Effects. *Sci. Total Environ.* **2016**, *571*, 955–962. DOI: 10.1016/j.scitotenv.2016.07.082.

[114] Rigano, F.; Albergamo, A.; Sciarrone, D.; Beccaria, M.; Purcaro, G.; Mondello, L. Nano Liquid Chromatography Directly Coupled to Electron Ionization Mass Spectrometry for Free Fatty Acid Elucidation in Mussel. *Anal. Chem.* **2016**, *88*, 4021–4028. DOI: 10.1021/acs.analchem.6b00328.

[115] Serra-Mora, P.; Herráez-Hernández, R.; Campíns-Falcó, P. Minimizing the Impact of Sample Preparation on Analytical Results: In-Tube Solid-Phase Microextraction Coupled on-Line to Nano-Liquid Chromatography for the Monitoring of Tribenuron Methyl in Environmental Waters. *Sci. Total Environ.* **2020**, *721*, 137732. DOI: 10.1016/j.scitotenv.2020.137732.

[116] Pan, H. T.; Guo, M. X.; Xiong, Y. M.; Ren, J.; Zhang, J. Y.; Gao, Q.; Ke, Z. H.; Xu, G. F.; Tan, Y. J.; Sheng, J. Z.; Huang, H. F. Differential Proteomic Analysis of Umbilical Artery Tissue from Preeclampsia Patients, Using ITRAQ Isobaric Tags and 2D Nano LC–MS/MS. *J. Proteomics* **2015**, *112*, 262–273. DOI: 10.1016/j.jprot.2014.09.006.

[117] Nägele, E.; Vollmer, M.; Hörth, P. Improved 2D Nano-LC/MS for Proteomics Applications: A Comparative Analysis Using Yeast Proteome. *J. Biomol. Tech.* **2004**, *15*, 134–143.

[118] Watson, G. W.; Wickramasekara, S.; Maier, C. S.; Williams, D. E.; Dashwood, R. H.; Ho, E. Assessment of Global Proteome in LNCaP Cells by 2D-RP/RP LC–MS/MS following Sulforaphane Exposure. *EuPA Open Proteomics* **2015**, *9*, 34–40. DOI: 10.1016/j.euprot.2015.08.002.

[119] Luo, Q.; Yue, G.; Valaskovic, G. A.; Gu, Y.; Wu, S.-L.; Karger, B. L. On-Line 1D and 2D Porous Layer Open Tubular/LC-ESI-MS Using 10-Mm-i.d. Poly(Styrene – Divinylbenzene) Columns for Ultrasensitive Proteomic Analysis. *Anal. Chem.* **2007**, *79*, 6174–6181. DOI: 10.1021/ac070583w.